INVESTIGATION OF HIPPOCAMPAL DEVELOPMENT DURING A PROTRACTED
POSTNATAL PERIOD IN CONTROL AND FETAL ALCOHOL WISTAR RATS

A THESIS SUBMITTED TO
THE GRADUATE SCHOOL OF NATURAL AND APPLIED SCIENCES
OF
MIDDLE EAST TECHNICAL UNIVERSITY

BY

BİRSEN ELİBOL-CAN

IN PARTIAL FULFILLMENT OF THE REQUIREMENTS
FOR
THE DEGREE OF DOCTOR OF PHILOSOPHY
IN
BIOLOGICAL SCIENCES

JANUARY 2013

Approval of the thesis:

INVESTIGATION OF HIPPOCAMPAL DEVELOPMENT DURING A PROTRACTED POSTNATAL PERIOD IN CONTROL AND FETAL-ALCOHOL WISTAR RATS

Submitted by **BİRSEN ELİBOL-CAN** in partial fulfillment of the requirements for the degree of **Doctor of Philosophy in Department of Biological Sciences, Middle East Technical University** by,

Prof. Dr. Canan Özgen   _____
Dean, Graduate School of **Natural and Applied Sciences**

Prof. Dr. Gülay Özcengiz   _____
Head of Department, **Biological Sciences**

Assoc. Prof. Dr. Ewa Jakubowska Doğru   _____
Supervisor, **Biological Sciences Dept., METU**

Prof. Dr. Ertuğrul Kılıç   _____
Co-Supervisor, **Physiology Dept., YU**

Examining Committee Members:

Prof. Dr. Emin Öztaş   _____
Medical Histology and Embryology Dept., GMMA

Assoc. Prof. Dr. Ewa Jakubowska Doğru   _____
Biological Sciences Dept., METU

Prof. Dr. Feride Severcan   _____
Biological Sciences Dept., METU

Assist. Prof. Dr. Tülin Yanık   _____
Biological Sciences Dept., METU

Assist. Prof. Dr. İlknur Dursun   _____
Molecular Biology Dept., Usküdar University

Date: 23.01.2013

I hereby declare that all information in this document has been obtained and presented in accordance with academic rules and ethical conduct. I also declare that, as required by these rules and conduct, I have fully cited and referenced all material and results that are not original to this work.

Name, Last name : BİRSEN ELİBOL-CAN

Signature　　　　　:

ABSTRACT

INVESTIGATION OF HIPPOCAMPAL DEVELOPMENT DURING A PROTRACTED POSTNATAL PERIOD IN CONTROL AND FETAL ALCOHOL WISTAR RATS

Elibol-Can, Birsen
Ph.D, Department of Biological Sciences
Supervisor : Assoc. Prof. Dr. Ewa-Jakubowska Doğru
Co-Supervisor: Prof. Dr. Ertuğrul Kılıç

January 2013, 134 pages

Behavioral deficits caused by fetal-alcohol are well expressed in juvenile subjects but usually ameliorate with maturation. It suggests some kind of postnatal regeneration. The aim of the present study was to examine the potential correlation between behavioral recovery and the postnatal hippocampal development in the fetal-alcohol rats. This study included behavioral tests applied to juvenile and adult subjects, unbiased stereology to investigate changes in neuron numbers and hippocampal volumes, the postnatal tracing and analysis of the hippocampal principal neuron's morphology, investigation of age-dependent changes in the distribution of doublecortin-expressing neurons, and evaluation of synaptic development by assessing age-dependent changes in the regional immunoreactivity/expression of synaptophysin and PSD95. Rats have been exposed to ethanol throughout 7-21 gestation days with daily ethanol dose of 6g/kg delivered by intragastric intubation to the pregnant dams. The morphological characteristics were examined on postnatal days P1, P10, P30, P60, in hippocampal CA1, CA3, and DG subregions, in fetal-alcohol and control rats. Both, stereological and doublecortin-immunoreactivity data pointed towards a possibility of limited neurogenesis taking place during a protracted postnatal period not only in the germinal zones (SGZ and SVZ) but also in the hippocampal CA regions. Ethanol effect on postnatal hippocampal development was limited to marginally lower number of granular cells in DG on P30. It correlated with poorer cognitive performance in the fetal-alcohol group. The treatment effect on the morphology of hippocampal neurons was observed mainly in CA region at P1 and seemed to be attributed more to the intubation stress than the ethanol itself.

Keywords: Fetal alcohol, postnatal brain development, hippocampus, rat, synaptic plasticity

ÖZ

NORMAL VE FÖTAL DÖNEMDE ALKOLE MARUZ KALMIŞ SIÇANLARDA DOĞUMDAN SONRAKİ İLK İKİ AYDA HİPPOKAMPUS GELİŞİMİNİN ARAŞTIRILMASI

Elibol-Can, Birsen
Doktora, Biyolojik Bilimler Bölümü
Tez Yöneticisi : Doç. Dr. Ewa-Jakubowska Doğru
Ortak Tez Yöneticisi : Prof. Dr. Ertuğrul Kılıç

Ocak 2013,   134 sayfa

Fötal alkole bağlı olarak gelişen davranışsal bozukluklar özellikle genç örneklerde görülmekte ve genellikle erginleşmeyle beraber azalmaktadır. Bu durum hemen doğum sonrasında beyinde görülen bazı yenilenme mekanizmalarına işaret etmektedir. Bu doğrultuda çalışmamızın amacı, fötal alkol grubundaki sıçanlarda görülen davranışsal bozukluklardaki iyileşme ile doğum sonrası hipokampal gelişim mekanizmaları arasındaki olası korelasyonların incelenmesidir. Bu çalışma, genç ve ergin sıçanlara uygulanan davranışsal testleri, hipokampus hacmindeki ve nöron sayısındaki değişimleri inceleyen tarafsız stereolojiyi, hipokampus ana nöronlarındaki morfolojik analizleri, doublekortin eksprese eden nöronların yaşa bağlı değişimlerinin incelenmesini ve sinaptofizin ile PSD95 proteinlerinin bölgesel immunoreaktivitilerinin/ekspresyonlarının yaşa bağlı değişimlerini inceleyerek sinaptik gelişimin değerlendirilmesini içermektedir. Bu amaçla, sıçanlar anne karnında gebeliğin 7–20'inci günleri arasında intragastrik besleme iğnesi ile günlük 6g/kg etanole maruz bırakıldılar. Fötal alkol ve kontrol sıçanlarındaki morfolojik özellikler hipokampusun CA1, CA3 ve DG bölgelerinde doğumdan sonra P1, P10, P30 ve P60 günlerinde incelendi. Sonuç olarak, hem stereoloji hem de doublekortin immunoreaktive verileri, doğumdan sonraki gelişim döneminde sadece sinir kök hücrelerinin bulunduğu ana alanlarda (SGZ ve SVZ) değil aynı zamanda hipokampusun CA bölgelerinde de sınırlıda olsa nörogenezin devam ettiğine işaret etmektedir. Fötal alkolün doğum sonrası hipokampal gelişimi üzerindeki etkisi sadece P30'da DG bölgesindeki granül hücrelerin sayısındaki marjinal düşüşle sınırlı kaldı. Bu sonuç fötal alkol grubunda görülen zayıf kognitif performansla ilişkilendirilebilmektedir. Diğer taraftan, fötal alkolün hipokampal ana nöronlarının morfolojik özellikleri üzerindeki etkileri özellikle P1'de CA bölgesinde gözlendi. Fakat analizler bu etkilerin sadece etanol alımından kaynaklanmadığını daha çok intübasyon stresiyle alakalı olabileceğini göstermektedir.

Anahtar Kelimeler: fötal alkol, doğum sonrası beyin gelişimi, hippokampüs, sıçan, sinaptik plastisite

To My Husband,
For his endless love

ACKNOWLEDGEMENTS

TABLE OF CONTENTS

LIST OF FIGURES

LIST OF TABLES

LIST OF ABBREVIATIONS

A	Alcohol
ADH	Alcohol Dehydrogenase
ANOVA	Analysis of Variance
ARBD	Alcohol-Related Birth Defects
ARND	Alcohol-Related Neurodevelopmental Disorder
BAC	Blood Alcohol Concentration
BDNF	Brain Derived Neurotrophic Factor
BSA	Bovine Serum Albumin
C	Control
CA	Cornu Ammonis (Ammon's Horn)
CAM	Cell Adhesion Molecule
CE	Coefficient of Error
CNS	Central Nervous System
CV	Coefficient of Variation
DAPI	4',6-diamidino-2-phenylindole
DCX	Doublecortin
DG	Dentate Gyrus
DNMTP	Delayed Non-Matching-To-Position
E	East
EC	Enthorhinal Cortex
ED	Embryonic Days
EDC	Ethanol Derived Calories
FAE	Fetal Alcohol Effects
FAS	Fetal Alcohol Syndrome
FASD	Fetal Alcohol Spectrum Disorders
G	Gestation
GABA	Gamma-Aminobutyric Acid
GD	Gestational Day
GL	Granular Layer
h	Hour
HRP	Horseradish Peroxidase
IC	Intubation Control
IgG	Immunoglobulin G
IOM	Institute of Medicine
i.p	Intraperitoneal
IR	Immunoreactivity
kDA	kilodalton
LA	Large Arena
LEC	Lateral Enthorhinal Cortices
LSD	Least Significant Difference
LTD	Long Term Depression
LTP	Long Term Potentiation
M	Molar
μg	Microgram
min	Minute

ML	Molecular Layer
mL	Milliliter
μL	Microliter
mm	Millimeter
μm	Micrometer
MOPP	Molecular Layer Perforant Path-Associated Cell
MWM	Morris Water Maze
N	North
NE	North-East
NGF	Nerve Growth Factor
NGS	Normal Goat Serum
NIH	National Institute of Health
NMDA	N-methyl-D-aspartate
NMJ	Neuromuscular Junction
NW	North-West
P	Postnatal Day
PBS	Phosphate Buffered Saline
PL	Polymorphic Layer
PP	Perforant Pathway
PSD	Postsynaptic Density
PSD-95	Postsynaptic Density 95 protein
PVDF	Polyvinylidene difluoride
ROI	Region of Interest
rpm	revolutions per minute
S	South
SA	Small Arena
SE	South-East
sec	second
SEM	Standard Error of Mean
SGZ	Subgranular Zone
SL	Stratum Lucidum
SO	Stratum Oriens
SP	Stratum Pyramidale
SR	Stratum Radiatum
SVZ	Subventricular Zone
SW	South-West
SYP	Synaptophysin
TBS-T	Tris Buffered Saline-Tween 20
V	Ventricule

CHAPTER 1

INTRODUCTION

1.1. Ethanol Teratogenity

Ethyl alcohol easily passes into the blood following rapid absorption from the stomach and gastrointestinal tract. Therefore, ethanol is evenly found in the body fluids and tissues. During the pregnancy, it also crosses from the placenta causing approximately equal maternal and fetal blood alcohol concentration (BAC) (Waltman and Iniquez, 1972). The embryo and fetus are dependent on the maternal liver to metabolize alcohol by hepatic alcohol dehydrogenase (ADH) enzyme which the fetus does not have. The elimination of alcohol from the fetus blood occurs through a passive diffusion of alcohol from placenta to the maternal blood. Therefore, the rate of alcohol elimination from amniotic fluid is approximately half that from maternal blood. This produces relatively high alcohol concentrations in amniotic fluid while alcohol levels are low in maternal blood. Thus, amniotic fluid may act as a reservoir for alcohol, and the fetus can be actually exposed to ethanol for a longer period than can be predicted from the maternal blood alcohol concentration (Brien *et al.,* 1983; Dursun *et al.,* 2006, 2011).

The neuroteratogenic effects of alcohol would depend on the amount and duration of prenatal alcohol exposure, but more than that on the timing of the exposure relative to the developmental stage of the cells and tissues involved (Goodlett *et al.,* 2005). The developmental periods of formation and/or maturation of organ systems are the critical periods for alcohol exposure. For example, in humans, the third trimester of gestation is the period for the major brain growth spurt (West, 1987). On the other hand, the major brain growth spurt in the rat occurs during the first 10-14 days of postnatal life, considered as equivalent of the human 3rd trimester (West *et al.,* 1989).

Another factor that is determining the adverse effects of ethanol insult is the peak blood alcohol concentration (BAC). The degree of severity of alcohol-related brain damage and behavioral deficits is related mostly peak BAC rather than daily alcohol dose. There is a handful of data suggesting that the pattern of alcohol consumption producing high BAC, such as binge-like drinking, may be especially harmful to the developing brain (West *et al.,* 1989). Peak BAC above 425 mg/dl was shown to be lethal, while BAC threshold for producing microencephaly was between 140 and 197 mg/dl (Pierce and West, 1986).

Thus the severity of the deficits may include the amount of ethanol dose and resulting BAC, the way of ethanol administration, duration and pattern of alcohol consumption, and the timing of the exposure relative to critical developmental stage, but also the inherent susceptibility to the adverse effects of ethanol. The dose/duration of alcohol exposure has been identified as an important factor in alcohol teratogenesis (Berman and Hannigan, 2000; Guerri, 2002; Mooney and Miller, 2007).

1.1.1. Fetal Alcohol Syndrome

Fetal alcohol syndrome (FAS) is defined as the systemic and ocular anomalies resulting from the teratogenic effect of maternal alcohol abuse during pregnancy. FAS is the most severe condition and clinically identifiable form of fetal alcohol spectrum disorders (FASD). A pattern of minor facial anomalies, prenatal and postnatal growth retardation, and functional or structural abnormalities in

central nervous system (CNS) are characteristic symptoms of FAS (Hoyme *et al.,* 2005, Wattendorf and Muenke, 2005). The term fetal alcohol effects (FAE) is used for children who are not as obviously impaired as children diagnosed with FAS. They usually lack the distinctive FAS facial features and have normal IQs. Therefore, FAE is sometimes described as less serious. Both conditions seem to be related to alcohol-induced cell deletions in the developing brain and result in the reduced brain mass at birth. Cells in the CNS show higher sensitivity to alcohol and therefore, experience more rapid cell death (apoptosis) than other cells in the developing embryo. In experiments on animal models of FAS/FAE, ethanol was shown to induce a massive wave of apoptosis (Goodlett *et al.,* 2005; Ikonomidou *et al*., 2000; Light *et al*., 2002). Alcohol exposure affects brain development via numerous pathways at all stages from neurogenesis to myelination. For example, the same processes that give rise to the facial characteristics of FAS also cause abnormal brain development. Behaviors as diverse as executive functioning to motor control are affected. It has been proposed that teratogenic effects of prenatal ethanol are mediated by increased free oxygen radicals. These free radicals are capable of generating highly reactive products that attack DNA, lipids, and other essential compounds of the cell and lipid peroxidation occurs.

In 1996, FAE was replaced the terms alcohol-related birth defects (ARBD) and alcohol-related neurodevelopmental disorder (ARND) by the Institute of Medicine (IOM) (Warren and Foudin, 2001). The term "alcohol-related birth defects" (ARBD) is used for children who have physical malformations or physiological abnormalities like abnormal structures of skeletal system and defects in major organ systems such as heart, kidneys, and/or auditory system. In addition, the term "alcohol-related neurodevelopmental disorder" (ARND) describes children with either physical CNS malformations (i.e., smaller head size) or with behavioral and/or cognitive abnormalities, such as deficits in memory, language skills or learning abilities (Stratton *et al.,* 1996). Special treatment is necessary for children exposed to alcohol prenatallly. Thus, alcohol abuse during pregnancy becomes a widespread issue of public interest. Today, FAS can be considered the most common nonhereditary cause of mental retardation.

1.1.2. Animal Models in Alcohol Studies

Today, both in the developed and developing countries, alcoholism is still a serious problem having a negative influence on the human health and countries' economy. Therefore, a lot of research is carried out regarding the ethanol's effects on the biological systems, the potential prevention strategies, and the therapeutic methods. Due to the legal and ethical constraints on research with humans, animals are used in most of the researches. Among different animal species, rodents and particularly rats have been most widely used in these studies because they have short gestation period, their handling is easy, and their cost to purchase, housing and feeding is relatively low (Keane and Leonard, 1989). Another fact of the using rats in alcohol studies is the similarity of humans and rats in mechanisms of alcohol metabolism, with the exception that man has slower metabolic rate than rats as being small endotherm, therefore, rats metabolize alcohol more quickly than humans.

There are different methods of alcohol administration to experimental animals such as subcutaneous/intraperitoneal injections, inhalation, liquid diet, and intraoral/intragastric infusion (gavage, intubation). Due to their advantages and disadvantages, there is no ideal method. The most commonly used methods are liquid diet and intragastric gavage. In the liquid diet, the animal's sole source of nutrition comes from the alcohol containing liquid diet. Alcohol is added to this diet either at a low concentration usually equivalent ~18% ethanol derived calories (EDC) or at a higher concentration usually equivalent ~35% EDC resulting in daily alcohol intake of ~12 and ~18 g/kg/day, respectively. In this method, generally, two control groups are used. The first control group is pair-fed receiving a similar liquid diet as 18% or 35% alcohol group. In this group a carbohydrate i.e. sucrose, is used instead of alcohol (Berman and Hannigan, 2000; Driscoll *et al.,* 1990). Therefore, the total daily caloric intake across groups becomes equal and thus, serves as a control for malnutrition that is characteristic for alcohol treated animals. The second control group, intact control group, has *ad libitum* access to standard laboratory chow and water. If the alcohol group differs from both control groups, and the two control groups do not differ from each other, the effect may be attributed to alcohol intake *per se*. It is noted that alcohol consumption with a liquid diet is more natural (Uzbay and Kayaalp, 1995). However, in this method, the amount of consumed alcohol shows great individual variations and therefore, the blood alcohol concentrations varied across the subjects. Additionally, the peak blood alcohol concentration (BAC) obtained with this method is relatively low.

To ensure equal ethanol intake by all the experimental animals, and obtain a high peak BAC direct intraoral or intragastric intubation (gavage method) is applied. This method is sometimes referred to as "binge-like drinking". Using a gavage method, alcohol mixed with a vehicle can be delivered in doses varying between 2 and 12 g/kg/day. The solution is administered directly to the stomach via a feeding needle and thus similar BAC is observed across the subjects. In this method, the absolute daily dose may be divided into two or three administrations to increase the portion of the day with elevated BAC. This method also includes two controls. One control is pair-fed to alcohol group which taking the equal volume of fluid that contains carbohydrate isocalorically substituted for alcohol via intubation. This group is at the same time a control for the effects of intubation-related stress. The other control group, intact control group, has no treatment and standard laboratory chow and water *ad libitum* (Driscoll *et al.,* 1990; Berman and Hannigan, 2000).

1.1.3. Critical Periods of Exposure to Alcohol in Animals

The fetal development of humans and rats follows similar stages, although they differ in the relative timing of birth. In human, the time of the fastest growth of the brain (brain growth-spurt period) associated with the development of a complex multicellular organization, correspond to the last trimester of gestation *in utero* (Rice and Barone, 2000; Bayer *et al.,* 1993). however, in the rodents, this period is restricted to the first 7-10 days after birth (Dobbing and Sands, 1979) which is referred to as the human 3rd trimester equivalent.

Animal studies of fetal development have indicated a critical period for the type of neuronal injury that causes FAS or FAE. The critical periods of alcohol exposure overlap with periods of greatest development and/or maturation of organ systems. In mice, for example, alcohol exposure around the 7th day of gestation can cause facial abnormalities, significant dysmorphia and neurological damage associated with FAS (Coles, 1994). In rats, alcohol exposure in the second half of gestation (equivalent to the second trimester in humans) results in reduction in brain weight (Miller, 1992) because this is when neurons in the cortex generate, differentiate and migrate to their appropriate functional areas. The presence of alcohol in this period disturbs both the timing and pattern of nerve cell generation and migration process both delaying the process and altering the number of cells that are produced (Miller, 1992). In small rodents (rats, mice), the "third trimester equivalent" includes the brain growth spurt and alcohol exposure during this period causes alterations in brain structure and function (West and Goodlet, 1990), mostly affecting cerebellum and hippocampus (Coles, 1994). Therefore, the alcohol exposure during this period results in behavioral deficits often manifested as locomotor hyperactivity and learning deficits (Aronson and Olegard, 1987; West and Goodlett, 1990). All the characteristic features of full FAS such as cranio-oral anomalies, growth deficits as well as behavioral dysfunctions were observed in a child when he/she exposed to alcohol during all three trimesters.

The studies on critical periods of organs' susceptibility to alcohol toxicity are especially important for better understanding alcohol-induced malformations and malfunctions. There is evidence that different aspects of the brain development are affected by perinatal (pre- and neonatal) exposure to alcohol at specific times. Initial studies indicating timing of alcohol exposure as an important factor responsible for differential ethanol effects led to discovery of facial dysmorphology, growth retardation and microcephaly in FAS patients.

1.1.4. Effects of Perinatal Ethanol Intoxication on The Brain Morphology

Quantitative magnetic resonance imaging studies have documented that certain structural anomalies can be detected in FAS subjects, including corpus callosum anomalies, reductions in the anteriorcerebellar vermis and basal ganglia (nucleus caudatus), and narrowing of gray matter density in certain regions of association cortex in parietal, temporal and frontal lobes (Archibald *et al.,* 2001; Riley *et al*., 2004). Alike in humans, also in the animal models of FAS, a microencephaly with significant growth deficits in the cerebrum including basal forebrain, cerebellum, and brain stem has been reported (Ryabinin *et al.,* 2006; Miller and Robertson 1993; Maier *et al*. 1999; Mattson *et al*. 1994). Neuronal loss is postulated to be one of the deleterious effects of perinatal exposure to ethanol (Goodlett *et al.,* 2005; Ikonomidou *et al*., 2000; Light *et al*., 2002). The possible mechanisms of pro-apoptotic effects of ethanol are induction of oxidative stress and activation of caspase-3 activation (Kotch *et al.,*1995; Ikonomidou *et al.,* 2000; Dunty *et al.,* 2001; Olney *et al.,* 2000, 2002a, 2002b, 2002c; Tenkova *et al.,* 2003; Young *et al.,* 2003; Olney, 2004; Dikranian *et al.,*2005; Goodlett *et al.,*

2005; Han *et al.,* 2005; Young and Olney, 2005; Young *et al.,* 2005; Ieraci and Herrera, 2007; Anthony *et al.,* 2008). It is found that NMDA glutamate receptors and GABA$_A$ receptors play important role in the toxic effects of alcohol on apoptotic neurodegeneration in the developing brain (Hughes *et al.,* 1998; Costa *et al.,* 2000; Ikonomidou *et al.,* 2000; Hsiao *et al.,* 2002; Nixon *et al.,* 2004; Riley *et al.,* 2001). Neurotrophic factors and their signal transduction pathways are also affected by pre or/and postnatal exposure to alcohol (Heaton *et al.,* 2003; Climent *et al.,* 2002; Moore *et al.,* 2004; Fattori *et al.,* 2008).

Alcohol exposure during brain development may produce neuron alteration in multiple ways, including inhibition of protein synthesis, alterations in lipid solubility, and thus disruption of cytoskeletal elements and/or membrane integrity. Other putative mechanisms through which chronic prenatal alcohol may show its adverse effects on the developing nervous system are: disrupted cellular energetic: altered energy metabolism (Snyder *et al.,* 1992) leading to oxidative stress and activation of the mitochondrial pathway of apoptosis (Cartwright *et al*., 1998; Ikonomidou *et al*., 2000; Light *et al.,* 2002; Zhang *et al*., 1998), suppression of protein and DNA synthesis (Shibley and Pennington, 1997), altered regulation of gene expression and reduced retinoic acid signaling (mainly due to the competitive interaction of ethanol with alcohol dehydrogenase (ADH), an enzyme critical for both, alcohol metabolism and synthesis of retinoic acid) (Deltour *et al*., 1996; Peng *et al.,* 2004), disruption of midline serotonergic neural development and thus serotonin signaling (Whitaker-Azmitia *et al.,* 1996) (both retinoic acid and serotonin signaling are important for normal neuronal differentiation and maturation in the developing brain), disruption of cell-to-cell interactions: inhibition of L1 cell adhesion molecule (L1 CAM) function (Charness *et al.,* 1994; Ramanathan *et al*., 1996; Wilkemeyer and Charness, 1998). Prenatal exposure to alcohol was also reported to interact with neurotransmitter systems and to interfere with growth-factor signaling or other cell-signaling pathways (Bonthius *et al*., 2004; Zhang *et al.,* 1998). After perinatal ethanol exposure, both suppression of NMDA receptor activation (Morriset *et al.,* 1989) and alterations in the expression of GABA$_A$ receptor (Iqbal *et al.,* 2004) was noted in the adult rat (P70-90) CA1 area of hippocampus. Alterations in these receptor functions may affect signal transduction in the hippocampus and result to hippocampal-related behavioral deficits described in fetal alcohol rats. It has been also reported that chronic but even acute (single intragastric alcohol infusion on the gestational day (GD) 15) prenatal administration of alcohol led to decreased expression and decreased brain levels of neurotrophins such as NGF and BDNF (Angelucci *et al.,* 1997; Climent *et al.,* 2002; Tapia-Arancibia *et al.,* 2001). Chronic alcohol intake during gestation and/or lactation was also shown to decrease expression of p75, low affinity NGF receptor (Seabold *et al.,* 1998), and increase the ratio of truncated to full-length brain-derived neurotrophic factor's (BDNF), TrkB receptors in the developing cerebral cortex (Climent *et al.,* 2002). These changes are accompanied by reduction in neurotrophin-activated extra- and intracellular signal transduction pathways leading to increased loss and/or dysfunction of cholinergic neurons, the neurons known to be highly dependent on neurotrophin support and critical for hippocampal functions. Reduction in the number of cholinergic neurons in the basal forebrain gives rise to the cholinergic deafferentation of the hippocampus and cortical mantle. In animals exposed to alcohol on GD6–21, an altered generation, proliferation and migration, and thus abnormal distributions and organization of neocortical neurons have been reported (Miller, 1988, 1989; Miller *et al.,* 1990; Miller and Nowakowski, 1991). An overall reduction in the brain weight (microencephaly or microcephaly) due to alcohol-induced neuronal loss has been also demonstrated in previous studies (Chiu *et al*., 1999; Maier *et al.,* 1997; Tran *et al.,* 2000).

''Secondary'' sources of brain damage during prenatal alcohol exposure are altered placental functions or other intrauterine factors (Randall *et al.,* 1989), hypoxia/ischemia (Savoy-Moore *et al.*, 1989), acetaldehyde formation (Sreenathan *et al*., 1982).

Morphological, neurochemical, and electrophysiological studies suggest that among brain structures the cerebellum and hippocampal formation are most vulnerable to the teratogenic consequences of perinatal exposure to ethanol (Bonthius and West, 1990; Goodlett *et al*., 1997; Livy *et al.,* 2003; Mihalick *et al.*, 2001; Miki *et al*., 2003). Alcohol exposure during development compromises the hippocampus (Miller, 1989; Gil-Mohapel *et al.,* 2010; Berman and Hannigan 2000) resulting in inhibited glutamatergic signaling, LTP induction (Puglia and Valenzuela, 2010) and permanent immature spines (Mameli and Valenzuela, 2006).

1.1.5. Effects of Perinatal Exposure to Ethanol on Motor and Cognitive Functions

In line with morphological data indicating great cell losses in cerebellum, basal ganglia, hippocampus, and some associative cortices due to perinatal alcohol intoxication, impairments of motor and cognitive functions belong to the most common alcohol-induced behavioral dysfunctions. Both in humans and in rodents, the locomotor hyperactivity is one of the most characteristic effects of perinatal alcohol exposure. Recent studies showed that locomotor hyperactivity has been frequently observed in children and in preweaning and juvenile rats (Mattson *et al*., 2001; Abel, 1982; Abel and Reddy, 1997; Tran *et al.*, 2000). In these studies, preweaning rats prenatally exposed to alcohol demonstrated worse performance than the controls on rotating drum, and fell off an inclined plane at a less steep angle, what suggested decrease in muscle strength and sensorimotor coordination due to prenatal alcohol exposure (Abel and Dintcheff, 1978). Cognitive deficits including attention and learning impairments were also reported in both humans and rodents after perinatal exposure to ethanol. It has been postulated that such deficits may be observed even in the absence of full-blown FAS (Girard *et al*., 2000). In animal experiments, learning deficits have been demonstrated especially in spatial tasks sensitive to hippocampal damage such as food-rewarded spatial navigation in the radial arm maze (Reyes *et al.*, 1989; Neese *et al.*, 2004), spatial navigation in the Morris Water Maze (MWM) (Girard *et al.*, 2000; Hamilton *et al*., 2003; Johnson and Goodlett, 2002) and place acquisition as well as conditional alternation in T-maze (Nagahara and Handa, 1997; Lee and Rabe, 1999). The endurance of adverse effects of fetal ethanol on both brain morphology and behavior is still an open issue. Generally more pronounced deficits in learning and memory tasks were noted in juveniles as compared to adult subjects (Girard *et al.*, 2000; Nagahara and Handa, 1997; Zimmerberg *et al*., 1991). However, some authors reported that adult animals show none or very small cognitive abnormalities, especially when alcohol was administered prenatally during the 2nd trimester equivalent (Cronise *et al.*, 2002; Clausing *et al.* 1995). Also, many authors reported lack of locomotor hyperactivity in fetal-alcohol rats when tested as adults (Bond and diGusto, 1977; Abel and Berman, 1994). These results have been confirmed in the previous studies carried out in our laboratory (Dursun *et al.*, 2006).

Amelioration of behavioral deficits with maturation may suggest some kind of recovery process from alcohol teratogenity pointing towards a potential for regeneration in the young brain. The nervous system may be able to overcome deteriorating effects of alcohol abuse more readily than the effects of certain other insults such as an ischemic infarct which, instead of subtly removing a percentage of neurons from many brain regions, totally destroys all neurons in a certain specific area and causes irreversible neurological deficits. Until now, however, there is little known about the mechanisms of the potential recovery process. On the other hand, the brain's ability to regain normal or almost normal capacity following severe apoptotic neuronal losses is of considerable interest. The studies on the innate regeneration mechanisms are important from clinical perspective as this knowledge may help with designing therapies against some other neurological disorders, too.

1.2. Hippocampal Formation

1.2.1. Anatomy

The hippocampus located in the center of the limbic system is a horseshoe shaped paired structure. Hippocampus is connected with subcortical limbic structures such as septum, hypothalamus, amygdala, striatum, mammillary bodies, and anterior thalamus. It is also connected with several neocortical areas including cingulate cortex, prefrontal/orbitorfrontal cortices, entorhinal, perirhinal and postrhinal cortices, and piriform cortex, (Fig. 1.1). It is connected to the hypothalamus by the fornix.

Figure 1.1. The Hipppocampal Anatomy (http://www.thebrainlabs.com/brain.shtml)
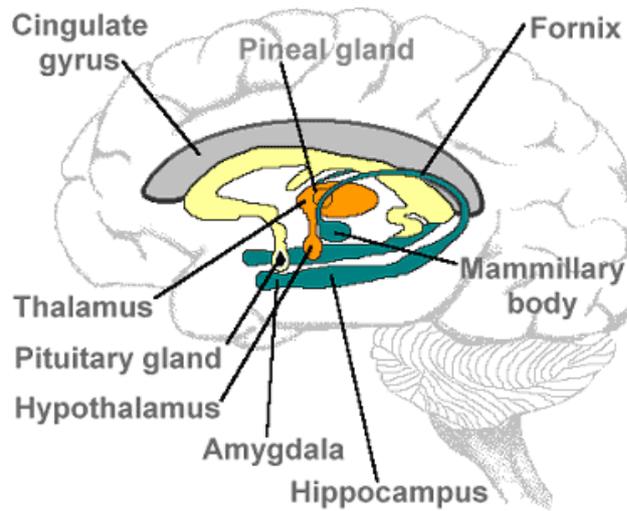
1.2.2. Hippocampal Layers

The hippocampal region includes hippocampal formation and parahippocampal region as a two sets of cortical structures. The major defining differences between the two are the number of cortical layers present and the overall principles of connectivity. The hippocampal formation comprises three cytoarchitectonically distinct regions: the dentate gyrus, the hippocampus proper, and the subiculum. The term "cornu ammonis" (Ammon's horn) (CA) is used to refer the hippocampus proper (Lorente de No, 1934). Four regions were identified in cornu ammonis (Fig. 1.2). The nearest region to the entorhinal cortex (EC) is called CA1 subregion. The narrow CA2 subregion is found between the CA1 and CA3 subregions. CA3 subregion continues to the hilus of dentate gyrus (DG) and CA4 subregion is the region between the arms of DG.
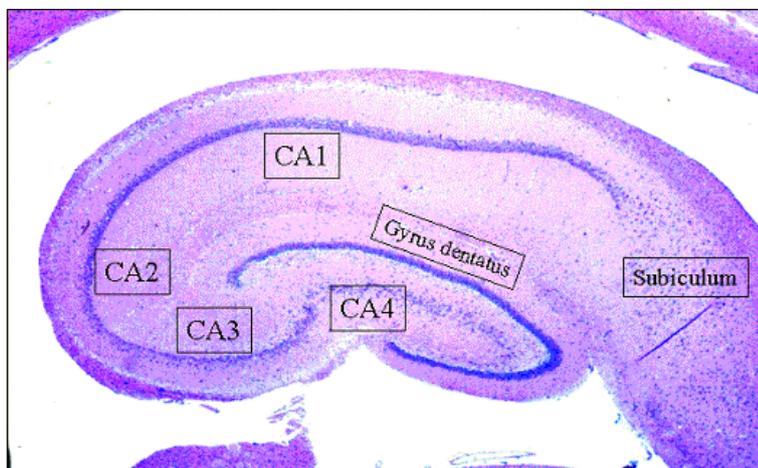
Figure 1.2. The Hipppocampal Layers
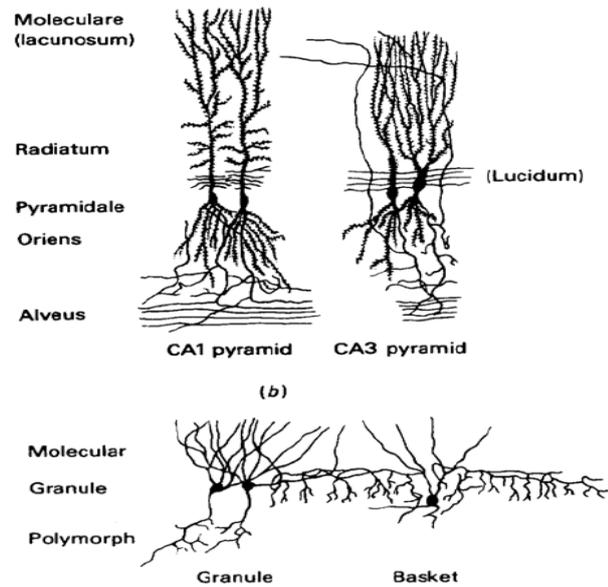
Figure 1.3. Examples of CA1 and CA3 pyramidal cells (upper), granule cells (bottom left) and a basket cell (bottom right) in DG (After Cajal, 1911).

1.2.2.1. Dentate Gyrus

The dentate gyrus (DG) is composed of three layers (Fig. 1.3). The outer cell-free region called molecular layer is the closest to the hippocampal fissure. The middle region of the DG is the principal cell layer or granular cell layer. Densely packed granule cells reside in the granular cell layer. The "U" or "V" shaped inner region of DG forms polymorphic cell layer also known as hilus.
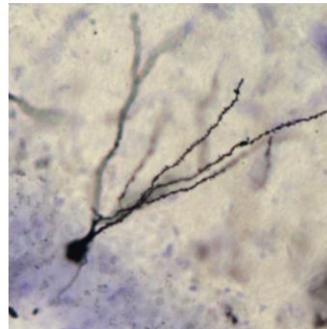
Figure 1.4. Example of a granule cell

The granule cell is the principal cell type of the DG. The dentate granule cell has an elliptical cell body (approximately 10 µm X 16 µm). The cells are closely packed and in most cases no glial sheath intervening between the cells is found. The packing density of granule cells is increasing towards septum (Gaarskjaer, 1978; Witter and Amaral, 2004). A granule cell has very characteristic cone-shaped dendritic tree containing spines with all of the branches directed toward the molecular layer (Claiborne *et al.,* 1990; Desmond and Levy, 1982; Witter and Amaral, 2004) (Fig. 1.4). In adult rodents, basal dendrites are absent while in young rats (P5-10) basal dendrites have been observed (Seress and Pokorny, 1981; Treves *et al.,* 2008). On the other hand, in monkeys and in humans, a substantial number of granule cells have basal dendrites extending into the hilus (Seress and Mrzljak, 1987; Treves *et al.,* 2008).

The second type of the cells in the DG is the basket cells. They are found in the deep surface of the granular layer. Basket cells have pyramidal-shaped cell bodies (25–35 µm in diameter) and a single aspiny apical dendrite with several aspiny branches directed into the molecular layer (Ramon y Cajal, 1911) and also two or three primary basal dendrites divindig to branches and extending into the polymorphic layer (Witter and Amaral, 2004). Within the same subgranular region, there are several

other cell types with different dendritic arrangements and soma structure. As Seress and Ribak (1990) have pointed out, all of these cells share fine structural characteristics such as infolded nuclei, extensive perikaryal cytoplasm with large Nissl bodies, and intranuclear rods. Some of these cells are multipolar with several aspiny dendrites entering the molecular and polymorphic layers while others tend to be more fusiform shaped with a similar dendritic distribution. It has become clear that many of these neurons are GABAergic and most likely modulate granular cell activity.

The cell-free molecular layer mainly consists of the dendrites of the granule, basket, and various polymorphic cells and terminal axonal arbors from several sources (Witter and Amaral, 2004). However, the molecular layer has a few neuronal cell types. One of them is located deep in the molecular layer, has a multipolar or triangular cell body and an axon contributing the basket plexus within the granule cell layer (Hazlett and Farkas, 1978; Kosaka *et al.,* 1987; Witter and Amaral, 2004). The second type is axo-axonic cell which is also known as "Chandelier" cell originally found in the neocortex (Kosaka, 1983; Somogyi *et al.,* 1985; Soriano and Frotscher, 1989) and their dendritic tree generally span the width of the molecular layer. The basal dendrites of axo-axonic cell are absent or not well-developed (Witter and Amaral, 2004). A third cell type named the molecular layer perforant path-associated cell (MOPP) has a characteristic axonal distribution within the outer two-thirds of the molecular layer (Han *et al.,* 1993; Witter and Amaral, 2004). The polymorphic cell layer is occupied by a variety of neuronal cell types (Amaral, 1978), however, little information is present about many of them. The mossy cell being the most impressive is the most common cell type in the polymorphic layer of DG. They have large (25–35 μm) cell bodies and their shape are often triangular or multipolar. Three or more thick dendrites originating from the cell body of mossy cell and take up long distances within the polymorphic layer; occasionally a dendrite will also reach to the molecular layer by extending through the granular layer (Witter and Amaral, 2004).

The granule cells have distinctive unmyelinated axons which Ramony Cajal called mossy fibers. Each principal mossy fiber (which is around 0.2–0.5 μm in diameter) has seven thinner collaterals within the polymorphic layer and then enters the CA3 field of the hippocampus (Claiborne *et al.,* 1986; Witter and Amaral, 2004).

The DG gives rise to no extrinsic projections other than the mossy fiber projection to the CA3 field of the hippocampus. The major input to the DG (the so-called perforant pathway) comes from layer 2 of the EC. No direct inputs come from other cortical structures to the DG. The perforant pathway (PP) is divided into the medial perforant path and the lateral perforant path, originating from the medial and lateral EC, respectively. The medial perforant path synapses onto the proximal dendritic area of the granule cells, whereas the lateral perforant path does so onto the distal dendrites of the same cells.

The terminals in the basket plexus are GABAergic and form symmetric, presumably inhibitory, contacts primarily on the cell bodies and shafts of apical dendrites of the granule cells (Kosaka *et al.,* 1984). A second inhibitory input comes from the the molecular layer, axoaxonic or "chandelier-type" cells (Han *et al.,* 1993; Kosaka, 1983; Soriano and Frotscher, 1989; Witter and Amaral, 2004). Another intrinsic projection within the DG is dispersed from the polymorphic layer (Bakst *et al.,* 1986; Morrison *et al.,*1982; Witter and Amaral, 2004). These cells give rise to a dense network of somatostatin-IR fibers and their dendritic terminals in the outer two-thirds of the molecular layer coincide with the terminal distribution of the PP (Witter and Amaral, 2004). The cells in the polymorphic layer send projections to the inner third of the molecular layer called the ipsilateral associational/commissural projection since this projection originates both on the ipsilateral and contralateral sides (Blackstad, 1956; Laurberg, 1979; Laurberg and Sorensen, 1981; Witter and Amaral, 2004). Previous studies showed the possibility that this projection originated, in part, from hippocampal CA3 cells (Witter and Amaral, 2004).
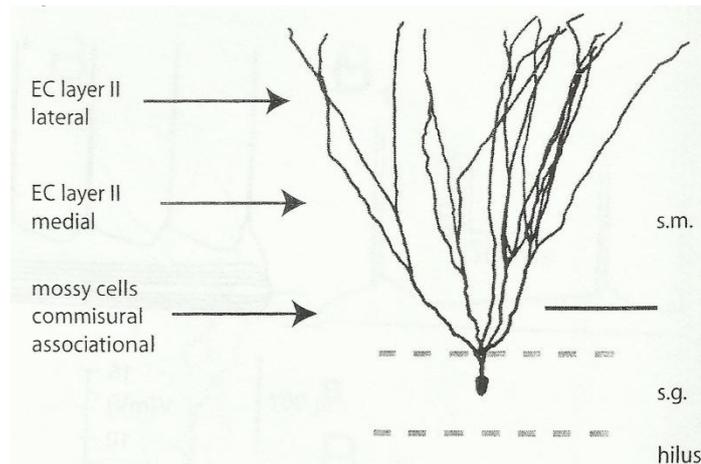
Figure 1.5. DG synaptic inputs and outputs (adapted from Claiborne *et al.,* 1990; Spruston and McBain, 2006)

The subcortical inputs to the DG originate mainly from the supramammillary region of the posterior hypothalamus, the septal nuclei, the raphe nuclei, the locus coeruleus. The supramammillary projection of hypothalamus terminates heavily in a narrow zone of the molecular layer of DG (Dent *et al.,* 1983; Haglund *et al.,* 1984; Riley and Moore, 1981; Vertes, 1993; Witter and Amaral, 2004). The septal projection arises from the cells of diagonal band of Broca nucleus and the medial septal nucleus and reaches to the hippocampal formation via dorsal fornix, the fimbria, supracallosal stria, and amygdaloid complex. These septal projections terminate heavily in the polymorphic layer, particularly in a narrow infragranular band, and more lightly in the molecular layer (Witter and Amaral, 2004). The nonserotonergic raphe nuclei projections originate from the medial raphe nucleus and terminate in the hippocampal formation (Vertes *et al.,* 1999; Köhler and Steinbusch, 1982; Montone *et al.,* 1988; Witter and Amaral, 2004). However, the raphe serotonergic fibers preferentially terminate on a class of interneurons in the DG which primarily influence the distal parts of the granular cell dendrites (Halasy *et al.,* 1992; Witter and Amaral, 2004). In addition, the pontine nucleus locus coeruleus sends a particularly prominent noradrenergic projection to the polymorphic layer of the DG (Haring and Davis, 1985; Moore *et al.,* 1978; Pickel *et al.,*1974; Witter and Amaral, 2004).

The DG is one of the few regions of the adult brain where neurogenesis (the birth of new neurons) takes place. The subgranular zone (SGZ) located at the hilar border of the granule cell layer consists of dividing precursor cells that produce new granule cells (Treves *et al.,* 2008) (Fig. 1.5). These precursor cells produce extra numbers of new neurons, and before maturation, a significantly great amount of them dies (Kempermann *et al.,* 2003; Treves *et al.,* 2008). The destiny of immature new neurons depends on their activation during hippocampal-dependent learning (Gould *et al.,* 1999; Dobrossy *et al.,* 2003; Dupret *et al.,* 2007; Epp *et al.,* 2007). Anatomical, electrophysiological, and computer simulation as well as behavioral data suggest an important role of DG in learning and memory by processing and representing spatial information on the basis of conjunctive encoding of multiple sensory inputs, pattern separation, and encoding of spatial information in conjunction with the CA3. The previous computational studies showed that the mossy fibers strengthen a new, well separated pattern of activity onto CA3 cells, perform a new memory by overcoming the interference of previous memories traces already stored on CA3 recurrent collateral connections. The critical role of mossy fibers dissociating new memory representations from previous ones is also supported by behavioral experiments (Treves *et al.,* 2008).

1.2.2.2. Hippocampus Proper

The hippocampus proper (CA regions) can be clearly divided into two major regions, a large-celled proximal region called regio inferior and a smaller-celled distal region called regio superior (Cajal, 1911). According to Lorento de No's (1934), regio inferior of Cajal corresponds CA3 and CA2 subregions whereas regio superior is equivalent to CA1 subregion.

The hippocampus proper has a similar laminar organization in all subregions. The pyramidal cell layer is the principal cellular layer. The layer located under the pyramidal cell layer is the stratum oriens which is a narrow, relatively cell-free layer. The fiber-containing alveus is found under the stratum

oriens layer. In the CA3 subregion, just above the pyramidal cell layer, a narrow acellular zone called stratum lucidum is found and it is occupied by the mossy fibers originating from the DG. This layer is absent in the CA2 or CA1. The CA3/CA2 border is marked by a slight thickening of the stratum lucidum layer at the distal end where the mossy fibers bend temporally (Witter and Amaral, 2004). The next layer which is above the stratum lucidum in CA3, and the pyramidal cell layer in CA2 and CA1, is called the stratum radiatum. Since CA3 to CA1 Schaffer collateral connections and CA3 to CA3 associational connections are located, the stratum radiatum can be defined as the suprapyramidal region.The layer called the stratum lacunosum moleculare corresponds the most superficial portion of the hippocampus. The perforant pathway (PP) fibers from the EC travel and terminate in the stratum lacunosum moleculare layer. The afferents from other regions, such as those from the nucleus reuniens of the midline thalamus, also terminate in this layer (Witter and Amaral, 2004).

The pyramidal cell which resides in the pyramidal cell layer is the principal neuronal cell type of the hippocampus. Pyramidal cells have an apical dendritic tree extending to the stratum radiatum and basal dendritic trees extending into stratum oriens (Witter and Amaral, 2004) (Fig. 1.6).
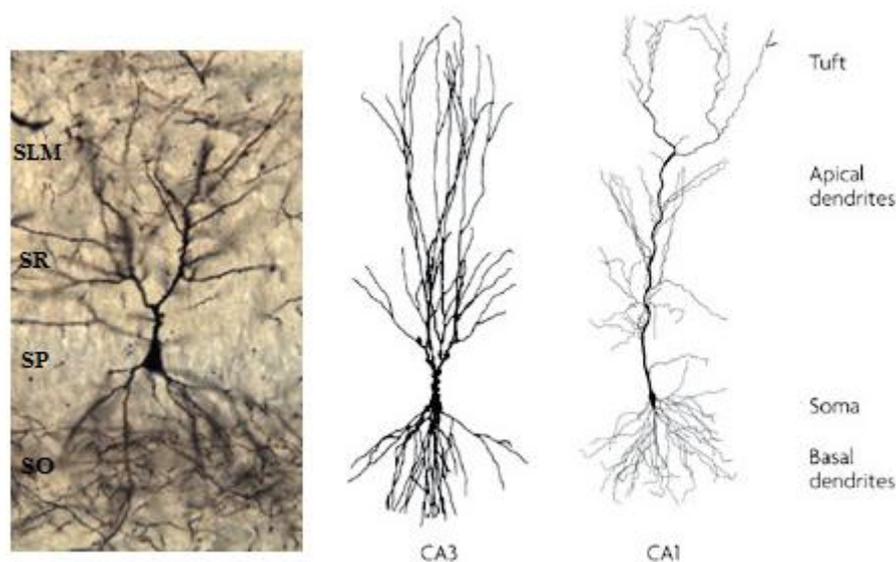
Figure 1.6. Exampleof pyramidal cells in CA3 and CA1 region of hippocampus

The second type of neurons in the pyramidal cell layer is the basket cells. There exists a heterogenous population of basket cells in various sizes and shapes in the pyramidal cell layer (Witter and Amaral, 2004; Freund and Buzsaki, 1996). Similar to pyramidal cells, the basket cells have apical and basal dendritic trees, however, their dendrites have few if any dendritic spines and have an overall beaded appearance (Witter and Amaral, 2004). The axon of basket cell extends in a transverse manner from the cell body of origin and forms a basket network innervating the cell bodies of pyramidal cells. Moreover, the O-LM cells are one class of interneurons in the hippocampus. Their dendrites are found in the stratum oriens. The axon of O-LM cells innervates the stratum lacunosum-moleculare layer of hippocampus (Blasco-Ibanez and Freund, 1995; Witter and Amaral, 2004). These cells generally appear to contain somatostatin and in some instances neuropeptide Y (NPY). The bistratified neuron is the second type of interneuron commonly found in the hippocampus. The axonal plexus of this type of neuron is distrubuted to the stratum radiatum and stratum oriens, innervating dendrites of pyramidal cells (Gulyas and Freund, 1996; Miles *et al.,* 1996; Witter and Amaral, 2004). Another type of hippocampal interneuron is trilaminar cells. They have axonal distribution extending for 2.5 mm in the septotemporal and transverse axes and axon collaterals targeting extrahippocampal regions (Toth and Freund, 1992). Both the bistratified and trilaminar cells form symmetrical synapses onto dendrites of presumed pyramidal cells (Halasy *et al.,* 1996; Witter and Amaral, 2004).

The hippocampus coordinates information from a variety of sources. A major flow of information through the hippocampus is a one-way circuit. Some inputs to the hippocampus from the EC (i.e. PP) pass through to the DG. From the DG connections are made to CA3 of the hippocampus proper via mossy fibers and to CA1 via Schaffer collaterals. Neural signals from these two CA fields pass through the subiculum and then are sent to other areas of the brain via alveus, fimbria, and fornix (Fig.

1.7). Hippocampal efferent projections return to the lateral septal nuclei, and from CA1 region through subiculum out of hippocampus on to the medial and lateral enthorhinal cortices (LEC) and via, respectively, post- and perirhinal cortices back to the subcortical structures of the extended hippocampal circuit, and to other neocortical areas (Burwell *et al.*, 1995). Hippocampus receives its major afferent input via the PP from EC which is a gateway from the many of other cortical areas. Direct inputs from layer III pyramidal neurons in the EC project to CA1 neurons via PP, so named because the fibers leaving the angular bundle perforate the subiculum (Cajal, 1911). The PP input from the EC to CA1 selectively innervates the distal apical dendrites in the stratum lacunosum-moleculare (Blackstad, 1956).

The mossy fiber projection is the dentate projection of the DG to the CA3 subregion of the hippocampus proper. The mossy fiber enters the CA3 subregion and forms few collaterals. They extend throughout the CA3 subregion in a transverse manner omitting the location of the granule cell of origin. The infrapyramidal bundle consists of the mossy fibers which travel deep to the pyramidal cell layer in the proximal part of CA3 subregion. The intrapyramidal bundle is formed from fibers which travel within the pyramidal cell layer while the fibers traveling superficial to the pyramidal cell layer form the suprapyramidal bundle which is the major constituent of stratum lucidum layer (Witter and Amaral, 2004). Fibers from all bundles, however, ultimately reach to stratum lucidum layer and stop at the CA3/CA2 border. The mossy fibers follow a relatively "lamellar" trajectory which is atypical for intrinsic connections of hippocampus. They remain at approximately the same septotemporal level as the cells of origin through the stratum lucidum layer (Claiborne *et al.,* 1986; Gaarskjaer, 1978; Witter and Amaral, 2004). In addition, the mossy fibers are thought to use glutamate as a primary neurotransmitter like other principal intrinsic connections of the rat hippocampal formation (Storm-Mathisen and Fonnum, 1972; Witter and Amaral, 2004). However, some mossy fibers reserve opiate peptides such as dynorphin (Gall, 1984; McGinty *et al.,* 1984; van Daal *et al.,* 1989).

Schaffer Collaterals and Commissural Fibers which are rather small in diameter (0.1-0.2 μm in the rat (Blackstad and Flood 1963)) are the branching axons of CA3 pyramidal neurons projecting to the ipsi- and contra-lateral hippocampal CA1 regions. The Schaffer collateral system arises from the CA4, CA3 pyramidal neurons and extends to the stratum radiatum layer of CA1 subregion, making powerful excitatory synapses en passant (Lorente de No 1934).
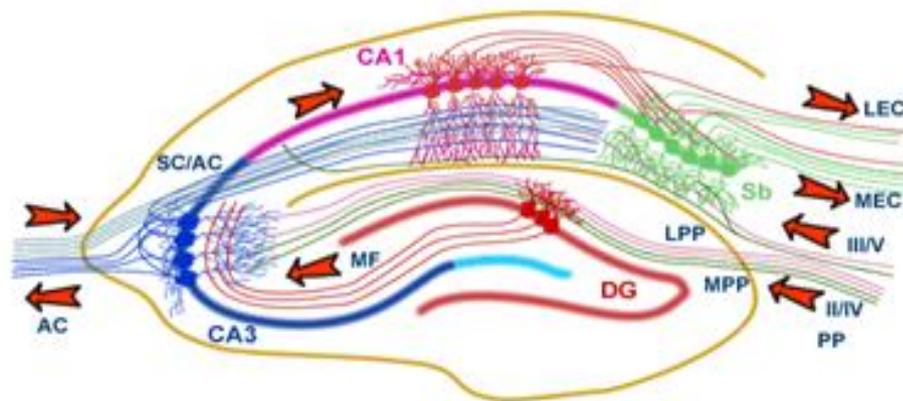
Figure 1.7. The Hippocampal Pathway (www.bristol.ac.uk/synaptic/pathways/)

1.2.2.2.1. Cornu Ammonis 1 (CA1)

In mature CA1 neurons, two branching dendritic trees emerge from the pyramidal-shaped soma. The basal dendrites of CA1 pyramidal neurons extend to the stratum oriens, and the apical dendrites of CA1 pyramidal neurons extend to the stratum radiatum (proximal apical) and the stratum lacunosum-moleculare (distal apical). Both the apical and basal dendritic trees occupy a roughly conical (sometimes ovoid) volume (Pyapali *et al.,* 1998). In adults, the total length of all branches in the CA1 dendrite is 12-13.5 mm. Basal dendrites contribute about 36% of the total length, apical dendrites in

the stratum radiatum contribute about 40%, and apical dendrites in the stratum lacunosum-moleculare contribute the remaining 24% (Bannister and Larkman, 1995; Ishizuka *et al.,* 1995; Megias *et al.,* 2001). Several dendritic branches extend to the stratum radiatum along the length of primary apical dendrite. The number of these oblique branches varies from 9 to 30 with a mean 17 (Bannister and Larkman, 1995; Pyapali *et al.,* 1998). An apical tuft is formed by the branching of apical dendrite in the stratum lacunosum-moleculare layer (Fig. 1.6) (Bannister and Larkman, 1995; Trommald *et al.,* 1995). Two-to-eight dendrites (a mean of five) emerge from the base of the pyramidal soma. Most of these dendrites branch several times (maximum 15 branch points), forming basal dendritic tree with about 40 terminl segment (Bannister and Larkman, 1995; Pyapali *et al.,* 1998). Most branches in the basal dendrites occur rather close to the soma so the terminal segments are quiet long, constituting about 80% of the total dendritic length (Bannister and Larkman, 1995; Trommald *et al.,* 1995).

The axon of CA1 pyramidal neurons arised from the pyramidal shaped soma and extends through the stratum oriens and into the alveus and bend sharply toward the subiculum (Amaral *et al.,* 1991; Finch and Babb, 1981; Witter and Amaral, 2004). The CA1 pyramidal cell axons branch widely and produce collaterals with several targets both within and beyond the hippocampus. In contrast to CA3 pyramidal neurons, CA1 pyramidal cells make no connections among themselves except in the developing hippocampus (Tamamaki *et al.,* 1987; Amaral *et al.,* 1991). This difference in intrinsic organization between CA3 and CA1 suggests that these two hippocampal subregions have different contributions to learning and memory processes (Treves and Rolls, 1992). Because the CA1 axon does not enter the stratum radiatum, local synaptic connections onto other CA1 neurons occur on basal dendrites. Particular interneurons located at the stratum oriens/alveus border in CA1 subregion project to CA3 subregion and the hilus of the DG. The major projection arising from the CA1 subregion goes to the adjacent subiculum in a topographic manner (Witter and Amaral, 2004).

The CA1 subregion has relatively more extrinsic projections than the CA3 or CA2 subregions. Both subcortical and cortical inputs from a variety of structures send projections to the CA1 subregion. Concerning subcortical inputs, CA1 subregion (stratum oriens) receives a projection from septum which is, however, less dense than in CA3 subregion (Nyakas *et al.,* 1987). Temporal two-thirds of CA1 neurons adjacent to the subiculum receive input from the amygdaloid complex (Krettek and Price, 1977; Witter and Amaral, 2004). Also, the small midline nucleus reuniens heavily projects to the stratum lacunosum-moleculare layer of CA1 subregion (Wouterlood *et al.,* 1990; Zheng, 1994). Like CA3, the CA1 subregion receives light dopaminergic, noradrenergic, and serotonergic projections (Swanson *et al.,* 1987). The main cortical inputs emerges from the parahippocampal region. The projections from CA1 region are quite similar, however generally less dense than the projections originating from the subiculum (Witter and Amaral, 2004).
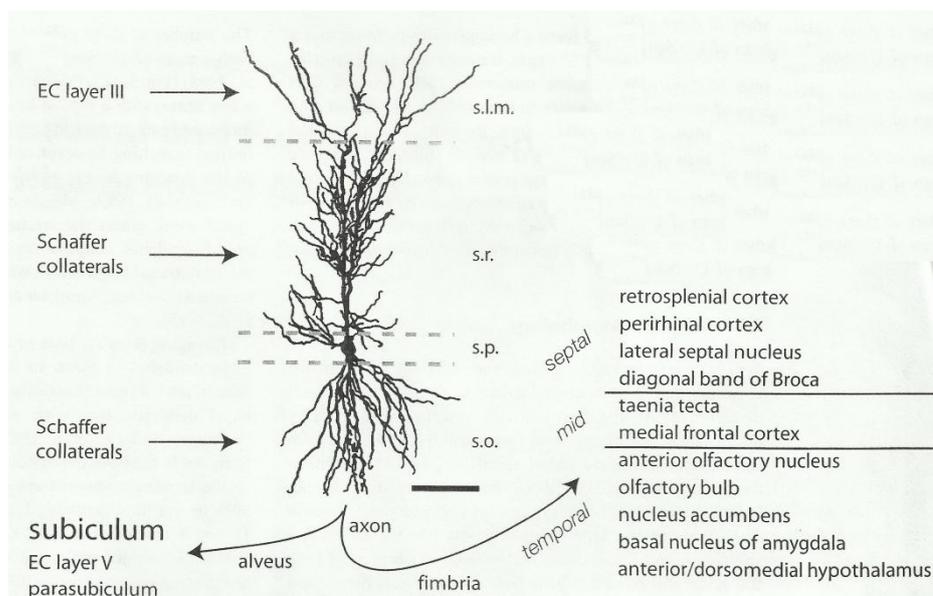
Figure 1.8. CA1 synaptic inputs and outputs (adapted from Bannister and Larkman, 1995; Spruston and McBain, 2006)

CA1 pyramidal neurons are composed of about 30,000 dendritic spines and most dendritic spines receive excitatory synaptic inputs, indicating that spine density can be used as a reasonable measure of excitatory synapse density (Megias *et al.,* 2001). The density of dendritic spines and synapses on CA1 pyramidal neurons is the highest in the stratum radiatum and stratum oriens layers.

1.2.2.2.2. Cornu Ammonis 2 (CA2)

As originally defined by Lorente de Nó (1911), CA2 subregion located between CA3 and CA1 regions is a narrow zone (no longer than approximately 250 μm (Witter and Amaral, 2004)) and has large cell bodies like in CA3 subregion, however, deprived mossy fiber projections just like CA1 subregion. As earlier mentioned, CA2 region consists of large, darkly staining pyramidal neurons, similar to pyramidal cells in CA3 region. Alike CA3 pyramidal neurons, the CA2 pyramidal cells have no the thorny excrescences in their dendrites (Lorente de Nó, 1934; Tamamaki *et al.,* 1987; Witter and Amaral, 2004). The CA2 cells give rise to a projection to CA1 region like CA3 neurons (Ishizuka *et al.,* 1990). In general, the connections of CA2 subregion are similar to those of CA3 subregion. However, the CA2 subregion appears to receive distinct projections from parts of the posterior hypothalamus, the tubero-mammillary nucleus (Köhler *et al.,* 1985), the supramammillary area (Haglund *et al.,* 1984). The borders of rodent CA2 area with CA3 and CA1 subregions are delineated by selective afferentation by the supramammillary nucleus of the hypothalamus (Magloczky *et al.,* 1994; Soussi *et al.,* 2010) and sparse innervation by nucleus reuniens of the thalamus (Wouterlood *et al.,* 1990; Halasy *et al.,* 2004). Although CA2 neurons are generally assumed to form a minor pathway linking CA3 to CA1 (Sekino *et al.,* 1997), *in vivo* stimulation of the inputs to EC can trigger the initial firing of CA2 neurons, followed by CA1 and then CA3 activation (Bartesaghi and Gessi, 2004), suggesting that CA2 neurons may create an indirect link between EC and CA1 region (Bartesaghi *et al.,* 2006). In a recent study (Chevaleyre and Siegelbaum, 2010), it was found that CA2 neurons are a major target of excitatory cortical input to the hippocampus and can potently excite their CA1 neuron targets. In contrast, CA2 neurons are largely inhibited by their intrahippocampal input from CA3 pyramidal neurons.

1.2.2.2.3. Cornu Ammonis 3 (CA3)

Pyramidal neurons in the CA3 region are structurally similar to CA1 neurons. They consist of pyramid-shaped soma that give rise to apical and basal dendritic trees, however, the cell body is larger and the apical dendritic tree bifurcates closer to the soma. CA3 pyramidal neurons possess extensive dendritic arborizations with four main features: 1) a basal arbor that extends throughout the stratum oriens, 2) a short apical trunk in the stratum lucidum branching two or more secondary trunks, 3) oblique apical dendrites in the stratum radiatum layer, and 4) an apical tuft that extends in the stratum lacunosum-moleculare layer. On average, the total dendritic length for the apical and basal dendritic arbors is similar to that in CA1 neurons, but with a larger range (9.3-15.8 mm) (Ishizuka *et al.,* 1995; Henze *et al.,* 1996). Despite the greater total length and surface area of the apical arbor, the number of terminal branch and number of dendritic segments are similar for both apical and basal arbors. However, basal dendrites have approximately three-fold fewer tips per primary dendrite (8.5 vs. 29.1). This together with the lower maximum branch order for the basal dendrites (7.0 vs. 10.8) suggests that the individual basal dendritic trees are significantly less complex than the apical trees. Finally, in addition to being less complex, the mean distance to the basal dendritic tips is shorter than for the apical tree (212 vs 425 μm) which suggests that synapses formed on the basal dendrites occupy a more restricted range of physical distances from the soma. The dendritic trees of CA3 pyramidal neurons also have a roughly symmetrical structure in their maximal transverse and septo-temporal extents (~ 300 and 270 μm, respectively).

The CA3 pyramidal cells give rise to highly collateralized axons that distribute fibers both within the ipsilateral hippocampus (to CA3, CA2, and CA1) and to the same fields in the contralateral hippocampus (the commissural projections) (Li *et al.,* 1994). There is a topographic organization of projections from CA3 to CA1 subregion. According to this, CA3 neurons located in a proximal region of CA1 produce collaterals that tend to terminate superficially in the stratum radiatum layer of the more distal portions of CA1 subregion (near the subicular border). On the contrary, neurons located more distal regions of CA3 send projections that terminate deeper in the stratum radiatum layer and in the stratum oriens layer of more proximal portions of CA1 (closer to the CA2 border) (Witter and Amaral, 2004). This axonal network may make various synapses on individual dendritic trees of CA1 pyramidal neuron (Sorra and Harris, 1993). Proximal CA3 neurons and CA2 cells promote a small

number of collaterals projecting to the polymorphic layer of the DG. Despite of some earlier postulates (Swanson *et al.,* 1978), it is observed that CA3 neurons have no projections to the subiculum, presubiculum, parasubiculum, or EC. In the rat (Amaral *et al.,* 1984; Demeter *et al.,* 1985), the CA3 pyramidal neurons send commissural projections to the CA3, CA2, and CA1 subregions of the contralateral hippocampal formation (Swanson *et al.,* 1978, Witter and Amaral, 2004). The lateral septal nucleus also provides the major subcortical input to CA3 subregion (Swanson and Cowan, 1977). This projection terminates most heavily in the stratum oriens layer and to a lesser extent in the stratum radiatum layer (Nyakas *et al.,*1987). Previous tracing studies showed that CA3 region also receives inputs from the amygdaloid complex which send projections mainly to CA1 and subiculum. The caudomedial portion of the parvicellular division of the basal nucleus produces these inputs which terminate in the the stratum radiatum and stratum oriens layers (Pikkarainen *et al.,*1999; Witter and Amaral, 2004). The piriform nucleus also sends weak inputs to the temporal part of CA3 region (Behan and Haberly, 1999). The CA3 subregion also receives inputs from the noradrenergic nucleus locus coeruleus and the nucleus subcoeruleus (Swanson *et al.,*1987; Datta *et al.,* 1998, Witter and Amaral, 2004) and these inputs terminate in stratum lucidum and stratum lacunosum-moleculare layers. Regarding internal connectivities within CA3 region, neurons located proximally in CA3 subregion only communicate with other neurons in the proximal portion of CA3 subregion at the same and adjacent septo-temporal levels. Associational projections arising from mid and distal portions of CA3 subregion, however, project transversely in CA3 subregion and also project much more widely along the septo-temporal axis (Ishizuka *et al.,* 1990; Witter and Amaral, 2004).
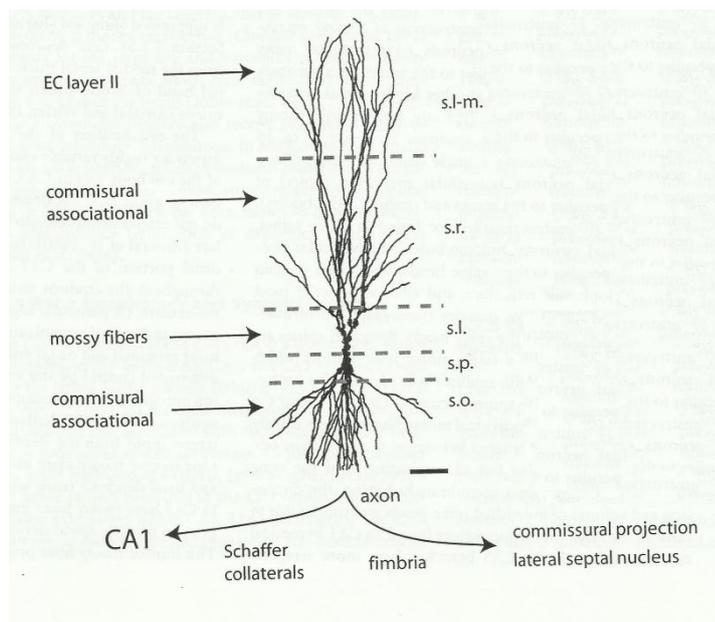
Figure 1.9. CA3 synaptic inputs and outputs (adapted from Gonzales *et al,* 2001; Spruston and McBain, 2006)

Like their CA1 counterparts, CA3 pyramidal neuron dendrites are studded with thousands of spines. Even greater diversity of spine morphology is appearent in CA3 neurons. In addition to the spine shapes observed in CA1 neurons, the CA3 neurons also have another major spine class, the "thorny excrescences". There are about 40 of these specialized spine clusters on each CA3 neuron (Blackstad and Kjaerheim, 1961; Gonzales *et al.,* 2001). These branched spines contain subcellular organelles typical of other spines but they also contain organelles not found other spines such as mitochondria and microtubules.

In particular, the extensive excitatory recurrent connections of CA3 subregion have been proposed to play a role in encoding and retrieval of associations, including autoassociative completion of a single pattern, or associative retrieval of the next pattern in a sequence (Jensen and Lisman, 1996; Levy, 1996; Lisman, 1999; Treves and Rolls, 1992). Computational studies suggest that the recurrent connections of CA3 cells operate as an attractor network that computes associations between elements

(Norman and O'Reilly 2003) and is suitable for representing sequences of events in episodic memories (Jensen and Lisman 1996; Levy 1996; Lisman 1999). In contrast, hippocampal CA1 subregion has been proposed to play a role in matching of CA3 output with afferent input from EC (Hasselmo and Wyble, 1997; Lisman and Otmakhova, 2001). Studies on the effects of selective damage within the hippocampus have shown that CA3 subregion is critical for remembering sequences of spatial locations (Hunsaker *et al.,* 2008), but not sequences of nonspatial events (Hoge and Kesner 2007). Other observations suggest that CA1 may be involved in memory for the order of both spatial (Hunsaker *et al.,* 2008) and nonspatial stimuli (Hoge and Kesner 2007; Manns *et al.,* 2007). However, it is not clear whether the contribution of CA1 involves integrating sequential elements of a memory or instead participates by active maintenance of event memories that underlies bridging sequential events in an episode (Kesner *et al.,* 2005).

1.2.2.2.4. Cornu Ammonis 4 (CA4)

The region known as CA4 is the deep region of polymorphic layer of the DG (Blackstad, 1956; Amaral, 1978) and often called the hilus or hilar region. CA4 neurons do not have pyramidal morphology like CA1 and CA3 neurons (Lorente de No, 1934; Amaral, 1978). This region contains mossy cells that primarily receive inputs from granule cells located nearby in the DG in the form of mossy fibers. They also receive a small number of connections from pyramidal cells located in CA3 subregion. They, in turn, project back into the DG at distant septo-temporal levels.

1.2.2.3. Subiculum

The subiculum lies on the opposite site of the CA1 region than CA3 region, directly adjacent to the distal extent of CA1 area. It begins where the Schaffer collaterals end, a point distinguishable by the transition from the tightly packed CA1 pyramidal layer to the more diffuse pyramidal layer of subiculum. The role of subiculum in the hippocampus is important because it receives convergent input from several sources and sends the major output to the target places (Naber *et al.,* 2000). The principal cell in the subiculum is the pyramidal neuron which has an apical dendrite extending into the molecular layer and mostly reaching the hippocampal fissure (Harris *et al.,* 2001). A quantitative comparison of dendritic branching in the subiculum and CA1 region revealed that subicular pyramidal neurons have slightly fewer branches in both the basal and apical dendritic trees, with the largest difference in the proximal apical dendrites (Staff *et al.,* 2000). Like the dendrites of CA1 and CA3 pyramidal neurons, the dendrites of pyramidal neurons in subiculum are studded with spines.
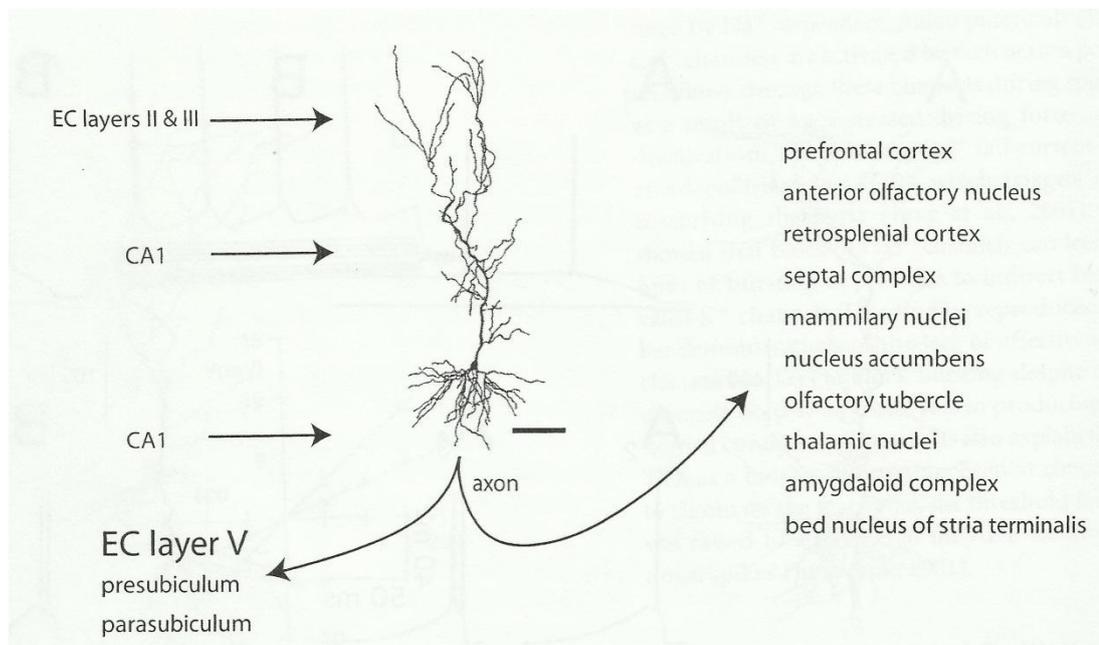
Figure 1.10. Subiculum synaptic inputs and outputs (adapted from Staff *et al,* 2000; Spruston and McBain, 2006)

The subiculum receives inputs from the subcortical structures like the thalamic nucleus reuniens, septal nucleus and the nucleus of the diagonal band. The latter ones send weak cholinergic projection to the subiculum. In addition, the brain stem also send modulatory inputs to the subiculum, including dopaminergic (ventral tegmental area), noradrenergic (the locus coeruleus), and serotonergic (raphe nuclei). The subiculum also receives inputs from many of the same cortical areas that project to the EC, in addition to a direct input from the EC. The subicular pyramidal neurons axons produce widespread collaterals in the subiculum and send projections out of the subiculum (Harris *et al.,* 2001). The local collaterals are believed to form glutamatergic synapses contacts (Harris and Stewart, 2001).

1.2.3. Hippocampal Development

In rat, hippocampal regions begin to form from embryonic days (ED) 15-21 and continue postnatally (Bayer, 1980a). Hippocampal neurons migrate from the hippocampal neuroepithelium which consists of three components: ammonic neuroepithelium which gives rise to pyramidal cells and large neurons of the stratum oriens and radiatum, dentate neuroepithelium which gives rise to granule cells and large neurons of stratum moleculare and hilus, and glioepithelium which gives rise to glial cells and fimbria. Pyramidal cells move out of the neuroepithelium and form a band of cells in the intermediate zone (Altman and Bayer, 1990; Danglot *et al.,* 2006). After that, cells leave this band to form the pyramidal cell layer, firsly CA1 then CA3.

At the beginning of its embriyonic development, left and right hippocampi invaginate into lateral ventricles with germinal hippocampal cells establishing layers called *matrix lamina* on the border with the ventricles (Bayer and Altman 1974). Here, the proliferation of precursor cells takes place. Newborn neurons migrate towards the pia mater to form the cortical plate in inside/out manner (Stensaas, 1967). With time, hippocampus proper starts taking its typical enfolded appearence. By that time, the future dentate gyrus represented by an aggregation of germinal cells (Schlessinger *et al.* 1975; Bayer and Altman 1975). The development of the DG is highly delayed compared to the hippocamspus proper and many other brain structures and extends to the protracted postnatal period. Approximately 85% of the dentate granule cells and high fraction of hippocampal interneurons originate after the birth. According to Bayer and Altman (1975), around 45% of postnatal granule cells originate during the first 8 postnatal days. The newborn precursors of dentate granule cells migrate and settle not above but beneath earlier established cell layer producing a spatial gradient (Altman and Das 1965, Schlessinger *et al.,* 1975).
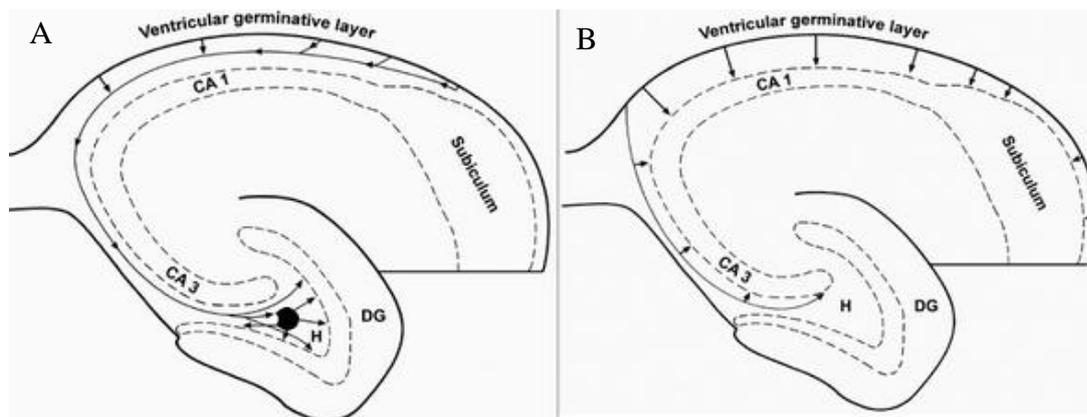
Figure 1.11. Route of migration of (arrows) granule cells (A) and pyramidal cells (B) (adopted from Spruston and McBain, 2006).

As in many other brain areas, here too, the location of a specific synaptic input to the neuron is very much determined by the timing of the afferents arrival. In example, earlier arriving commissural afferents originating in the contralateral hippocampus occupy dendritic segments close to the cell perikaryon, while enthorhinal afferents arriving later on locate their terminals at more distal dendritic segments. However, some new findings argue with the Gottlieb-Cowan principle "first- come, first-served" (Gottlieb and Cowan 1972). It has been reported that in rats, despite the neonatal damage to

the commissural fibers belonging to the PP were still located on the distal portion of the dendrite (Hjorth-Simonsen and Jeune 1972, Lynch *et al.*, 1973). Opposite, an early postnatal lesion to the PP did not cause a spread of commisural terminals on the distal dendritic fragments (Lynch *et al.,* 1973, Zimmer 1973). It has been also found that in mutant 'reeler' mouse (Bliss *et al.,* 1974) with disturbed control over neuroblasts migration, granule cells scattered throughout the whole DG area and PP axons preserve their usual positions with regard to the pial surface while the granule cells extend their dendrites to make contacts with them. Conversely to this, formation of synaptic contacts between the CA3 Schaffer collaterals and the CA1 dendrites occur because the axons search for the dendrites. According to the electrophysiological data, in both case functional synapses are established. It has been also postulated that the reason for PP not occupying termination sites typical to commissural fibres after commissural lesion could be the competition from the ipsilateral association fibres which are earlier arriving to the newly available sites (Zimmer, 1974). This notion has drawn attention of researches to the potential importance of the spatial proximity in determination of the location of a synaptic input to the neuron (Hjorth-Simonsen and Zimmer, 1975; Zimmer and Hjoith-Simonsen, 1975).

Dentate gyral neurons born prenatally are generated from the ventricular zone, whereas those born postnatally are derived from a secondary proliferative zone, the intrahilar subgranular zone. On the other hand, for many years it has been believed that the, hippocampal pyramidal neurons are generated only prenatally from the ventricular zone.

Interstingly, the maturation stage of newly born dentate neurons are similar in both, the developing and the adult brain (Esposito *et al.,* 2005; Zhao *et al.,* 2006; Treves *et al.,* 2008). Shortly being born, new neurons extend axons down to CA3 subregion and extend dendritic processes into the DG molecular layer (Hastings and Gould, 1999; Zhao *et al.,* 2006; Treves *et al.,* 2008). After 2 weeks, the new neurons start receiving GABAergic and glutamatergic innervation (Ge *et al.,* 2006). By that time, there is observed a rapid increase in the number of dendritic spines (Zhao *et al.,* 2006). Granule cells of DG were reported to reach their adult phenotype approximately one month after the birth (van Praag *et al.,* 2002; Zhao *et al.,* 2006; Treves *et al.,* 2008) although the spine changes may still continue (Zhao *et al.,* 2006; Toni *et al.,* 2007; Treves *et al.,* 2008).

1.2.3.1. Synapse Formation in Hippocampus

Synaptogenesis is the formation of synapses between neurons in the nervous system. Although it occurs throughout a healthy person's lifespan, an explosion of synapse formation occurs during early postnatal development. During the developmental "critical periods", there is a certain degree of neuronal pruning due to competition for neural growth factors by neurons and synapses.

According to the results of early studies tracing the changes in the number of synaptic contacts across the postnatal development in the DG, synapse number at P4 constituted less than 1% of that in adults (Crain *et al.*, 1973; Marrone and Petit, 2002). Despite of a rapid increase in the numeric synapse density between P4 and P11 (20 fold increase), on P11, the recorded synapse count was only 5% of that in the adults. At P25, the overall increase in synapses was more than one hundred-fold, with no further increase until P90. In contrast to this, in hippocampal region CA1, the total density of synapses in the neuropil between P15 and adult ages was doubled (Harris *et al.,* 1992). These results show that the time course of the increases in synapse numbers may be different among different hippocampal regions, however, in all hippocampal regions the most rapid synaptogenesis is observed during early postnatal development. In the hippocampus, Cotman *et al.* (1973) reported a decrease in the synapse size along with an increase in the synapse count. However, later on during the postnatal life, an increase in the size of synapses may be driven by the neural activity (Marrone and Petit, 2002). Electron microscopic studies showed that the adult level of synaptic complexity was obtained at about P25 (Crain *et al.* 1973).

After a contact is made between axon terminals and their targets, the presynaptic growth cones differentiate into specialized synaptic boutons containing clustered at a membrane-associated fusion apparatus. At the same time, postsynaptic densities containing a variety of proteins including neurotransmitter receptors and cytoskeletal proteins are formed. The postsynaptic densities are localized to so called junctional folds at the neuromuscular synapses and dendritic spines at excitatory CNS synapses.

The changes in spine morphology were shown to occur with development and in activity-dependent fashion in the adult brain (Segal, 2001; Matsuzaki *et al.,* 2001). It was manifested that dendritic filopodia attract axons to the dendrite (Dailey and Smith, 1996), and may give rise to spines of varying morphologies (Harris *et al.,* 1992). Initially, most synapses occur directly on the dendritic shaft. Then, shaft synapses give rise to stubby spines, which predominate for the next few weeks. At juvenile age (at P21-30), the shaft and stubby spine synapses are markedly reduced while thin and mushroom spines are formed, and eventually the thin spines become the dominant spine shape. On P21, the thin and mushroom spines reach numbers comparable with those found in the mature hippocampus *in vivo* and *in vitro* (Harris *et al.,* 1992, Harris and Stevens, 1989).

In the mature brain, new spines may form from pre-existing spines by splitting (Geinisman *et al.,* 1996; Jones and Harris, 1995). The consecutive steps of this process are as follows: perforation of PSD, extending a spinule from the perforation gap into the presynaptic bouton and in this way dividing the presynaptic terminal into two synaptic compartments. This is followed by a retraction of a spinule, and creation of a branched spine and finally two synaptic buttons (Fig. 1.12). It is generally accepted that the perforations in PSDs are not permanent features of the synapse, but instead occur transiently in response to synaptic activation (Cohen and Siekevitz, 1978). Spliting of the synapses has been proposed as one of the mechanisms of new synapses formation during the late phase LTP in hippocampal CA1 area (Bolshakov *et al.,* 1997). An increase in in branched spines was also reported in DG after LTP (Trommald *et al.,*1990).
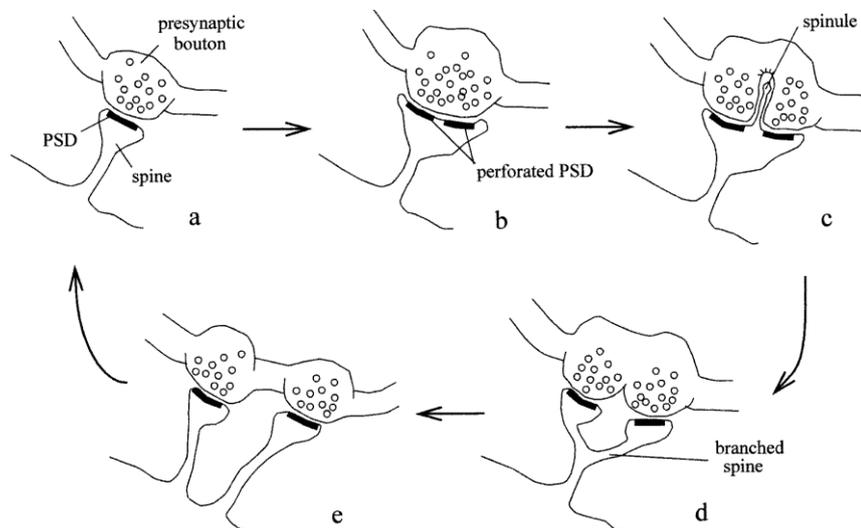
Figure 1.12. Model of synapse splitting (Sorra and Harris, 1998).

During postnatal synaptogenesis, the new granular cells, approximately one week after being generated, receive GABAergic input to their dendrites. This innervation is initially depolarizing until 2-4 postnatal weeks, when it becomes hyperpolarizing (Esposito *et al.* 2005). The initial excitatory character of these synapses is related with the transient expression of the inward chloride transporter NKCC1 in immature neurons, which results in an elevated intracellular chloride concentration as compared with mature neurons (Ge *et al.* 2006). Expression of this transporter is necessary for normal development because its inactivation leads to severely delayed neuronal maturation (Ge *et al.* 2006). In the second week after their birth, dendrites of granule cells start to form spines and to receive glutamatergic input, and their GABAergic input becomes predominantly perisomatic (Esposito *et al.,* 2005; Ge *et al.,* 2006). At the same time, axonal projections from new neurons extend the CA3 region and begin to form contacts that continue to mature for months (Toni *et al.*, 2007). By two months of age, adult-born neurons have similar morphological and electrophysiological properties to those formed during perinatal development (Ge *et al.,* 2006; Laplagne *et al.,* 2006). Levels of neurogenesis and subsequent survival of granular cells are strongly influenced by neuronal activity.

1.2.4. Hippocampal Function

The hippocampus plays an important role in the process of learning and memory (El-Falougy and Benuska, 2006). The hippocampus also functions as a part of the limbic system in regulation of sexual

and emotional behaviors (El-Falougy and Benuska, 2006). Therefore, hippocampus is related with multiple neurological disorders such as epilepsy, Alzheimer's disease, and depression (Benedetti *et al.,* 2006; Scheff and Price, 2006). The hippocampal functions can be summarized as:

- Consolidation of New Memories
- Emotional Responses
- Spatial Orientation and Navigation

Since long it has been accepted that at the basis of learning and memory formation, there are changes (increase or decrease) in synaptic strength (Hebb, 1949). The cellular model of learning and memory is "long-term potentiation" (LTP) first demonstrated by Bliss and Lomo in 1973. They showed that at many synapses in the hippocampus, a short pulse of high-frequency stimulation (50-100Hz) applied to presynaptic fibers leads to a long-lasting increase in synaptic signal recorded from the postsynaptic neurons efficacy. To demonstrate that LTP is gateway to memory formation, extensive studies have been carried out on molecular cascades activated by LTP induction, changes in LTP resulting from pharmacological or genetic manipulations, and correlation of these changes with behavioral learning.

According to their mechanisms, there are two types of LTP in hippocampus. In CA3 region, at mossy fibers' synapses, NMDA-independent type of LTP relying on presynaptic mechanism with cAMP as a second messenger was described (Kessey *et al*., 1997). In contrast, NMDA-dependent LTP characterized by input specificity, rapid induction, cooperativity, and variable persistence (early-LTP and late-LTP), relying on both pre- and postsynaptic mechanisms was described at PP synapses in DG and at Schaffer collaterals in CA1 region (Morris, 2006). While NMDA-dependent LTP is associative, NMDA-independent LTP is known to be nonassociative. In various brain pathways, NMDA receptor (NMDAR) activation is the first step of the induction of synaptic potentiation. Being a slow-acting, ionotropic glutamatergic receptor, NMDAR is known as the most potent Ca^{2+} ionophore and play a selective role in induction of LTP. NMDAR is identified as a "coincidence detector" since NMDAR stimulation needs presence of two events concurrently; binding of glutamate to the receptor and the depolarization of postsynaptic membrane by the same or another synaptic input. Upon receptor stimulation by these two events, the Mg^{2+} block inside the channel are opened and Ca^{2+} ions cross through the channel and enter the postsynaptic cell. The previous studies using pharmacological blocking agents or inactivating the NMDARs genetically demonstrated the importance of the NMDAR-dependent mechanisms in LTP induction and behavioral learning (Davis *et al*., 1992; Tsien *et al*., 1993). The activation of several synaptic proteins by protein-protein interaction and posttranslational modification occurs due to an increase in the intracellular Ca^{2+}. These two processes confirm the biochemical reactions providing persistent modifications of synapse.

Previous studies showed that long term depression (LTD) is responsible for the memory formation. However, there is a controversial opinions about the LTD function in the learning and memory. Some researches thougt that LTD is a cellular storage mechanism and others considered that it mainly works with LTP to adjust the synaptic strength. In hippocampus, Kemp and Manahan-Vaughan (2007) reported that LTD may be induced by low-frequency stimulation only when rats explore new environments. This result indicated the role of LTD in complex spatial mapping. Furthermore, in the studies of mutant mice having deficiency in memory for novel context, LTD is impaired while there is no change in LTP (Etkin *et al*., 2006). It is assumed that LTD-like mechanisms during the acquisition of contextual memory make ready synapses to LTP-like mechanisms expected to take place in their following enhancements. For hippocampus, a modest and more lasting increase in intracellular Ca^{2+} levels together with phosphatase activity creates LTD whereas kinase activation and rapid increase of Ca^{2+} levels points out LTP (Bruel-Jungerman *et al*., 2007).

1.3. Aim of the Study

Fact that adverse effects of fetal alcohol exposure tend to be more pronounced in immature than adult animals is pointing either towards alcohol-induced developmental delay or a "recovery" from alcohol-induced impairments due to some regeneration process. Indeed, some authors were reporting recovery of morphological parameters such as numbers of principal neurons, dendritic arborization, or spine densities in the adult subjects (Davies and Smith, 1981; Ferrer *et al.,* 1988; Miki *et al.,* 2003). However, there is still very little known about the morphological and functional recovery of the brain from teratogenic effects of prenatal alcohol taking place with maturation.

The aim of the present study was to compare developmental changes in the hippocampus, over a protracted postnatal period between control and fetal-alcohol rat pups to reveal potential compensatory processes underlying amelioration of cognitive deficits occuring with maturation. In this study, the behavioral and morphological recovery was examined after fetal ethanol intoxication during the 7-20 gestation period. In this project, morphology of the hippocampus was examined in fetal alcohol and control rat pups at four postnatal ages: P1, P10, P30, and P60. As earlier mentioned, hippocampus is a brain structure critical for the declarative learning and memory and at the same time belongs to those brain regions that were reported to be most susceptible to the adverse effects of fetal ethanol. In the present study, morphological examination of the hippocampal tissue included investigation of age- and ethanol-dependent changes in the counts of principal neurons in the hippocampus proper (CA1, and CA2+3 subregions) and DG by unbiased stereology technique using StereoInvestigator software; tracing hippocampal neurogenesis by estimating doublecortin immunoreactivity; examination of 11 morphometric parameters of hippocampal principal neurons such as the soma size, number of dendrites, number of branches/dendrite, dendritic length, branch angle and dendritic tortuosity, size of the overall dendritic field, and spine densities and morphology using Fast Golgi Stain and Neurolucida software; and finally, evaluation of immunoreactivity and concentration of synaptic protein: presynaptically expressed synaptophysin and postsynaptically expressed PSD-95 protein. Histological data obtained from P30 and P60 age groups of control and fetal alcohol rats were correlated with animal performance in a variety of behavioral tasks including Plus Maze anxiety test, Open Field locomotor activity test, place learning and memory under both allo- and idiothetic stimulus conditions in the Morris Water Maze. In addition to careful examination of ethanol effects, this study gave us also an opportunity to examine several different aspects of hippocampal development over a protracted postnatal period in the same random population of intact Wistar rats.

CHAPTER 2

MATERIALS AND METHODS

2.1. Subjects

Large number of 3.5 - 4 months old, naive, female and male Wistar rats, obtained from the Gulhane Millitary Medical Academy (GMMA) Animal Breeding Facility (Ankara), was used in the present study. Throughout the experiments, rats were kept in the METU animal facilities at the Department of Biological Sciences, under the stable temperature of $22 \pm 1°C$ and 12 h/12 h light/dark cycle, and with *ad libitum* food and water supply.

2.2. Breeding

Individual female rats were placed in transparent Plexiglas cages. For mating, a male rat, picked at random, was housed with a female in the female's cage for maximum a week. Each morning, female rats were examined for the presence of the vaginal plug (Fig. 2.1) which was an evidence of successful fertilization and this day was marked as gestational day 0 (GD0). On GD7, pregnant dams were assigned (counterbalanced for initial body weight) to one of three treatment groups: Alcohol Group (A), pair-fed Intubated Control Group (IC), a control for possible intubation-induced stress effects, and Control Group (C).

Figure 2.1. The appearance of vaginal plug

The day of birth was referred to as postnatal day 0 (P0). At birth, the number of pups in each litter was counted. The body weight gains of dams and then offspring were monitored on daily basis. Until weaning at P25, pups (except those used in experiments at earlier ages) remained with their natural mothers. Afterwards pups were group-housed by litter and sex in transparent Plexiglas cages (46×24×20 cm).

2.3. Ethanol Treatment

Starting from the gestational day (GD) 7 throughout GD20, dams from alcohol (A) group were daily administered 6 g ethanol/kg body weight by intragastric intubations (Fig. 2.2). Ethyl alcohol 96.5% v/v, Merck was used in the study. Animals in IC group received the same volume of fluid with sucrose substituted isocalorically for ethanol; they were given the same amount of food as that

consumed by their weight-matched A group females. Animals in C group received *ad libitum* access to laboratory chow and water with no additional treatment. The protocol of alcohol administration was as earlier described (Dursun *et al*., 2006). The alcohol/isocaloric sucrose solution was delivered by intragastric intubations using stainless curved feeding needle (18 ga, 3 in, Stoelting Co., Wood Dale, IL). Daily portion of alcohol/sucrose solution was divided into two equal doses given to animals 1 h apart. The alcohol solution was prepared daily as a 25% (vol/vol) ethanol mixed with distilled water and stored at room temperature. All animals were daily weighted and the ethanol solution was fresh prepared each day.

Figure 2.2. The moment of intragastric intubation

2.4. Determination of Blood Alcohol Concentration

Blood alcohol concentration (BAC) was assessed on GD20 in a different group of pregnant dams (n=4). Blood samples (1–2 ml) were taken from the rat-tail vein 3 h after the last intragastric intubation (Tran and Kelly, 2003). Blood samples were then centrifuged for 10 min. at 1000 *g*, blood plasma separated and stored at -80^0C until BAC determination was carried out. BAC (mg/dl) was determined by an alcohol assay kit (Biolabo, France) at the Gülhane Military Medical Academy (Sag *et al.,* 2006).

2.5. Experiment 1: Behavioral Testing

2.5.1. Pups

Behavioral tests were started at two ages of pups: at P30 (juveniles) and at P75 (young adults) in two intubation control groups (IC30 (n=7), and IC75 (n=6)) and fetal alcohol rats (A30 (n=7), and A75 (n=6)). Since in our previous studies (Jakubowska-Dogru, 2010) no substantial sex-related differences were observed in the rat's performance on the tasks similar to those applied in this study, in the present study, the female offspring were used in behavioral experiments while male offspring in the neuroanatomical investigations. Since in our previous study (Dursun *et al.,* 2006) no significant difference was found in behavioral measures between intact and intubated control groups, considering the restriction on animals use by the NIH *Guide for the Care and Use of Laboratory Animals* (1996) and METU Ethic Committee Directory, a single control group was enrolled into the behavioral tests in the present study. To limit the effects attributable to contributions from individual litters the rats from each treatment group were intermixed between litters. All experimental procedures were approved by the Ethics Committee of the Middle-East Technical University, Ankara, Turkey. In this study, all efforts were made to minimize animal suffering and to keep the number of animals used as low as possible.

2.5.2. Open Field Test

The open field test (Hall and Ballachey, 1932) is used to measure general locomotor activity and at the same time anxiety in rodents. Test was carried out according to the Latin square design in two square boxes of different size: a large box (120 x 120 cm) and a small box (60 x 60 cm) on two consecutive days. The test boxes had the side walls 50 cm high, made of plain wood painted black and illuminated by a bright light from the ceiling (Fig. 2.3). The rat was placed at the middle of one of the side walls facing the wall. Its locomotor activity was recorded by the computerized video tracking system (EthoVision System by Noldus Information Technology, Holland). The open field was divided by virtual lines into 16 equal squares, 12 of which constituted the peripheral zone, and remaining 4, the central zone of the arena. The system recorded time spent and distance moved (ambulation) in each of the zones for 20 min. in 5 min. intervals.

Figure 2.3. The open field instrument

2.5.3. Elevated Plus Maze Test

The plus maze, designed to measure anxiety level in small rodents, was constructed of polyester. It includes a central platform (10×10 cm), two open arms (50×10 cm) and two closed arms (50×10 cm). Plexiglas walls of maze arms extend 30 cm high and have no ceiling (Fig. 2.4). The arms were arranged in a cross shape with the two open arms facing each other and two closed arms facing each other. The height of maze from the floor is 80 cm. During a single testing session, each animal was put by an experimenter in the center of the maze facing an open arm. Each testing trial lasts in 5 min. During this time, the number of entries with all four paws of rat to the open and closed arms, the total time spent in open and closed arms individually, and total time spent on the central platform were recorded by the computerized video tracking system (EthoVision System by Noldus Information Technology, Holland).

Figure 2.4. The Elevated Plus Maze Apparatus

2.5.4. Morris Water Maze

Morris Water Maze (MWM) was used to monitor spatial learning and memory in small rodents (Morris, 1984). The maze is a circular tank (150 cm X 60 cm in diameter) and filled to the depth of 45 cm with water with a temperature of 23 °C (±1). To make the water opaque, a nontoxic food coloring was used (Fig. 2.5). Computerized video tracking system (EthoVision System by Noldus Information Technology, Holland) was set to track the animal in the pool and to record data. The pool was divided into four quadrants (NE, NW, SE, and SW) by two imaginary perpendicular lines crossing in the center of the pool. A movable platform (11 cm × 11 cm) made of transparent Plexiglas and thus invisible to the animals, was located in the center of one of the quadrants. The top of the platform was 2 cm below the surface of the water such that the animal could not see it but could climb on it in order to escape from the water. Experimental room was furnished with several extra-maze cues immobile throughout the entire experimental period. These distal extramaze cues were either available to the animals and could be used as a spatial reference frame in place learning (an allothetic paradigm), or eliminated by nontransparent curtains surrounding the pool (idiothetic paradigm). Training and testing in the MWM comprised of 6 consecutive stages: Shaping Training; Place Learning under Allothetic Paradigm; Allothetic Probe Trial; Place Learning under Idiothetic Paradigm; Idiothetic Probe Trial, Working Memory Test.

Figure 2.5. The Morris Water Maze Apparatus

2.5.4.1. Shaping training

Shaping training was applied to minimize the confounding effect of non-mnemonic factors arising from being introduced to a novel stressful situation (Dursun *et al*., 2006). On the first day in the pool, each rat was trained to swim in the water and climb on the escape platform. The raised platform was put 30 cm from the edge of the pool in a randomly choosen position. Nontransparent curtains were used around the tank to eliminate the distal cues that were important for the subsequent place learning sessions. Animals were placed into the pool four times from different starting points: first in the vicinity of the platform, then from a gradually increased distance from the platform. Each time an

animal swam in the water until it found the platform. If an animal did not find the platform within 60 s the experimenter guided it gently to learn the platform place.

2.5.4.2. Allothetic (Allocentric) Training and Probe Trial

The platform was placed in the center of one of the quadrants where it stayed throughout the whole experiment. In a daily single session, rats were trained four trials, for 4 consecutive days. Each rat was put into the water gently facing the pool wall at one of the four starting points (S, N, W, E) which were chosen in a pseudorandom order such that each start position was used only once during the daily experimental session. The trial was finished when the animal found the platform or 60s passed. Afterwards the rat was returned to its cage for a 5 min. inter-trial interval. The video-tracking system was automatically recording the swim trajectory (Fig. 2.6), swim velocity, escape latency and the swim distance to reach the invisible platform.
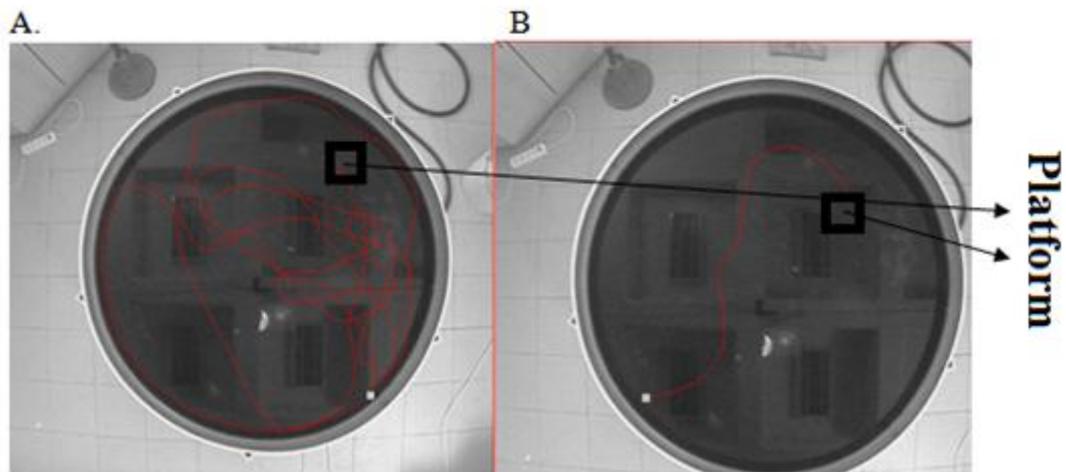
Figure 2.6. The pathways of the first (A) and the last (B) trials of MWM training. The white squares were the start points

On the completion of the 4 consecutive training days, to assess the strength of the acquired place preference, a probe trial, was carried out (Fig. 2.7). On a 60 s probe trial, the platform was removed from the pool and the percentage time spent by the animal in the platform quadrant and in the imaginary 40 cm diameter annulus (annulus 40) virtually drawn around the platform position was recorded.
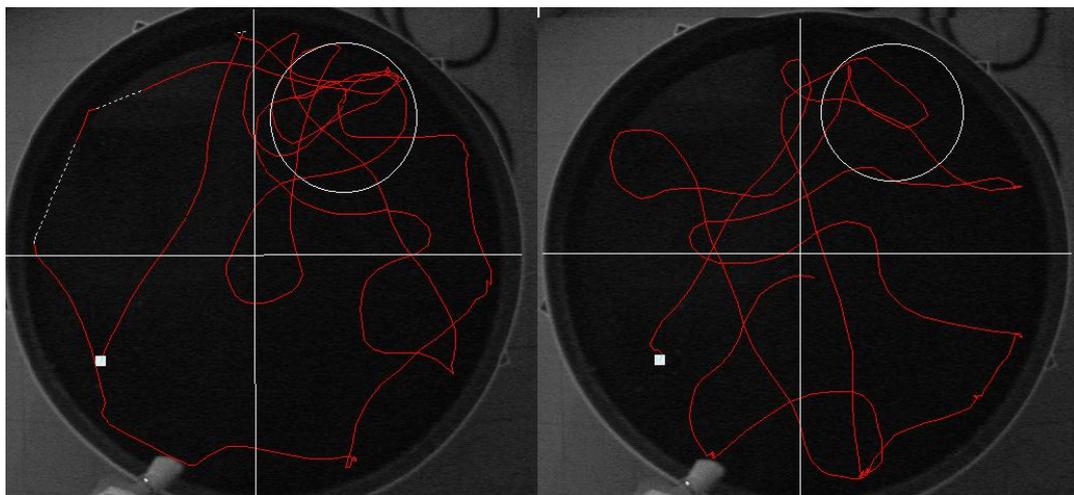
Figure 2.7. The good(left) and the bad (right) probes in MWM. The circles show the annulus 40. The small white squares indicate the start points.

2.5.4.3. Idiothetic (Egocentric) Training and Probe Trial

This training procedure was basically the same as the one previously described for allothetic training except that the platform was moved into different location and the water pool was surrounded by nontransparent curtains eliminating the distal visuo-spatial cues belonging to the room. In this situation, instead of spatial mapping the distal environment, rats were forced to apply another strategy to find the hidden platform. This time, the guiding cues would come from the proximal environment (i.e. from the pool itself) and from the proprioceptive and vestibular feedback (idiothetic or egocentric signals) from the executed movements. Place learning in the absence of the distal visuo-spatial cues was apparently more difficult and it took 6 days to reach the same level of performance as in the previous task. The idiothetic training was followed by the probe trial.

2.5.4.4. Delayed Non-Matching-To-Position (DNMTP) Working Memory Test

Delayed non-matching to position (DNMTP) task was used to measure the spatial working memory. In this test, two visible platforms marked with a flag were used. The training comprised of several pairs of "sample" and "test" trials applied in succession with stepwise increased delay in-between. On a "sample" trial rat swam to a visible platform which position changed between "sample" trials but stayed the same on the following "test" trial. On the "test" trial, the animal was confronted with two identical visible platforms, one in the same location as on the last "sample" trial and the other in a new location. However, only the escape platform in the new location was stable and thus accessible to the animal. The optimal performance was to choose the new platform position. 2 days of shaping training (four trials per daily session) was applied to teach to the rats to swim to a visible platform regardless of its position. During the initial "rule learning", the interval between sample and test swim was kept short (2 min.). In the course of the training, the delay between the trials was increased from 2 to 15 min. The training ended when the animal reached a performance criterion of 75% correct choices in the three successive daily sessions with four "sample" and four "test" trials per session. Since the sample platform position changed between the trials this test was scanning the short-term (working) spatial memory.

2.6. Experiment 2: Morphological Studies

2.6.1. Pups

Male pups belonging to the mothers from each of treatment groups (A, IC, and C) were randomly assigned to 4 age subgroups and sacrificed at P1 (n=87), P10 (n=88), P30 (n=90), and P60 (n=90), respectively. To limit the effects attributable to contributions from individual litters the rats from each age group were intermixed between litters with one or maximum two pups from a single litter assigned to each of the age groups. In the present study including 12 treatment/age groups, the reason for using the male pups only was to avoid the gender effect analysis and in this way not to further inflate the "multiplicity" problem.

2.6.2. Stereology

2.6.2.1. Fixation

Pups belonging to either each age (P1 (n=19), P10 (n=23), P30 (n=23), P60 (n=23)), were deeply anesthetized with a mixture containing ketamine hydrochloride (80 mg/kg Alfamine 10%, Alfasan International B.V. Holland) and xylazine (10 mg/kg Alfamine 2% Alfasan International B.V. Holland) (i.p.) and perfused intracardially with 0.1 M phosphate buffer (pH 7.4) followed by 4% paraformaldehyde solution in 0.1 M phosphate buffer. The brains were removed from the skulls, and postfixed overnight in 4% paraformaldehyde. After that, brains were cryoprotected with 10% sucrose solution for 1 h and then 30% sucrose solution until the brain was sank. Then it was quickly frozen in liquid nitrogen and then stored at -80^0C.

Figure 2.8. Fixed brains at different ages. From left to right: P60, P30, P10, P1.

2.6.2.2. Sectioning, Sampling, and Staining

The fixed brains were cut coronally at 50-µm on a Shandon Cryotome (Thermo Fisher Scientific Inc., USA). Stereological studies use both plastic embedding and frozen sections methods. Frozen sections are easier to obtain but they may create problems resulting from the shrinking of tissue samples. This may affect the estimation of cell density but not the estimates of the total cell counts. The stereological studies on frozen sections have previously been successfully performed by other research groups (Boldrini *et al.,* 2012; Bonthius *et al.,* 2004; Dong *et al.,* 2003; Dursun *et al.,* 2011; Fitting *et al.,* 2010; Goodlett *et al.,* 1997; Lemmens *et al.,* 2011; Vazquez-Roque *et al.,* 2012). In the present study, too, we neither had difficulties with applying a dissector with a height of 10 µm (the dissector height used in the present study), nor we had resolution problems when viewing the cells. Initially, all sections that included the entire hippocampal formation were collected starting from the dorsal tip of the hippocampus, where the corpus callosum begins to form, past the end of the posterior ventral hippocampus. A systematic random sampling of one section out of every 3rd in P1, every 4th in P10 and P30 brains, and every 5th in the P60 brains (16-22 section per rat) was done. The sections were floated in 0.1 M PBS in 24-well plates, mounted on polylysine covered glass slides, dried at room temperature, and stained with cresyl fast violet (Nissl staining). The staining solution contained 1 g of cresyl violet acetate (Merck), 2-3 drops of glacial acetic acid and distilled water. The mounted sections were dehydrated in increasing alcohol concentrations (70%: 2 min., 95%: 2 times, 2 min. each time; and eventually 100%: 2 times, 2 min. each time), defatted in xylene solutions (3 times, for 5, 10 and 1 min.) and eventually rehydrated in decreasing alcohol concentrations (100%: 2 times, 1 min. each time; 95%: 2 times, 1 min. each time; and 70%: 1 min.). The slides were washed in distilled water (2 times, 30 sec. each time). Afterwards, the slides were placed in the staining solution for 2-10 min., dependent on tissue thickness and stain freshness, and washed again in distilled water (2 times, 15 sec. each time). During differentiation step the sections were immersed in dilute acetic acid solution for 2-10 min., dependent on tissue thickness and cresyl violet staining time. Finally, the samples were dehydrated in 95% and 100% ethanol (2 times, 30 sec. each time) and cleared in xylene (2 times, 5 min. each time). Sections were then cover-slipped using Entellan (Merck) mounting medium.
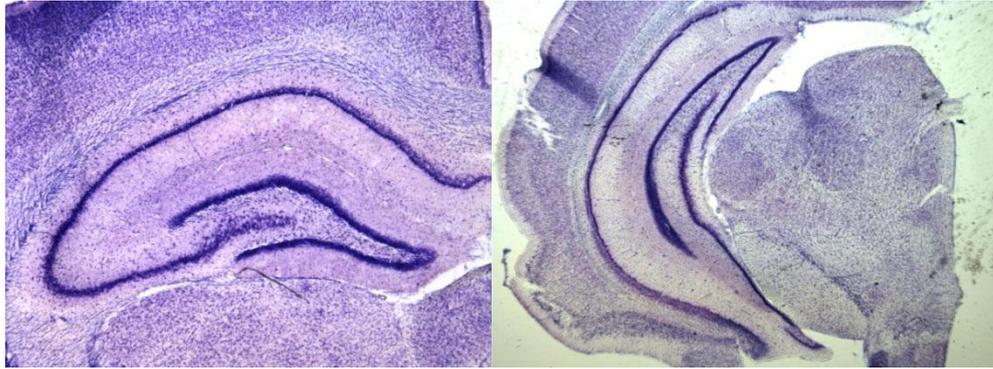
Figure 2.9. The examples of Nissl stained dorsal (on the left, Bregma -3.60, magnification at 2.5X) and ventral (on the right, Bregma 5.80, magnification at 1.25X) hippocampus. (Paxinos and Watson, 2004).

2.6.2.3. Cell Counting

All stereological procedures were applied using a commercial computer-assisted stereological workstation (StereoInvestigator, Microbrightfield, Williston, VT) including a high-resolution computer monitor DM5500 and a Leica light microscope equipped with a Leica DFC320 R2 digital firewire camera. The neurons of different hippocampal regions were clearly differentiated by their characteristic shapes and sizes according to morphological criteria described by West and colleagues (1991) (Fig. 2.10). Nevertheless, in addition to principal neurons, the counts probably also include basket interneurons which are difficult to discriminate. Basket cells, however, constitute only a very small fraction (less than 1%) of all neurons in granular and pyramidal cell layers.
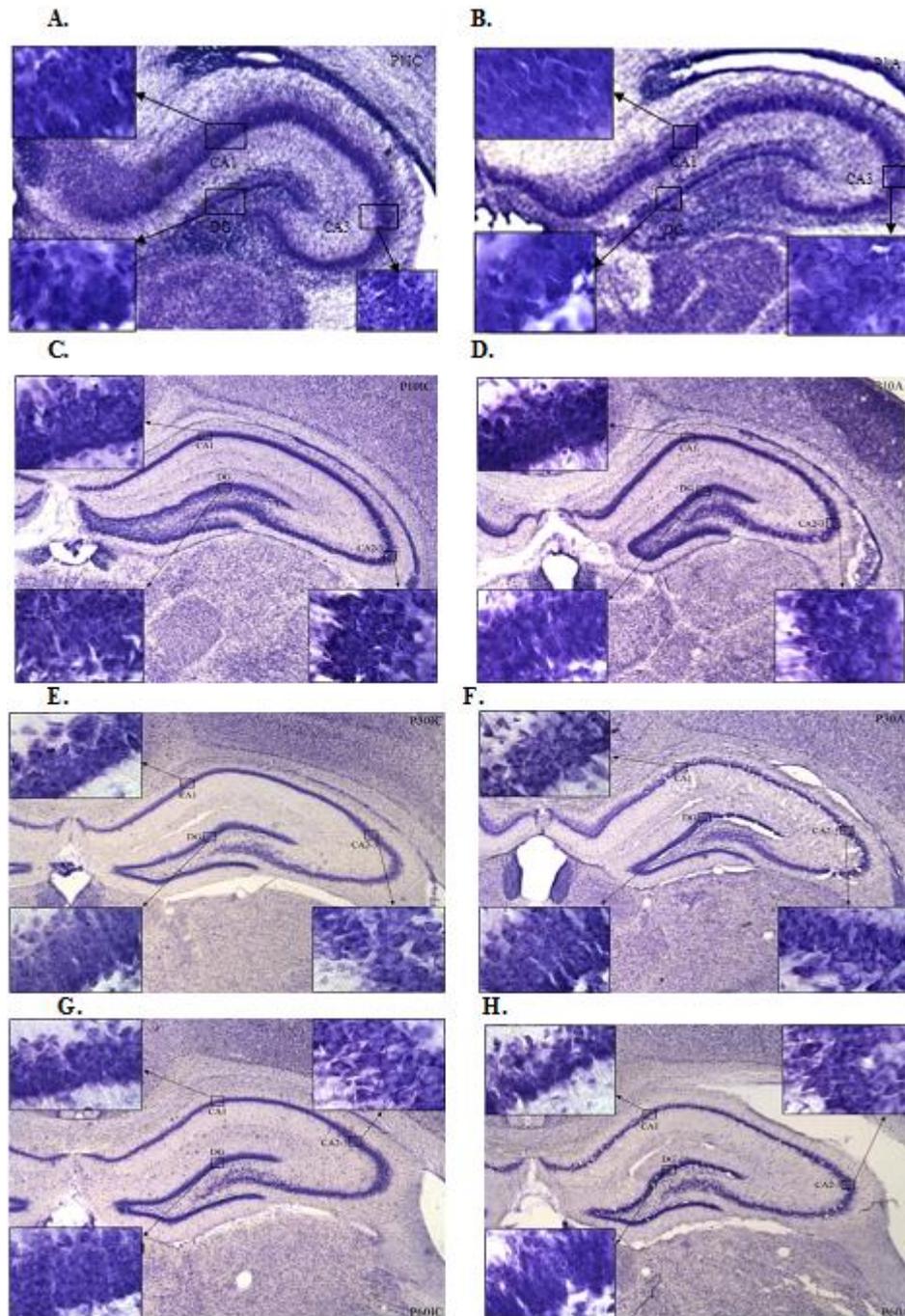
Figure 2.10. Photomicrographs showing hippocampal slices from a control (left) and fetal ethanol rat (right) for different postnatal days: P1 (A ve B), P10 (C ve D), P30 (E ve F), and P60 (G ve H) DG: dentate gyrus; CA1: Cornu Ammonis area 1, CA2: Cornu Ammonis area 2; CA3: Cornu Ammonis area 3

The neuroanatomical borders of the principal cell layers of the hippocampus were outlined under a low-power (4X) objective and the selected areas were systematically sampled with the aid of StereoInvestigator software. Areal outlines and volumes were confined to the stratum pyramidale in regions CA1 and CA2+3 and the stratum granulosum in the DG according to Paxinos and Watson rat brain atlas (2007). Similarly, cell counts were limited to the pyramidal cells in regions CA1 and CA2+3, and granule cells from the DG. Unbiased stereological procedures were used to estimate the total number of principal neurons within the DG and hippocampal CA1 and CA2+3 regions. Figure 2.10 presents a photomicrograph of a representative Nissl stained coronal section at magnification of 100X through CA hippocampal region on which pyramidal and glial cells can be easily discriminated.
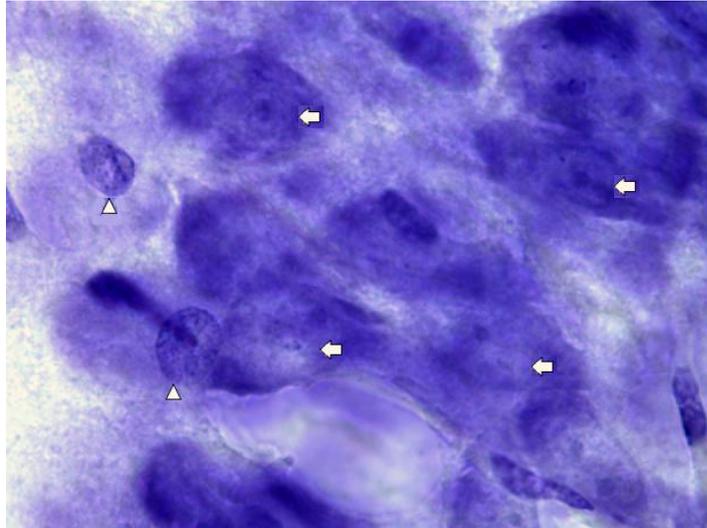
Figure 2.11. Photographs showing neuron (arrow) and glia (arrowhead) in CA3 region of adult hippocampus.

These procedures attempt to maximize precision and efficiency using systematic random sampling of sections and unbiased sampling of nuclei (Gundersen and Jensen, 1987). The neuronal counts were done within these areas under a high-power oil immersion lens (100X, N.A. 1.25), using motorized X-Y-Z stage controlled through the StereoInvestigator software package. The optical fractionator workflow extension of the StereoInvestigator software was used to quantify the total number of neurons. The area of the unbiased counting frame for CA1 and CA2+3 regions where the cell size is larger was set to 625 μm^2 with a grid (sampling step) size of 22500 μm^2, and for DG region where the cell size smaller to 144 μm^2 with a grid size of 14400 μm^2. Counting was performed in each sampling step according to the rules of the unbiased counting frame and the optical dissector (West *et al.,* 1991).
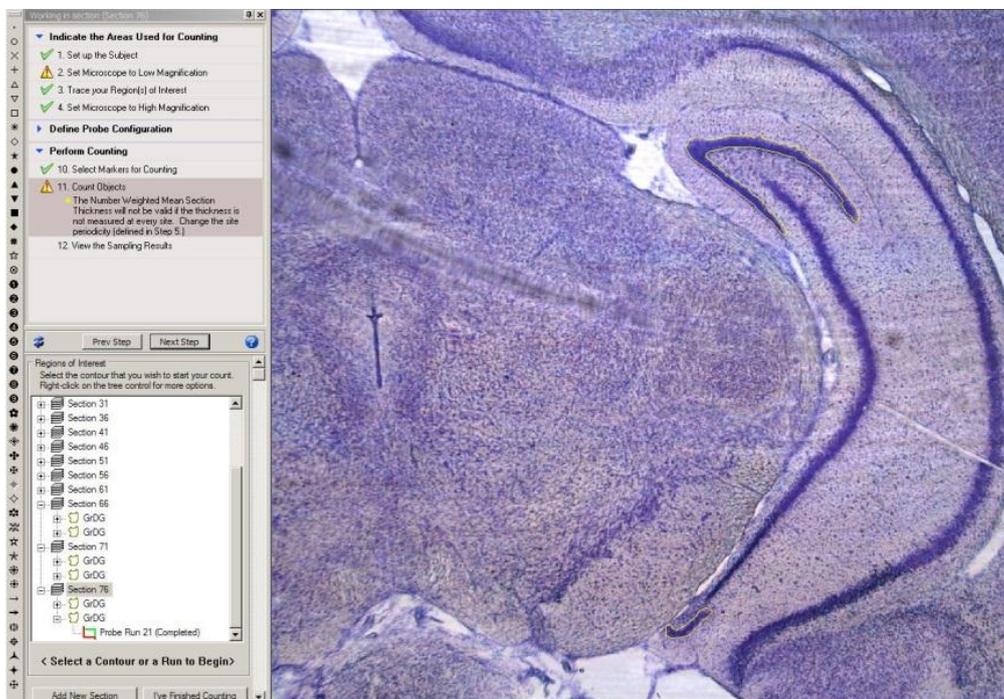
Figure 2.12. Optical fractionator workflow
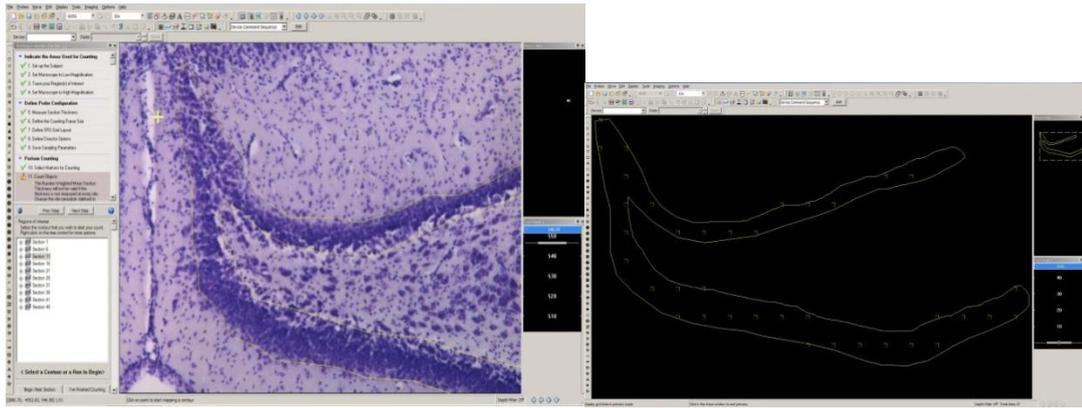
Figure 2.13. Determination and visualization of ROI (region of interest) and the grid size in the DG of hippocampus with the help of StereoInvestigator software

A fixed dissector height of 10 µm was used in every counting step with a guard height of 2 µm from the top surface of each section in order to avoid errors when counting the cells at the cut surface. In order to calculate the mean section thickness ([t]), first, the thickness of each sampled section was estimated at every sampled dissector location and then the thickness estimates were averaged across the whole set of sampled sections. The thickness sampling fraction was estimated as the dissector height relative to the mean section thickness (tsf=10/[t]). An unbiased estimate of the total number of hippocampal pyramidal and dentate granular cells (N) was calculated by multiplying the sum of the neuronal counts over all sections ($\sum Q$) with the reciprocals of the sampling fractions as follows: $N=\sum Q^{-}.(1/ssf).(1/asf).(1/tsf)$, where ssf is the section sampling fraction (the actual number of sections sampled in relation to the total number of sections), asf - the areal sampling fraction (the area of the counting frame relative to the sampling area per each sampling step), and tsf -the thickness sampling fraction. Statistical evaluation and error determination of obtained estimates were determined by the coefficients of error (CE) (Gundersen *et al.,* 1999).
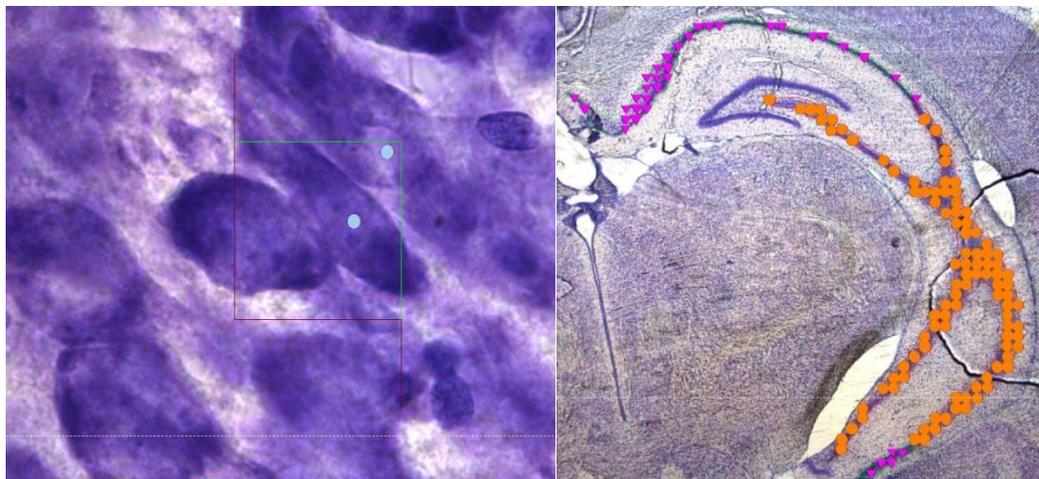
Figure 2.14. A representative counting window and completed count of hippocampal CA1 and CA2+3 regions.

2.6.3. Golgi Staining and Neuron Morphometry

2.6.3.1. Tissue Preparation

The pups belonging to either A, IC, or C group used in this study were deeply anesthetized and sacrificed at P1 (n=22), P10 (n=22), P30 (n=21), and P60 (n=21). They were first intracardially perfused with saline to remove the blood from the brain. The brain was removed from the skull as quickly as possible but handled carefully to avoid damaging or pressing the tissue. The part of the brain containing hippocampus was dissected. The rapid Golgi staining was performed by using FD Rapid GolgiStain™ kit. The dissected part of the brain was immersed in the impregnation solution,

prepared by mixing equal volumes of Rapid GolgiStain A and B solutions (containing mercuric chloride, potassium dichromate and potassium chromate) and then stored for 2 weeks at room temperature in darkness. Afterwards, the tissues were transferred into Solution C of the kit and stored for at least 48 hours at 4^0C in darkness. After that the brain specimens were cut into 100 μm sections on a Leica cryostat at -22^0C. Each section was transferred with a glass specimen retriever and mounted on gelatin-coated microscope slides with solution C. Then, sections were allowed to dry naturally in a dark place at room temperature.

2.6.3.2. Staining Procedure

Following drying the sections were washed with distilled water (2 times, 2 min. each time) and stained with mixture of Solution D and Solution E of the kit (1 part solution D, 1 part solution E and 2 parts distilled water) for 10 min. Again the sections were rinsed with distilled water (4 times, 5 min. each time) and counterstained with cresyl violet. After dehydrating in increasing concentrations of alcohol (50%, 75%, 95% (4 min. each time) and absolute (4 times, 4 min. each time) ethanol and clearing in xylene (3 times, 4 min. each time), the sections were coverslipped with Permount mounting media. Golgi-stained sections were kept in a dark place until further analysis of hippocampal neurons.

2.6.3.3. Imaging and Morphometric Measures

The morphometric analysis and Sholl analysis of the hippocampal principal neurons was carried out using Neurolucida/Neuroexplorer softwares (MBF Inc., Williston, VT), the gold standards for neuron tracing and neuron analysis.

The stained cells from both left and right hippocampus were first traced with Neurolucida software under a light microscope at 100X magnification and then analyzed with Neuroexplorer software. The same criteria were used for the selection of the pyramidal neurons in CA1 and CA3 hippocampal regions and granular neurons in DG region of hippocampus (Ruan *et al.,* 2006). According to these criteria:

➢ The neurons should be densely stained so all the processes could be followed to the end at high magnification. The clear image of dendritic spines on these processes is the indication of good staining

➢ No abrupt truncation of dendritic branches should be present

➢ Only one neuron should be located within the viewing area to avoid possible mismatches of dendrites from other neurons.

In this study, there were at least 7 subjects in each treatment/age group (total 12 groups). From each hippocampal region (CA1, CA3, and DG) of each animal generally 5-8 neurons meeting the above stated staining criteria were selected (total 1574 neuron) (Fig. 2.15). Only neurons from the both left and right dorsal hippocampus (the region known to be more critical than the ventral hippocampus for spatial learning and memory) were used in evaluation of morphological parameters.
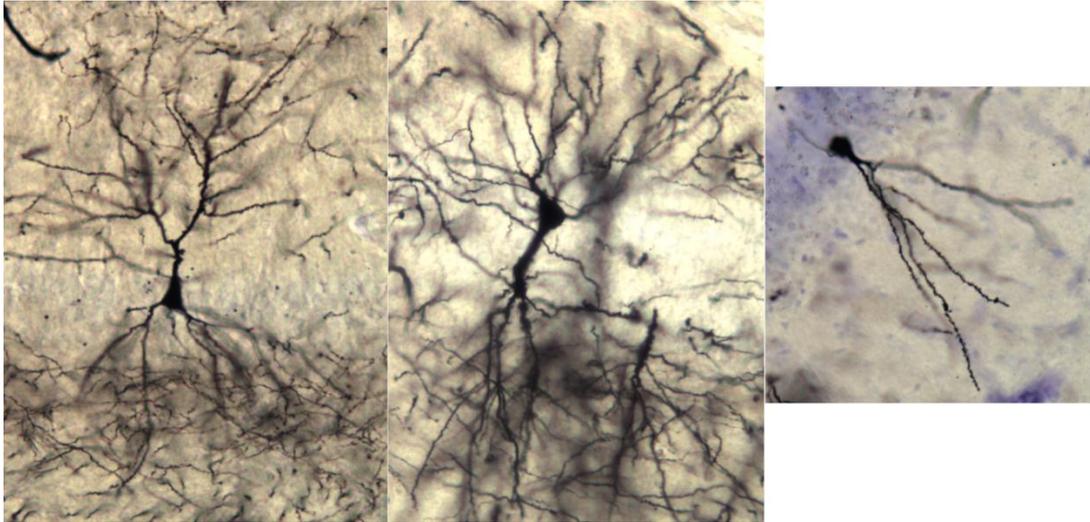
Figure 2.15. A representative picture golgi-stained CA1, CA3 and DG neurons, respectively

Eleven standard parameters were measured and analyzed as described in earlier studies (Coombs *et al.,* 2006; Ishizuka *et al.,* 1995; Dursun *et al.,* 2011; Altemus *et al.,* 2005). All diagrams adopted with permission from Ilknur Dursun (2012). The measured parameters were;

1. **Soma size:** A topographic series of contour lines were drawn around each soma to outline the shape in three-dimensions with the largest contour used to calculate the area (Fig. 2.16)
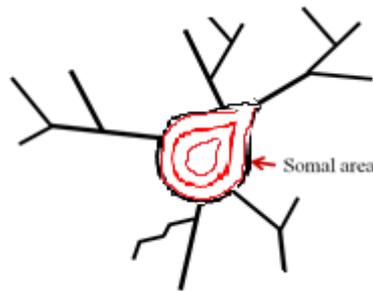
Figure 2.16. Schematric diagram of somal area

2. **Dendritic field area:** A line was drawn connecting the outermost tips of the dendrites around the edge of the arbor with dendritic field area defined as the area within this contour (Fig. 2.17).
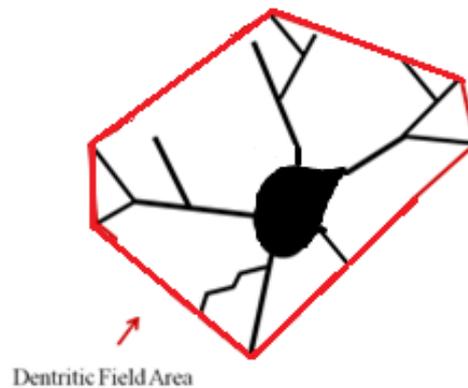
Figure 2.17. Schematric diagram of dendritic field area

3. **Total dendrite length:** The sum of the lengths of all the dendrites (a+b+c+d+e+…) (Fig. 2.18).
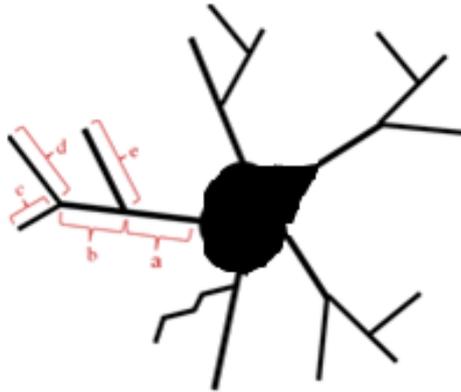
Figure 2.18. Schematric diagram of total dendrite length

4. **Number of dendritic branches:** All branches of all dendrites per cell (1, 2, 3, 4, 5, 6, 7,…) (Fig. 2.19).
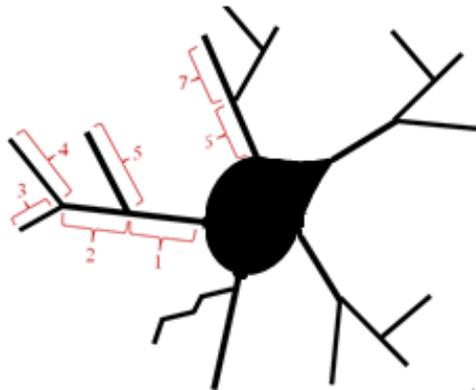
Figure 2.19. Schematric diagram of total dendrite length

5. **Branch order:** The highest number of times a dendrite branches, with the primary branch emerging from the soma defined as branch order 1 (Fig. 2.20).
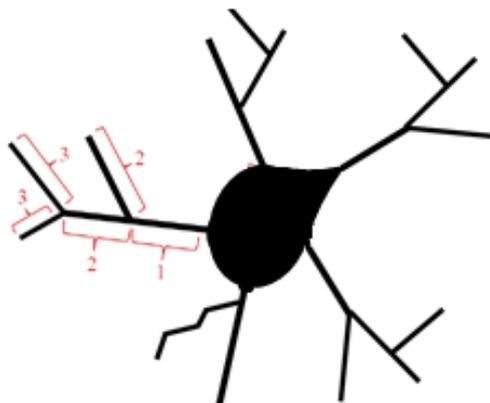
Figure 2.20. Schematric diagram of branch order

6. **Branch angle**: The angle (in three-dimensions) formed by two lines that each pass through the same branch point (Fig. 2.21).
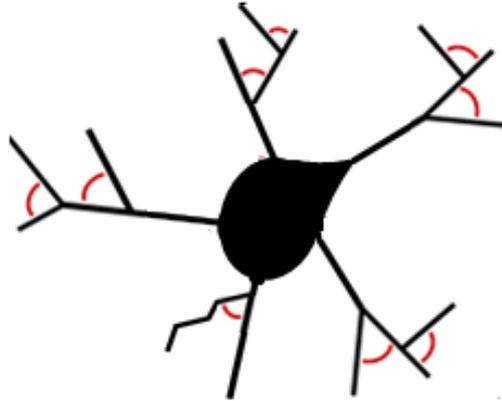
Figure 2.21. Schematric diagram of branch angle

7. **Mean internal branch length:** Average distance along the dendrite between the soma and the first branch point and between branch points (Fig. 2.22).
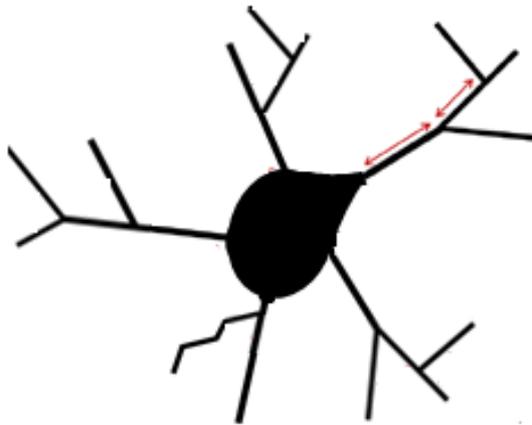
Figure 2.22. Schematric diagram of mean internal branch length

8. **Number of dendrites:** Number of primary dendrites emerging from the soma (Fig. 2.23).
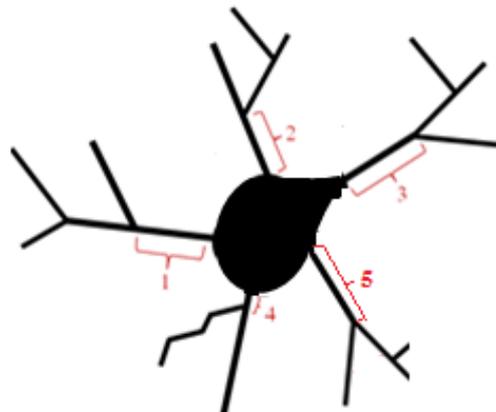
Figure 2.23. Schematric diagram of number of dendrites

9. **Spine density:** The total number of spines divided by the total dendrite length. Spines were defined as terminal dendritic projections less than 5 μm long (Fig. 2.24).
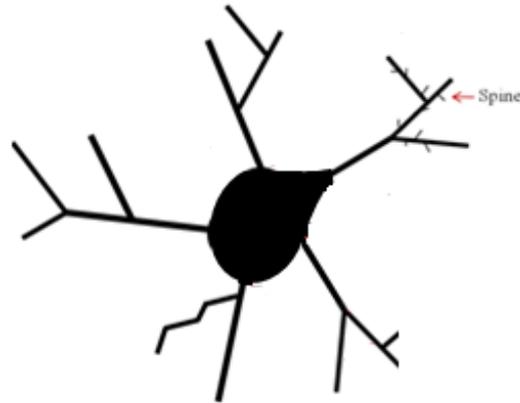
Figure 2.24. Schematric diagram of spine density

10. **Dendrite diameter:** The mean diameter of the three branch orders closest to the soma(Fig. 2.25).
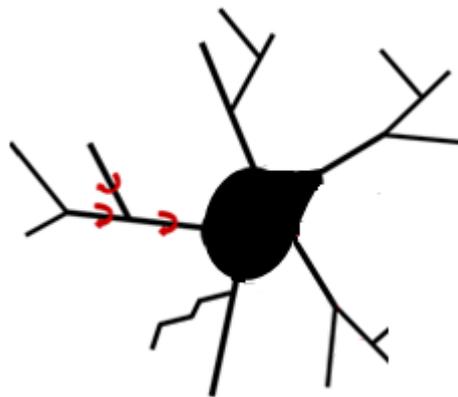
Figure 2.25. Schematric diagram of dendrite diameter

11. **Tortuosity:** The ratio (a/b) of the length along each dendritic branch (a) and the length of the straight line drawn between the two nodes (b) that define the branch(Fig. 2.26).
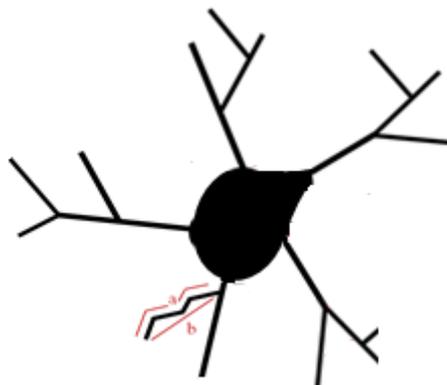
Figure 2.26. Schematric diagram of tortuosity

2.6.4. Immunohistochemical Studies

2.6.4.1. Tissue Preparation for Immunofluorescence

Another group of pups belonging to A, IC, and C groups were sacrificed at P1 (n=22), P10 (n=19), P30 (n=23), and P60 (n=22) to be used in immunohistochemical studies. Animals, under deep anesthesia, wereintracardially perfused with saline and then 4% paraformaldehyde. The fixed and cryoprotected brains were cut coronally on aShandon Cryotome at 20-μm. The dorsal part of each hippocampus were investigated by taking 3 or 4 section (sampling was 1/24) for each antibodies.

First of all, tissue sections were mounted on polylysine-coated glass microscope slides. Then, the sections were dried at 37^0C in an incubator for 20-25 min. After rinsing with 0.1 M phosphate buffered saline (PBS) once, the antigen retrieval was performed by citrate buffer to uncover epitopes. Sections were kept inside the boiling citrate buffer for 15 min. then they cooled down inside citrate buffer for 15 min. After rinsing in PBS (3 times, 5 min. for each time), the sections were incubated for 1 h at room temperature with blocking solution containing 5% normal goat serum (NGS) with 0.3% Triton-X-100 in PBS. Afterwards, at 4^0C, the sections were incubated for 48 h with primary antibodies against synaptophysin (SYP) (cell signaling #4329, 1:100) and postsynaptic density 95 protein (PSD95) (cell signaling #2507, 1:100), and for 24 h with primary antibodies against for doublecortin (DCX) (cell signaling #4604, 1:200). The antibody dilution buffer contained 1% BSA dissolved in 0.3% Triton-X-100 in PBS for SYP and PSD95, and 2% NGS dissolved in 0.3% Triton-X-100 in PBS for DCX. When the primary antibody incubation completed, after being rinsed in 0.1M PBS (3 times for 5 min. each time), sections were incubated for 2 h at room temperature in a dark place with fluorescent-conjugated secondary antibody, Alexa Fluor 488, goat anti-rabbit IgG (1:100 for SYP and PSD95 and 1:250 for DCX) diluted with 1% BSA dissolved in 0.3% Triton-X-100 in PBS for SYP and PSD95, and 2% NGS dissolved in 0.3% Triton-X-100 in PBS for DCX. The secondary antibody incubation was followed by washing the sections with PBS (3 times for 5 min. each time) and counterstaining the cell nucleus by DAPI (Kılıç *et al.,* 2010). After washing the slides with PBS, slides were coverslipped by fluoromount, a water soluble mounting media. Negative control was provided for each staining by omitting the primary antibody in antibody dilution buffer.
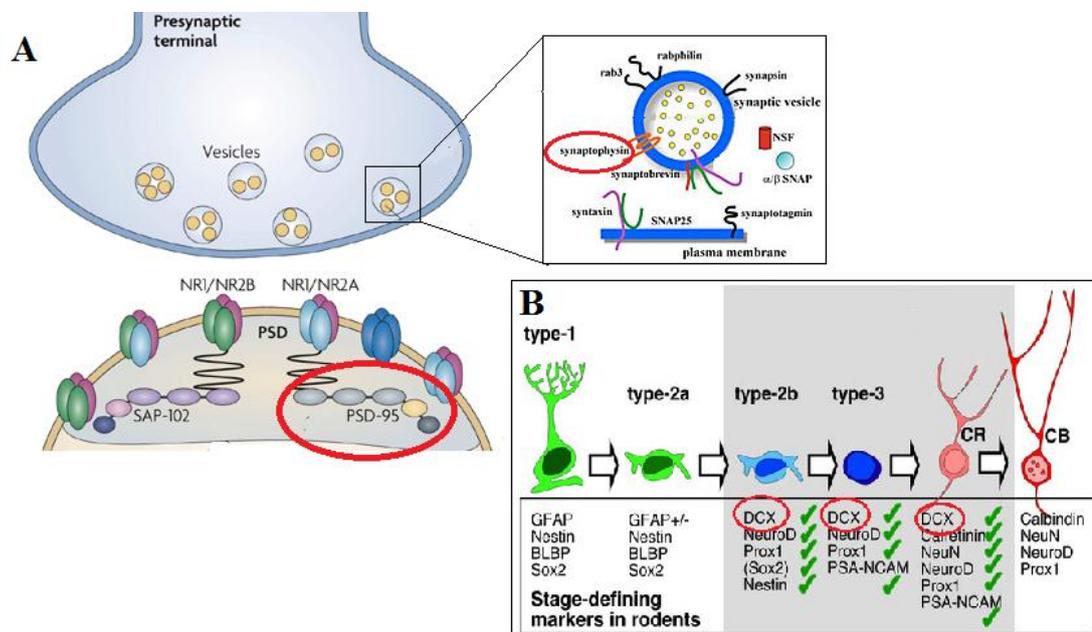
Figure 2.27. **A)** The schematic diagram showing presynaptic synaptophysin protein and postsynaptic PSD-95 protein in neuron **B)** DCX expressing stages during developmentcovered in this study

2.6.4.2. Visualization and Analysis of Immunolabelled Images

Coronal brain sections obtained from subjects were visualized using a Nikon Microscope equipped with a fluorescent attachment at 40X magnification. For each brain section, left and right hippocampi were visualized separately. Corpus callosum which contains no presynaptic or postsynaptic protein was used as a background. The pictures of each hippocampal region (CA1, CA3, DG, V) for each hemisphere (3-7 pictures/each hippocampal region, 3265 pictures for SYP, 3459 pictures for PSD95, 4051 pictures for DCX) were taken under fluorescence microscope at 40X magnification. The optical density measurements of SYP and PSD95 and the count of DCX-positive cells were done by using ImageJ software. Optical density measurements were done by converting the pictures in grayscale (0-255). For each image obtained, 5 representative areas (100 X 100 pixel each) were chosen for every cell layer to be studied (SO, SP, SR for CA1; SO, SP, SL for CA3; ML, GL, PL for DG) (Fig. 2.28) and averaged. To eliminate contribution of background fluorescence from obtained images, background fluorescence subtraction was applied for each image. To determine the number of DCX positive cells, the cell counter option of ImageJ software was used.
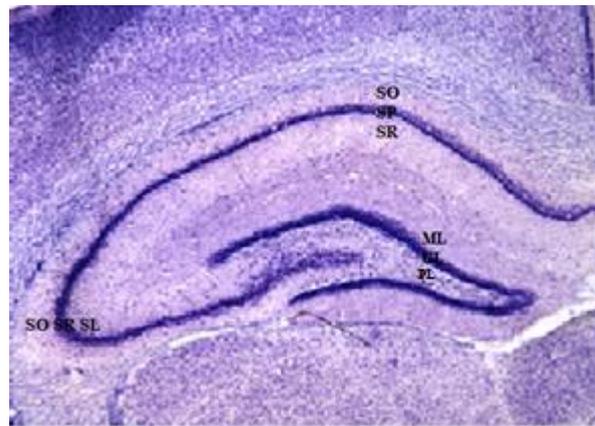
Figure 2.28. Photomicrograph showing SO (stratum oriens), SP (stratum pyramidale), SR (stratum radiatum) layers of CA1 region, SO (stratum oriens), SP (stratum pyramidale), SL (stratum lucidum) layers of CA3 region, ML (molecular layer), GL (granular layer), PL (polymorphic layer) of DG region.

2.6.4.3. Western Blotting Studies

In these studies, 8 pups intermixed between litters were used per single treatment/age group. Rats belonging to either A, IC, or C were sacrificed by decapitation at P1, P10, P30, and P60. The brains were rapidly removed and placed on ice-cold petri dish, hippocampi dissected by the help of isotonic sucrose solution and immediately frozen in liquid nitrogen and then stored at -80ºC until the biochemical assay were performed.

Left hippocampi of rats belonging to the same control or experimental group were pooled (Kılıç *et al.,* 2012), complemented with lysis buffer (RIPA buffer Sc2498) and homogenized by mortor and pestle in the presence of protease inhibitors. Tissue samples were incubated for 20 min. and then centrifuged at 14000 rpm for 20 min at 4°C, and then supernatant was removed and stored at -80°C until use.

2.6.4.4. Determination of Protein Concentration

Protein concentrations were determined by using Qubit assay kit and Qubit Fluorometer. First of all, the working solution was prepared by mixing 199 µL protein buffer (Quant-it) and 1 µL protein reagent (Quant-it) for every sample and mixed by vortex. For standards, 190 µL of working solution was aliquoted into three assay tubes special for Qubit. Then, 10 µL of each standard (standard #1- 0 ng/ µL, standard #2- 200 ng/ µL and standard #3- 400 ng/ µL) were added to the assay tube and mixed by vortex. After that, 1 µL sample of each group was mixed with 199 µL working solution and mixed by vortex. The final volume in each tube after adding sample should be 200 µL. All the tubes were incubated 15 min. at room temperature. Lastly, the protein concentrations were read in the Qubit® 2.0

Fluorometer, and the loaded amounts of sample and buffer for gel electrophoresis were determined. The fluorometer gives values for the Qubit protein assay in μg/mL which described as the formula;

$$\text{Concentration of sample} = \text{QF value.} \frac{(200)}{x}$$

where QF value = the value given by the Qubit® 2.0 Fluorometer

 x = the number of microliters of sample you added to the assay tube

2.6.4.5. Gel Electrophoresis

Sample proteins were separated by polyacrylamide gel electrophoresis. XCell SureLock™ Mini-Cell Electrophoresis System(Invitrogen) was used for gel preparation and electrophoresis. NuPAGE® Novex® 4-12% Bis-Tris Gels (1.0-mm thick, 15-well) the pre-cast polyacrylamide gels designed to give optimal separation of small- to medium-sized proteins under denaturing conditions were used in this study.

Table 1. The properties of gel used in this study

Gel Type	Formulation	Stacking Gel	Separating Gel	pH
NuPAGE® Novex® Bis-Tris Gels	Bis-Tris-HCl buffer (pH 6.4), Acrylamide, Bis-acrylamide, APS, Ultrapure water	4%	10%, 12%, 4–12%	7.0

After inserting the gels to the XCell SureLock™ chamber, put the 200 ml running buffer (1X NuPAGE MES SDS Running Buffer diluted by deionized water) was put to the chamber. Then 500 μL NuPAGE antioxidant was added to the chamber and with the help of a pipette, the wells of gel were gently washed with 1X running buffer including antioxidant without any air bubles. Finally, the gel running module was filled with a sufficient volume of electrode running buffer.

Protein samples were diluted with 4X NuPAGE LDS sample buffer and sterile distilled water and samples were heated in water bath at 70^0C for 10 min. Then, 10 μL of protein samples (20 μg) and 5 μL of commercially available protein molecular weight marker (invitrogen) were loaded to different wells (Fig. 2.29).
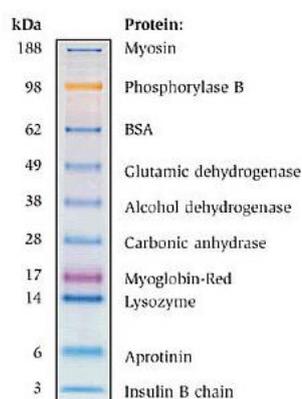
Figure 2.29. Protein molecular weight marker

After application of the samples, gel running module was placed to main buffer tank containing sufficient amount of electrode running buffer. The electrophoresis unit was connected to the power supply to run electrophoresis at 200 V for 35 min.
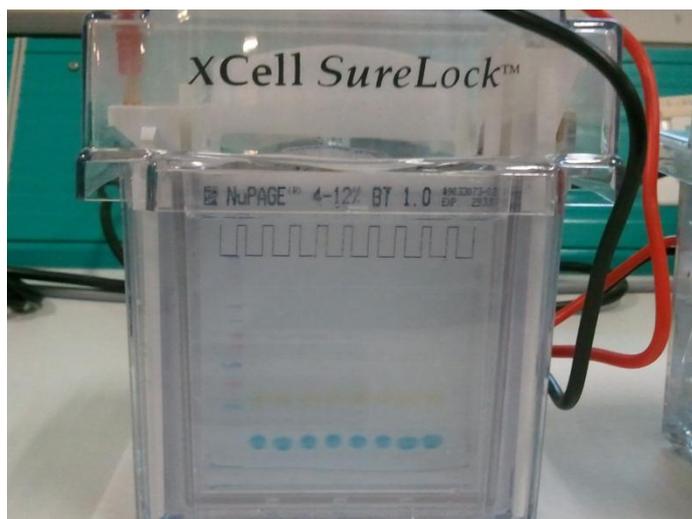
Figure 2.30. A representative picture for gel electrophoresis

2.6.3.6. Western Blotting

After electrophoresis was completed, gels were removed from set-up by the help of knife to separate the plates around the gel for western blotting. The iBlot® Gel Transfer Device was used to transfer the proteins from gel to membrane. The system consisted of disposable blotting stacks that contain the buffers and the transfer membrane (nitrocellulose or PVDF). After placing gel and membrane to the device without any air bubbles which were removed with the help of a rolling device, blotting was performed by starting the device for 7 min. At the end of this process, the membrane carrying the transferred protein on it, i.e. "blot" was obtained and removed from the device. The gel stained by coomassie blue to check whether the transfer was successful or not. Then, membrane was transferred to a plastic dish with protein side facing upwards and washed with TBS-T (Tris Buffered Saline plus Tween 20: 20 mM Tris-HCL, pH 7.4, 0.5 M NaCl and 0.05 % Tween 20) for 10 min. on a shaker. This washing step removes the salts and buffers from transfer medium. Then, the blot was incubated with blocking solution (2% ECL advance Blocking Reagentin TBS-T) for 1 h at room temperature so that empty spaces between transferred proteins were filled. This filling inhibits the non-specific binding of antibodies to the membrane. After that, the blot was incubated with primary antibody (SYP and PSD95, cell signaling, 1:1000) at 4^0C for overnight on a shaker. On the following day, the blot was washed 3 times with TBS-T for 10 min each time. The washing steps were necessary for removal of excess of antibody from the membrane. The blot was then incubated with secondary antibody (HRP-linked anti-rabbit amersham, 1:2500) for 1 h at room temperature. The blot was then washed 3 times with TBS-T for 10 min each time to remove excess antibody. The complete removal of TBS-T between each washing steps was extremely important since non-specifically bound regions can give reaction with substrate solution.

Blots were then incubated with substrate solution (RPN2135V1 Sol A (1000 µL) and Sol B (1000 µL) and 2000 µL distilled water for 1 min. Protein loading was controlled using a monoclonal mouse antibody against β-actin which was used as a control to normalize protein expression levels. The final images were photographed using a computer-based gel imaging instrument (DNR). Immunoreactive protein bands were then quantified by densitometric scanning method using an ImageJ software package program developed by NIH.

2.7. Statistical Analyses

Group means ± SEM were calculated from all measures. The dams, pups, and behavioral data were analyzed by two-way ANOVA with treatment (A, IC, C) as independent factor, and experimental sessions as repeated measures. The dams' data were analyzed by two-way ANOVA with treatment (A, IC, C) as independent factor, and days as a repeated measure. Pups' weights were analyzed for each postnatal age separately by one-way ANOVA with treatment as independent variable. The analyses of morphological data performed for each hippocampal subregion independently included cross-sectional

comparisons of treatment effects at different ages and longitudinal comparisons of age effect in different treatment groups. In the current study, the group sizes were similar with number of subjects per group varying between 6 and 8. The morphological data showed normal distribution as assessed by Kolmogorov-Smirnov normality test. Under these conditions two-way ANOVA (treatment x age) was used to evaluate the main effects of age and treatment as well as age x treatment interaction. Additionally, the between-group differences in the estimates of volumes and cell counts for each hippocampal region and postnatal age, and between different ages for the same hippocampal region in each treatment group separately were analyzed by one-way ANOVA using treatment or pups' age as an independent factor. The post-hoc comparisons of simple effects were conducted using Fisher's Least Significant Difference (LSD) test. The SPSS 15 statistical package was used for statistical analysis of the data. The criterion of statistical significance was p≤0.05.

CHAPTER 3

RESULTS

3.1. Subjects

Table 2. Animals used in experiments

Groups	No. of mated dams	No. of dams giving birth	Rate of succesful pregnancy (%)	Total no. of Used dams	Total no. of Pups	Total no. of female pups	Total no. of male pups	No. of surviving male pups	Surviving rate of male pups (%)
A	190	60	**31.58**	38	373	191	160	121	**75.63**
IC	95	43	**45.26**	30	325	178	147	115	**78.23**
C	50	35	**70.00**	33	246	118	120	119	**99.17**
Total	335	138		101	944	487	427	355	83.14

As seen from the Table 2, in C group as compared to A group, there was a higher proportion of incidents of successful pregnancies indicating towards higher rate of abortion in dams administered ethanol and/or subjected to the intubation-related stress during pregnancy. The survival rate of pups was also lower in IC and A groups as compared to the intact control.
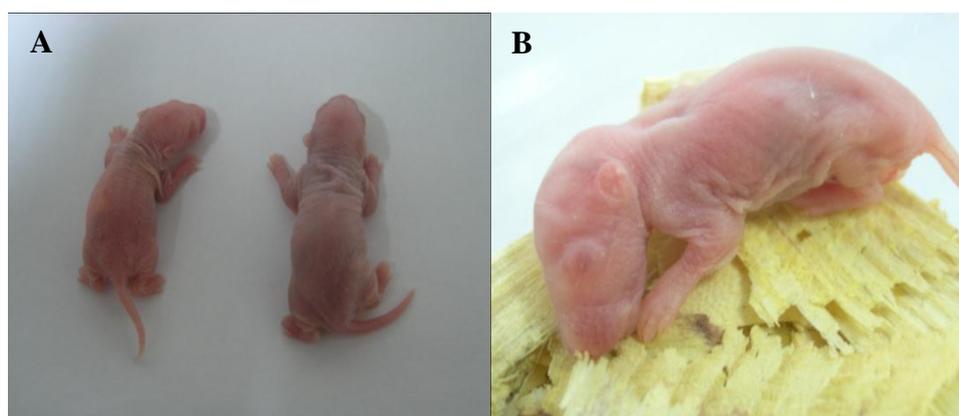
Figure 3.1. A. New-born pups from the control (C) group (right) and the fetal alcohol (A) group (left). **B.** The head anomaly in one of the fetal alcohol pups.

As demonstrated in Fig. 3.1, the body size of some fetal alcohol pups at birth was much smaller than that of control pups. Some of the fetal alcohol pups also showed typical for FAS head and oral abnormalities.

3.1.1. Body Weights of Dams and Pups

In Fig. 3.2, in both control and alcohol-treated groups, an increase in body weight of pregnant rats was observed. The relative increase in the body weight between the GD7 and GD20, in alcohol, intubation control, and control groups were, 13%, 13% and 17% respectively. The repeated measure ANOVA yielded the day effect ($F_{(20:1960)}$=119.250, $p\leq0.001$) and the day x group interaction ($F_{(40:1960)}$=3.100, $p\leq0.001$) highly significant. By the start of intragastric intubation, a small decrease was observed in the body weights of intubated groups but not in control group. In addition, the main group effect was insignificant ($F_{(2:98)}$=2.106, p=0.127).
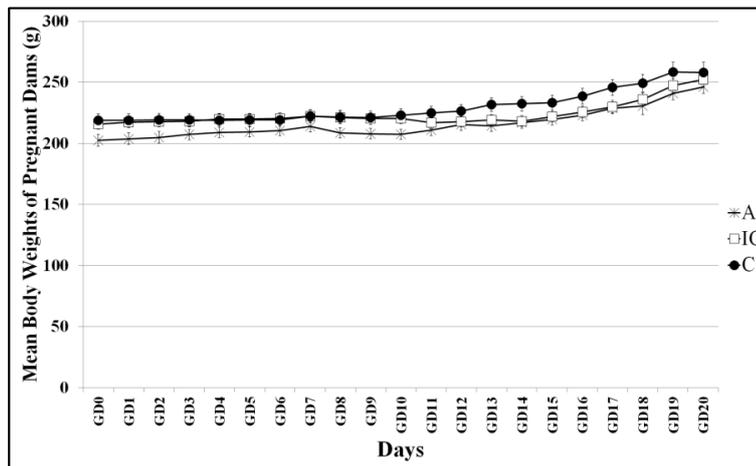
Figure 3.2. The mean body weight gain in alcohol and control groups of pregnant dams throughout gestation days 0-20 (the data pooled from all experiments).

The pups' weights were also analyzed by two-way ANOVA with age and treatment as independent variables and revealed the age effect ($F_{(3:633)}$=3724.050, $p\leq0.001$) and treatment effect ($F_{(2:633)}$=7.144, p=0.001) highly significant. The age x group interaction was insignificant. Afterwards, one-way ANOVA with treatment as independent variable following post hoc LSD test was applied to each postnatal age independently. The pups' body weight at birth and at P10 was significantly lower in A group as compared to the control groups ($F_{(2:228)}$=103.933, $p\leq0.001$; $F_{(2:195)}$=17.165, $p\leq0.001$ respectively). This difference disappeared at P30 and at P60 ($F_{(2:120)}$=2.388, p=0.096; $F_{(2:90)}$=1.083, p=0.343, respectively) (Fig. 3.3).
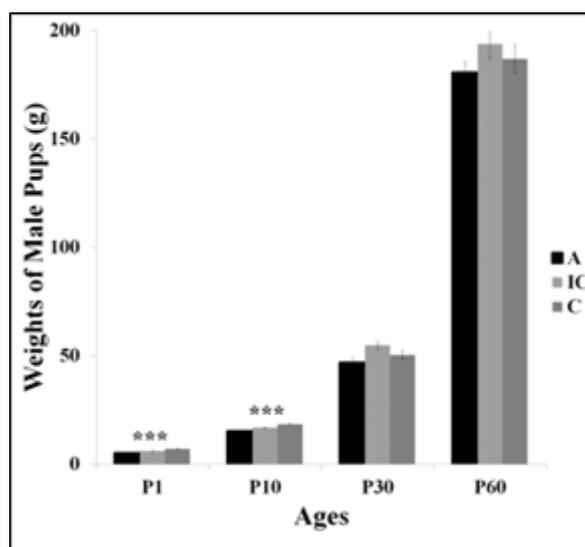
Figure 3.3. Changes in the mean body weight ($\pm$SEM) of control (IC and C) and fetal alcohol (A) rat groups at different postnatal ages. Error bars denote SEM. Asterisks denotes p<0.001***.

3.1.2. Blood Alcohol Concentration (BAC)

At the GD20, the mean BAC in pregnant rats from A group estimated 3 h after the second intubation on the GD20, was found as 246.6 ± 40.9 mg/dl.

3.2. Behavioral Experiments

Behavioral experiments were performed on female pups from A and IC groups at P30 and P75.

3.2.1. Open Field Test

The open field test was carried out in two arenas of different size, the small and the large one, on the two consecutive days, for 20 min each day. According to the Latin square paradigm, on the first day the half of the pups from each group was tested in the small arena and the other half was tested in the large arena. On the following day, the arenas were changed.
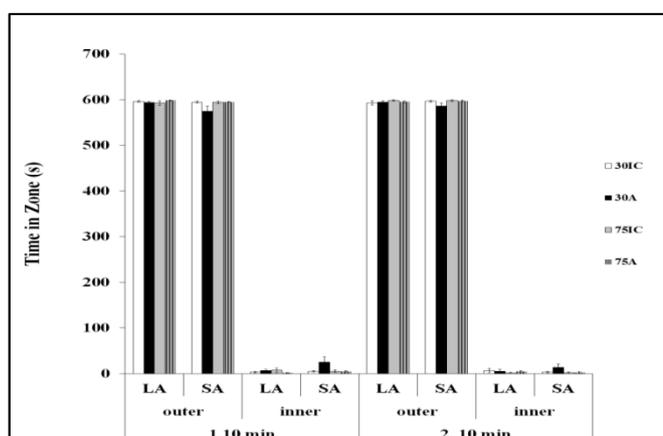
Figure 3.4. The mean time ($\pm$ SEM) spent in the different zones of the large (LA) and the small (SA) arena, during the two consecutive 10 min time intervals, in juvenile and adult control and fetal-alcohol rats. Error bars denote SEM.

As it can be seen from the Fig. 3.4, independently of the arena's size, in both treatment and age groups, the rats spent significantly more time in the outer zone, close to the arena's walls (tigmotaxy) ($F_{(1:48)} = 3352.6$, p=0.0001, and $F_{(1:40)}$=2996.5 p=0.0001, for juvenile and adult rats respectively). These result confirmed the lack of a significant difference in the anxiety level between the treatment groups.
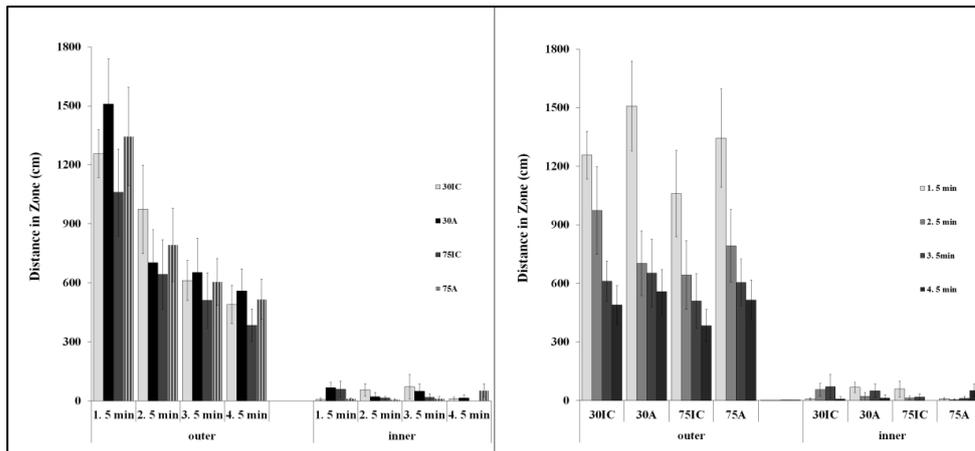
Figure 3.5. The mean distance (± SEM) moved in the outer and the inner zone of the open field, respectively, during the consecutive 5-min intervals of the total 20-min. testing period for juvenile (P30) and adult (P75) control (IC) and fetal-alcohol (A) rats. B. Error bars denote SEM.

The Fig. 3.5. shows the mean distance moved in two zones of the large open arena, by each of the treatment group, during the consecutive 5 min. intervals of the total 20 min. testing period. The distance moved is an index of animals' locomotor activity. Two-way ANOVA (age x treatment) done for each of the consecutive 5 min. intervals and each zone of the large arena independently, did not reveale significant between-group differences in the animals' locomotor activity. Two-way repeated measures ANOVA for groups and the four 5-min. intervals in the OF yielded significant effect of interval ($F_{(3:66)}=10.829$, $p=0.001$).

3.2.2 Elevated Plus Maze Test
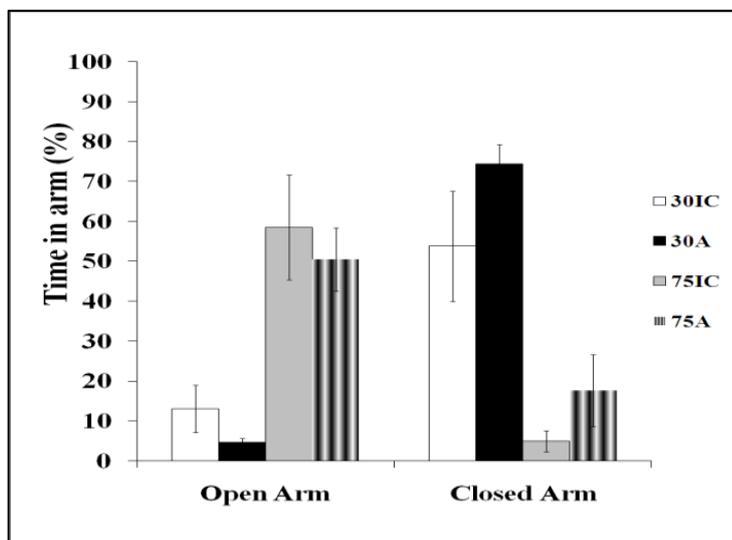
Figure 3.6. Comparison of the animal's behavior in the elevated plus maze test as a function of age (P30 vs P75) and treatment (A vs IC). The bars represent mean time percent spent in open and closed arms of the plus maze. Error bars denote SEM.

Two-way ANOVA (treatment x arm of the plus maze) performed for each age group independently did not reveale a significant difference between the treatment groups in the arm preferences either at P30 or at P75. Interestingly, in both treatment groups, the opposite patterns of behavior were noted at two tested ages. As seen from the Fig. 3.6., juvenile rats from both groups showed significantly higher preference for the closed arms ($F_{(1:12)}=34.34$, $p=0.001$), while the adult animals spent significantly more time in the open arms ($F_{(1:10)}=15.5$, $p=0.003$).

3.2.3 Morris Water Maze Test

3.2.3.1. Allothetic (Allocentric) Paradigm
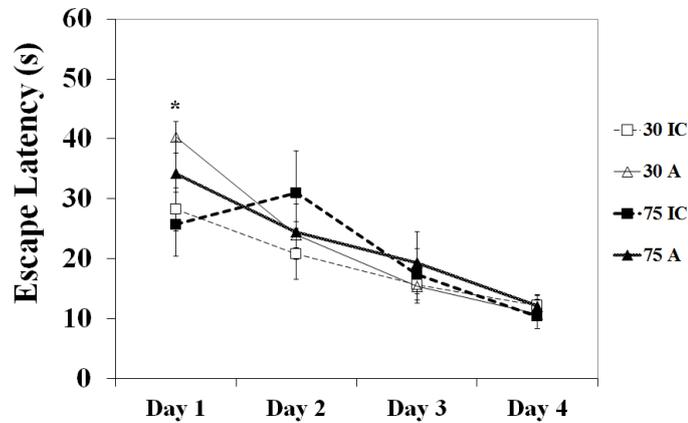
Figure 3.7. Mean escape latency (± SEM) calculated for the first four days of MWM training carried on under allothetic stimulus conditions in the intubation control and alcohol rat groups at P30 and P75. Error bars denote SEM. * indicates significant difference at $p \leq 0.05$.

In all groups, a decrease in the swim latency to reach the hidden platform was observed across the days of training (Fig. 3.7). There was no significant difference in the task acquisition between adult control and adult fetal-alcohol rats. Two-way repeated measure ANOVA with day and group as independent factors revealed the day effect significant ($F_{(3:66)}=23.448$ $p\leq0.001$), main group effect and the day x group interaction were insignificant. However, one-way ANOVA performed for each training day and each age group independently, confirmed significantly worse performance in juvenile fetal alcohol pups compared to their age-matched controls ($F_{(1:12)} =7,352$ $p=0.019$).
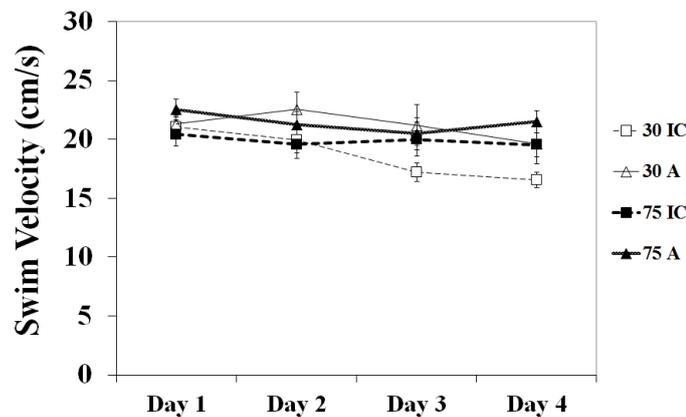
Figure 3.8. Mean swim velocity (± SEM) calculated for the first four days of MWM training carried on under allothetic stimulus conditions in the intubation control and alcohol rat groups at P30 and P75. Error bars denote SEM.
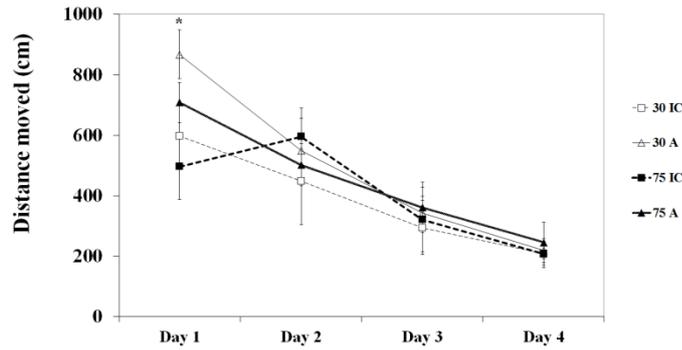
Figure 3.9. Mean swim distance (± SEM) calculated for the first four days of MWM training carried on under allothetic stimulus conditions in the intubation control and alcohol rat groups at P30 and P75. Error bars denote SEM. * indicates significant difference at p ≤ 0.05.

There was no significant between-group difference in the swim velocity on the first day of training (Fig. 3.8). Therefore, the significant difference in the escape latency between 30A and 30IC groups noted on the 1st day of training was paralleled by a significant (p≤0.05) difference in the distance moved to the hidden platform (Fig. 3.9).
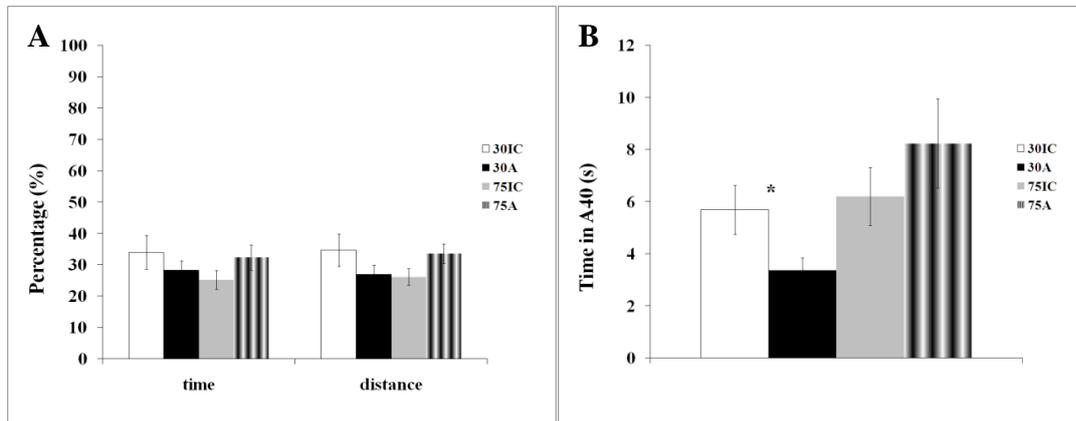
Figure 3.10. A. Mean percent time spent and the distance swam in the platform quadrant, and **B.** mean time spent in the annulus 40 (±SEM) on the 60-sec probe trial in control (IC) and alcohol (A) groups at the age P30 and P75. Error bars denote SEM. * indicates significant difference at p≤0.05

The probe trial was done to assess the place preference for the platform quadrant and thus, to measure the habit strength. For all three measures (percent time spent in the platform quadrant, percentage of distance swam in the platform quadrant, and time in the annulus 40), the fetal-alcohol juvenile rats showed worse performance as compared to the age-matched intubation control pups (Fig. 3.10). However, the only the difference in the time spent in Annulus 40 was yielded significant ($F_{(3:22)}=3.528$, p=0.049). No significant difference in the probe trial performance was found between adult control and fetal-alcohol rats.

3.2.3.2. Idiothetic (Egocentric)Paradigm

In this paradigm, when the animal can only use the egocentric cues, finding the hidden platform is apparently more difficult. Therefore, under this training condition, reaching the performance level with escape latency equal to or less than 10 s took 6 instead of 4 days as it is in the classical MWM (Fig. 3.11).

48
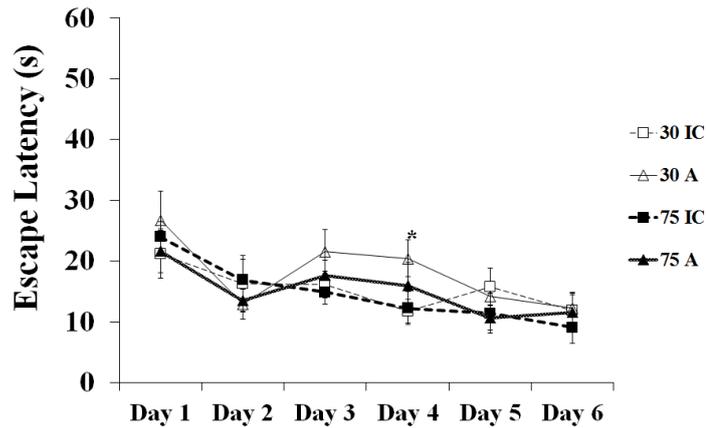
Figure 3.11. Mean escape latency (±SEM) calculated for six consecutive days of MWM training carried on under idiothetic stimulus conditions in intubation control and fetal-alcohol rat groups at P30 and P75. Error bars denote SEM. * indicates significant difference at $p \leq 0.05$.

Under these more difficult test conditions, the difference in the task performance between fetal-alcohol and intubation control juvenile rats was more pronounced. Two-way repeated measure ANOVA with day and group as independent factors revealed the day effect significant ($F_{(5:110)}=9.699$ $p \leq 0.001$), main group effect and the day x group interaction were insignificant.

In the juvenile group, one-way ANOVA showed that the treatment factor was significant for the distance swam to reach the escape platform ($F_{(1:12)}=7.4$, $p=0.019$) (Fig. 3.12). Among adult animals, fetal-alcohol rats showed worse performance only on the third day of training.
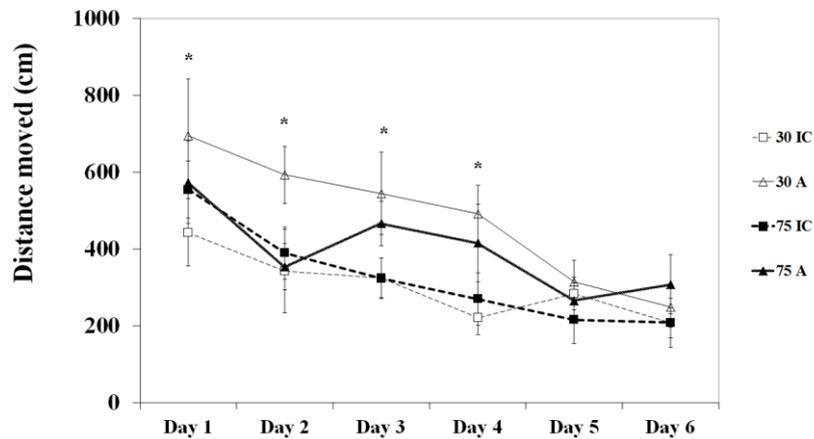
Figure 3.12. Mean swim distance (±SEM) calculated for six consecutive days of MWM training carried on under idiothetic stimulus conditions in control and fetal-alcohol rat groups at P30 and P75. Error bars denote SEM. * indicates significant difference at $p \leq 0.05$.

As seen in Fig. 3.13 this time swim velocity of juvenile fetal alcohol rats was generally faster than that of age-matched controls. Two-way repeated measure ANOVA with day and group as independent factors revealed the day effect significant ($F_{(5:60)}=4.64$, $p=0.001$), main group effect and the day x group interaction were insignificant.
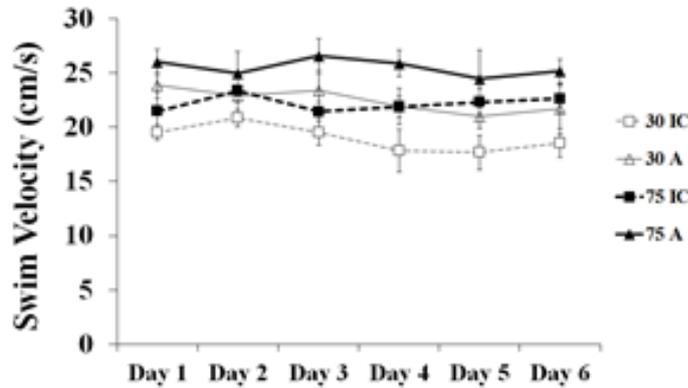
Figure 3.13. Mean swim velocity (±SEM) calculated for six consecutive days of MWM training carried on under idiothetic stimulus conditions in intubation control and fetal-alcohol rat groups at P30 and P75. Error bars denote SEM. * indicates significant difference at p≤0.05.

On the probe trial (Fig. 3.14), in both age groups, generally the fetal-alcohol rats showed worse performance as compared to controls. However, only the difference in the swim distance in the platform quadrant between the juvenile fetal-alcohol pups and their age-matched controls was yielded significant ($F_{(1:12)}$=7.580, p=0.017).
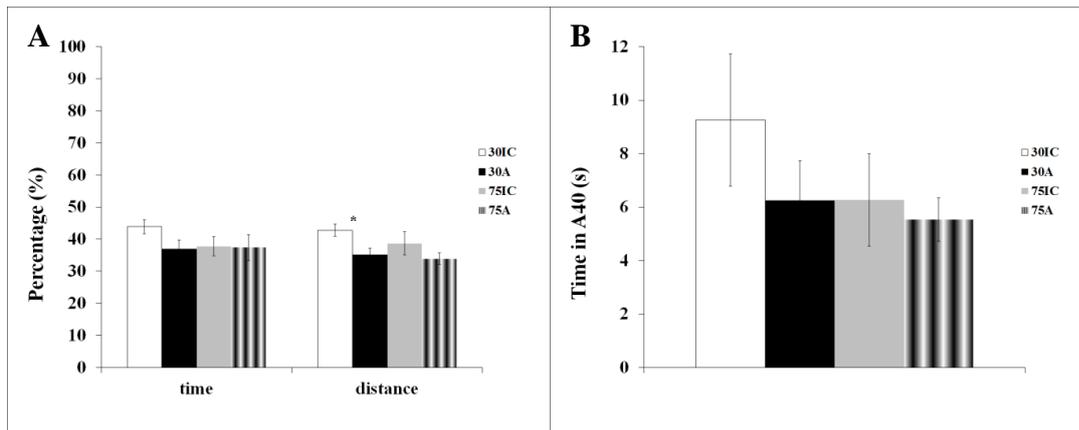
Figure 3.14. A. Mean percent time spent and the distance swam in the platform quadrant, and **B**. mean time spent in the annulus 40 (±SEM) on the 60-s probe trial in intubation control (IC) and alcohol (A) groups at the age P30 and P75. Error bars denote SEM. * indicates significant difference at p≤0.05.

3.2.3.3. Delayed Non-Matching-To-Position (DNMTP) Working Memory Test

This test was applied to the young adult rats only. As it can be seen from the Fig. 3.16, there was no significant difference between fetal-alcohol and control rats, either in the rule learning with the short 2 min. delay or when the delay between sample and test swim was prolonged to 15 min.
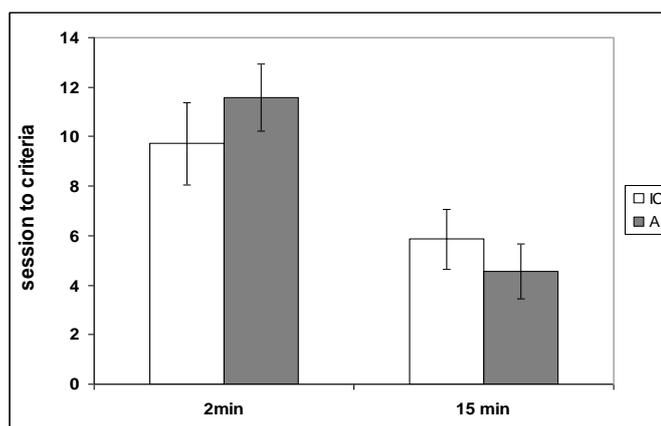
Figure 3.15. Mean number of sessions (±SEM) to reach the performance criterion in Delayed Non-Matching-To-Position test with 2 and 15 min. delay between sample and test swim in control and fetal-alcohol groups at P75.

3.3. Morphological Experiments

3.3.1. Unbiased Stereology and Estimates of Hippocampal Neuron Counts

Estimates of the numbers of the principal hippocampal neurons were done using StereoInvestigator (MBF Inc.), the most-cited stereology software. Using unbiased stereological methods, neuron counts were performed separately for the granular layer of DG and the pyramidal layer of hippocampal CA1 and CA2+3 subregions in fetal-alcohol and control rats throughout the postnatal developmental period at P1, P10, P30, and P60. Total numbers of neurons for each hippocampal region, each treatment group, and each postnatal age independently, are presented in the Figures 3.16 and 3.17 and in the Table 3. For all estimates, CEs were between 0.02-0.04. Table 3 presents also the coefficient of variance (CV) indicating inter-individual variation for each group. The observed between-subject variation in the total number of granular and pyramidal cells was generally similar in the fetal alcohol and control groups.
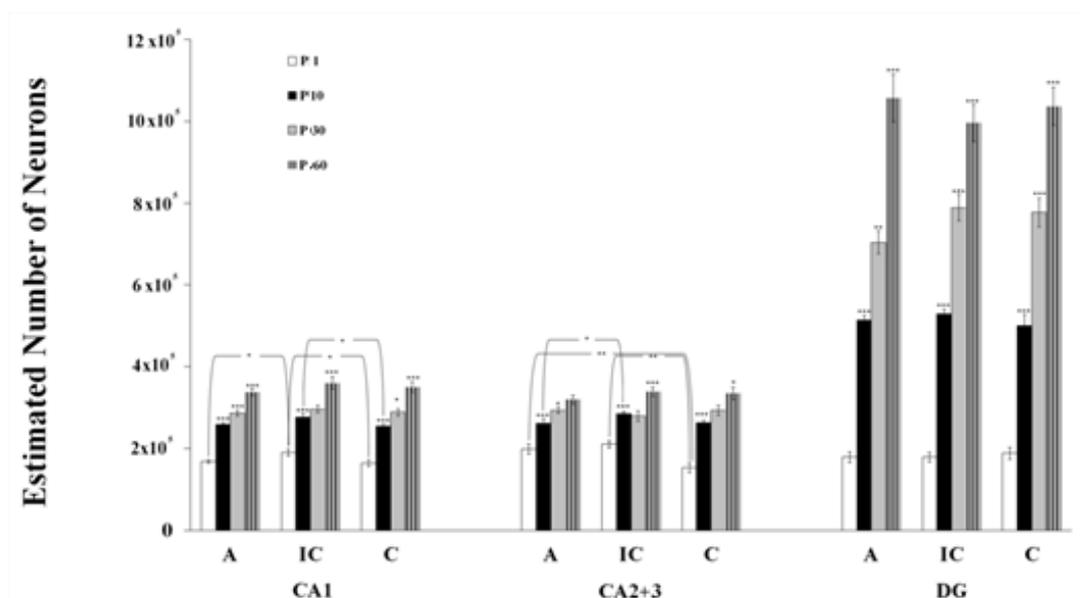
Figure 3.16. Comparison of mean total neuron numbers (±SEM) within hippocampal CA1, CA2+3, and DG regionsin fetal alcohol (A) and control (IC and C) rat pups at different postnatal ages: P1, P10, P30, and P60, respectively. Error bars denote SEM. Asterisks indicate significant difference between the two consecutive age groups (P1 versus P10, P10 versus P30, and P30 versus P60): *p ≤ 0.05, ** p ≤ 0.01, *** p ≤ 0.001.

As seen from the Figures 3.16, 3.17 and the Table 3, on P1, no significant difference in cell numbers was noted between the three hippocampal regions. During the following two months, in all treatment groups and in all three hippocampal subregions, a significant increase in the number of principal neurons was observed (in A group: $F_{(3:26)}= 94.115$, $p \leq 0.001$, $F_{(3:26)}= 23.768$, $p \leq 0.001$, and $F_{(3:26)}= 98.636$, $p \leq 0.001$; in IC group: $F_{(3:24)}= 36.261$, $p \leq 0.001$, $F_{(3:24)}= 26.613$, $p \leq 0.001$, and $F_{(3:24)}= 120.213$, $p \leq 0.001$; in C group: $F_{(3:26)}= 68.545$, $p \leq 0.001$, $F_{(3:26)}= 43.467$, $p \leq 0.001$, and $F_{(3:26)}= 117.079$, $p \leq 0.001$, for CA1, CA2+3, and DG, respectively).

Table 3. Mean volumes and total neuron number estimates (±SEM) for granular and pyramidal layers in DG and CA subregions of the hippocampus. CE represents coefficient of error. CV represents coefficient of variation.

		CA1				CA2+3				DG			
		Neuron number (10^5)	CE	CV	Volume (mm^3)	Neuron number (10^5)	CE	CV	Volume (mm^3)	Neuron number (10^5)	CE	CV	Volume (mm^3)
P1	A	1,7±0,04	0,03	0,06	0,5±0,02	2,0±0,12	0,03	0,15	0,6±0,04	1,8±0,13	0,04	0,18	0,3±0,02
	IC	1,9±0,08	0,03	0,09	0,5±0,02	2,1±0,09	0,03	0,11	0,6±0,03	1,8±0,12	0,04	0,16	0,3±0,02
	C	1,6±0,08	0,03	0,12	0,4±0,02	1,5±0,11	0,03	0,19	0,6±0,16	1,9±0,14	0,04	0,20	0,3±0,02
P10	A	2,6±0,05	0,03	0,05	1,1±0,04	2,6±0,10	0,03	0,11	1,5±0,07	5,1±0,11	0,03	0,06	0,9±0,03
	IC	2,8±0,09	0,03	0,09	1,1±0,04	2,8±0,05	0,03	0,05	1,6±0,07	5,3±0,12	0,03	0,06	1,0±0,03
	C	2,6±0,05	0,03	0,06	1,0±0,03	2,6±0,06	0,03	0,06	1,5±0,03	5,0±0,27	0,03	0,15	1,0±0,03
P30	A	2,9±0,07	0,03	0,07	1,2±0,05	2,9±0,07	0,03	0,07	1,9±0,07	7,0±0,28	0,03	0,11	1,4±0,06
	IC	3,0±0,09	0,02	0,08	1,3±0,06	2,8±0,13	0,03	0,12	1,8±0,04	7,9±0,32	0,03	0,11	1,4±0,04
	C	2,9±0,09	0,03	0,09	1,3±0,06	2,9±0,12	0,03	0,12	2,0±0,11	7,8±0,35	0,03	0,13	1,4±0,06
P60	A	3,4±0,09	0,03	0,08	1,5±0,04	3,2±0,11	0,03	0,10	2,3±0,11	10,6±0,59	0,02	0,16	1,7±0,07
	IC	3,6±0,15	0,03	0,12	1,5±0,07	3,4±0,11	0,03	0,09	2,3±0,10	10,0±0,45	0,03	0,13	1,7±0,06
	C	3,5±0,13	0,03	0,10	1,6±0,05	3,3±0,13	0,03	0,12	2,4±0,13	10,4±0,46	0,03	0,12	1,8±0,05

The greatest increase was recorded in DG wherein already on P10, the neuron number was almost twice of that in CA subregions. A further, relatively fast increase in neuron counts was recorded in DG region throught the whole remaining postnatal period between P10-P60. However, a significant increase in the cell count estimates was also noted in both CA subregions of the hippocampus (p≤0.05) (Table 4).
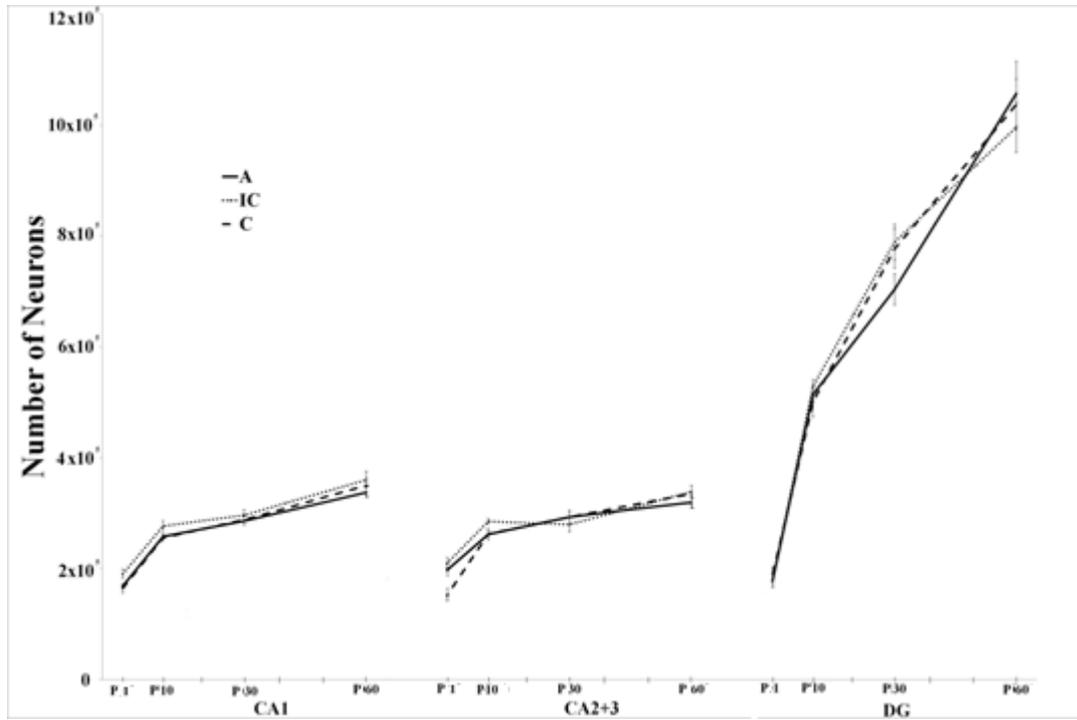
Figure 3.17. Illustration of the temporal pattern of an increase in neuron numbers in CA1, CA2+3, and DG hippocampal subregions throughout 2 postnatal months in fetal alcohol and control rat groups.

Table 4. Percent increase in the number of principal neurons within three postnatal time windows in CA and DG hippocampal subregions (the data collapsed across the treatment groups).

	P1-P10	P10-P30	P30-P60	Total
CA1	58%	12%	36%	106%
CA2+3	42%	10%	22%	74%
DG	283%	139%	150%	572%

Two-way (age x treatment) ANOVA performed for cell counts within CA1 region yielded a significant main effect of both age ($F_{(3:76)}$=171.243, p≤0.001) and treatment ($F_{(2:76)}$=3.446, p=0.037). The treatment x age interaction was statistically insignificant. One-way ANOVA applied to these data yielded a significant group effect on P1 ($F_{(2:14)}$=3.837, p=0.047). On P10, the main group effect approached ($F_{(2:20)}$=2.964, p=0.075) but did not reached the arbitrary significance level of p≤0.05. Post hoc analyses revealed asignificantly higher number of neurons in group IC compared to group C on both P1 and P10 (p=0.020 and p=0.035, respectively). In addition, on P1, the total number of neurons in group IC was significantly higher (p=0.046) than that in group A. On P10, the number of neurons in group IC was also higher compared to group A, but this difference did not reach the required level of significance remaining at p=0.064.

A similar data analysis carried out for the hippocampal CA2+3 region yielded significant main effect of age ($F_{(3:76)}$=89.818, p<0.001) and significant treatment x age interaction ($F_{(6:76)}$=2.665, p=0.021). However, the main effect of treatment remained only marginally significant ($F_{(2:76)}$=2.706, p=0.073). A subsequent analysis performed by one-way ANOVA revealed a significant main effect of treatment

on P1 ($F_{(2:16)}$=7.925, p=0.004) and a marginally significant treatment effect on P10 ($F_{(2:20)}$=2.798, p=0.085). Post-hoc comparisons confirmed significantly higher numbers of neurons on P1 in both A and IC groups compared to group C (p=0.009 and p=0.002, respectively) and a significantly higher number of neurons in group IC compared to both A and C groups on P10 (p=0.047 and p=0.05, respectively).

In contrast to CA1 and CA2+3 regions, two-way ANOVA performed for the DG region yielded a significant main effect of age ($F_{(3:76)}$=328.584, p<0.001) with the treatment effect and treatment x age interaction insignificant. One-way ANOVA and subsequent post-hoc comparisons of simple effects revealed the cell count to be marginally lower in the fetal alcohol group as compared to IC group (p=0.078). On P30, the total number of neurons in group A was also lower than that in group C, however, this difference also did not reach the accepted level of significance, remaining at p=0.114. The difference between IC and C groups was insignificant.
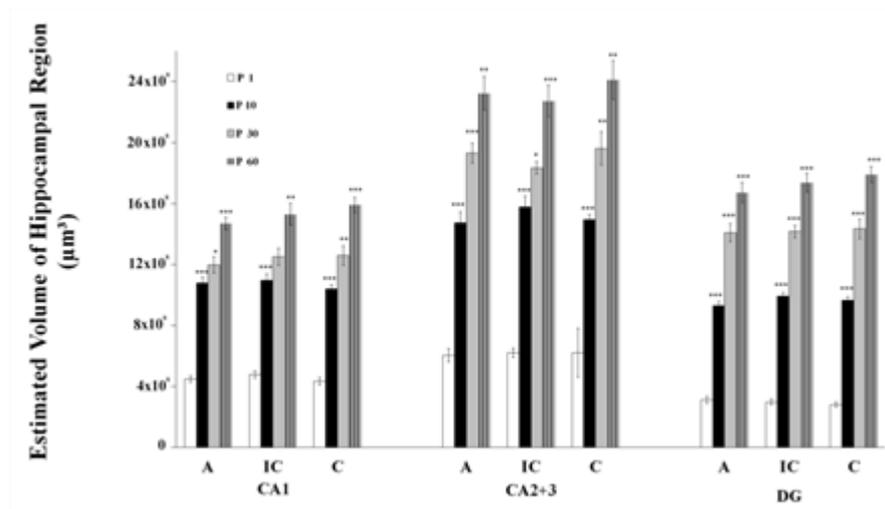
Figure 3.18. Comparison of mean volume (±SEM) of hippocampal CA1, CA2+3, and DG regions in fetal alcohol (A) and control (IC and C) rat pups at different postnatal ages: P1, P10, P30, and P60, respectively. Error bars denote SEM. Asterisks indicate significant difference between the two consecutive age groups (P1 versus P10, P10 versus P30, and P30 versus P60): *p ≤ 0.05, ** p ≤ 0.01, *** p ≤ 0.001

Fig. 3.18 and Table 3 present volume estimates for each hippocampal region, each treatment group, and each postnatal age independently. Two-way ANOVA performed for volume data from all three hippocampal regions yielded a significant main effect of age at p≤0.001. However, no significant between-group differences were found in any of the developmental time windows studied. The fastest volume increase was shown for the CA2+3 region and the slowest for the DG region which may contribute to the lowest cell density in CA2+3 and the highest cell density in the DG area.

3.3.2. Quantitative Morphometry of Hippocampal Pyramidal and Granular Cells
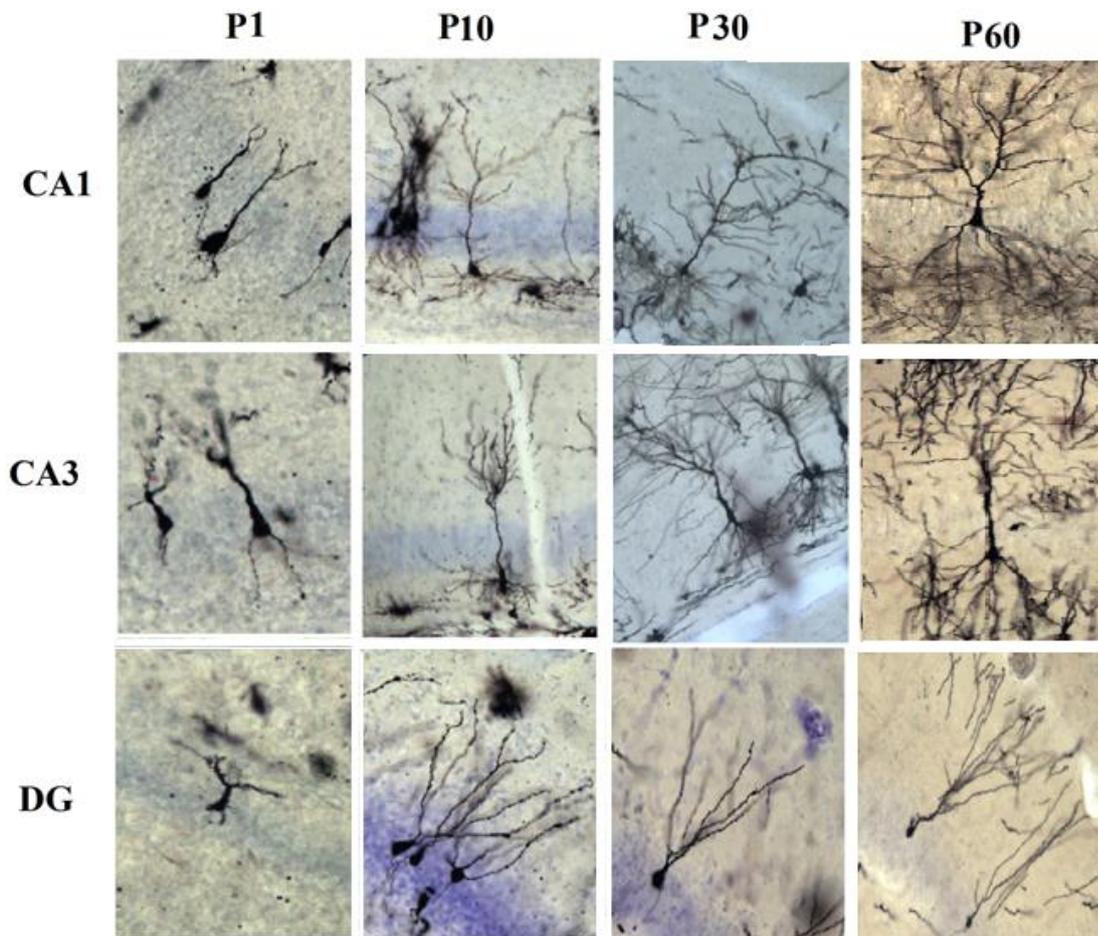
Figure 3.19. Representative photomicrographs showing Golgi-impregnated cellsfrom hippocampal CA1, CA3 and DG regions at P1, P10, P30, and P60 (Magnification 20X).
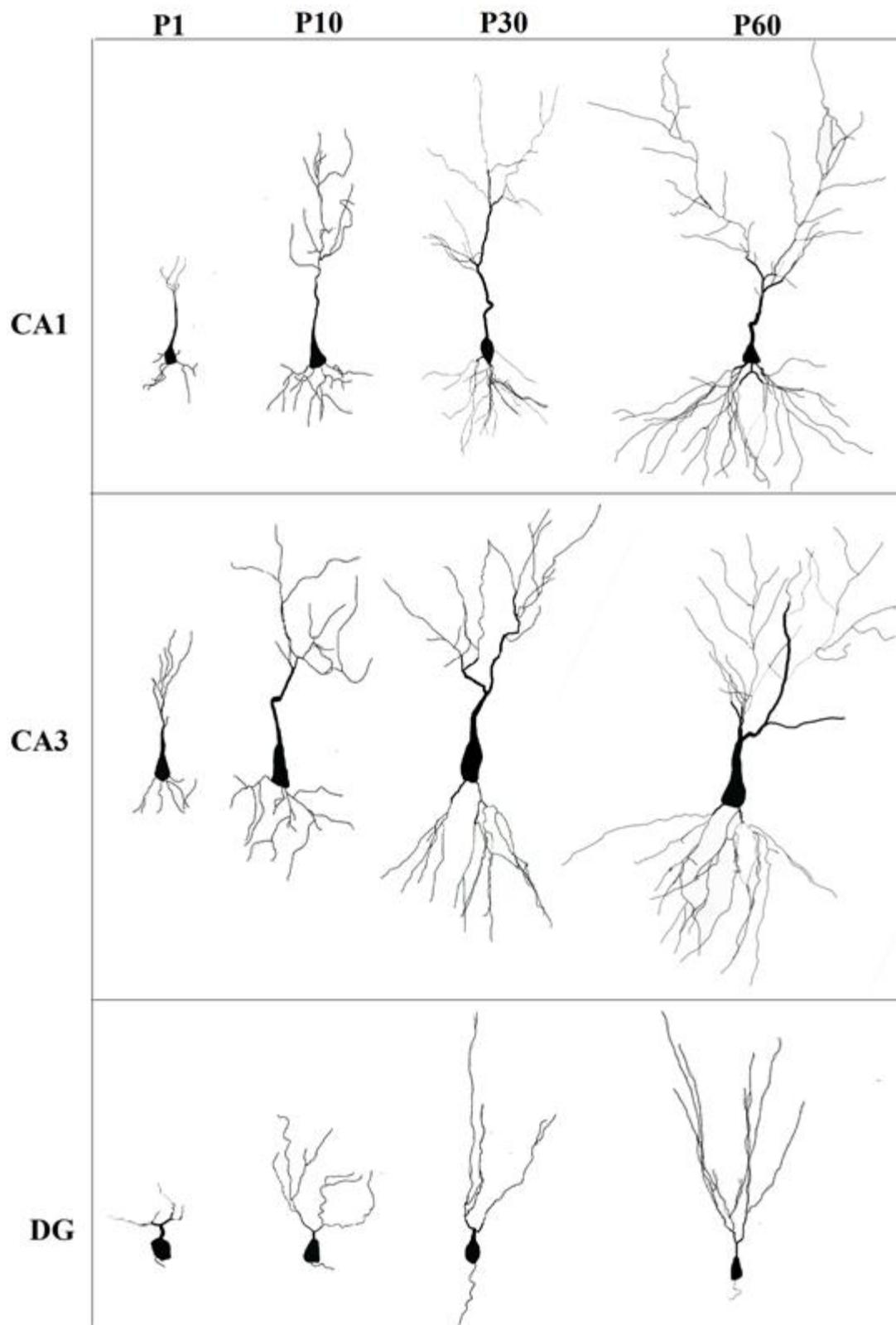
Figure 3.20. Line drawings of Golgi-impregnated cells of CA1, CA3 and DG region of intact control hippocampus for all ages (P1, P10, P30, and P60) studied.

The dendrites of pyramidal neurons meeting the criteria for being traced were labelled as apical and basal according to their location either in stratum oriens or in stratum radiatum (Fig. 3.21).
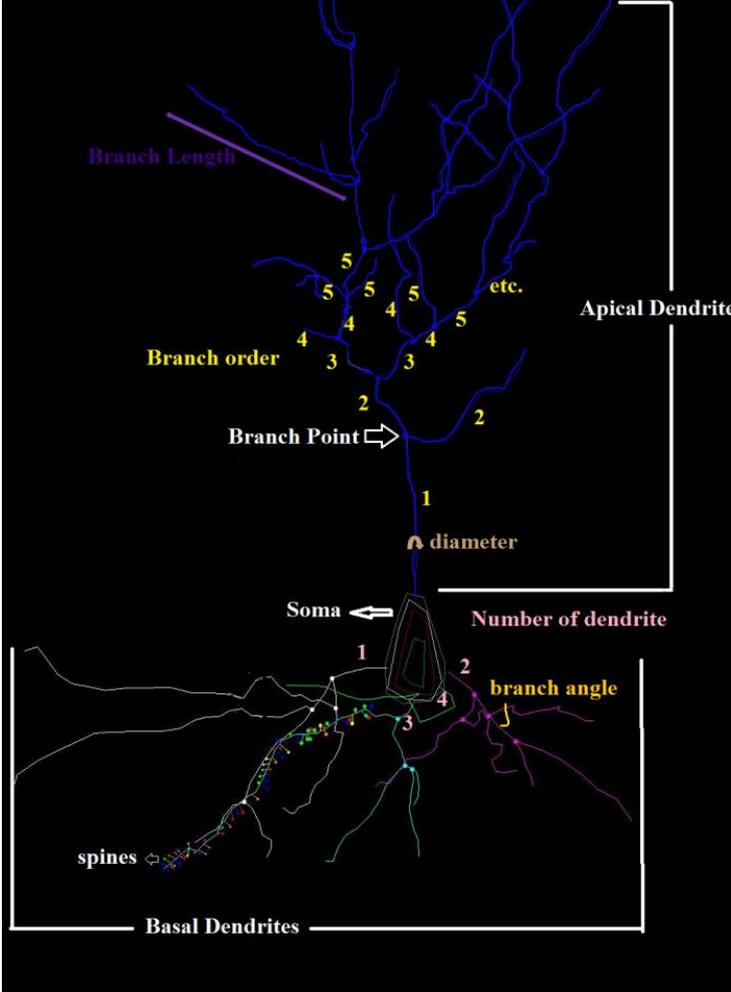
Figure 3.21. Diagramatic representation of a pyramidal neuron of hippocampus showing some morphological parameters
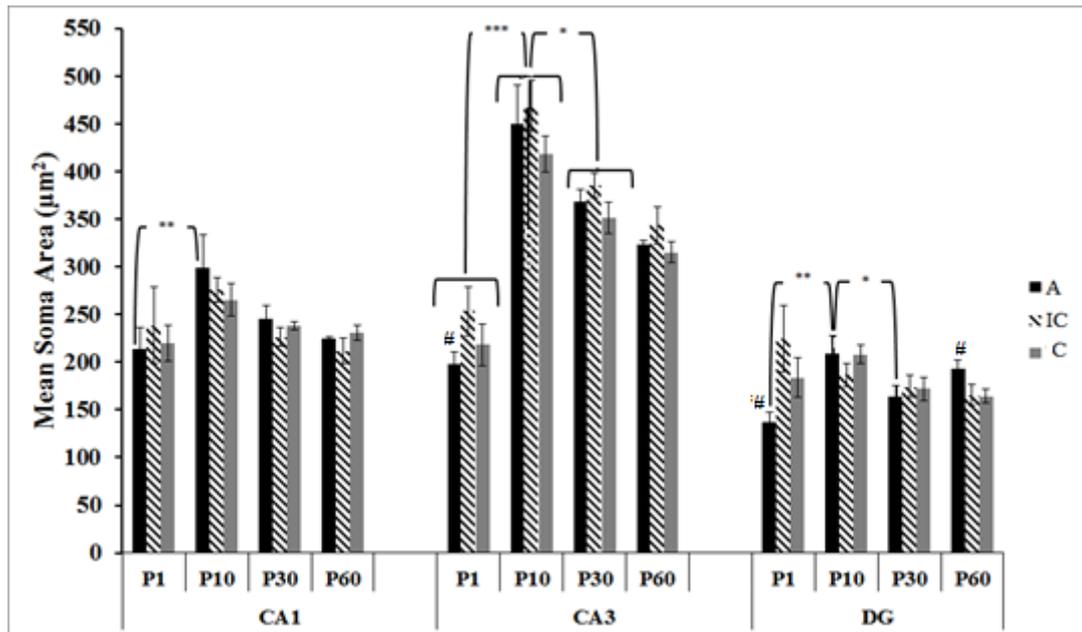
Figure 3.22. **S**oma area estimates made for each postnatal age, each treatment group, and each hippocampal region, independently. The degree of significance is denoted as p≤0.1$^{\#}$, p≤0.05*, p≤0.01**, p≤0.001***.Error bars denote SEM.

As seen from Fig. 3.22, alcohol treatment did not affect significantly the mean soma area of hippocampal CA1 pyramidal neurons. However, the soma area of CA3 pyramidal neurons and DG granular neurons were marginally smaller in alcohol group at birth.

Two-way ANOVA with age and treatments as independent variable performed on CA1 soma data yielded significant age effect ($F_{(3:74)}$=5.727, p=0.001) and insignificant treatment effect. The age x treatment interaction was also statistically insignificant. One-way ANOVA with age as independent variable yielded the main effect of age significant in A group only ($F_{(3:26)}$=3.049, p=0.047). Post-hoc comparisons by LSD test confirmed significantly smaller soma area on P1 when compared to P10 in alcohol group (p=0.009).

Two-way (age x treatment) ANOVA performed for CA3 soma data yielded a significant main effect of both age ($F_{(3:74)}$=59.845, p≤0.001) and treatment ($F_{(2:74)}$=3.402, p=0.039). The treatment x age interaction was statistically insignificant. One-way ANOVA with age as independent variable found soma size increase observed in all groups between P1-P10 and soma size decrease observed in all groups between P10-P30 significant ($F_{(3:25)}$=23.426, p≤0.001 for A group; $F_{(3:25)}$=16.413, p≤0.001 for IC group; $F_{(3:24)}$=22.457, p≤0.001 for C group). One-way ANOVA and subsequent post hoc LSD comparisons revealed the soma size to be marginally lower in the alcohol group as compared to IC group at P1 (p=0.065).

A similar data analysis carried out for the hippocampal DG region yielded marginally significant main effect of age ($F_{(3:73)}$=2.378, p=0.078) and significant treatment x age interaction ($F_{(6:73)}$=2.995, p=0.011). The main effect of treatment was insignificant. Nevertheless, one-way ANOVA applied to DG soma data yielded group effect at P1 and P60 marginally significant ($F_{(2:18)}$=3.365, p=0.057, and $F_{(2:18)}$=2.892, p=0.081, respectively). Post hoc comparisons with LSD test showed that alcohol group soma size was significantly smaller at P1 (p=0.018 when compared IC group) and larger at P60 (p=0.056 when compared IC group and p=0.048 when compared C group). The significant treatment x age interaction shows that the temporal profiles of soma size changes were different between the groups. One-way ANOVA yielded a significant main effect of age in A group only ($F_{(3:24)}$=5.880, p=0.004). In A group, comparison of simple effects with LSD test revealed significantly smaller mean soma area of DG granular cells at P1 compared to P10 (p=0.001). However, in granular neurons, the soma size significantly decreased between the P10-P30 period (p=0.022).

Resuming these results we can say that developmental changes in the soma size were most pronounced in CA3 region where in all treatment groups, a significant increase in this parameter was

observed during the brain growth spurt period, followed by a significant reduction in soma size between P10-P60, nevertheless, on P60, an overall soma size of CA3 neurons remained larger than that in CA1 or DG regions. The effect of fetal alcohol was manifested by a marginally smaller soma size of CA3 pyramidal and DG granular cells at birth, which, however, showed significant increase between P1-P10 to catch up with the soma size in control subjects already at P10
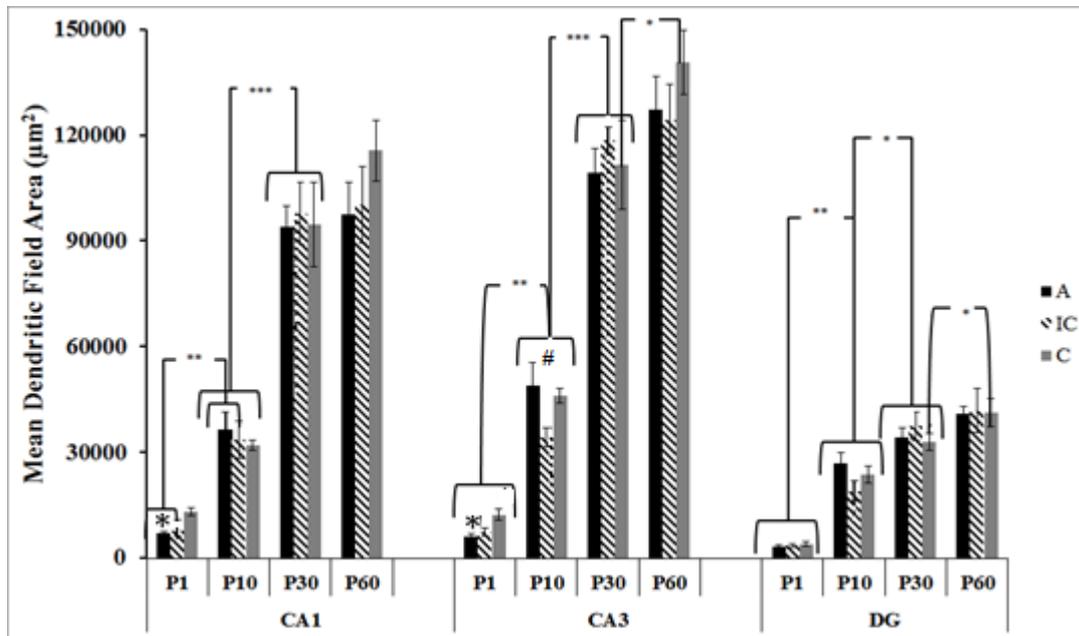
Figure 3.23. Morphometric estimates of the mean dendritic field area made for each postnatal age, each treatment group, and each hippocampal region, independently. The degree of significance is denoted as $p \leq 0.1^{\#}$, $p \leq 0.05^{*}$, $p \leq 0.01^{**}$, $p \leq 0.001^{***}$. Error bars denote SEM.

Two-way ANOVA with age and treatment as independent variables performed for all three hippocampal subregions independently on the dendritic field data yielded a highly significant age effect ($F_{(3:74)}=134.156$, $p \leq 0.001$ for CA1; $F_{(3:74)}=224.511$, $p \leq 0.001$, for CA3; ($F_{(3:74)}=88.243$, $p \leq 0.001$, for DG) with age x treatment interaction insignificant. The significant age effect was confirmed by the results of one-way ANOVA analysis which revealed significant age-dependent changes in all treatment groups (CA1: $F_{(3:28)}=58.170$, $p \leq 0.000$ for A group; $F_{(3:28)}=38.654$, $p \leq 0.000$ for IC group; $F_{(3:27)}=43.290$, $p \leq 0.000$ for PC group; CA3: $F_{(3:28)}=76.576$, $p \leq 0.000$ for A group; $F_{(3:28)}=113.618$, $p \leq 0.000$ for IC group; $F_{(3:27)}=55.422$, $p \leq 0.000$ for PC group; DG: $F_{(3:27)}=52.479$, $p \leq 0.000$ for A group; $F_{(3:28)}=19.767$, $p \leq 0.000$ for IC group; $F_{(3:27)}=37.320$, $p \leq 0.000$ for PC group) with the significant increase in the dendritic field area between P1-P10 and P10-P30 (Fig. 3.23).

Two-way (treatment x age) ANOVA yielded main effect of treatment insignificant. Nevertheless, one-way ANOVA with treatment as an independent factor applied to these date yielded treatment effect significant in CA1 and CA3 but not DG subregions at P1 ($F_{(2:19)}=8.893$, $p=0.002$ for CA1 and $F_{(2:19)}=8.127$, $p=0.003$ for CA3). Comparison of simple effects with LSD tests found that the mean dendritic field area in CA regions in C group marginally larger than in A and IC groups ($p \leq 0.01$).

Resuming these results, independent of treatment, a significant increase in the dendritic field area was observed in all hippocampal regions, mainly during the first postnatal month (between P1-P10 and P10-P30). This increase was 13.9 folded in CA1 pyramidal cells, 20.2 folded in CA3 pyramidal cells, and 12.9 folded in DG between P1-P60. On P1, the dendritic field of CA1 and CA3 pyramidal cells was significantly smaller in intubated groups (A and IC), compared to C group, but on P10, it reached the size of intact control.
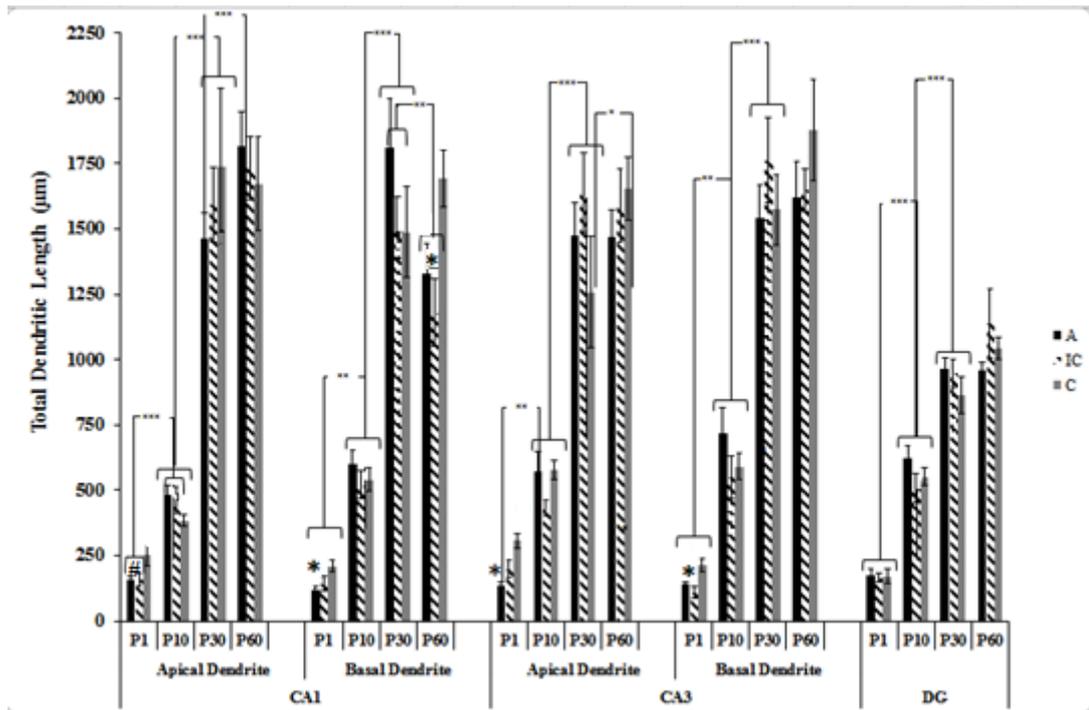
Figure 3.24. Morphometric estimates of total apical and basal dendritic length of pyramidal and granular neurons made for each postnatal age, each treatment group and each hippocampal region, independently. The degree of significance is denoted as $p \leq 0.1^{\#}$, $p \leq 0.05^*$, $p \leq 0.01^{**}$, $p \leq 0.001^{***}$. Error bars denote SEM.

Two-way ANOVA with age and treatment as independent variables performed for the dendritic length in all hippocampal region yielded a significant age effect (apical dendrites: $F_{(3:74)}$=124.386, $p \leq 0.001$ for CA1; $F_{(3:74)}$=122.992, $p \leq 0.001$, for CA3; $F_{(3:72)}$=141.929, $p \leq 0.001$, for DG;basal dendrites: $F_{(3:74)}$=136.866, $p \leq 0.001$ for CA1; $F_{(3:74)}$=151.026, $p \leq 0.001$, for CA3) and insignificant treatment effect. The age x treatment interaction was significant only for the basal dendrites of CA1 ($F_{(6:74)}$=2.625, p=0.023) where a significant decrease in the total dendritic length was noted in intubated groups but not in intact control.

As seen from Fig. 3.24, an overall increase in the total dendritic length was observed between P1-P10 and P10-P30, with little between-regional differences in the total dendrite length at P1 and P10 and great difference emerging between pyramidal and granular cells' dendrites at P30.

According to the results of one-way ANOVA applied to these data, at P1, alcohol and intubation control groups showed significantly shorter apical and basal dendrite in both CA1 and CA3 region of hippocampus as compared to intact control group ($F_{(2:19)}$=3.232, p=0.062 for CA1 apical, $F_{(2:19)}$=5.284, p=0.015 for CA1 basal; $F_{(2:19)}$=11.118, p=0.001 for CA3 apical, $F_{(2:19)}$=7.353, p=0.004 for CA3 basal). In addition, at P60, basal dendritic length of CA1 pyramidal neurons of PC group was significantly longer than other two groups ($F_{(2:18)}$=4.989, p=0.019).

In summary we can say that parallel to an increase in the total dendritic field area, the total length of both pyramidal and granular dendrites significantly increased during P1-P30 period with pyramidal dendrites significantly longer at P30 but not at P10. The combined ethanol/intubation effect was manifested as significantly shorter dendritic length on P1 in CA but not DG region. The effect was transient and disappeared on P10.
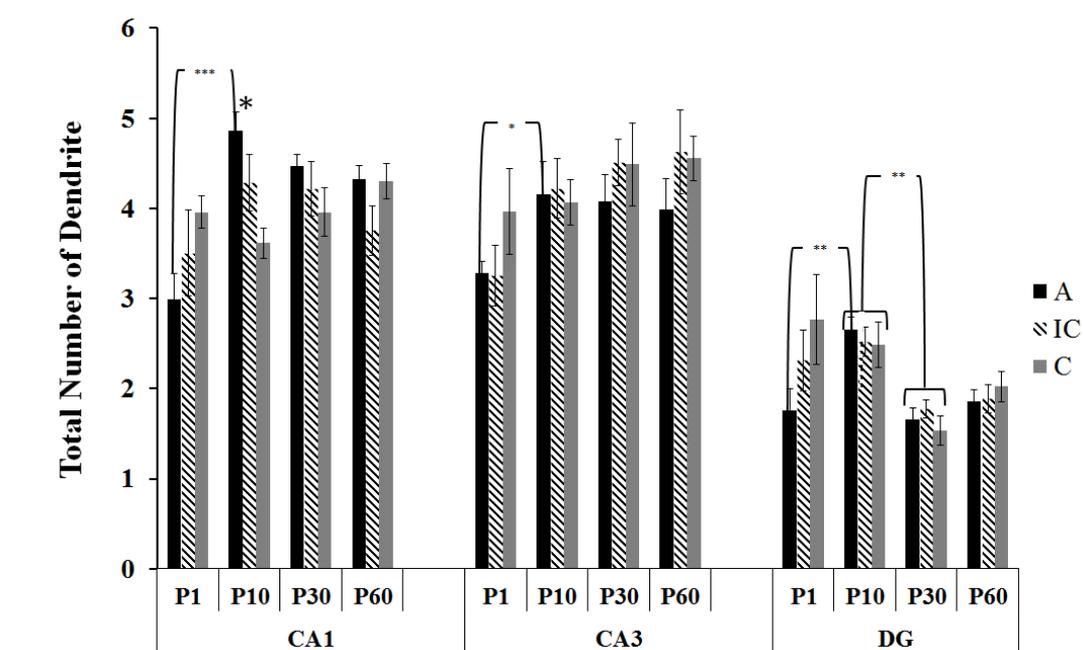
Figure 3.25. Morphometric estimates of total number of basal dendrites in pyramidal and granular neurons made for each postnatal age, each group and each hippocampal region, independently. The degree of significance is denoted as p≤0.05*, p≤0.01**, p≤0.001***. Error bars denote SEM.

Since pyramidal neurons have a single apical dendrite, this analysis was done for basal dendrites of pyramidal neurons and granular neurons.

Two-way ANOVA with age and treatment as independent variables performed on the numbers of basal dendrites in pyramidal and granular cells yielded a significant age effect ($F_{(3:74)}$=5.611, p=0.002 for CA1; $F_{(3:74)}$=4.436, p=0.006, for CA3; $F_{(3:72)}$=8.776, p≤0.001, for DG) and insignificant treatment effect. The age x treatment interaction was significant ($F_{(6:74)}$=3.531, p=0.004) in CA1 region.

One-way ANOVA with age as independent factor and subsequent post hoc LSD test revealed a significant increase in dendrite numbers taking place on P10 in all hippocampal regions in A group (p≤0.05). Changes in dendrite numbers between different ages in CA subregions in control groups were insignificant. However, a significant (p≤0.01) decrease in the dendrite number in granular neurons was found in all groups between P10-P30.

One way ANOVA with treatment as independent factor showed a significant between-group difference only for CA1 basal dendrites at P10 ($F_{(2:19)}$=5.978, p=0.010). As seen from the Fig. 3.25, at P10, alcohol group showed significantly higher number of basal dendrites compared to C group (p=0.003).

Resuming these results we can say that dendrite number in hippocampal pyramidal neurons generally did not change after the birth while in the granular cells it significantly decreases between P10-P30. The alcohol effect was manifested as a significant increase in the total dendrite number both in pyramidal and granular cells between P1-P10, and a significantly higher total dendrite number in CA1 pyramidal cells at P10 as compared to the intact control.
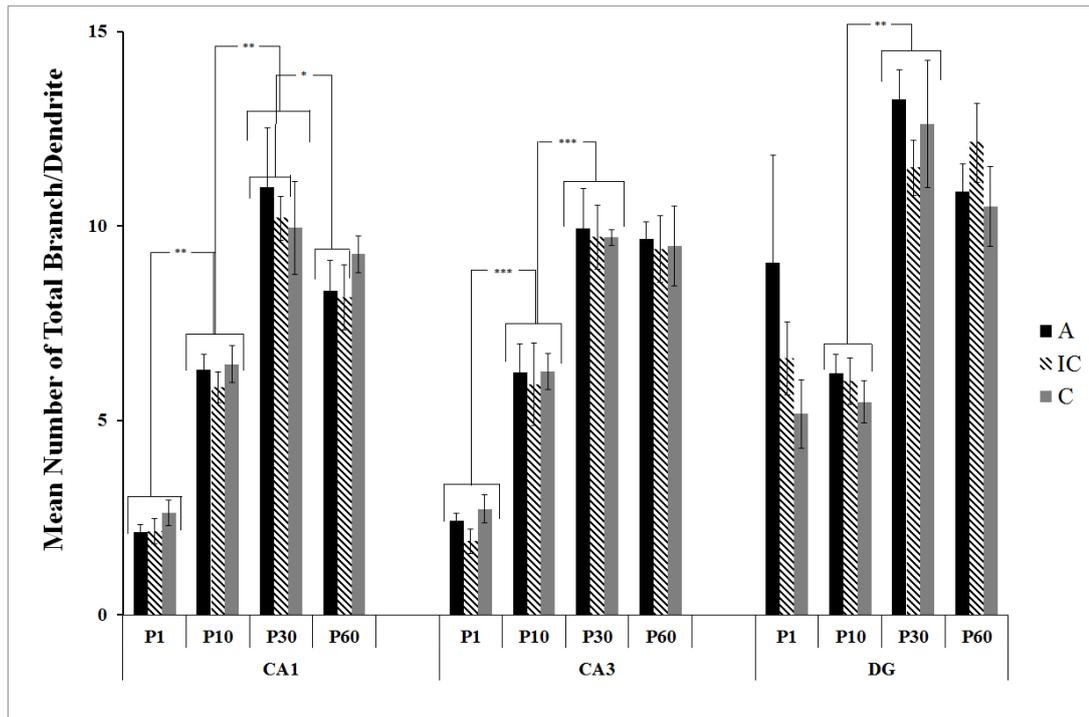
Figure 3.26. Morphometric estimates of mean number of branches per dendrite made for each postnatal age, each group, and each hippocampal region, independently. The degree of significance is denoted as p≤0.05*, p≤0.01**, p≤0.001***. Error bars denote SEM.

This parameter was again estimated for basal dendrites of pyramidal and granular neurons.

Two-way ANOVA with age and treatment as independent variables performed for dendritic branch/dendrite yielded a significant age effect ($F_{(3;74)}=71.737$, p≤0.001 for CA1; $F_{(3;74)}=74.157$, p≤0.001, for CA3; $F_{(3;73)}=22.780$, p≤0.001, for DG). The age x treatment interaction and the main effect of treatment remained insignificant.

According to one-way ANOVA results, alcohol treatment did not have a significant effect on this parameter. In all treatment groups, a significant increase in dendrite density was observed between the P1-P30 in CA region and between P10-P30 in DG region (Fig. 3.27). No significant effect of treatment was found.

In summary, it was found that although after the birth, the total number of dendrites was either stable (CA pyramidal neurons) or show decrease (granular cells), the average number of branches per dendrite show a highly significant increase between P1-P30 in pyramidal neurons and between P10-P30 in granular cells. Interestingly, the final branch density was higher in granular cells compared to pyramidal cells. The ethanol and/or intubation stress had no.effect on this parameter.
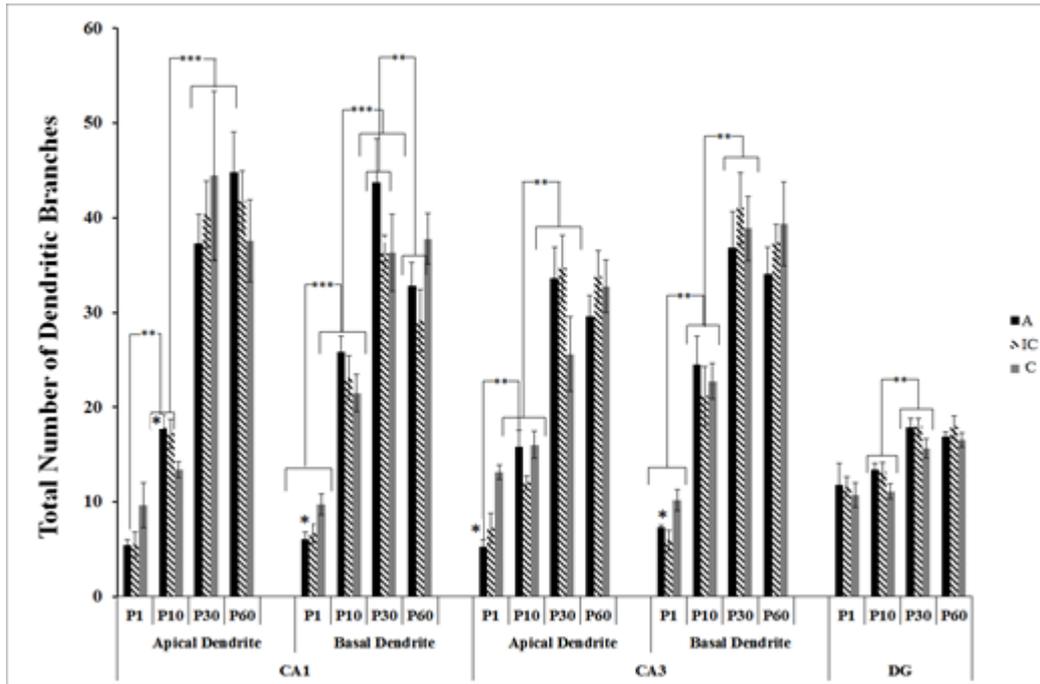
Figure 3.27. Morphometric estimates of total number of dendritic branches made for each postnatal age, each treatment group, and each hippocampal region, independently. The degree of significance is denoted as p≤0.05*. Error bars denote SEM.

Two-way ANOVA with age and treatment as independent variables performed for dendritic branch number in hippocampal CA and DG regions yielded a significant age effect (apical dendrites: $F_{(3:74)}=70.991$, p≤0.001 for CA1; $F_{(3:74)}=77.085$, p≤0.001, for CA3; $F_{(3:73)}=21.333$, p≤0.001, for DG; basal dendrites: $F_{(3:74)}=85.903$, p≤0.001 for CA1; $F_{(3:74)}=79.932$, p≤0.001, for CA3). The age x treatment interaction was significant only for apical dendrite of CA3 region ($F_{(6:74)}=3.071$, p=0.010). The main effect of treatment appeared marginally significant only in granular neurons ($F_{(2:73)}=2.519$, p=0.087).

As seen from the Fig. 3.27, an overall increase in the number of denrite branches was observed in all groups and in all hippocampal regions. The total number of apical dendrite branches in pyramidal neurons and of dendrite branches in granular cells was significantly increased during P10-P30, while the total number of basal dendrite branches in pyramidal neurons was significantly increased during the P1-P30 period

A subsequent analysis performed by one-way ANOVA revealed a significant main effect of treatment of the total number of branches of CA1 basal dendrite and CA3 apical and basal dendrite on P1 ($F_{(2:19)}=4.457$, p=0.026, $F_{(2:19)}=14.558$, p≤0.001, $F_{(2:19)}=6.360$, p=0.008, respectively). Post hoc LSD test showed that on P1, basal dendrites in CA1 and both basal and apical dendrites in CA3 had significantly lower number of branches in both alcohol and intubation control group compared to the intact control group (p≤0.05).
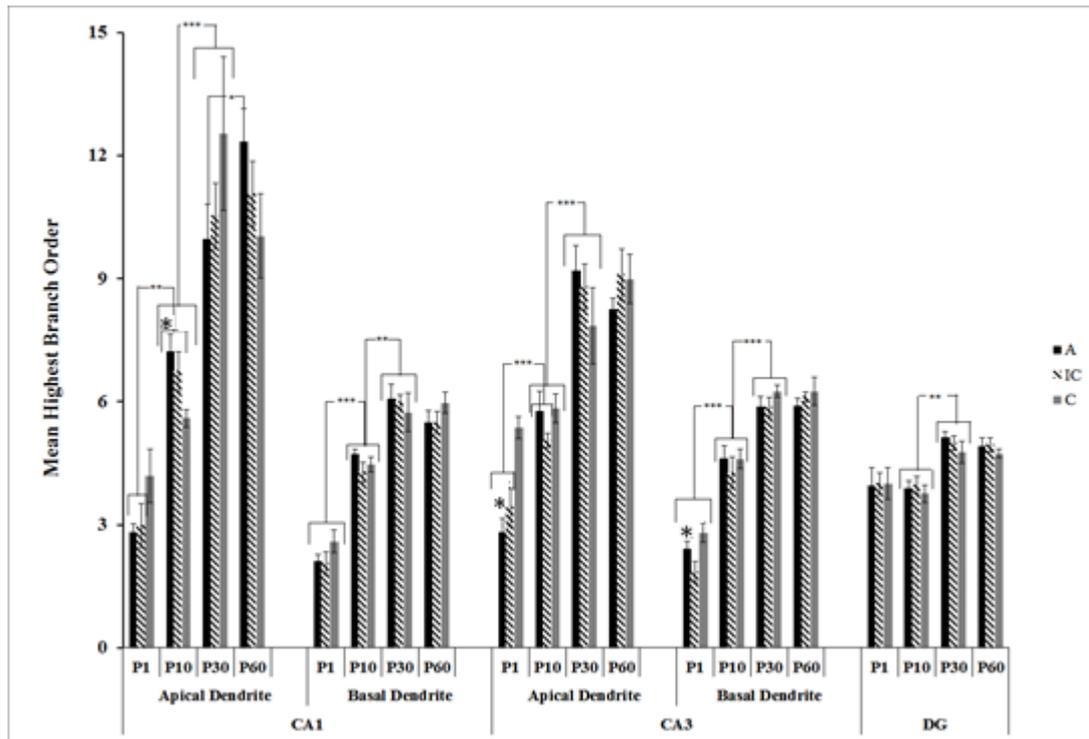
Figure 3.28. Morphometric eastimates of the mean highest branch order made for each postnatal age, each group, and each hippocampal region, independently. The degree of significance is denoted as $p \leq 0.05*$, $p \leq 0.01**$, $p \leq 0.001***$. Error bars denote SEM.

Two-way ANOVA with age and treatment as independent variables performed for highest number of dendritic branch order of hippocampus yielded a significant age effect (apical dendrites: $F_{(3:74)}=64.097$, $p \leq 0.001$ for CA1; $F_{(3:74)}=68.490$, $p \leq 0.001$, for CA3; $F_{(3:73)}=16.280$, $p \leq 0.001$, for DG; basal dendrites: $F_{(3:74)}=118.644$, $p \leq 0.001$ for CA1; $F_{(3:74)}=143.709$, $p \leq 0.001$, for CA3). The age x treatment interaction was significant in apical dendrites of pyramidal neurons ($F_{(6:74)}=2.124$, $p=0.060$ for CA1;$F_{(6:74)}=3.112$, $p=0.009$ for CA3). The main effect of treatment was significant only in basal dendrites of CA3 neurons ($F_{(2:74)}=3.223$, $p=0.045$).

An overall increase in the highest dendrite order was observed in all hippocampal regions during the first postnatal month (Fig. 3.28). One-way ANOVA with age as independent factor revealed significant increase in the highest branch order between P1-P30 in basal dendrites of CA1/CA3 pyramidal neurons, and between P10-P30 in pyramidal cells' apical dendrites and dendrites of dentate granular cells. ($p \leq 0.01$).

On P1, the highest order of branches in CA regions in intubated, A and IC groups, was lower compared to intact control group. One-way ANOVA with treatment as independent variable revealed at P1, significantly lower the highest number of both apical and basal dendrite bifurcations in the pyramidal cells of CA3 region in alcohol group compared to control group ($F_{(2:19)}=13.823$, $p \leq 0.001$ and $F_{(2:19)}=4.615$, $p=0.023$, respectively). At P10, in alcohol group, the number of branch order of apical dendrites of CA1 neurons was significantly higher compared to control group ($F_{(2:21)}=4.109$, $p=0.033$).
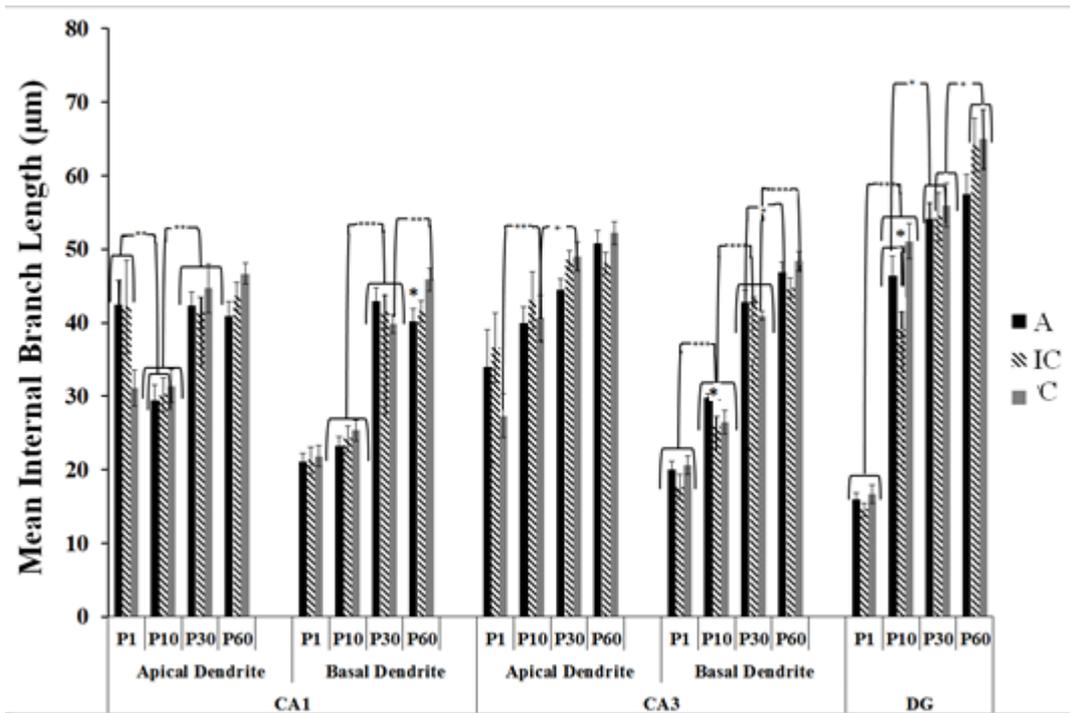
Figure 3.29. Morphometric estimates of mean internal dendritic branch length made for each postnatal age, each group, and each hippocampal region, independently. The degree of significance is denoted as p≤0.05*, p≤0.01**, p≤0.001***. Error bars denote SEM.

In all groups and hippocampal regions except CA1 apical dendrites, an overall increase in the internal branch length was observed (Fig.3.29). Two-way ANOVA with age and treatment as independent variables performed for internal length of dendritic branches of hippocampus yielded a significant age effect (apical dendrites: $F_{(3:74)}=13.319$, p≤0.001 for CA1; $F_{(3:74)}=19.698$, p≤0.001, for CA3; $F_{(3:73)}=179.643$, p≤0.001, for DG; basal dendrites: $F_{(3:74)}=143.565$, p≤0.001 for CA1; $F_{(3:74)}=298.367$, p≤0.001, for CA3). The age x treatment interaction was marginally significant only in apical dendrites of CA1 ($F_{(6:74)}=2.105$, p=0.063). The main effect of treatment was marginally significant in basal dendrites of CA3 neurons ($F_{(2:74)}=2.638$, p=0.078) and granule neurons ($F_{(2:73)}=2.970$, p=0.058). One way ANOVA with age as independent revealed the increase in the internal branch length during P1-P10 period in DG neurons and during P10-P30 period in basal dendrites of pyramidal neurons significant (p≤0.001).

One way ANOVA with treatment as independent factor and the subsequent post hoc comparison of simple effects with LSD test confirmed significantly longer internal branch length in A group compared to IC group on P10 in CA3 basal dendrites and shorter internal branch length in the same group compared to control at P60 in CA1 basal dendrites (p=0.022) and in IC group compared to both A and C groups at P10 in DG dendrites (p=0.048 and p=0.003, respectively).
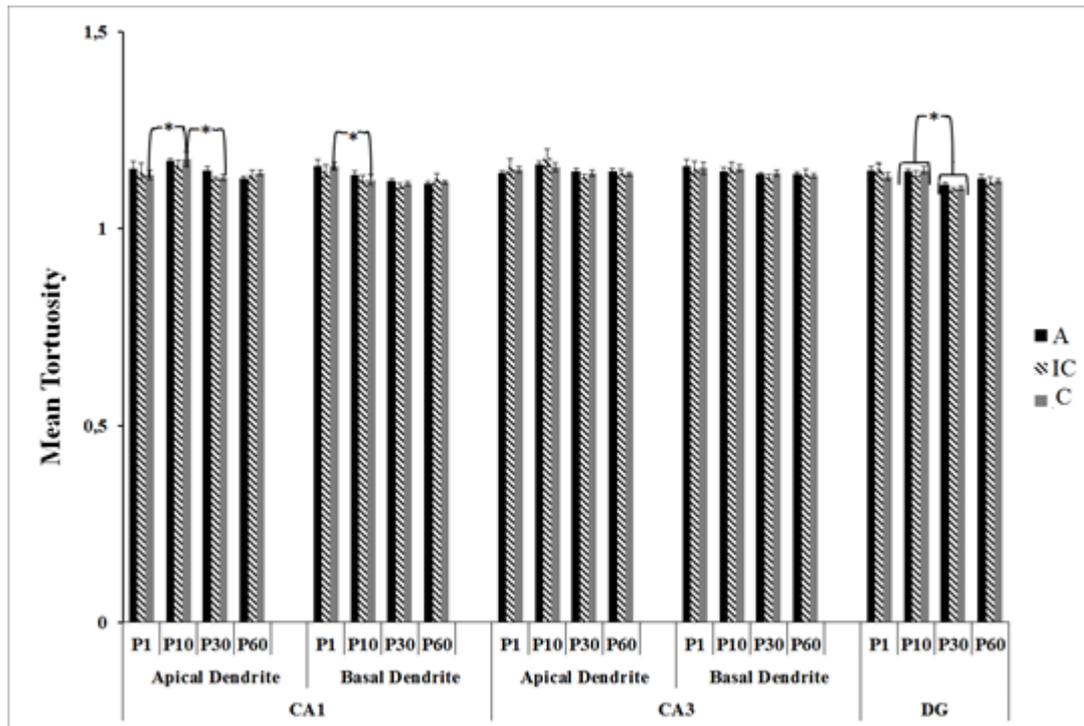
Figure 3.30. Morphometric estimates of mean dendritic tortuosity made for each postnatal age, each group, and each hippocampal region, independently. The degree of significance is denoted as $p \leq 0.05^*$. Error bars denote SEM.

Two-way ANOVA with age and treatment as independent variables performed for tortuosity of dendrites of hippocampus yielded a significant age effect in apical and basal dendrites of pyramidal neurons and granular neurons (apical dendrites: $F_{(3:74)}=5.298$, p=0.002 for CA1; $F_{(3:74)}=3.112$, p=0.031, for CA3; $F_{(3:73)}=15.160$, p≤0.001, for DG; basal dendrites: $F_{(3:74)}=4.575$, p=0.005 for CA1) except the basal dendrites of CA3 region. The age x treatment interaction and main effect of treatment were insignificant.

One-way ANOVA with age as independent variable revealed that in intact control group, the dendritic tortuosity of apical dendrite of CA1 pyramidal neuron was larger at P10 ($F_{(3:27)}=2.632$, p=0.073, and $F_{(3:27)}=5.144$, p=0.007, respectively) than both the dendritic tortuosity at P1 and P30 (p≤0,05). On the other hand, the basal dendritic tortuosity of CA1 neurons at P1 was higher than the tortuosity at P10 (p≤0.05). In DG granular neurons, the age effect was observed at P10-P30 period (Fig. 3.30).

To summarize these results, we can say that the prenatal ethanol administration and/or intubation stress did not have a significant effect on tortuosity of hippocamapl dendrites The developmental changes in tortuosity of dendrites in hippocampus were very small. There was .a mild trend towards greater tortuosity at early postnatal ages.
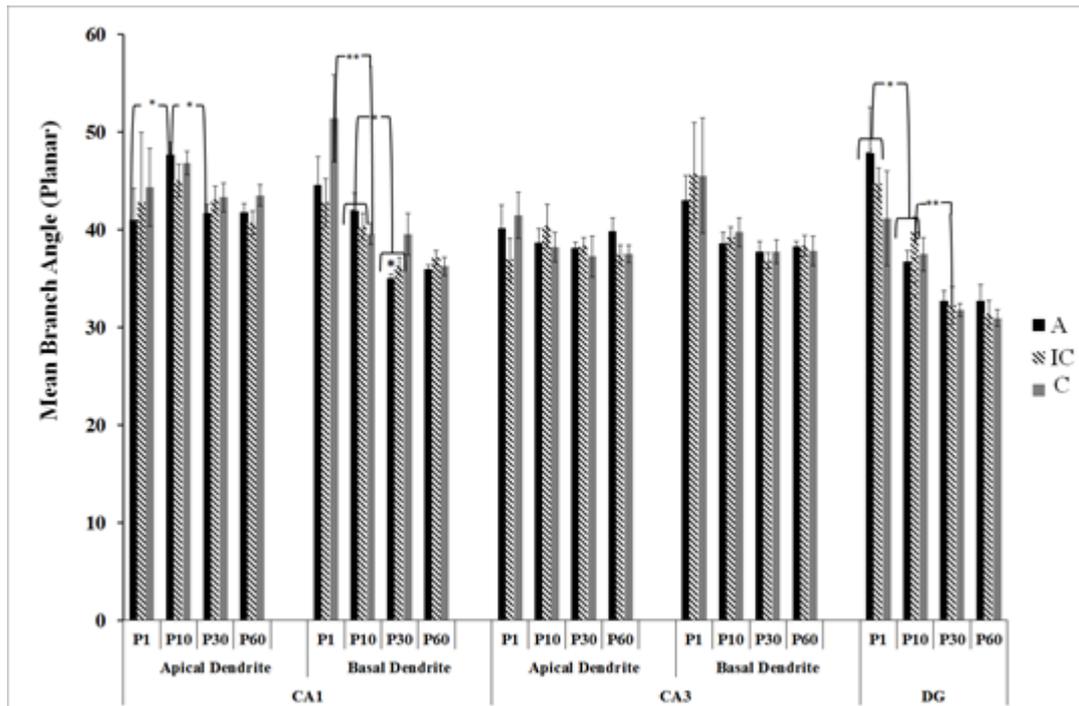
Figure 3.31. Morphometric estimates of mean planar branch angle made for each postnatal age, each group, and each hippocampal region, independently. The degree of significance is denoted as $p \leq 0.05^*$ and $p \leq 0.01^{**}$. Error bars denote SEM.

Two-way ANOVA with age and treatment as independent variables performed for branch angle of dendrites yielded a significant age effect in basal dendrites of pyramidal neurons and granular neurons (basal dendrites: $F_{(3:74)}=15.993$, $p \leq 0.001$ for CA1; $F_{(3:74)}=5.303$, $p=0.002$, for CA3; and $F_{(3:73)}=20.516$, $p \leq 0.001$, for DG). The age x treatment interaction and main effect of treatment were insignificant.

As seen from the Fig. 3.31, a significant trend for decrease in branch angle during the postnatal development was observed especially in DG and in basal CA3 dendrites. One-way ANOVA showed the main treatment effect on the planar branch angle significant at P30 in the basal dendrite of CA1 neurons ($F_{(2:20)}=2.874$, $p=0.083$), with a decreased branch angle in intubated groups compared to intact control but this effect was yilded significant only in A group ($p \leq 0.05$).
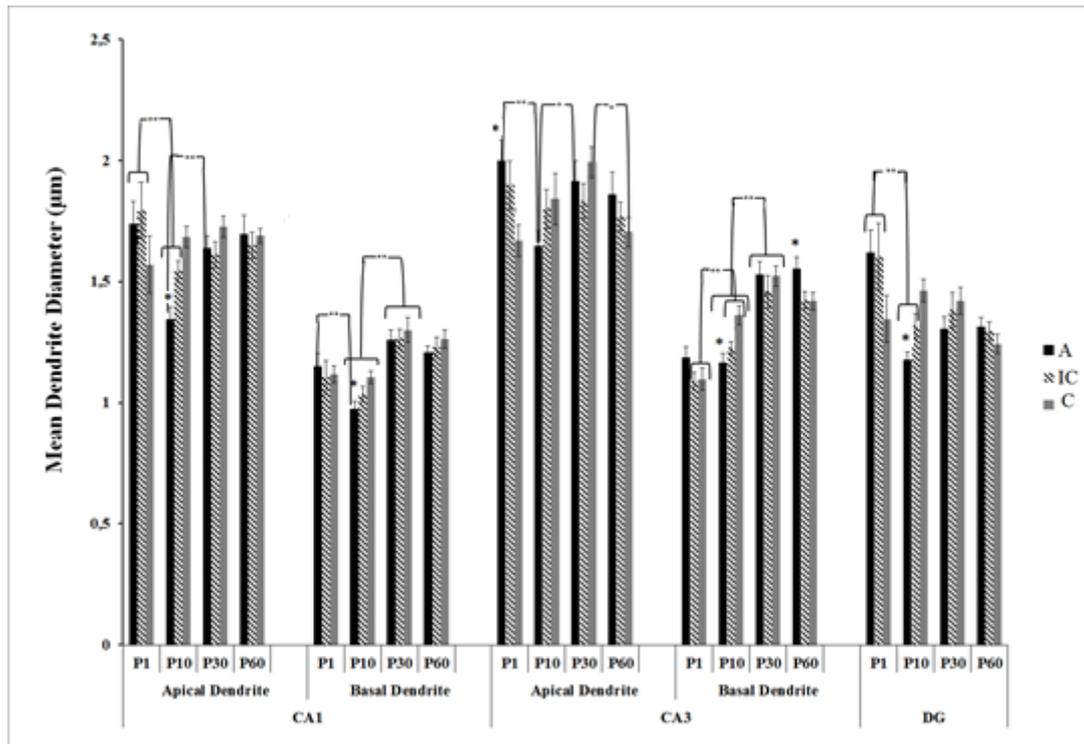
Figure 3.32. Morphometric estimates of mean dendrite diameter made for each postnatal age, each group, and each hippocampal region, independently. The degree of significance is denoted as $p \leq 0.05*$ and $p \leq 0.01**$. Error bars denote SEM.

Two-way ANOVA with age and treatment as independent variables performed for dendrite diameter yielded a significant age effect (apical dendrites: $F_{(3:74)}=2.780$, $p=0.047$ for CA1; $F_{(3:74)}=2.315$, $p=0.083$, for CA3; $F_{(3:73)}=6.884$, $p \leq 0.001$, for DG; basal dendrites: $F_{(3:74)}=19.301$, $p \leq 0.001$ for CA1; $F_{(3:74)}=51.643$, $p \leq 0.001$, for CA3). The age x treatment interaction was also significant in apical dendrites of CA1 and CA3 ($F_{(6:74)}=2.134$, $p=0.059$, and $F_{(6:74)}=2.555$, $p=0.026$, respectively), in DG granule neurons ($F_{(6:73)}=3.203$, $p=0.008$), and in basal dendrites of CA3 ($F_{(6:74)}=2.856$, $p=0.015$). The main effect of treatment was insignificant. There was seen a trend for an increase in branch angle especially for CA basal dendrites between P10-P30 and a steady decrease in this measure across postnatal ages in DG.

According to one-way ANOVA with treatment as independent variable, at P10, the dendrite diameter of both apical and basal dendrites of CA1 ($F_{(2:21)}=13.313$, $p \leq 0.001$, $F_{(2:21)}=4.585$, $p=0.024$, respectively), basal dendrites of CA3 ($F_{(2:21)}=7.764$, $p=0.003$) and granule cells' dendrites ($F_{(2:21)}=11.020$, $p=0.001$) were significantly decreased upon prenatal ethanol administration (Fig 3.32).
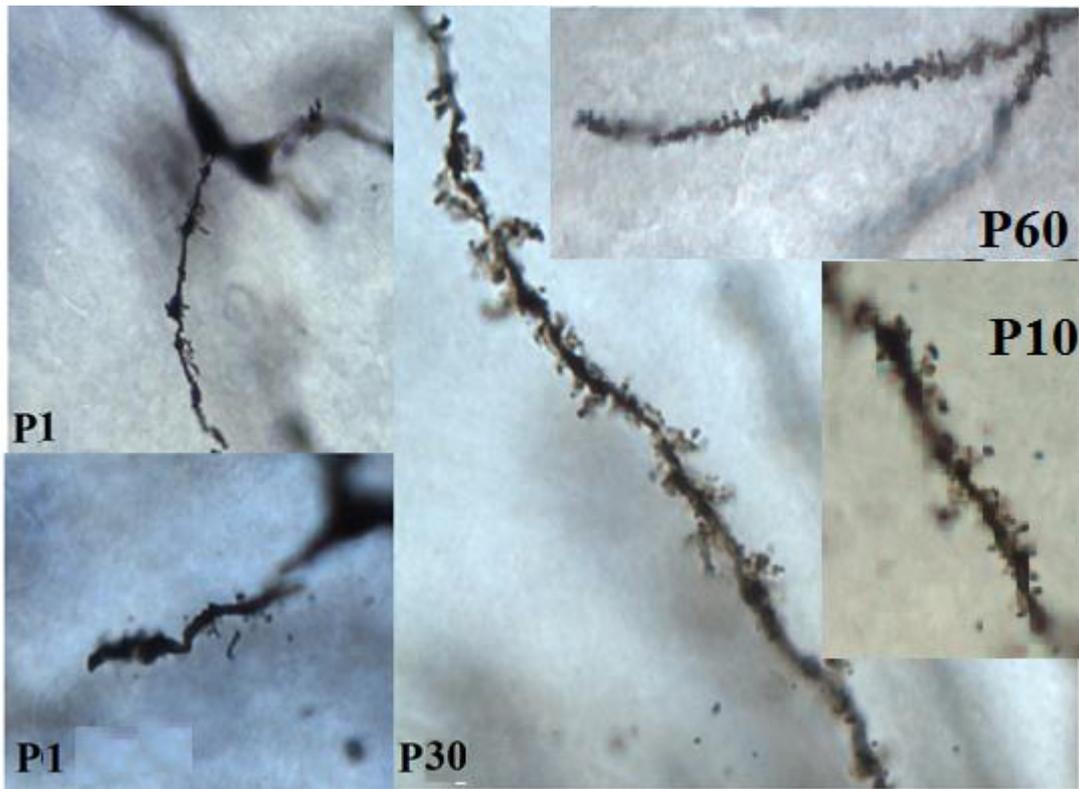
Figure 3.33. Representative photomicrographs showing the spines of apical dendrites of pyramidal neurons at birth (P1), P10, P30, and P60 (Magnification- 100X).
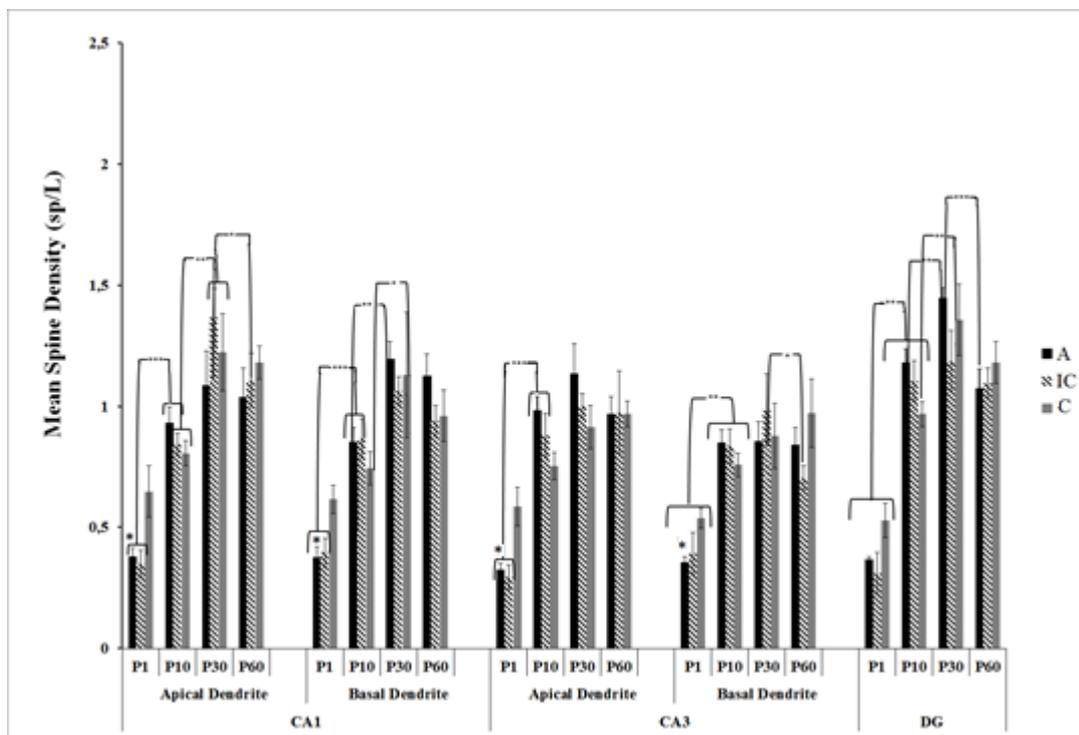
**Figure 3.34.** Morphometric estimates of mean total spine density made for each postnatal age, each group, and each hippocampal region, independently. The degree of significance is denoted as $p \leq 0.05$*, $p \leq 0.01$**, $p \leq 0.001$***. Error bars denote SEM.

The density of spines was measured in the third branch of apical dendrite and second branch of basal dendrite of pyramidal neurons and third dendritic branch of granular neurons for each cell. As seen Fig. 3.33, the density of spines was increased with increasing age.

Two-way ANOVA with age and treatment as independent variables performed for spine density yielded a significant age effect (apical dendrites: $F_{(3:66)}$=44.550, $p \leq 0.001$ for CA1; $F_{(3:69)}$=37.098, $p \leq 0.001$, for CA3; $F_{(3:68)}$=66.175, $p \leq 0.001$, for DG; basal dendrites: $F_{(3:65)}$=34.457, $p \leq 0.001$ for CA1; $F_{(3:67)}$=11.286, $p \leq 0.001$, for CA3). The age x treatment interaction was only significant in apical dendrites of CA3 ($F_{(6:69)}$=2.426, p=0.035). The main effect of treatment was insignificant.

As seen Fig. 3.34, the density of spines significantly increased between P1-P30 in CA regions and between P1-P10 in DG.

According to one-way ANOVA with treatment as independent variable, at P1, the total spine density of pyramidal neurons both apical dendrite and basal dendrite was lower in alcohol and intubation control group compared to intact control group (CA1: $F_{(2:21)}$=5.345, p=0.014 for apical dendrite, $F_{(2:20)}$=6.225, p=0.009 for basal dendrite, CA3: $F_{(2:21)}$=8.377, p=0.002 for apical dendrite, $F_{(2:21)}$=3.076, p=0.070 for basal dendrite) (Fig. 3.34). However, there is no alcohol effect on the spine density of granular neurons at any ages.

In this study, in addition to total spine densities, the densities of different spine types were also evaluated. The representative pictures were presented in Fig. 3.35 and the densities of major type of spines (thin, mushroom, stubby, and branched) were shown in the Fig. 3.36.
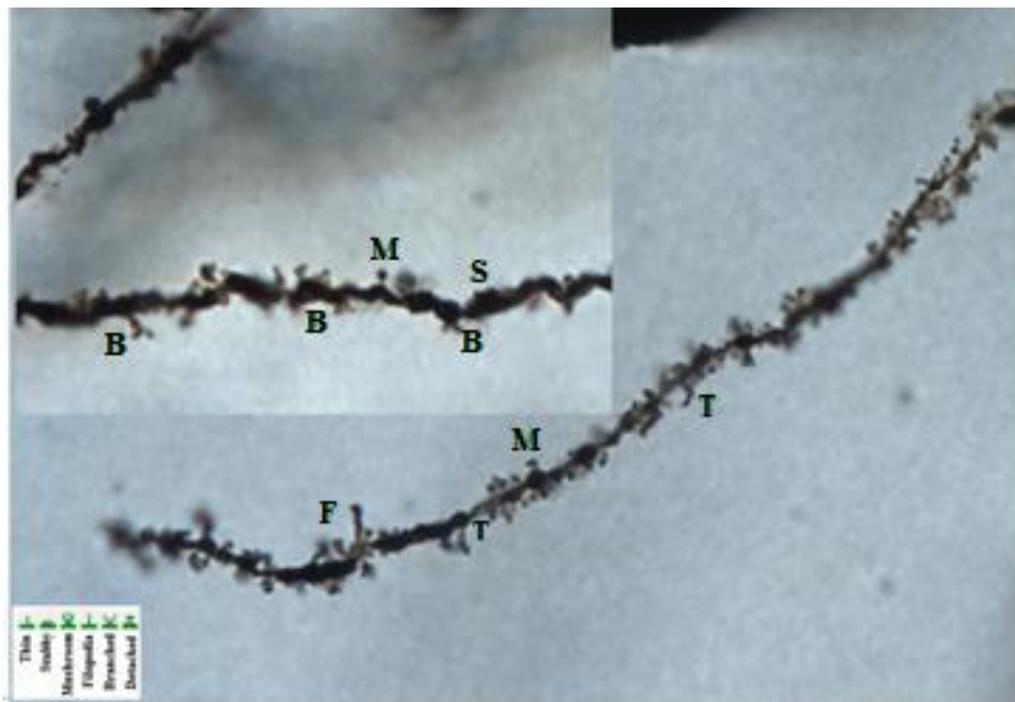
Figure 3.35. Representative photomicrographs showing different types of spines in the neuropile of the hippocampal CA and DG region at P60 under 100X magnification. (T: Thin spine, S: Stubby spine, M: Mushroom spine, B: Branched spine, F: Filopodia spine).
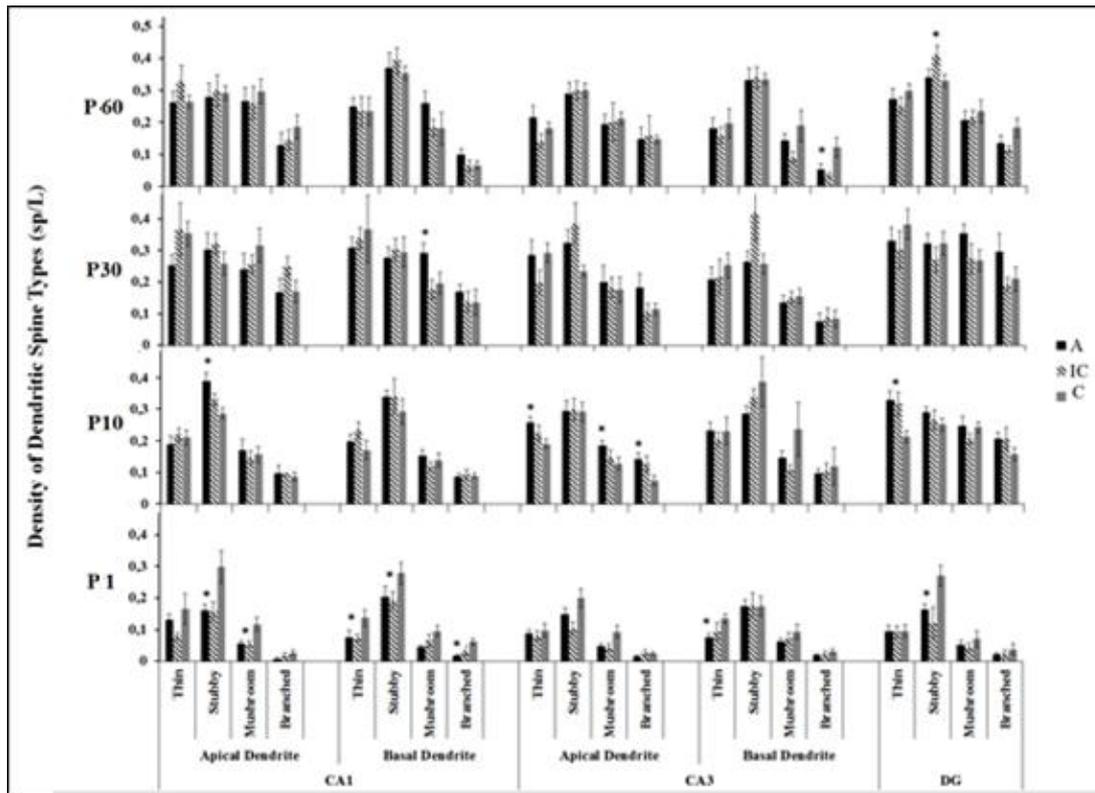
Figure 3.36. Morphometric estimates of the density of thin, stubby, mushroom, and branched spines made for each postnatal age, each treatment group, and each hippocampal region, independently. Error bars denote SEM and the asterisks denote significance at $p \leq 0.05$ with respect to control.

Only one-way ANOVA with treatment as independent variable and subsequent post hoc LSD test was applied as a statistical test to determine the each type of spine density fluctuation due to prenatal ethanol consumption.

As seen from Fig. 3.36, in all hippocampal regions, an overall increase in the spine density was noted throughout P1-P30. At P1, stubby spines prevailed. With maturation, thin spines emerged to be the second most crowded spine type. The overall frequency of branched spines, an indirect index of synaptogenesis, was the lowest.

At P1, the density of predominating stubby spines (spines with head widths equal to neck lengths) in CA1 and DG regions was significantly higher ($p \leq 0.05$) in intact control compared to intubated groups. At P10, the number of these spines in A and IC groups caught up or even overrode that in C group. At P10, the density of stubby spines on apical dendrite of CA1 neurons, density of thin, mushroom and branched spines on apical dendrites of CA3 neurons, and the density of thin spines on granular neurons was found to be significantly higher ($p \leq 0.05$) in the alcohol group compared to the intact control group. At P30, the density of mushroom spines on CA1 basal dendrites in A group was significantly higher ($p \leq 0.05$) compared to controls. Interestingly, at P60, the density of branched spines on CA3 basal dendrites was significantly higher in C group compared to A and IC groups.

72

In this study, sholl analysis was also done to evaluate the complexity of dendritic tree. This method is performed by counting the number of dendrite intersections for concentric circles of gradually increasing radius usually centered at the centroid of the cell body. The sholl ring radia applied in this analysis had 10 µm increments (Fig 3.37).
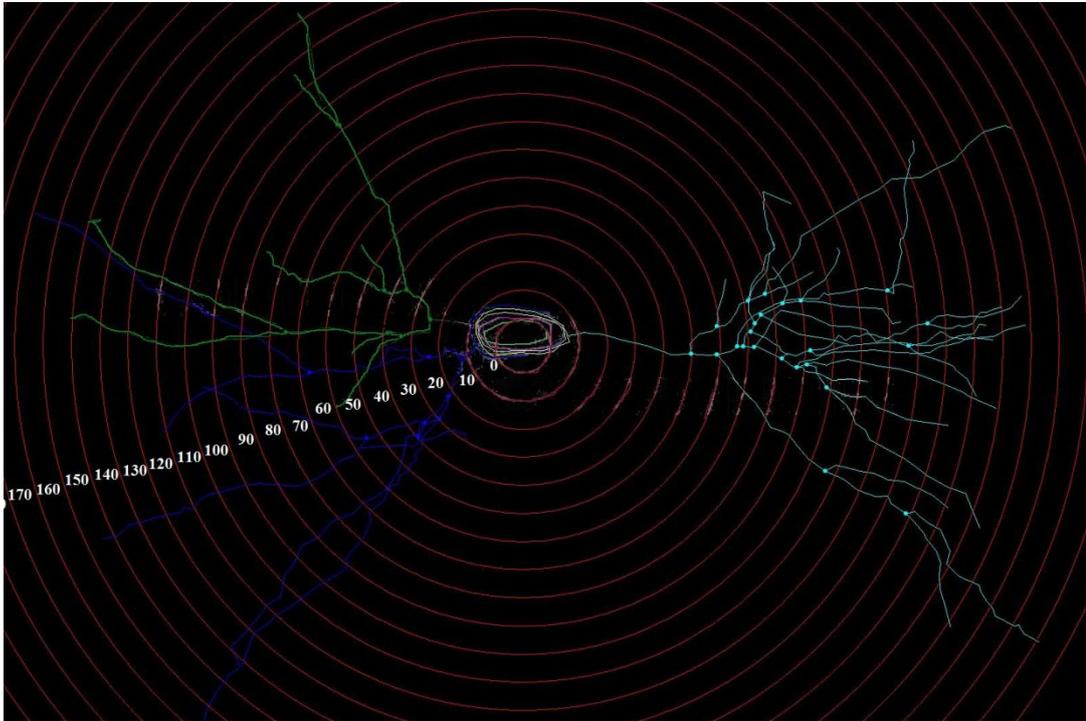
Figure 3.37. Representative diagram showing an overlay of concentric rings centered at the cell body for Sholl analysis.
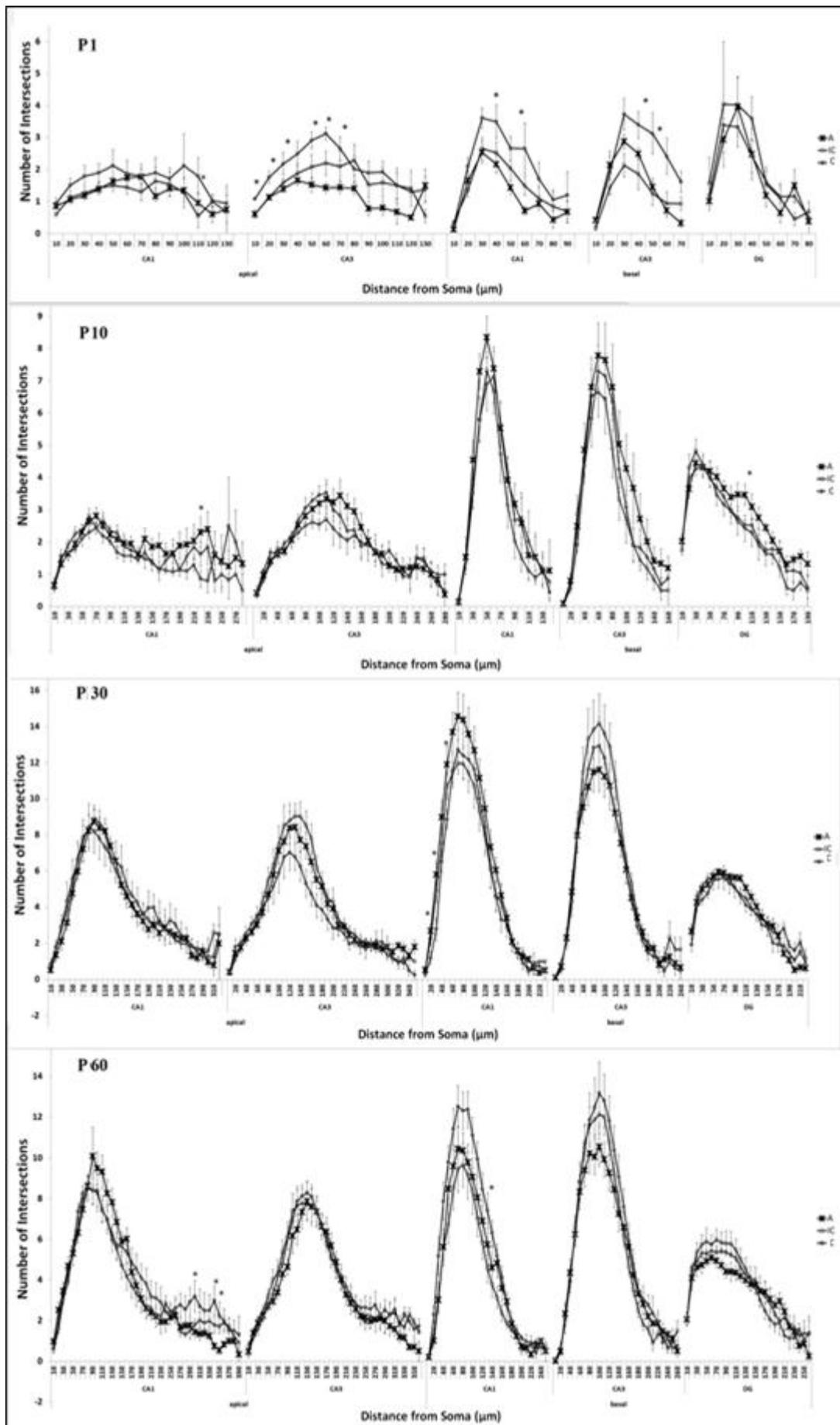
Figure 3.38. Sholl analysis of number of intersections of dendritic branches measured for each group, each hippocampal region, and each postnatal age, independently. The degree of significance is denoted as p≤0.05*, and error bars denote SEM.

The treatment effect was mostly seen at P1 dendrites. Two-way repeated measure ANOVA with sholl ring and treatment as independent variables yielded significant decrease in the intersections on the basal dendrites of CA1 neurons ($F_{(2:16)}$=7.576, p=0.005) and CA3 neurons ($F_{(2:19)}$=9.111, p=0.002). One-way ANOVA followed by post hoc LSD test revealed on P1, a significant decrease of the number of intersections between 40 and 60 μm from the soma (p≤0.05) in the basal dendrites of CA1 neurons and also between 50 and 60 μm from the soma (p≤0.05) in the basal dendrites of CA3 neurons in A group as compared to controls. It also showed a significant decrease of the intersections in alcohol group as compared to control groups, at P1, in the apical dendrites of CA1 neurons in the sholl ring at 220 μm from the soma (p=0.011) and in the sholl ring between 300 and 350 μm from the soma (p≤0.05) at P60. Moreover, in the basal dendrite of CA1 neurons at P30 between 20 and 50 μm from the soma (p≤0.05) and at P60 in the sholl ring at 120 μm from the soma (p=0.039), a significant decrease in the complexity of dendrites in the alcohol group was observed. On the contrary, in the DG neurons, a significant increase in the number of intersections was noted in the A group as compared to controls at P10 in the sholl ring at 100 μm from the soma (p≤0.05).

3.3.3. Immunohistochemistry Experiments

3.3.3.1. Synaptophysin Immunoreactivity

3.3.3.1.1. Cornu Ammonis 1 (CA1)
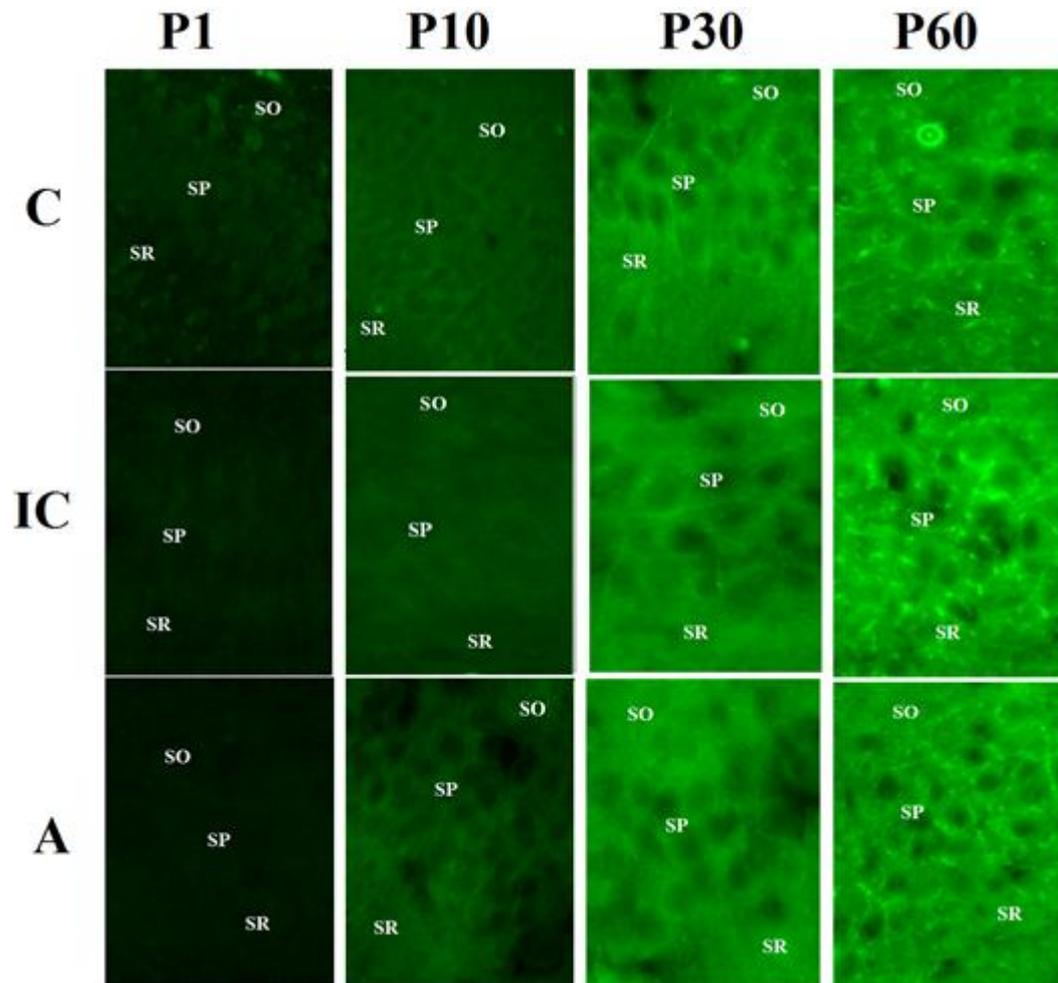
Figure 3.39. Photomicrographs showing SYP-immunoreactivity in CA1 region in alcohol (A) and control (IC and C) groups at different postnatal ages under 40X magnification. Abbreviations: SO (stratum oriens), SP (stratum pyramidale), SR (stratum radiatum).

As seen from Fig. 3.39, SYP immunostaining showed punctuated labeling pattern. Figure 3.40 presents the SYP-IR scores for each treatment group and each postnatal age in stratum oriens, stratum pyramidale, and stratum radiatum of the CA1 region.
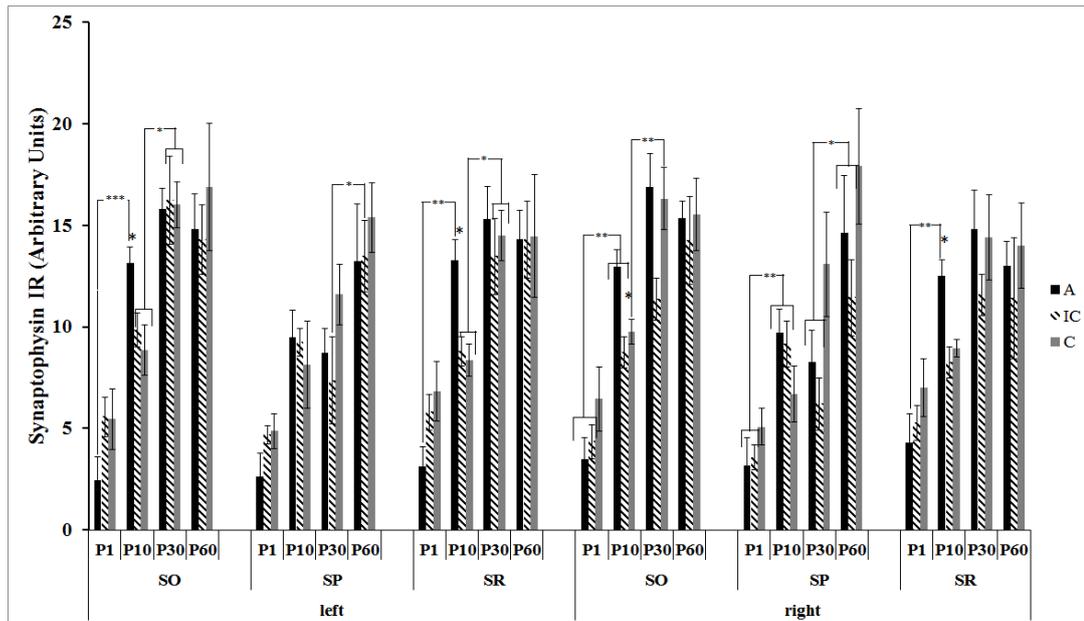
Figure 3.40. Comparison of SYP immunoreactivity in alcohol (A) and control (IC, PC) groups at different postnatal ages for both left and right in CA1 region of the hippocampus. Error bars denote ±SEM. Asterisks denote the level of significance at * p<0.05. Abbreviations: SO (stratum oriens), SP (stratum pyramidale), SR (stratum radiatum).

The overall level of SYP IR was higher in SO and SR than in SP of CA1 area.

Two-way ANOVA with age and treatment as independent factors was carried out on SYP-IR scores separately for SO, SP, and SR, in the left (L) and the right (R) CA1 region of the hippocampus. In both left and right hippocampus, in all hippocampal subregions, the main effect of age was highly significant ($p \leq 0.001$) while the age x treatment interaction was insignificant. The main effect of treatment was significant only in SO ($F_{(2:54)}=3.299$, $p=0.045$) and marginally significant in SP ($F_{(2:53)}=2.646$, $p=0.080$) of the right hippocampus.

In CA1 hippocampal subregion, a steady increase in SYP-IR was observed between P1-P30 in SO and SR, and throughout the whole 2 mo. postnatal period in SP (Fig. 3.40). One-way ANOVA with age as independent factor confirmed a significant increase in SYP-IR ($p \leq 0.01$) in A group, in all CA1 layers (except left SP), during P1-P10. In contrast to this, a greater increase in SYP-IR in the control groups, was taking place between P10-P30. Different temporal patterns of increase in SYP-IR in CA1 subregion in A and control groups resulted in a significant difference in SYP-IR level at P10 between these groups.

One way ANOVA performed on SYP-IR data for each age and each cell layer of CA1 subregion independently, revealed a significant main group effect on P10 in SO and SR layers in both left and right hippocampus ($F_{(2;15)}=6.362$, $p=0.009$; $F_{(2;18)}=10.118$, $p=0.001$, respectively for left hippocampus and $F_{(2;15)}=8.101$, $p=0.005$; $F_{(2;15)}=9.702$, $p=0.003$, respectively for right hippocampus). On P10, the recorded SYP-IR signal in SO and SR of both L and R hippocampi was significantly stronger in A group as compared to both controls ($p \leq 0.05$). In contrast to this, on P1, SYP-IR level in A group was lower than in control groups but this difference did not reach a required significance level.

3.3.3.1.2. Cornu Ammonis 3 (CA3)
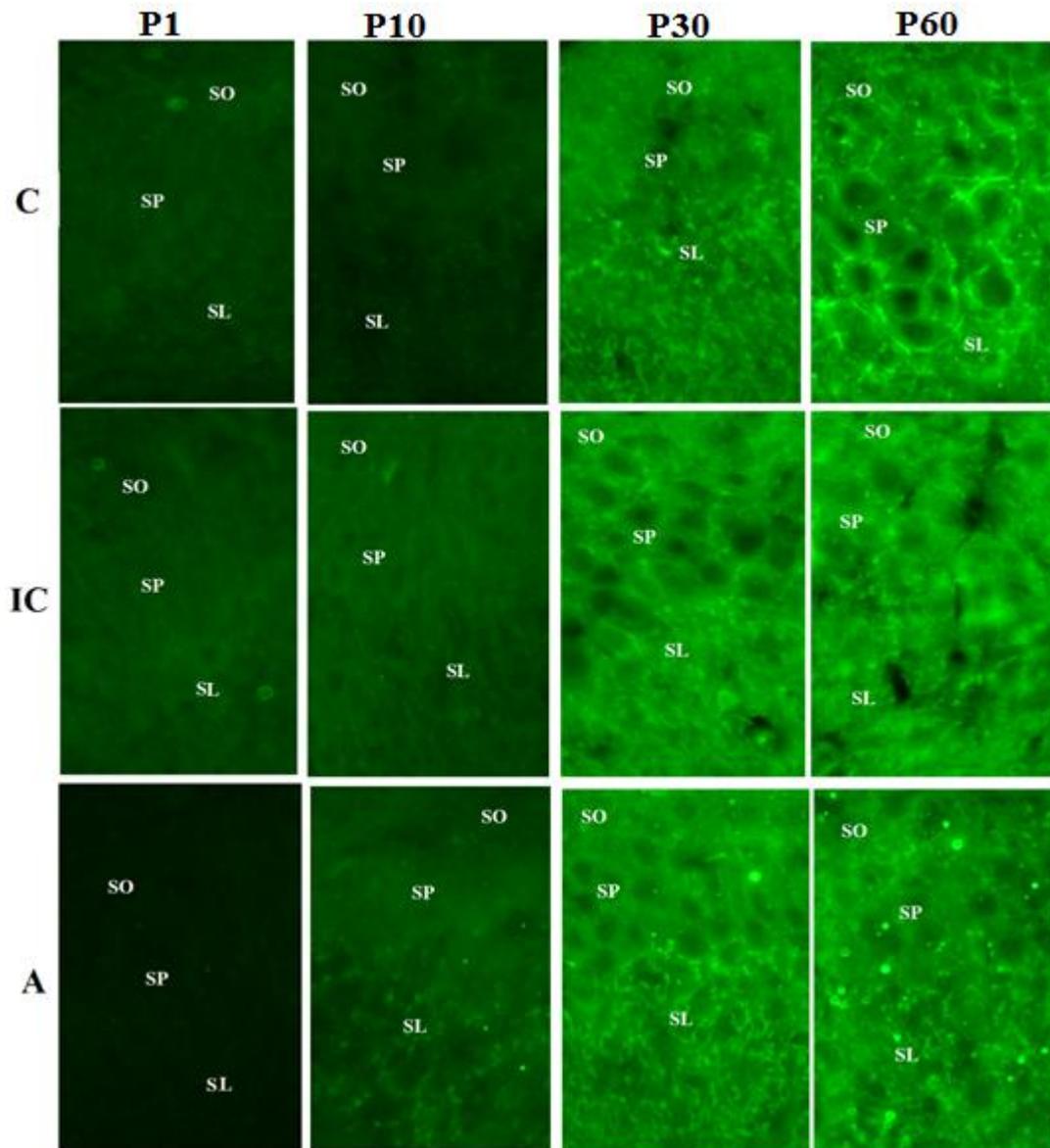
Figure 3.41. Photomicrographs showing SYP-immunoreactivity in CA3 region in alcohol (A) and control (IC and C) groups at different postnatal ages under 40X magnification. Abbreviations: SO (stratum oriens), SP (stratum pyramidale), SL (stratum lucidum).

Figures 3.41 and 3.42 present the tissue immunostaining against SYP and SYP-IR scores, respectively, in stratum oriens, stratum pyramidale, and stratum lucidum of the CA3 region for each treatment group and each postnatal age, independently
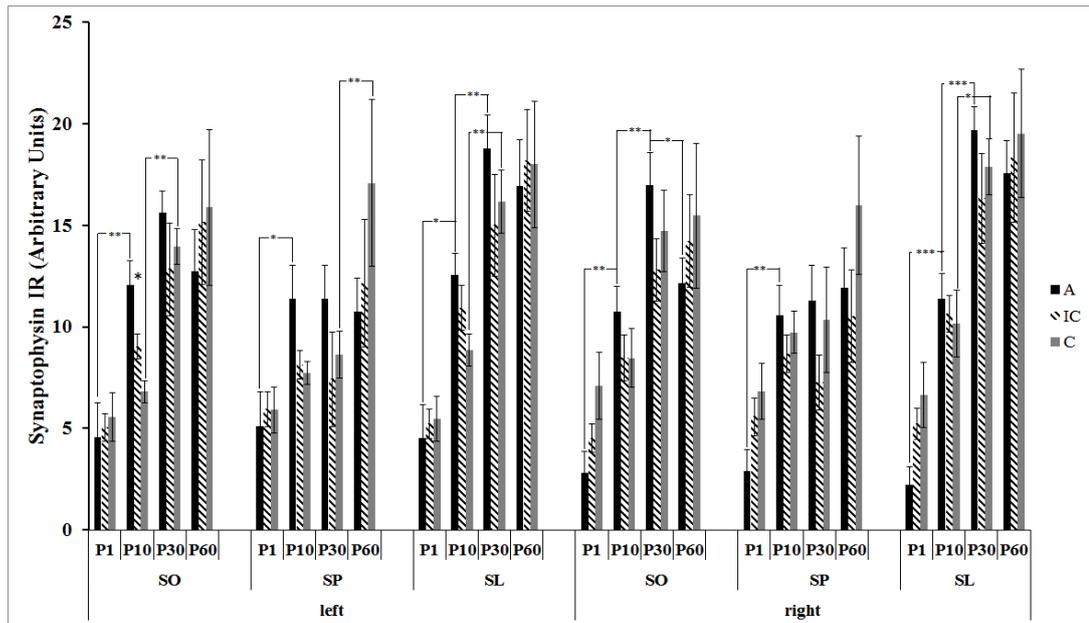
Figure 3.42. Comparison of SYP immunoreactivity in alcohol (A) and control (IC, PC) groups at different postnatal ages for both left and right CA3 regions of the hippocampus. Error bars denote ±SEM. Asterisks denote the level of significance at p<0.05. Abbreviations: SO (stratum oriens), SP (stratum pyramidale), SL (stratum lucidum).

Two-way ANOVA with age and treatment as independent factors was carried out on SYP-IR scores separately for SO, SP, and SL, in the left (L) and right (R) CA3 region of the hippocampus. In both left and right hippocampus, in all regions, the main effect of age was highly significant (p≤0.001) and the main effect of treatment and the age x treatment interaction were insignificant.

One-way ANOVA with age as independent factor applied to these data confirmed a similar temporal pattern of SYP-IR changes in CA3 layers to that observed in CA1 region. While in A group, a significant increase (p≤0.01) in SYP-IR was recorded in all layers of hippocampal CA3 area already at P10, in control groups it was recorded at P30 (p≤0.01). An increase in SYP-IR in the left CA3 SP continued until P60.

One-way ANOVA with treatment as independent factor performed on SYP-IR data for each age and each cell layer of CA3 subregion independently, revealed a significant group effect only in SO of left hippocampus at P10 with SYP-IR score significantly higher in the alcohol group as compared both control groups (p≤0.05) (Fig. 3.43).

3.3.3.1.3. Dentate Gyrus (DG)
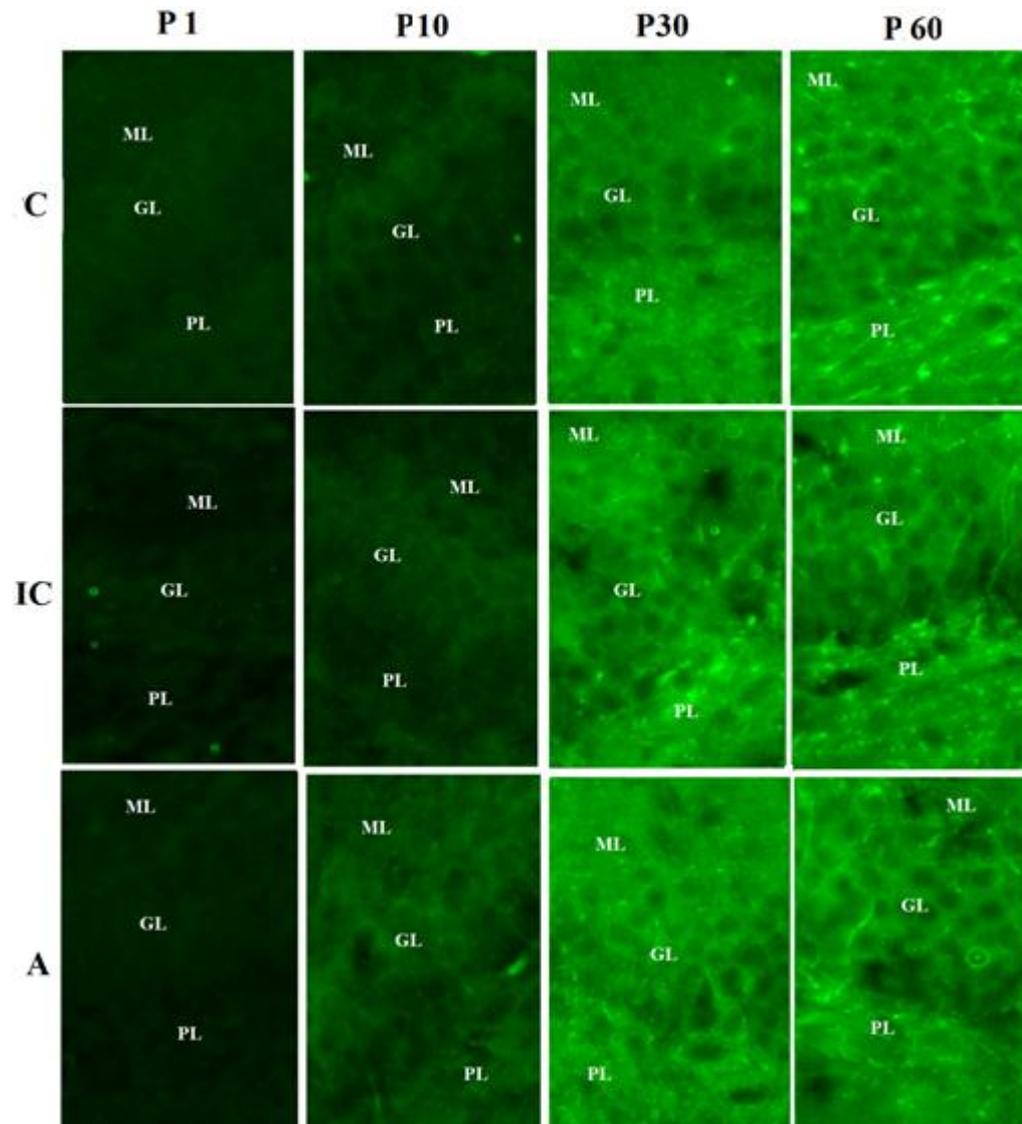
Figure 3.43. Photomicrographs showing SYP-immunoreactivity in DG region in alcohol (A) and control (IC and C) groups at different postnatal ages under 40X magnification. Abbreviations: ML (molecular layer), GL (granular layer), PL (polymorphic layer).

Figures 3.43 and 3.44 present the tissue immunostaing against SYP and SYP-IR scores, respectively, in molecular, granular, and polymorphic layer of the DG region for each treatment group and each postnatal age, independently.
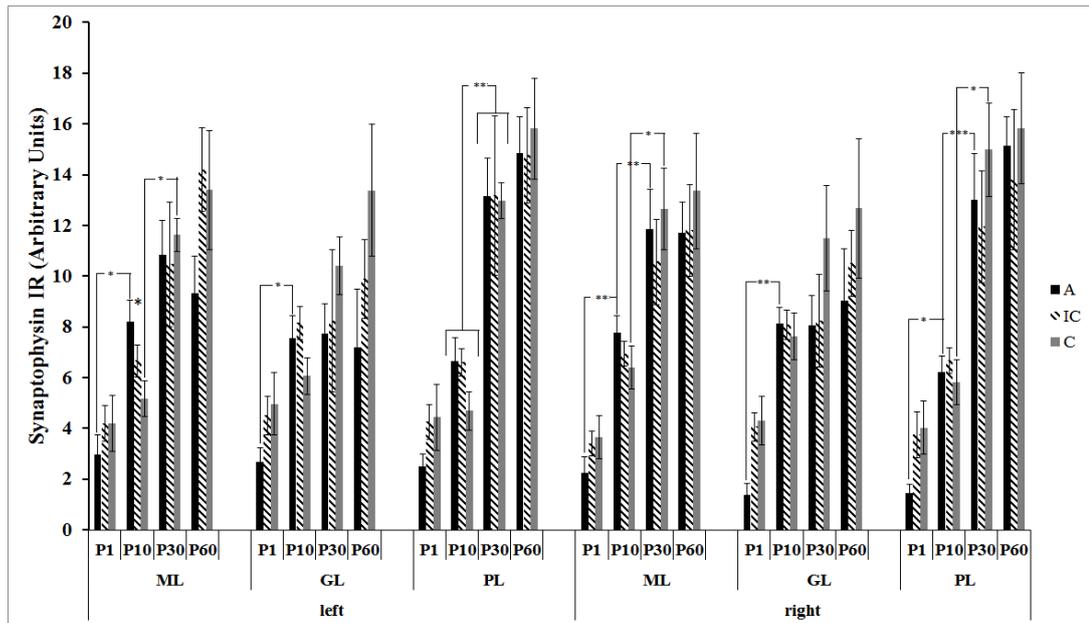
Figure 3.44. Comparison of SYP immunoreactivity in alcohol (A) and control (IC and C) groups at different postnatal ages for both left and right DG regions of the hippocampus. Error bars denote ±SEM. Asterisks denote the level of significance: $p<0.05^*$, $p<0.01^{**}$, $p<0.001^{***}$. Abbreviations: ML (molecular layer), GL (granular layer), PL (polymorphic layer).

Two-way ANOVA with age and treatment as independent factors was carried out on SYP-IR scores separately for ML, GL, and PL, in the left (L) and right (R) DG region of the hippocampus. In both left and right hippocampus, in all regions, the main effect of age was highly significant ($p\leq0.001$) and the main effect of treatment and the age x treatment interaction was insignificant.

As seen from the graphics, the overall levels of SYP-IR were lower in DG compared to CA subregions. Statistical analysis of SYP-IR in DG layers showed higher overall levels of SYP-IR in ML and PL compared to GL. Changes in SYP-IR across ages had similar temporal pattern as those observed in CA subregions with a significant SYP-IR increase in all DG layers, except PL, at P10 in A group and at P30 in controls (Fig. 3.44). A significant main effect of treatment (one-way ANOVA) was found only in ML of the left DG at P10 ($F_{(2;18)}=3.642$, $p=0.050$) with the higher level of SYP-IR in A group compared to C group ($p\leq 0.05$). At P1, the level of SYP-IR was generally lower in alcohol group as compared to controls. However, these differences did not reach the accepted level of significance.

3.3.3.2. Postsynaptic Density 95 (PSD-95) Immunoreactivity
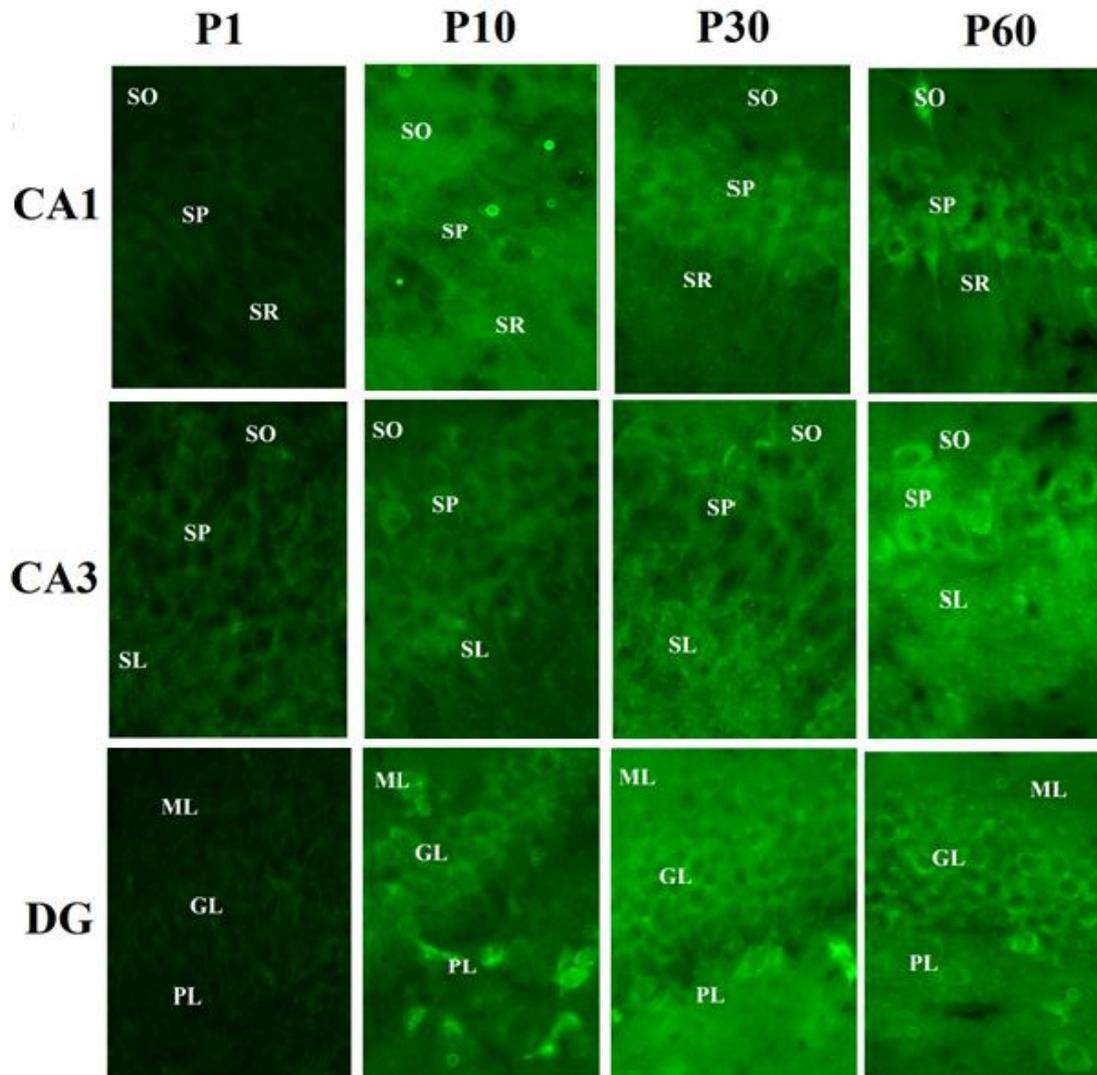
Figure 3.45. Representative photomicrographs showing PSD95-immunoreactivity in CA1, CA3, and DG regions at different postnatal ages in C group under 40X magnification. Abbreviations: SO (stratum oriens), SP (stratum pyramidale), SR (stratum radiatum), SL (stratum lucidum), ML (molecular layer), GL (granular layer), PL (polymorphic layer).

3.3.3.2.1. Cornu Ammonis 1 (CA1)

Fig. 3.46 presents levels of PSD-95 IR in different layers of the left and right hippocampal CA1 regions in A and control groups at different postnatal ages.
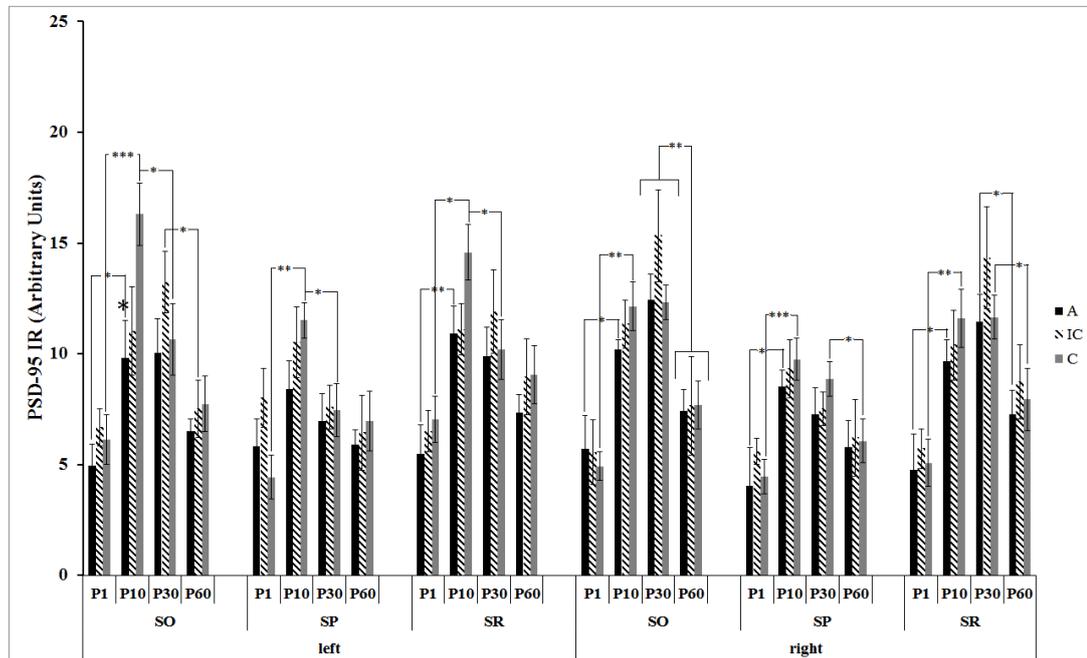
Figure 3.46. Comparison of PSD-95 immunoreactivity in alcohol (A) and control (IC and C) groups at different postnatal ages for both left and right CA1 regions of the hippocampus. Error bars denote ±SEM. Asterisks denote the level of significance: p<0.05*, p<0.01**, p<0.001***. Abbreviations: SO (stratum oriens), SP (stratum pyramidale), SR (stratum radiatum).

Two-way ANOVA with age and treatment as independent factors was carried out on PSD95-IR scores separately for SO, SP, and SR, in the left (L) and right (R) CA1 region of the hippocampus. In both left and right hippocampus, in all regions, the main effect of age was highly significant (p≤0.001) and the age x treatment interaction was insignificant.

As seen from the Fig, 3.46, the temporal pattern of postnatal changes in PSD95-IR levels in CA1 layers was different than that of SYP-IR changes. One-way ANOVA with age as independent factor applied to PSD-95 data confirmed a significant increase (p≤0.05) in PSD95-IR in all CA1 layers (except SP), and in all treatment groups during P1-P10 and then a significant decrease between P30-P60 (p≤0.05). The differences in the PSD95-IR between P1 and P60 were insignificant. The temporal pattern of PSD95-IR changes in CA1 subregion demonstrated reverse U shape with maximum PSD-95 expression at P10-P30.

One-way ANOVA analysis with treatment as independent factor performed for each age group and each cell layer separately yielded the main effect of treatment significant in the left CA1 SO ($F_{(2;67)}=3.326$, $p=0.042$) only where at P10, the density of PSD95-IR was lower in alcohol group compared to control (p≤0.05) (Fig. 3.47).

3.3.3.2.2. Cornu Ammonis 3 (CA3)

Fig. 3.47 presents levels of PSD95-IR in different layers of the left and right hippocampal CA3 region in A and control groups at different postnatal ages.
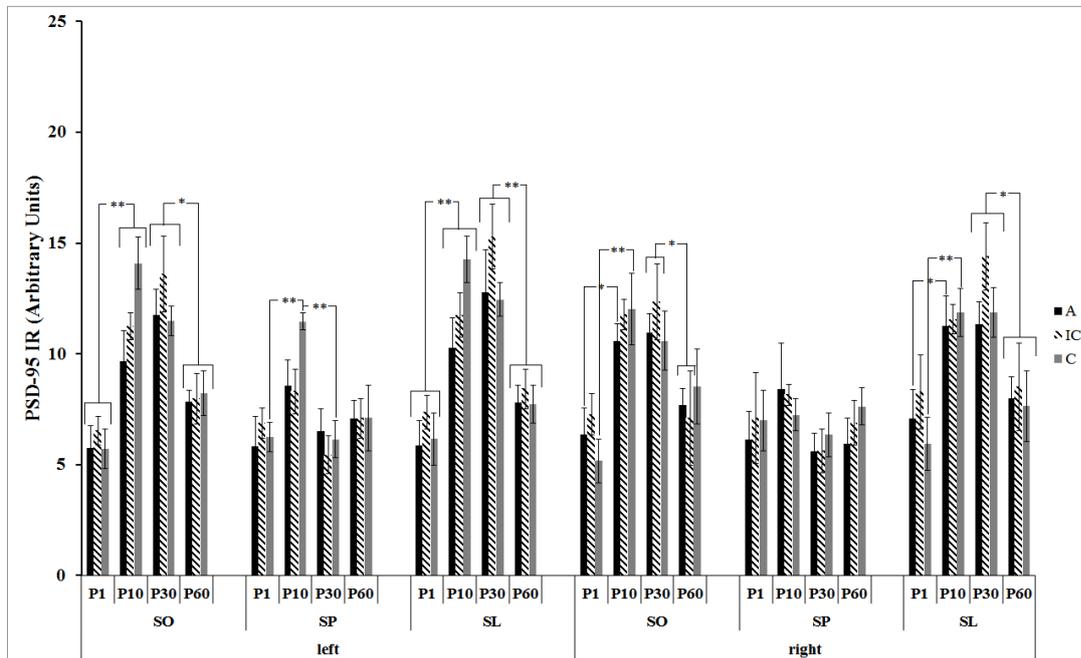
Figure 3.47. Comparison of PSD-95 immunoreactivity in alcohol (A) and control (IC and C) groups at different postnatal ages for both left and right CA3 region of the hippocampus. Asterisks denote the level of significance: p<0.05*, p<0.01**. Error bars denote ±SEM. Abbreviations: SO (stratum oriens), SP (stratum pyramidale), SL (stratum lucidum).

Two-way ANOVA with age and treatment as independent factors was carried out on PSD95-IR scores separately for SO, SP, and SL, in the left (L) and right (R) CA3 region of the hippocampus. In both left and right hippocampus, in all regions, the main effect of age was highly significant ($p \leq 0.001$) and the age x treatment interaction was insignificant. However, the main effect of treatment was marginally significant in PSD95-IR of left CA3 SL ($F_{(2;71)}=2.669$, p=0.076).

The temporal pattern of PSD-95 IR changes across postnatal ages in SO and SL was the same as in CA1 region. The age-dependent changes in PSD-95 IR in SP were negligible. According to one way ANOVA results, in all layers, there was no significant between-group differences in both left and right CA3 (Fig. 3.47).

3.3.3.2.3. Dentate Gyrus (DG)

Fig. 3.48 presents levels of PSD95-IR in different layers of the left and right DG in A and control groups at different postnatal ages.
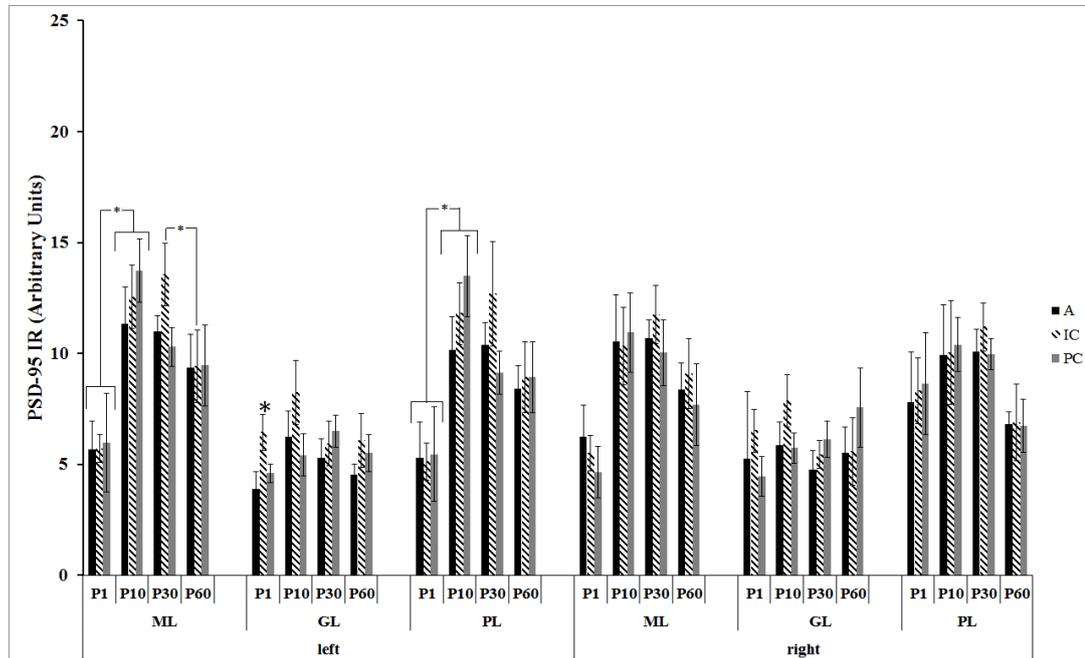
**Figure 3.48.** Comparison of PSD-95 immunoreactivity in alcohol (A) and control (IC and C) groups at different postnatal ages for both left and right DG regions of the hippocampus. Error bars denote ±SEM. Asterisks denote the level of significance: * p<0.05. Abbreviations: ML (molecular layer), GL (granular layer), PL (polymorphic layer).

Two-way ANOVA with age and treatment as independent factors was carried out on PSD-95 IR scores separately for ML, GL, and PL, in the left (L) and right (R) DG. In both left and right hippocampus, in ML and PL, the main effect of age was highly significant (p≤0.001) and the age x treatment interaction was insignificant. However, the main effect of treatment was significant in PSD95-IR of left DG GL ($F_{(2;65)}$=3.263, p=0.045) (Fig. 3.48).

The temporal pattern age-dependent changes in PSD-95 IR similar to that observed in CA subregions were noted in ML and PL of both L and R DG, however these changes reached a required level of significance only in L DG ($F_{(2;17)}$=3.726, p=0.049).

85

3.3.3.3. Doublecortin (DCX) Immunoreactivity
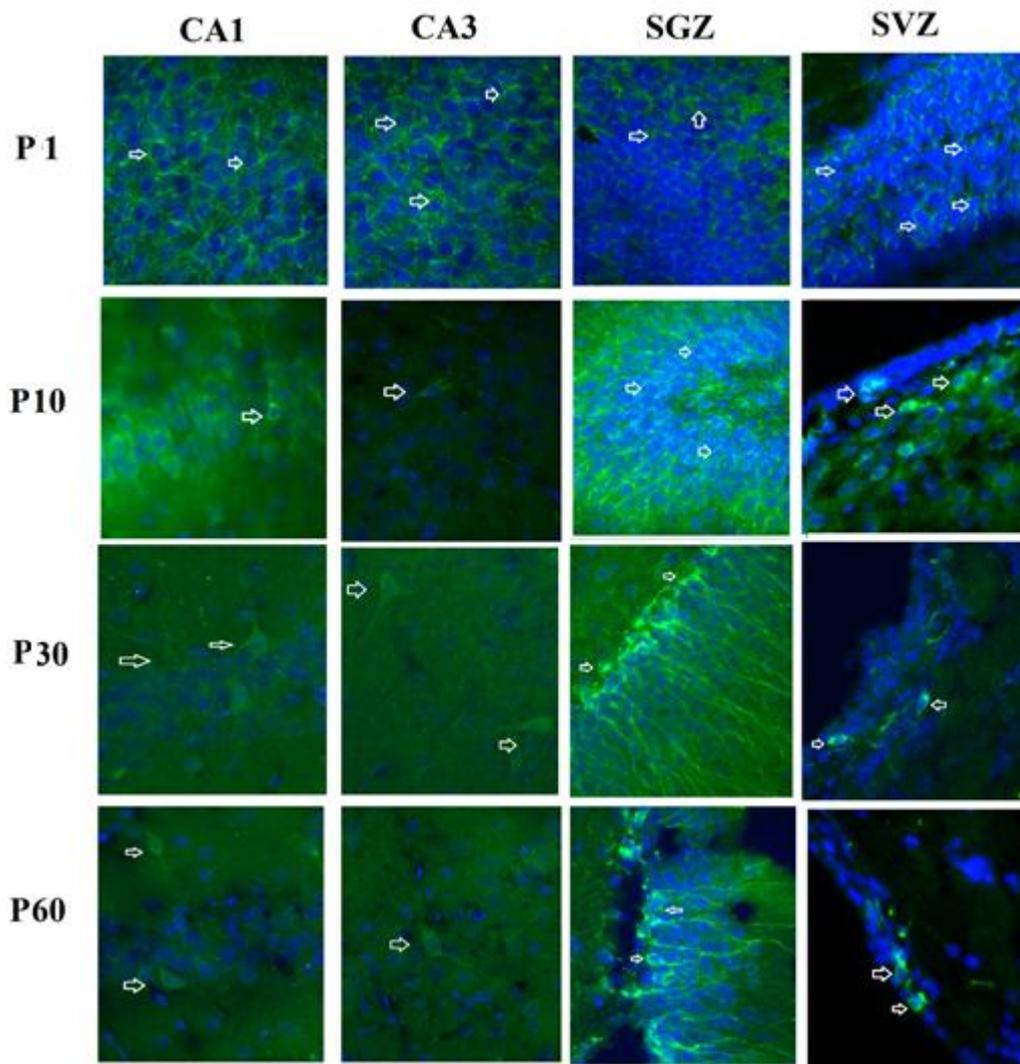
Figure 3.49. Representative photomicrographs showing DCX-immunoreactivity of CA1, CA3, SGZ, and SVZ regions for all experimental ages under 40X magnification in control group (arrows shows the DCX-positive cells) (green: DCX, blue: DAPI (nuclear stain).

Figures 3.49 and 3.50 present the tissue immunostaing against DCX and DCX-IR scores, respectively, in CA1, CA3, SGZ, SVZ region of hippocampus for each treatment group and each postnatal age, independently.
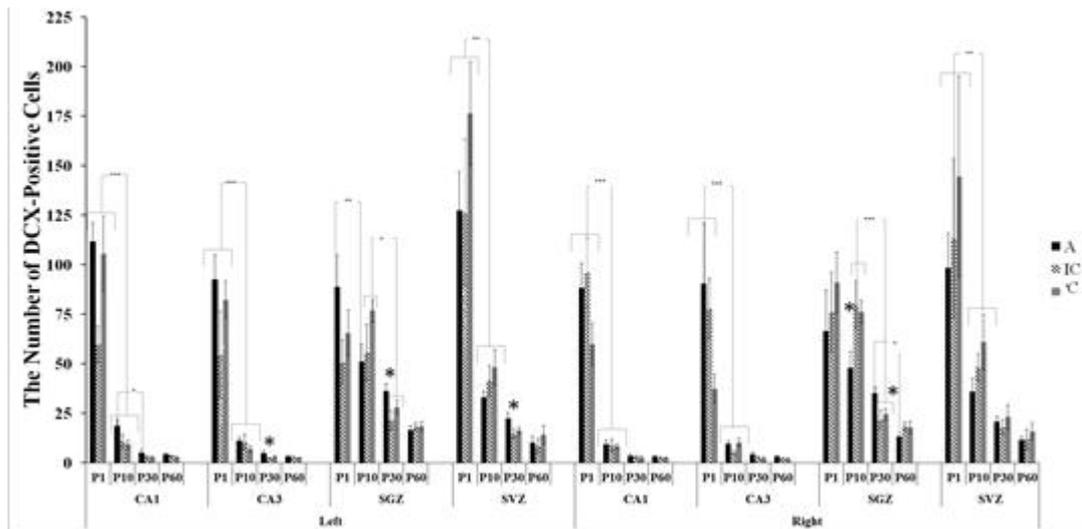
**Figure 3.50**. Comparison of the numbers DCX-IR neurons immunoreactivity in alcohol (A) and control (IC and C) groups at different postnatal ages for both left and right CA1, CA3, SGZ, SVZ regions of the hippocampus. Error bars denote ±SEM. Asterisks denote the level of significance: p<0.05*, p<0.01**, p<0.001***.

Two-way ANOVA with age and treatment as independent factors was carried out on DCX IR scores separately for all four regions in the left (L) and right (R) hippocampus. In both left and right hippocampus, in all regions, the main effect of age was highly significant ($p \leq 0.001$). In both left and right CA1 region and right CA3, the main effect of treatment was significant ($F_{(2;70)}=3.669$, p=0.031, $F_{(2;54)}=3.090$, p=0.054, and $F_{(2;54)}=3.567$, p=0.035, respectively). The age x treatment interaction was significant in left and right CA1 ($F_{(6;70)}=2.468$, p=0.032, $F_{(6;54)}=2.218$, p=0.055, respectively) and in right CA3 ($F_{(6;54)}=3.204$, p=0.009), and it was marginally significant in left SGZ ($F_{(6;70)}=1.980$, p=0.080).

The estimates of DCX-IR cell counts were the highest at P1 and then showed a linear decline in SGZ and exponential decline in hippocampal CA regions and SVZ. Regardless of treatment, in all regions, except SGZ, a significant decrease in DCX-IR cell counts was recorded between P1-P10. In SGZ, the greatest decrease was observed between P10-P30.

According to the results of one-way ANOVA with treatment as independent variable, at birth and on P10, there were no significant between-group differences found in the left hippocampus. However, at P30, there was a marginally significant difference between alcohol and control groups in CA3, SGZ and SVZ layers ($F_{(2;21)}=3.265$, p=0.060; $F_{(2;21)}=3.364$, p=0.056; and $F_{(2;21)}=3.100$, p=0.068, respectively). Post hoc LSD test showed that the alcohol group had significantly higher number of DCX-positive neurons compared to both IC and C control groups in CA3 (p=0.025, p=0.069, respectively), in SGZ (p=0.018 for IC), and in SVZ (p=0.029, and p=0.074, respectively). There was no statistically significant difference between control groups (Fig. 3.50).

On the right hippocampus, at P10, a decrease in the DCX-positive neurons in SGZ in alcohol group reached a statistically significant level ($F_{(2;15)}=3.827$, p=0.049). According to post hoc LSD results alcohol group was statistically lower than both control groups (p=0.027 for IC and p=0.058 for C). However, to compensate this decrease, a fast increase in the migrating neurons in the alcohol group produced a significant between group differences at P30 ($F_{(2;20)}=3.686$, p=0.046). This change was reached significant level between alcohol and both control groups (p=0.019 for IC and, p=0.055 for C).

In the right SGZ, at P10, the count of DCX-positive neurons in alcohol group was statistically lower than in both control groups (p=0.027 for IC and p=0.058 for C). However, on P30, the count of DCX-IR cells was significantly higher as compared to both controls (p=0.019 for IC and, p=0.055 for C).

3.3.4. Western Blotting Studies

3.3.4.1. Quantitative Immunoblot Analysis of SYP Levels in The Left Hippocampus

In the Western blot analysis, SYP protein band was detected at 38 kDa (Fig.3.51). Relative SYP protein concentrations were determined by comparing band intensities with that of β-Actin. β-Actin having a molecular weight of 42 kDa was used as the internal sample loading control (Fig.3.52).
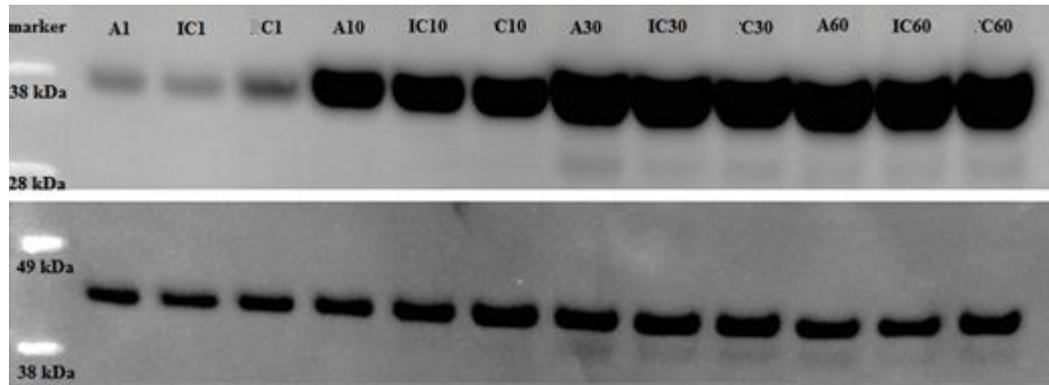
Figure 3.51. Immunoreactive protein bands representing SYP (38kDa) from the left hippocampus in control (IC and C) and alcohol (A) groups at the ages of P1, P10, P30, and P60. The β-Actin band (42 kDa) was used as an internal control.
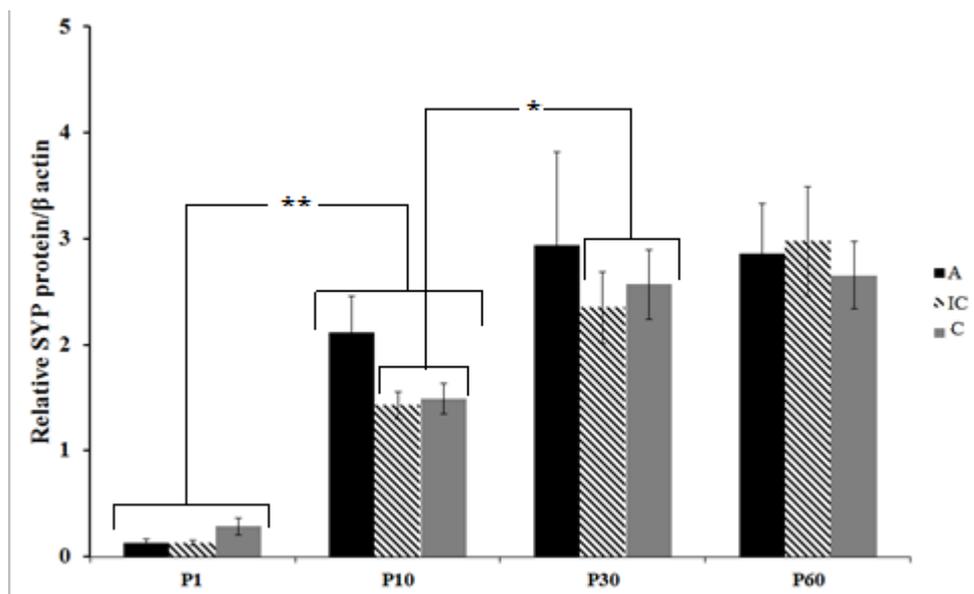
Figure 3.52. Comparison of the SYP levels in the left hippocampus of control (IC and C) and alcohol (A) groups at the ages of P1, P10, P30, and P60. Band quantification is expressed as the mean ± SEM of the relative intensity with respect to that of β-Actin.

Two-way ANOVA with age and treatment as independent factors was carried out on Western blot data for the whole left hippocampus. The main effect of age was highly significant ($F_{(3;60)}$=30.011, p≤0.001), and the main effect of treatment and the age x treatment interaction were insignificant.

According to the results of one-way ANOVA with age as independent factor performed for each treatment group separately, in all groups, there was a significant increase in the expression of SYP between P1-P10 and P10-P30 ($F_{(3;23)}$=6.140, p=0.004 for A; $F_{(3;23)}$=15.481, p≤0.001 for IC; $F_{(3;23)}$=20.945, p≤0.001 for C). However, the temporal pattern of these changes differed between groups. As seen from Fig. 3.52, while in the alcohol group, a significant increase was recorded during

P1-P10 period, in both control groups, a significant increase in the hippocampal expression of SYP protein continued during P10-P30 period.

Quantitative immunoblot analysis of SYP levels in the left hippocampus done by one-way ANOVA revealed marginally significant between-group difference in the expression of SYP protein only in P1 and P10 ($F_{(2;17)}$=2.926, p=0.085, $F_{(2;17)}$=2.887, p=0.087, respectively). At P1 in alcohol group a level of SYP protein was lower and at P10 higher compared to both control groups (Fig. 3.52).

3.3.4.2. Quantitative Immunoblot Analysis of PSD-95 Levels in the Left Hippocampus

In the Western blot analysis, PSD-95 protein band was detected at 95 kDa (Fig. 3.53). Relative PSD-95 protein concentrations were determined by comparing band intensities with that of β-Actin. β-Actin having a molecular weight of 42 kDa was used as the internal sample loading control (Fig. 3.54).
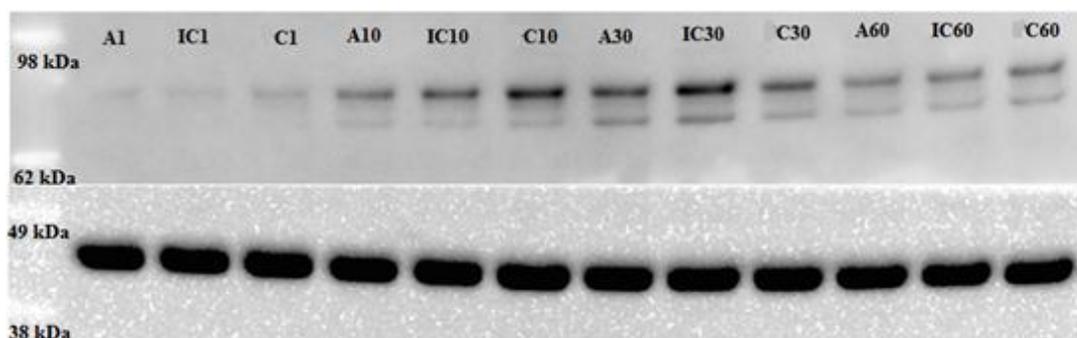
Figure 3.53. Immunoreactive protein bands representing PSD-95 (95kDa) from the left hippocampus in control (IC and C) and alcohol (A) groups at the ages of P1, P10, P30, and P60. The β-Actin band (42 kDa) was used as an internal control.
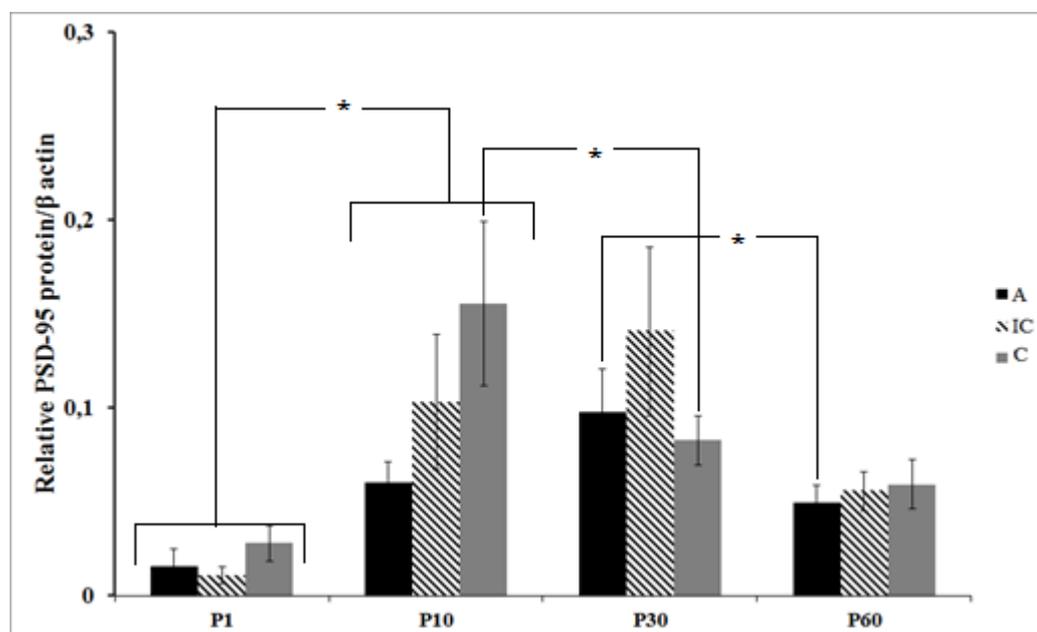
Figure 3.54. Comparison of the levels of PSD-95 protein in the left hippocampus of control (IC and C) and alcohol (A) groups at the ages of P1, P10, P30, and P60. Band quantification is expressed as the mean ±SEM of the relative intensity with respect to that of β-Actin.

Two-way ANOVA with age and treatment as independent factors was carried out on Western blot data for PSD-95 in the whole left hippocampus. The main effect of age was highly significant

($F_{(3;60)}=10.196$, p≤0.001), and the main effect of treatment and the age x treatment interaction were insignificant.

To analyze the temporal pattern of changes in PSD-95 levels during postnatal development, one-way ANOVA with age as independent factor applied to each treatment group, separately. According to the results of this analysis, a significant increase in the hippocampal PSD-95 concentration was observed in A, IC, and C groups (($F_{(3;19)}=5.810$, p=0.007, $F_{(3;19)}=3.700$, p=0.034. and $F_{(3;19)}=4.996$, p=0.012, respectively) between P1-P10. This was followed by an overall decrease in the hippocampal PSD-95 level. This decrease reached an accepted significance level in C group between P10-P30 and in A group between P30-P60.

Resuming the results of Western blot analysis, a significant overall increase in the hippocampal expression of SYP protein was observed between P1-P30 reaching a plateau level between P30-P60, while the changes in the overall hippocampal levels of PSD-95 demonstrated inverted U shape with an initial significant increase during P1-P30 followed by a significant decrease during P30-P60.

CHAPTER 4

DISCUSSION

4.1. Behavioral changes observed during postnatal development in fetal-alcohol and control rats

The administration of ethanol to the pregnant rat dams at the dose of 6g/kg body weight/day throughout the gestation days 7-20 resulted in the mean BAC of 246.6 ± 40.9 mg/dl and caused an increase in the abortion incidents and a decrease in the neonatals' survival rate. In addition, pups from A group showed lower body weight during early postnatal ages (P1 and P10) and some individuals displayed oral anomalies. These observations are consistent with previous reports about increased fetal death and birth defects as well as reduction in the litter size and body weight at birth among pups exposed to alcohol *in utero* (Ba, 2009; Spong *et al.,* 2001).).

Fetal intoxication by ethanol was also reported to cause diverse behavioral deficits including hyperactivity, affective disorders, and cognitive impairments (Abel and Reddy, 1997; Abel and Dintcheff, 1978; Girard *et al.,* 2000). However, in the present study, neither juvenile nor adult fetal-alcohol rat pups manifested the locomotor hyperactivity. Instead, they showed a normal course of habituation to a new environment demostrated by a steady decrease in the overall locomotor activity as a function of time spent in the open field. In the literature, the effects of prenatal ethanol exposure on activity in rats is an controversial issue. Some authors reported an increased activity (Martin *et al.*, 1978; Osborne *et al.*, 1979; Bond, 1981; Ulug and Riley, 1983; Meyer and Riley, 1986; Vorhees and Fernandez, 1986), others did not (Vorhees, 1989; Wigal and Amsel, 1990; Westergren *et al.*, 1996; Carneiro *et al.*, 2005). In their recent publication, Downing and co-workers (2009) also reported lack of an effect of fetal ethanol administration on the locomotor activity in 30 and 60 days old mice pups with overall locomotor activity significantly higher in juveniles as compared to young adults.

In the present study, no significant difference was also found between the A and IC groups in the level of anxiety as assessed by the rats' behavior in the plus maze task. Interestingly, independent of the treatment, juvenile rats showed higher level of anxiety compared to young adults spending relatively more time in closed than in the open arms of the plus maze. The latter finding demonstrates that age-specific behavioral patterns may easily confound the drug effects.

The controversial results regarding fetal ethanol effects on animals' locomotor activity and anxiety may be related to ethanol dose applied and timing of ethanol exposure,. The prenatal period in small rodents was previously reported to be less sensitive to teratogenic ethanol effects than the early postnatal, brain growth spurt period corresponding to the third thrimester in human (Shah and West 1984, Smith *et al.,* 2012, Tran and Kelly, 2003).

In the present study, the effect of fetal-alcohol on behavior was limited to a significantly worse performance of juvenile rat pups in the hippocampus-dependent spatial reference memory task, the place learning in the MWM, carried out under both allothetic and idiothetic stimulus conditions. This was an expected result considering previously reported high vulnerability of the hippocampus to the teratogenic alcohol effects (Bonthius and West, 1990**;** Goodlett *et al.,* 1997; Livy *et al.,* 2003; Mihalick *et al.*, 2001; Miki *et al*., 2003). However, these learning deficits ameliorated with maturation and could not be detected in the young adult subjects. The behavioral results presented in this study are consistent with our previous findings (Dursun *et al.,* 2006) and some earlier reports by other authors (Blanchard *et al.,* 1987; Cronise *et al.,* 2002; Gianoulakis, 1990; Girard *et al.,* 2000; Goodlett

and Peterson, 1995; Goodlett and Johnson, 1997, Nagahara and Handa, 1997; Pauli *et al.,* 1995; Thomas *et al.,* 1996, Clausing *et al.,* 1995, Minetti *et al.,* 1996) and suggest a functional recovery taking place with maturation in the animals exposed *in utero* to ethanol.

Therefore, as it was earlier stated, the aim of this study was to examine developmental changes occurring postnatally in the hippocampus of normal and fetal-alcohol rat pups to find developmental delays or deficits, as well as potential compensatory processes that would correlate with cognitive impairments frequently observed in juveniles and ameliorating in young adults.

The morphological studies included unbiased stereology to investigate changes in neuron numbers and hippocampal volumes, the postnatal tracing and analysis of the morphology of the principal hippocampal neurons, investigation of age-dependent changes in the distribution of doublecortin expressing neurons (an index of neurogenesis), and evaluation of synaptic development by assessing age-dependent changes in the regional immunoreactivity/expression of synaptophysin and PSD-95.

4.2. Changes in hippocampal volumes and neuron counts observed during postnatal development in fetal-alcohol and control rats

In this study, using unbiased stereology technique, changes in neuron numbers in the granular layer of DG and the pyramidal layers of CA1 and CA2+3 hippocampal subregions were investigated throughout a protracted postnatal period from birth to maturity, in control and fetal-alcohol rat pups belonging to the same laboratory rat strain.

In the present study, on P1, no significant difference was found in the cell counts between the three hippocampal subregions in fetal alcohol and control rats. In all groups, regardless of the treatment, an increase in the counts of principal hippocampal neurons was observed between P1-P60; however, the temporal pattern of these changes was region- and treatment-specific. The greatest overall increase in neuron counts was recorded in the time period between P1-P10 ($p \leq 0.001$) referred to as the brain growth spurt. This increase was much faster in DG compared to CA subregions resulting in a significant difference in cell counts between DG and CA regions already at P10. In CA1 and CA2+3 areas, the postnatal increase in neuron numbers slowed between P10-P30 again accelerating between P30-P60 ($p \leq 0.05$). This bi-phasic pattern of neuron number increase was observed in control groups but not in the alcohol group wherein a more linear rise in cell counts was noted. Over the first two postnatal months, the number of pyramidal cells in CA regions doubled, while the increase in the number of granular cells in DG was 5.8 fold.

In all three groups, during the first two postnatal months, a steady increase in the estimated volume of the three hippocampal regions was recorded. The time courses of the changes in neuron count (biphasic) and volume of the pyramidal layer (linear) are not always parallel. It may suggest that the volume increase between P10-P30 is primarily due to an increase in neuron size and/or gliogenesis.

Our findings are consistent with previous reports showing that in many mammals including human and rat, the brain growth and the increase in neuron number are not completed at birth but continue postnatally (Bandeira *et al.,* 2009; Bayer, 1980b). In the present study in accordance with the literature, the fastest increase in neuron counts was recorded within P1-P10 time window covering so called brain growth spurt period (Bonthius and West, 1991; Dobbing and Sands, 1979; Goodlett *et al.,* 1990; Napper and West, 1995). According to our estimates, regardless of the treatment, the increase in neuron number was by 50% in CA and almost 3-fold in DG during the first 10 postnatal days, and approximately 85% of all hippocampal neurons were generated within the time window between P1 and P30 which is highly consistent with the previous estimates by Bayer (1980a). An increase in the neuron number within DG, observed in this study throughout the first two postnatal months, also agrees with previous reports by other authors. Already in 1965, Altman and Das postulated the presence of newly generated dentate granule cells in the postnatal rat hippocampus. Later on, Bayer and co-workers (1982) demonstrated an increase in the total number of granular cells in rat dentate gyrus from birth up-to one year of life. Our results together with the low coefficient error (0.03) confirm the accuracy of the neuron number estimates in the present study. There is, however, a contradiction between a significant increase in the neuron counts in the hippocampal CA regions observed in the present study during P10-P30 and P30-P60 time windows and some previous reports according to which the increase in the neuron numbers in cornu ammonis is completed by the end of the first postnatal week (Bandeira *et al.,* 2009, Bayer *et al.,* 1993). There are, however, very few

studies wherein the changes in the numbers of hippocampal neurons were traced throughout an extended postnatal period and the discrepancies in the obtained results may arise from the variation in estimation methods. For instance, Bandeira *et al.,* (2009) reporting the completion of neuron addition in rat CA region during the first postnatal week estimated neuron numbers by counting only nuclear antigen (NeuN) marked isolated nuclei in suspension using the isotropic fractionator method. Restricting the cell counting to NeuN marked nuclei may produce underestimated results since a developmental delay in acquisition of NeuN by neurons has been previously reported. Lyck *et al.,* (2007) showed that on P8, only 65% of the whole neuron population in the neocortex, expressed the marker characteristic for postmigratory mature neurons. On the other hand, however, in another recently published study by Morterá and Herculano-Houzel (2012) who applied the same method of cell counting as Bandeira and co-workers (2009), a continuous increase in neuron numbers was demonstrated in varies brain regions including hippocampus throughout the period from birth to adolescence (2-3 months of age). Afterwards, a progressive decline in neuronal counts occurring with aging was observed. Gokcimen and colleagues (2007) using optical fractionator technique also have found the total pyramidal cell number in hippocampal CA area in 20 weeks old rats as compared to 4 weeks old rats. Parallel to this, using the same technique, Smith *et al.,* (2008) found an increase in the cell number of hippocampal CA area between P9 and P68.

If neuronal death is one of the essential processes during postnatal brain development (Buss *et al.,* 2006; Clarke, 1985; Low and Cheng, 2006), a net increase in the number of principal neurons observed in the present and some other studies during the first two months after the birth in all hippocampal subregions studied suggests that, during this period, neuron addition may be prevailing over neuron deletion. Net increase in the cell number apparently implicates neurogenesis. An increase in the numbers of granular cells in both control and experimental animals throughout the two postnatal months is not surprising since the life-long neurogenesis in dentate gyrus has been well documented (Bayer *et al.,* 1982, Kaplan and Bell, 1983; Veena *et al.,* 2011). According to the results of these studies, an increase in the total number of dentate neurons taking place after P10 corresponds to the formation of the thicker inner shell of the granular layer deriving from an intrinsic, tertiary germinal matrix (Altman and Bayer, 1990). After P30, the tertiary dentate matrix was reported to disappear in the basal polymorph layer and proliferative cells became largely confined to the subgranular zone in the intrahilar region thereby becoming the final source of granular cells produced during the juvenile and adult periods. In contrast to dentate gyrus, neurogenesis in the cornu ammonis was postulated to terminate during early postnatal period. However, when employing a prolonged bromodeoxyuridine (BrdU) labeling protocol facilitating detection of cells which cell cycle increased with age, Rietze and colleagues (2000) identified mitotic activity in multiple regions of the adult mice hippocampus, including CA region, with some of newly generated neurons detected directly within the pyramidal cell layer. In addition, a massive migration of neuroblasts from the subventricular zone (SVZ) not restricted to the rostral migratory stream (RMS) but dispersing into several adjacent cortical and subcortical areas was shown in mice during postnatal life (Inta *et al.,* 2008). In the latter study, the postnatal genesis and migration of a distinct GABAergic phenotype was traced, however, these experiments demonstrated that during postnatal life, the SVZ in addition to supplying neurons to the RMS and olfactory bulb may supply newborn cells also to other brain areas.

The neuron number estimates obtained in our study for the intact control group at different postnatal ages, in different hippocampal subfields are generally comparable with the results of previous studies that also used unbiased stereology methods (Table 5).

Some discrepancies in cell counts reported by different research groups may arise from using different animal strains, the differences in applied stereological methodology, and including or excluding CA2 field from cell counting. Additionally, a significant lateral asymmetry was demonstrated for CA1 and CA2+3 subfields, with the right hemisphere containing respectively 21% and 6% fewer neurons (Lister *et al.,* 2006). If so, cell counts confined to the left hippocampi, just like in the present study, may result in higher cell numbers.

Table 5. Comparison with Previous Stereological Estimates of Neuronal Number in Subregions of the Male Rat Hippocampus in Control Rats Using the Optical Fractionator Technique

Hipp. Areas	Cell number	Rat strain	Age	Reference
CA1	150,000	W	**1 day**	Elibol-Can *et al.* present
			10±5 days	
	250,000	W	10 days	Elibol-Can *et al.* present
	177,000	SD	9 days	Smith *et al.*, 2008
	201,291	SD	10 days	Livy *et al.*, 2003
	239,000	SD	10-12 days	Maier and West, 2001b
			30± 5 days	
	280,000	W	30 days	Elibol-Can *et al.*, present
	403,930	W	30 days	Sousa *et al.*, 1998
	382,000	W	30 days	West *et al.*, 1991
			≥ 60 days	
	350,000	W	60 days	Elibol-Can *et al.*, present
	262,181	SD	154–160 days	Fitting *et al.*, 2010
	238,000	SD	68 days	Smith *et al.*, 2008
	330,998	SD	90 days	Lister *et al.*, 2005
	420,524	W	180 days	Sousa *et al.*, 1998
CA2+3	150,000	W	**1 day**	Elibol-Can *et al.* present
			10±5 days	
	250,000	W	10 days	Elibol-Can *et al.* present
	146,000	SD	9 days	Smith *et al.*, 2008
	347,157	SD	10 days	Livy *et al.*, 2003
	293,000	SD	10-12 days	Maier and West, 2001b
			30± 5 days	
	280,000	W	30 days	Elibol-Can *et al.*, present
	244,647	W	30 days	Sousa *et al.*, 1998
	250,000	W	30 days	West *et al.*, 1991
			≥ 60 days	
	340,000	W	60 days	Elibol-Can *et al.*, present
	416,498	SD	154–160 days	Fitting *et al.*, 2010
	368,000	SD	68 days	Smith *et al.*, 2008
	181,570	SD	90 days	Lister *et al.*, 2005
	239,615	W	180 days	Sousa *et al.*, 1998
DG	200,000	W	**1 day**	Elibol-Can *et al.* present
			10±5 days	
	520,000	W	10 days	Elibol-Can *et al.* present
	423,417	SD	10 days	Livy *et al.*, 2003
	466,000	SD	10-12 days	Maier and West, 2001b
			30± 5 days	
	800,000	W	30 days	Elibol-Can *et al.*, present
	944,030	W	30 days	Sousa *et al.*, 1998
	1,200,000	W	30 days	West *et al.*, 1991
			≥ 60 days	
	1,000,000	W	60 days	Elibol-Can *et al.*, present
	654,000	SD	68 days	Smith *et al.*, 2008
	1,172,290	SD	154–160 days	Fitting *et al.*, 2010
	1,182,100	W	180 days	Sousa *et al.*, 1998

Interestingly, control pups born from intubated dams manifested significantly higher cell counts in CA regions on P1 and P10, compared to intact control and fetal alcohol pups. Fetal alcohol pups also showed asignificantly higher pyramidal cell count in CA2+3 regions on P10 as compared to the intact control. The difference in the neuron count between intubated and intact control animals can be related to the prenatal stress induced by intubation. In the alcohol group, intubation-induced prenatal

stress is attenuated by sedative and anesthetic effects of ethanol which, in the present study, was administered in two doses 1h apart. However, in contrast to our record of significantly higher neuron counts in IC group at P1 and P10 and in A group at P10, a substantial body of evidence indicates that prenatal stress inhibits rather than stimulates neurogenesis, and thus, adversely affects neuron counts in the hippocampus (Lemaire *et al.,* 2000; Mirescu and Gould, 2006; Sliwowska *et al.,* 2010). However, most of the experimental data on the effects of prenatal stress on hippocampal neuron numbers were collected from adult animals. On the other hand, there is an evidence that the effects of prenatal stress on neurogenesis in hippocampus are age-, gender-, and strain-dependent (Darnaudéry and Maccari, 2008; Koehl *et al.,* 2009; Lucassen *et al.,* 2009; Schmitz *et al.,* 2002). Schmitz and colleagues (2002) reported that prenatal stress more readily affected female than male rats. It was also shown that suppressing effects of prenatal stress on hippocampal neurogenesis may be highly delayed and not occur before senescence (Koehl *et al.,* 2009). Interestingly, it was also reported that some adverse factors, for instance moderate ethanol intake, may increase rather than decrease neurogenesis (Aberg *et al.,* 2005; Miller, 1995). Taking all these into consideration, it is possible that moderate prenatal stress may increase rather than decrease neurogenesis during the critical postnatal period of rapid brain growth. It can be also viewed as an escape from stress-induced inhibition after cessation of ethanol administration. Our results suggest that developmental neurogenesis, much like adult neurogenesis, is a highly regulated process.

The expected adverse effect of fetal ethanol on the numbers of hippocampal neurons was very mild and confined to DG granular layer at P30 only. In juvenile fetal alcohol pups (P30), the granular cell count was lower than that in control groups; however, the difference remained at a level of marginal significance ($p \leq 0.078$).

The type and severity of ethanol-induced hippocampal damage depends on timing, duration and/or frequency of ethanol exposure, ethanol dose and BAC, as well as maternal and genetic factors (Gil-Mohapel *et al.,* 2010; Livy *et al.,* 2003; Maier and West 2001a; West *et al.,* 1990). Previous studies showed that chronic alcohol intake in adulthood decreases the number of stem/progenitor cells in the dentate gyrus, decreases neurogenesis and survival rate of new cells in the hippocampus, and alters morphological maturation of newborn neurons (He *et al.,* 2005; Herrera *et al.,* 2003; Lukoyanov *et al.,* 1999; Nixon and Crews, 2002). Although experiments conducted to assess the neurotoxic effects of ethanol exposure on hippocampus development not always brought consistent results, it is generally accepted that a developing brain is even more sensitive to adverse effects of ethanol. Even a few binge-like drinking episodes or a single alcohol exposure during the early postnatal period (the brain growth spurt) were reported to activate caspase-3, decrease the number of primary neurospheres derived from the hippocampi, decrease the number of stem/progenitor cells in the dentate gyrus, and finally decrease neurogenesis and survival rate of new cells in the adult hippocampus (Hamilton *et al.,* 2011; Ieraci and Herrera, 2007; Klintsova *et al.,* 2007; Wozniak *et al.,* 2004). In the present study, the effects of prenatal ethanol exposure during the period corresponding to the 2nd half of the first and the whole second trimester-equivalent were examined. Our results show that prenatal exposure to ethanol resulting in a moderate BAC (246.6 mg/dl) did not affect the numbers of principal neurons in the hippocampal CA1 and CA2+3 regions at any of the postnatal ages examined. In contrast to some previous studies, wherein prenatal ethanol treatment resulted in a decrease in the total number of neurons in the CA1 segment of the hippocampus having little impact on neuronal number in DG as assessed at P30-P35 (Barnes and Walker, 1981; Miller, 1995), in the present study a marginal reduction in neuron count was found only in DG by P30. This transient reduction in DG granular cell number by P30 correlates with spatial learning and memory deficits observed by us and other authors in juvenile fetal alcohol rat pups (Nagahara and Handa, 1997; Zimmerberg *et al.,* 1991).

The mild effect of fetal ethanol on the neuron numbers in hippocampal subregions observed in the present study is consistent with some previous reports demonstrating areduction in neuron numbers only in rats treated with alcohol during the third trimester-equivalent but not prenatally (González-Burgos *et al.,* 2006; Livy *et al.,* 2003; Maier and West, 2001b; Tran and Kelly, 2003).

Taken as a whole, our results suggest an extended postnatal neurogenesis in both DG and CA hippocampal subregions with the time course of postnatal increase in neuron counts being region specific. Lack of a significant treatment effect supports the notion that alcohol abuse during the second-trimester equivalent has a minor effect on the postnatal neuron counts and/or hippocampal volumes. In this study, in pups prenatally exposed to ethanol, a marginally significant reduction in neuron number was found on P30 in DG only, which correlates with but can hardly be shown as the

only reason of poorer cognitive performance observed in our laboratory and by many other authors in fetal-alcohol juvenile rats.

4.3. Doublecortin immunostaining: Tracing hippocampal neurogenesis during postnatal development in fetal-alcohol and control rats

In relation with the results obtained in the stereological study demonstrating an increase in neuron counts during a protracted postnatal period not only in DG but also in CA subregions, it was of interest to investigate the postnatal changes in the hippocampal counts and distribution of doublecortin immunoreactive cells representing population of an immature migratory neurons (Brown *et al.,* 2003). It was shown that the number of cells expressing DCX closely correlated with proliferation, migration and differentiation of neurons in the central nervous system (Francis *et al.,* 1999; Rao and Shetty, 2004). Due to the fact that DCX expression predominantly occurs in the developing neurons and that an increase in DCX-IR was shown to be parallel with increased BrdU labelling this protein is increasingly used as a marker for neurogenesis (Couillard-Despres *et al.,* 2005).

As expected, in all brain regions studied, the highest numbers of DCX-expressing neurons were found at P1. At P1, the highest overall count of DCX-IR neurons was recorded in SVZ. At birth, no regional differences in the numbers of DCX-IR cells were observed within the hippocampus. During the postnatal development, in all brain regions, a decline in the DCX-IR neuron's counts took place. This decline was exponential in CA subregions and SVZ and more linear in SGZ. Interestingly, a significantly lower count of DCX-IR neurons in SGZ was noted at P10 in fetal-alcohol pups as compared to controls. It can suggests a delayed, negative impact of fetal-alcohol on the dentate neurogenesis. It can also be a reason of relatively lower count of granular cells recorded in A group 20 days later, at P30. As mentioned earlier, some previous studies demonstrated a suppression of adult hippocampal neurogenesis following perinatal exposures to ethanol in rodents (Ieraci and Herrera, 2007; Klintsova *et al.,* 2007; Redila *et al.,* 2006; Sliwowska *et al.,* 2010; Uban *et al.,* 2010). This negative effect of fetal-ethanol on the neuron counts may be related with alterations of cell signalling due to interaction of ethanol with γ-aminobutiric acid (GABA). It is known that immature GABA neurons are excitatory (Ben-Ari *et al.,* 2007). As neurons mature, GABA's action shifts from excitatory to inhibitory (Ben-Ari *et al.,* 2007; Ge *et al.,* 2006). The functional shift in GABA's action is correlated with the development of mGlu and dopamine neurons that have been shown to modulate GABA activity. These sequential neurochemical changes are essential for normal neurogenesis and synaptogenesis (Ge *et al.,* 2006). Previous studies have shown that alcohol drinking increased the brain GABA levels and up-regulated GABAergic signaling in the CNS (Silberman *et al.,* 2008; Zhu and Lovinger, 2006). An increase in GABAergic activity increases inhibitory actions in the adult and excitatory actions in the immature nervous system. The latter may result in abnormal synapse maturation and/or an increase in neuronal death via apoptosis (Andres *et al.,* 2005).

Interestingly, at P30, a significantly higher number of DCX-IR cells was recorded in A group as compared to controls. This between-group difference disappeared at P60. Our findings are consistent with some other studies wherein a significant increase in the number of immature neurons in the DG was also recorded in juvenile but not any more in ethanol-exposed adult rats (Gil-Mahopel *et al.,* 2010; Chang *et al.,* 2012; Singh *et al.,* 2009). These results may suggest an escape from fetal ethanol-induced inhibition of neurogenesis occuring in the course of postnatal development and representing an intrinsic compensatory process counteracting the deleterious ethanol effects. Alternatively, these results may also suggest an ethanol-induced developmental delay in the maturation of new migratory neurons. To better understand the mechanism underlying fluctuations in the postnatal hippocampal neurogenesis in the fetal-alcohol subjects further investigations are required.

The presence of DCX-IR cells at more advanced postnatal ages (P30 and P60) in the hippocampal CA area is consistent with the increase in the neuron counts observed in CA1 and CA2+3 regions between P10-P60 in both fetal-alcohol and control rat pups. All these findings suggest that limited neurogenesis may take place during protracted postnatal periods also in the brain areas other than DG and olfactory tract. As it was discussed in the previous chapter, some other recent studies also demonstrated the existence of adult neurogenesis in the brain areas outside the germinal zones (Inta *et al.,* 2008; Morterá and Herculano-Houzel, 2012; Rietze *et al.,* 2000).

.

4.4. Changes in the morphology of hippocampal neurons during postnatal development in fetal-alcohol and control rats.

In the previous studies, it has been shown that changes in neuron morphology including fluctuations in dendritic complexity, spine density, and soma size may be associated with cognitive functions (Moser *et al.,* 1994; Woolley, 1998; O'Malley *et al.,* 2000) and be affected by perinatal ethanol intoxication (Davies and Smith, 1981: Dursun *et al.,* 2011). In the present study, for the quantitative morphometric analysis of hippocampal pyramidal and granular cells performed across different postnatal ages in control and fetal-alcohol rats, 11 different morphological parameters were considered.

Most of the morphometric parameters considered in this study underwent rapid changes during early postnatal development of hippocampal neurons. The least affected parameters were dendrite tortuosity (meandering) showing only a mild decreasing tendency between P1 and P10, and the planar branch angle (the bifurcation angle) demonstrating a decrease tendency through P10-P30 in the dendrites of granular cells and in the basal dendrites of CA3 pyramidal cells. These results are roughly consistent with previous studies on retinal ganglion cells (Coombs *et al.,* 2006) and the kitten cerebellar Purkinje cells (Calvet and Calvet, 1984) where these two parameters were reported to reach adult values shortly after birth and remain relatively unchanged throughout postnatal development. On the other hand, just like in the present study, both the branch angle and dendrite tortuosity in Y-like geniculocortical relay neurons in cat have been shown to decrease in the course of postnatal development (Coleman and Friedlander, 2002).

During neural development, a decrease in the branch angle represents an increase in the distance between the dendrite terminal tips and the soma. The straightening of dendritic segments associated with reduced tortuosity would have a similar effect. On the other hand, during early developmental stages, the meandering of growing fibers may favor location of specific cellular targets, which would be more difficult if dendrite elongation took place along a straight manner. In previous studies, it has been noted that tortuosity might be critical for searching of specific targets or inputs (Stepanyants *et al.,* 2004). Moreover, it has been also postulated that increased tortuosity can be used as a morphologic marker of nerve regeneration (Kallinikos *et al.,* 2004).

Most of the significant changes in the neurons' morphometry took place between P1-P30 in CA regions and P10-P30 in DG. Soma size underwent changes only in the pyramidal cells from CA3 region (a significant increase between P1-P10 followed by some decrease between P10-P30) finally demonstrating the largest size among all hippocampal neurons. The importance of neuron soma as a factory where the neurotrophic factors and most of proteins for the dendrites, axons and synaptic terminals are produced and where the signals from the dendrites are joined and passed on is well known. The developmental changes in the soma size of CA3 pyramidal neurons observed in the present study are in accord with the previous literature data reporting 2 folded increase in soma area of cortical pyramidal neurons between postnatal days 3 and 21 (Zhang, 2004). However, as seen in the present study, the increase in the soma size during development is not a general phenomenon observed in all types of neurons. It has been shown that changes in soma size in different classes of neurons are regulated by differential gene expression. In a recent study done by Ransdell *et al.* (2010), a significant positive correlations was found between neurons' 18s rRNA expression and their soma size.

Interestingly, in pyramidal neurons, the total dendrite number did not change after the birth, while in the granular cells it significantly decreased throughout P10-P30 period.

Among the morphometric parameters showing the most pronounced changes were the dendritic field area, the mean total dendritic length, the internal branch length, total number of dendritic branches, mean number of branches per dendrite, the highest branch order, and the spine density, all manifesting a significant increase in all hippocampal regions and all treatment groups during early postnatal life. The neurons' dendritic tree is known to play an important role in establishing and regulation of neural networks properties and dynamics, and during normal development, the dendritic field area and related parameter were reported to increase in different classes of neurons (Coombs *et al.,* 2006; McAllister, 2000; Uylings *et al.,* 1994).

In the central nervous system, dendritic spines are the primary recipients of excitatory input. They provide biochemical compartments that locally control the signaling mechanisms at individual synapses. In the adult brain, activity-dependent modulation of spine numbers is a common phenomenon. Hippocampal spines show structural plasticity as the basis for the physiological changes in synaptic efficacy underlying learning and memory. As mentioned earlier, there is a variety of spine types, thin (immature), stubby, mushroom (mature), branched (newly formed). Each of the spine types due to the spine shape shows different resistance to the flow of electric current: 105-106 Ω for stubby spines, 106-108 Ω for mushroom-shaped spines and 108-109 Ω for long-thin spines (Segev and Rall, 1998) and thus have different contribution to neural signaling at dendritic synapses. The distribution of different spine types among different hippocampal regions was similar, with stubby spines predominating at P1, and thin spines constituting the second, most crowded spine category at P30. A significant increase in the numbers of mushroom and branched spines was also observed during P1-P30 postnatal period especially on apical dendrites in CA1 pyramidal cells, and dendrites of granular cells. Among all four spine types, the overall frequency of branched spines, an indirect index of synaptogenesis, was the lowest, although their numbers too substantially increased in the course of postnatal development between P1-P30, especially on apical CA dendrites and granular cells' dendrites. The latter results are consistent with previous studies reporting that stubby spines predominate early after the birth but with maturation (at P21-30), the stubby spine synapses may be reduced in numbers while thin and mushroom spines are formed, and eventually the thin spines become the dominant spine shape (Chicurel and Harris; 1992; Fiala *et al.,* 1998; Harris and Stevens, 1989; Harris *et al.,* 1992; Sorra *et al.,* 1998; Tarelo-Acuna *et al.,* 2000; Trommald and Hulleberg, 1997; Kirov *et al.,* 1999). It has been also reported that almost no splitting dendritic spines were found in the hippocampus until postnatal day 15 which is somewhat contradictory to the present observations indicating an increase in the numbers of branched synapses already at P10.

The treatment effect was mild and mostly noted at birth (P1) only. Since in most cases, the difference was found between intubated groups (A and IC) versus intact control, the observed effect could be attributed to both ethanol and the intubation stress. The effects of prenatal ethanol exposure and prenatal stress may be cumulative since both prenatal ethanol exposure and prenatal stress were demonstrated to cause deficits in feedback control of pituitary-adrenal activity and thus produce pituitary-adrenal hyperresponsiveness (Schneider *et al.,* 2004; Van den Hove *et al.,* 2006; Zhang *et al.,* 2005). On the other hand, the hippocampal formation was reported to be highly sensitive to the effects of adrenal glucocorticoids (McEwen, 2001).

The up-to-day knowledge about the effects of prenatal stress on neuronal morphology at early postnatal ages (P1 or P10) is rather limited (Van Den Hove *et al.,* 2006; Fujioka *et al.*, 2006). In contrast to this, there have been more studies scanning the effects of prenatal stress at more advanced postnatal ages (Bock *et al.*, 2011; Mychasiuk *et al.*, 2011; Jia *et al.,* 2010; Barros *et al.*, 2006; Hayashi *et al.,* 1998). According to the available literature, prenatal stress has several important consequences in neonatals including reduction in the birth weight, disruption of HPA axis activity, a strong decrease in the brain cell proliferation, increased caspase-3-like activity, and reduced brain BDNF levels (Van Den Hove *et al.,* 2006). However, the effects of prenatal stress on hippocampus in neonatal rats can be bimodal depending on stress intensity and duration with mild, short-lasting prenatal stress enhancing neonatal neurogenesis and cell differentiation and severe, long-lasting prenatal stress having opposite effects (Fujioka *et al.,* 2006). When the effects of prenatal stress have been tested at more advanced postnatal ages, prenatal stress was reported to induce a reduction in dendritic arborization by 73%, in the CA1 hippocampal area at P90 (Barros *et al.*, 2006) and to cause a significant reduction (by 32%) in synaptic density within the hippocampal CA3 area at P35 (Hayashi *et al.,* 1998). It was also reported that prenatal stress decreased spine densities in pyramidal neurons in both, juvenile and adult rats (Hossein-Sharifabad and Hadinedoushan, 2007) and altered dendritic length and the complexity of both pyramidal and granular neurons (Bock *et al.,* 2011; McKittrick *et al.,* 2000; Watanabe *et al.,* 1992; Jia *et al.*, 2009; Mychasiuk *et al.,* 2011). The changes in the morphology of principal hippocampal neurons observed in the present study at P1 in both A and IC groups were similar to those previously reported in animals subjected to prenatal stress and included a decrease in the mean dendritic field area and the mean dendritic length in CA regions, a decrease in the total number of dendritic branches, the highest branch order and the total number of spines in pyramidal but not granular cells, decrease in the number of stubby spines in CA and DG regions, and also in the number of thin spines on CA3 basal dendrites. It has been postulated that the shrinkage of dendritic trees and decrease in spine density in the hippocampus in response to stress serve as an adaptive mechanism

reducing input of the over-active stress response into hippocampal neurons (McKittrick *et al.,* 2000, Silva-Gomez *et al.,* 2003).

However, perinatal ethanol *per se* was also reported to produce a decrease in spine density and synaptic contacts in hippocampal neurons at different postnatal ages (Ferrer *et al.,* 1988, Kuge *et al.,* 1993), and to reduce the spine density in the hippocampal neurons exposed to ethanol in culture (Yanni and Lindsley, 2000).

In this study, a marginal deteriorating effect of ethanol *per se* was found in the soma size of CA3 pyramidal neurons and DG granular cells on P1. The soma area of CA3 and DG neurons was marginally smaller in A group as compared to both controls. In addition, on P1, the Sholl analysis revealed a significantly smaller number of intersections between 40 and 60 μm Sholl rings for the basal dendrites of CA1 neurons and between 50 and 60 μm Sholl rings for the basal dendrites of CA3 neurons, in the alcohol group compared to both controls.

These results are partially in accord with the effects of early postnatal ethanol intoxication on developing retinal ganglion cells in mouse, where a significant reduction in soma size and total dendritic field area were noted (Dursun *et al.,* 2011) and with the findings by other authors reporting reduction of the soma size and dendritic fields of the neurons in the rat oculomotor nucleus (Burrows *et. al.,* 1995), Bergmann glial cells (Perez-Torrero *et al.,* 1997), and cerebellar granule cells (Smith *et al.,* 1986) due to perinatal alcohol exposure. The atrophy dendritic processes in hippocampal pyramidal neurons of fetal-alcohol subjects were also reported by Saunders *et al.* (1995) and Gonzalez-Burgos *et al.* (2006). It was also shown that ethanol addition to the hippocampal cell cultures led to a decrease in number and length of dendrites (Yanni and Lindsley, 2000). It is well known that both, neurite extension and bifurcation are strongly influenced by the fibroblast growth factor (bFGF), and ethanol inhibits the activity of bFGF (Luo and Miller, 1998). In addition, it has been reported that high intracellular Ca^{2+} levels have a suppressive effect on the neurite growth (Kostyuk, 1986). The suppresion of neurite growth could be mediated by interaction of ethanol with GABA receptors. At early stages of development, GABA receptors show excitatory rather than inhibitory properties (Prendergast *et al.,* 2004; Harris and Kather; 1994; Papa *et al.,* 1995; Rogers and Hunter, 1992) and when stimulated lead to a rise in the intracellular Ca^{2+} levels (Prendergast *et al.,* 2004) negativelly affecting dendrite growth and bifurcation (Mameli *et al.,* 2005).

In our study, the adverse effects of prenatal ethanol and stress exposure were transient, observed only at birth. All the changes in the hippocampal cells' morphology observed on P1, disappeared during the following postnatal period, mostly already at P10, with some parameters in A group over passing those in controls. The latter included, mean dendritic field area in CA3 region, total number of dendrites in CA1, mean branch number, the highest branch order in apical CA1 dendrites, and the number of stubby spines on apical CA1 dendrites at P10, the number of mushroom spines on basal CA1 dendrites at P30, and the soma size of granular cells at P60. This significant increase in the values of some morphological parameters of hippocampal pyramidal neurons observed at more advanced stages of postnatal development in A group compared to controls may represent a compensatory "rebound" from the fetal alcohol abuse. Interestingly, an increase in some neuronal parameters after perinatal ethanol exposure was observed also in other studies. For instance, the dendrite elongation, increase in the mean branch angle, and increase in dendritic tortuosity were found in retinal ganglion cells after early postnatal ethanol exposure (Dursun *et al.,* 2011). An alternative explanation of the observed temporal pattern of neuronal changes in fetal-alcohol subjects could be ethanol-induced developmental delay (Davies and Smith, 1981). Some studies showed that alcohol administration during prenatal period delays the neuron development by 1–2 days (Miller, 1988). Another possibility is that an increase in some dendritic paremeters observed in fetal-acohol subjects during postnatal development is mediated by upregulated levels of neurotrophins. It is well documented that the formation of dendritic arbor is mediated by neurotrophic actions. On the other hand, it was shown that chronic ethanol exposure causes alteration in the neurotrophin levels (Maier *et al.,* 1997; Tran *et al.,* 2000). Indeed, some studies indicated that following prenatal alcohol treatment, neurotrophin levels measured postnatally in the cortex and hippocampus were significantly higher compared to controls (Angelucci *et al.,* 1997; Nakano *et al.,* 1996; Parks *et al.,* 2008).

The absence of quantitative deficits in the neurons' morphology in the hippocampus of young-adult ethanol-exposed rats exhibitig a kind of maturational retardation when examined at birth, suggests that

prenatal ethanol intoxication and/or prenatal intubation-stress applied in the present study did not produce an irreversible maturational deficits.

4.5. Changes in the distribution and the overall levels of synaptic proteins, synaptophysin and PSD-95, during the postnatal development of hippocampus in fetal-alcohol and control rats.

Synapse density is believed to correlate with cognitive status (DeKosky and Scheff, 1990; Terry *et al.,* 1991) and it can be indirectly evaluated by measuring the levels of synapse proteins (Siew *et al.,* 2004). Synaptophysin (SYP) and other synaptic vesicle proteins as well as proteins belonging to postsynaptic densities have been implicated in mechanisms of activity-dependent neuroplasticity underlying learning and memory formation (Lynch *et al.,* 1994; Mullany and Lynch, 1998; Janz *et al.,* 1999). Synaptophysin is a presynaptic protein implicated in vesicular docking and considered a reliable marker of synaptogenesis (Bergmann *et al.,* 1993; Grabs *et al.,* 1994; Papa and Segal, 1996). It is a major integral transmembrane protein (molecular weight 38 kDa) of synaptic vesicles (Wiedenmann and Franke, 1985; Südhof *et al.,* 1987). Several studies have demonstrated the role of synaptophysin in the regulation of exocytosis and endocytosis of neurotransmitters (Alder *et al.,* 1992; Edelmann *et al.,* 1995; Sugita *et al.,* 1999; Valtorta *et al.,* 2004). It was also suggested that SYP plays a role in formation and stabilization of synapses (Tarsa and Goda, 2002). As it is known, Schaffer collaterals originating from CA3 principal neurons terminate in stratum radiatum (SR) of the CA1 region, while mossy fibers originating from granule cells of the DG terminate in stratum lucidum (SL) of the CA3 area. Consequently, measurement of synaptophysin expression in stratum radiatum of the CA1 area refers to protein expression in boutons of CA3 pyramidal cells and in stratum lucidum of CA3 synaptophysin expression refers to terminals of granule cells.In the previous studies, SYP-IR was mostly seen within the hilus of the DG, in CA3 SL where mossy fiber terminals are abundant, and in SR and SO of CA1 (Fykse *et al.,* 1993; Waters *et al.,* 2009). These results are generaly consistent with the findings in the present study.

In the present study, at P1, the SYP IR was lower in the alcohol group as compared to controls in all layers and hippocampal regions studied, however, these difference did not reach the accepted level of significance. At P10, in the alcohol group compared to control, a sharp increase in SYP-IR was observed in the oriens and radiatum layers of both left and right CA1 region, oriens layer of the left CA3 region, and molecular layer of left DG region while in control groups, the simlar changes in the SYP expression occured mostly between P10-P30. This resulted in significantly higher SYP levels at P10 in A group as compared to control. A slight increase in the expression level of synaptophysin in the cortex and hippocampus of fetal-alcohol rats during postnatal development was also reported by Kim *et al.* (2010).

Parallel to the immunoreactivity results, the western blot analysis revealed at P1 marginaly significantly lower SYP levels in the alcohol group as compared to the intact controls, and, at P10, marginally significantly higher SYP levels in alcohol as compared to both control group. Also, the significant increase in protein concentration during development was observed between P1-P30 in control groups, and between P1-P10 in the alcohol group. Generally, in all groups, the changes in SYP expression are correlate with changes in spine densities and dendritic arbor. Our results, however, are contradictory to the results of a previous study reporting a lack of significant changes in the hippocampal levels of synaptophysin at different ages after the birth in fetal alcohol subjects (Maciejewski–Lenoir, 1993). Nevertheless, it should be remembered that either pre- or postnatal ethanol effects depend on several factors such as alcohol dose, timing of alcohol exposure, peak BAC, animals vulnerability to ethanol toxic effects, etc.

PSD-95 is a scaffolding protein involved in the organization of glutamate receptors and other constituents of the postsynaptic density (Kim and Sheng, 2004). It plays a major role in synapse organization and functions by determining the size and the strength of synapses (Funke *et al.,* 2005; Ehrlich and Malinow, 2004). It was also shown to play an important role in the spine-maturation process including changes in the spine shape and volume, and an enlargement of the PSD (Kennedy, 1998, Nikonenko *et al.,* 2008). An increased expression of PSD-95 protein was reported to be associated with the formation of synapses with complex, perforated or segmented PSDs. PSD-95 is a protein associated with glutamatergic NMDA and AMPA receptors found in postsynaptic densities at excitatory synapses. It was shown to regulate the densities and subcellular localization of these receptors (Gardoni *et al.,* 2009; Tang *et al.,* 1999; Zhang *et al.,* 2008; Zhao *et al.,* 2005) and to

function as an adapter protein that couples signaling molecules to NMDA receptors (Garner *et al.,* 2000). All this has a profound impact on the cellular processes underlying various forms of synaptic plasticity including learning and memory formation (Nyffeler *et al.,* 2007). During development, PSD-95 expression facilitates maturation of excitatory synapses in hippocampal neurons (El-Husseini *et al.,* 2000).

In the present study, in the contrary to SYP protein showing an increase in all hippocampal regions between P1-P30 to reach a plateau level afterwards, the PSP-95 expression sharply increased between P1-P10 to decline during the 2nd postnatal month. Similar inverse U shape of the temporal profile of PSD-95 expression in the hippocampus was reported also by other authors (Chang *et al.,* 2009; Zhu *et al.,* 2010).

In the present study, at P1, the intial levels of PSD-95 protein were not different between the treatment groups. A significantly lower level of this protein in the fetal-alcohol as compared to intact control was noted in the stratum oriens of the CA1 region only. In parallel to the immunofluorescence results, in the Western blot analysis, a significant increase in PSD-95 protein concentration was also found between P1-P10. However, no significant differences in the concentration of PSD-95 protein between alcohol and control groups were found at any postnatal age and/or hippocampal region.

The lack of fetal- ethanol effect on the postnatal PSD-95 levels was also observed by other authors (Samudio-Ruiz *et al.,* 2010; Hughes *et al.,* 2001) what is a bit surprising considering a significant effect of prenatal alcohol intoxication on NMDA receptors as reported by some previous studies (Costa *et al.,* 2000).

The differences in the expression of PSD-95 and SYN suggest that the postnatal dendritic remodeling is accompanied by the differential reorganization and redistribution of synaptic proteins. A significant increases in both pre-synaptic (SYN) and post-synaptic (PSD-95) proteins' levels between P1-P10 overlap with so called brain growth spurt period and suggest that synaptogenesis is actively taking place already at a very early stage of postnatal life. The increase in SYP and PSD-95 levels in hippocampus is parallel to a rapid increase in spine densities recorded also between P1-P10.

CHAPTER 5

CONCLUSION

In animal models of Fetal Alcohol Syndrome, ethanol causes a number of changes in brain development, with many of these changes being very transient. Many functional deficiencies following prenatal alcohol exposure are thought to be cumulative results of developmental changes in subtle processes. In our study, the behavioral results suggest that a moderate ethanol intoxication during second trimester equivalent in rats neither significantly affects general arousal manifested by changed spontaneous locomotor activity nor emotionality manifested by increased anxiety. The differential age-dependent behavioral display observed in the plus-maze (an anxiety test) manifests the presence of age-specific behavioral patterns which may confound the drug effects. The ethanol-related behavioral deficit was observed only in the learning tasks and only in juvenile rats and it was proportional to the task difficulty. The observation that learning and memory deficits were noted only in juvenile but not any more in young-adult subjects was consistent with several previous findings and may suggest a functional recovery occurring with maturation in the animals exposed to ethanol *in utero*.

In summary, our results suggest an extended postnatal neurogenesis in both DG and CA hippocampal subregions with the time course of postnatal increase in neuron counts being region specific. The postnatal changes in stereological estimates in the hippocampal neuron counts were generally consistent with the parallel changes in the counts of DCX-IR neurons, an index of neurogenesis. In all hippocampal regions, the highest numbers of DCX-IR neurons were recorded at P1 which corresponded to the rapid increase in neuron counts between P1-P10. The subsequent decline in DCX-IR neuron counts was exponential in CA areas and SVZ, and linear in SGZ. Nevertheless, DCX-IR cells were still found at more advanced postnatal ages (P30 and P60) in the hippocampal CA area indicating a limited neurogenesis taking place during a protracted postnatal period in the brain areas outside DG and olfactory tract. A mild effect of ethanol administration during the second-trimester equivalent on the postnatal neuron counts in the rat hippocampus was observed in DG only, wherein, on P30 a marginally significant reduction in the granular cell number was found. Reduced neuron count in DG on P30 correlated with impaired spatial learning and memory observed in our laboratory and by other authors in fetal alcohol juvenile rats. In alcohol group as compared to controls, a relatively lower number of DCX-IR cells was found in SGZ, on P10, which may explain a relatively lower number of DG granule cells 20 days later (at P30) in this area. In contrast to this, at P30, a significantly higher DCX-IR cell counts were recorded in SGZ in A group compared to controls. Taken together, these results may indicate an alcohol-induced developmental delay or a kind of intrinsic compensatory process against the adverse ethanol effects

During 2 mo. of postnatal development, the morphology of principal hippocampal neurons underwent profound changes to reach an adult phenotype at P30. The least affected parameters were dendrite tortuosity (meandering), and the planar branch angle (the bifurcation angle). Soma area showed a significant increase only in the CA3 pyramidal cells between P1-P10 finally demonstrating the largest size among all hippocampal neurons. Interestingly, the total dendrite number did not change in pyramidal neurons, and significantly decreased in the granular cells. Among the morphometric parameters showing a significant increase were the dendritic field area, the dendritic length, number of branches, and the spine density. In accordance with literature, the distribution of different spine types among different hippocampal regions was similar, with stubby spines predominating at P1, and a significant increase in the density of the other spine types (thin, mushroom, and branched) between

P1-P30. The treatment effects on the morphology of hippocampal neurons was seen mainly at birth (P1) in CA region, with the dendritic field area, the mean dendritic length, total number of dendritic branches, and the total number of spines (especially stubby and thin) significantly lower in A and IC groups as compared to intact controls. Since in most cases, the difference was found between intubated groups (A and IC) versus intact control, the observed effects could be attributed to both ethanol exposure and the intubation stress. Since the mentioned above morphological differences disappeared at P30, they could not be correlated with behavioral deficits observed in juvenile fetal-alcohol pups. Interestingly, between P10-P30, some morphometric parameters (dendritic field area in CA3, total number of dendrites in CA1, mean branch number, the highest branch order, and the number of stubby spines on apical and, the mushroom spines on basal CA1 dendrites) showed significantly higher values in A group compared to controls, which may indicate a compensatory "rebound" effect in developing hippocampus: an escape from ethanol-induced inhibition.

The changes in the expression of synaptic proteins were roughly parallel to the changes in the cell counts, dendritic arbor, and spine densities (the latter representing excitatory synapses). A significant increases in both, pre-synaptic (SYN) and post-synaptic (PSD-95) proteins' IR and tissue levels between P1-P10 overlap with so called brain growth spurt period and confirm the presence of active synaptogenesis in neonatal hippocampus. Interestingly, the pattern of temporal changes in SYP and PSD-95 IR/tissue levels was highly different suggesting that the postnatal dendritic remodeling is accompanied by the differential reorganization and redistribution of synaptic proteins. The SYP expression (especially in CA1 area) was much more affected by fetal alcohol than PSD-95 expression. At P1, in alcohol group, the SYP-IR was generally lower while at P10, significantly higher as compared to controls which repeats the pattern of changes in spine density and several dendritic parameters once more indicating a compensatory escape from fetal-ethanol induced inhibition. The absence of quantitative deficits in hippocampal morphology and the levels of synaptic proteins in young-adult fetal-alcohol animals which exhibited a kind of maturational retardation when examined at earlier postnatal ages, suggests that prenatal ethanol intoxication and/or prenatal intubation stress applied in the present study did not produce irreversible maturational deficits during hippocampal development.

Except a marginally lower cell counts in DG at P30, no other profound developmental anomalies were observed in fetal-alcohol pups that could account for the behavioral deficits observed in the hippocampus-dependent learning tasks in juvenile fetal-alcohol subjects and for amelioration of these deficits in young adults.

REFERENCES

Abel EL., Dintcheff BA. 1978. "Effects of prenatal alcohol exposure on growth and development in rats" The Journal of Pharmacology and Experimental Therapeutics. 207(3):916-921.

Abel EL. 1982. "In utero alcohol exposure and developmental delay of response inhibition" Alcoholism Clinical and Experimental Research. 6(3):369-376.

Abel EL, Berman RF. 1994 "Long-term behavioral effects of prenatal alcohol exposure in rats" Neurotoxicology Teratology. 16(5):467-470.

Abel EL., Reddy PP. 1997. "Prenatal high saturated fat diet modifies behavioral effects of prenatal alcohol exposure in rats" Alcohol. 14(1):25-29.

Aberg E, Hofstetter CP, Olson L, Brené S. 2005. "Moderate ethanol consumption increases hippocampal cell proliferation and neurogenesis in the adult mouse" Int J Neuropsychopharmacol. 8:557-567.

Alder J, Xie ZP, Valtorta F, Greengard P, Poo M. 1992. "Antibodies to synaptophysin interfere with transmitter secretion at neuromuscular synapses" Neuron. 9(4):759-768.

Altemus KL, Lavenex P, Ishizuka N, Amaral DG. 2005. "Morphological characteristics and electrophysiological properties of CA1 pyramidal neurons in macaque monkeys" Neuroscience. 136(3):741-756.

Altman J, Das GD. 1965. "Autoradiographic and histological evidence of postnatal hippocampal neurogenesis in rats" J Comp Neurol. 124:319-335.

Altman J, Bayer SA. 1990. "Migration and distribution of two populations of hippocampal granule cell precursors during the perinatal and postnatal periods" J Comp Neurol. 301:365-381.

Amaral, DG. 1978."A Golgi study of the cell types in the hilar region of the hippocampus in the rat" J. Comp. Neurol. 182, 851–914.

Amaral DG., Insausti R., Cowan WM. 1984. "The commissural connections of the monkey hippocampal formation" J. Comp. Neurol. 224, 307–336.

Amaral DG, Dolorfo C, Alvarez-Royo P. 1991. "Organization of CA1 projections to the subiculum: a PHA-L analysis in the rat" Hippocampus. 1(4):415-435.

Andres RH, Ducray AD, Huber AW, Pérez-Bouza A, Krebs SH, Schlattner U, Seiler RW, Wallimann T, Widmer HR. 2005. "Effects of creatine treatment on survival and differentiation of GABA-ergic neurons in cultured striatal tissue" J Neurochem. 95(1):33-45.

Angelucci, F., Cimino, M., Balduini, W., Piltillo, L., Aloe, L., 1997. "Prenatal exposure to ethanol causes differential effects in nerve growth factor and its receptor in the basal forebrain of preweaning and adult rats" Journal of Neural Transplantion and Plasticity. 6(2):63-71.

Anthony B., Zhou F.C., Ogawa T., Goodlett C.R., Ruiz J. 2008. "Alcohol exposure alters cell cycle and apoptotic events during early neurulation" Alcohol & Alcoholism. 43 (3):261–273.

Archibald SL, Fennema-Notestine C, Riley EP, Jernigan TL. 2001. "Brain dysmorphology in individuals with severe prenatal alcohol exposure" Dev Med Child Neurol. 43:148–154.

Aronson M., Olegard R. 1987. "Children of alcoholic mothers" Pediatrician. 14: 57–61.

Bâ A. 2009. "Alcohol and B1 vitamin deficiency-related stillbirths" J Matern Fetal Neonatal Med. 22(5):452-457.

Bakst, I., Avendano, C., Morrison, JH., and Amaral, DG. 1986. "An experimental analysis of the origins of somatostatin-like immunoreactivity in the dentate gyrus of the rat" J. Neurosci. 6:1452–1462.

Bandeira F, Lent R, Herculano-Houzel S. 2009. "Changing numbers of neuronal and non-neuronal cells underlie postnatal brain growth in the rat" Proc Natl Acad Sci U S A. 106:14108-14113.

Bannister NJ, Larkman AU. 1995. "Dendritic morphology of CA1 pyramidal neurones from the rat hippocampus: I. Branching patterns" J Comp Neurol. 360(1):150-160.

Barnes DE, Walker DW. 1981. "Prenatal ethanol exposure permanently reduces the number of pyramidal neurons in rat hippocampus" Brain Res. 227:333-340.

Barros VG, Rodríguez P, Martijena ID, Pérez A, Molina VA, Antonelli MC. 2006. "Prenatal stress and early adoption effects on benzodiazepine receptors and anxiogenic behavior in the adult rat brain." Synapse. 60(8):609-618.

Bartesaghi, R. and Gessi, T. 2004. "Parallel activation of field CA2 and dentate gyrus by synaptically elicited perforant path volleys" Hippocampus. 14, 948–963.

Bartesaghi R, Migliore M, Gessi T. 2006. "Input-output relations in the entorhinal cortex-dentate-hippocampal system: evidence for a non-linear transfer of signals" Neuroscience. 142(1):247-265.

Bayer SA, Altman J. 1974. "Hippocampal development in the rat: cytogenesis and morphogenesis examined with autoradiography and low-level X-irradiation" J Comp Neurol. 158(1):55-79.

Bayer SA, Altman J. 1975. " The effects of X-irradiation on the postnatally-forming granule cell populations in the olfactory bulb, hippocampus, and cerebellum of the rat" Exp Neurol. 48(1):167-174.

Bayer SA. 1980a. "Development of the hippocampal region in the rat. I. Neurogenesis examined with 3H-Thymidine autoradiography" J Comp Neurol. 190:87-114.

Bayer SA. 1980b. "Development of the hippocampal region in the rat II.Morphogenesis during embryonic and early postnatal life" J Comp Neurol. 190:115-134.

Bayer SA, Yackel JW, Puri PS. 1982. "Neurons in the rat dentate gyrus granular layer substantially increase during juvenile and adult life" Science. 216:890-892.

Bayer SA., Altman J., Russo RJ., Zhang X. 1993. "Timetables of neurogenesis in the human brain based on experimentally determined patterns in the rat" Neurotoxicology. 14 (1): 83–144.

Behan M, Haberly LB. 1999. "Intrinsic and efferent connections of the endopiriform nucleus in rat" J Comp Neurol. 408(4):532-548.

Ben-Ari Y, Gaiarsa JL, Tyzio R, Khazipov R. 2007. "GABA: a pioneer transmitter that excites immature neurons and generates primitive oscillations" Physiol Rev. 87(4):1215-1284.

Benedetti F, Bernasconi A, Pontiggia A. 2006. "Depression and neurological disorders" Curr Opin Psychiatry. 19(1):14-18.

Bergmann M, Schuster T, Grabs D, Marquèze-Pouey B, Betz H, Traurig H, Mayerhofer A, Gratzl M. 1993. "Synaptophysin and synaptoporin expression in the developing rat olfactory system" Brain Res Dev Brain Res. 74(2):235-244.

Berman RF., Hannigan JH. 2000. "Effects of prenatal alcohol exposure on the hippocampus: Spatial behavior, Electrophysiology, and Neuroanatomy" Hippocampus. 10: 94–110.

Blackstad TW. 1956. "Commissural connections of the hippocampal region in the rat, with special reference to their mode of termination". J. Comp. Neurol. 105, 417–537.

Blackstad TW, Kjaerheim A. 1961. "Special axo-dendritic synapses in the hippocampal cortex: electron and light microscopic studies on the layer of mossy fibers" J Comp Neurol. 117:133-159.

Blackstad T W., Flood PR. 1963. "Ultrastructure of hippocampal axo-somatic synapses" Nature. 198:542-543.

Blanchard BA, Riley EP, Hannigan JH. 1987. "Deficits on a spatial navigation task following prenatal exposure to ethanol" Neurotoxicol Teratol. 9(3):253-258.

Blasco-Ibanez, J. M., and Freund, T. 1995. "Synaptic inputs of horizontal interneurons in stratum oriens of the hippocampal CA1 subfield: Structural basis of feed-back activation" Eur. J. Neurosci. 7, 2170–2180.

Bliss TV, Lomo T. 1973. "Long-lasting potentiation of synaptic transmission in the dentate area of the anaesthetized rabbit following stimulation of the perforant path" J Physiol. 232(2):331-356.

Bliss TV, Chung SH, Stirling RV. 1974. " Proceedings: Structural and functional development of the mossy fibre system in the hippocampus of the post-natal rat" J Physiol. 239(2):92P-94P.

Bock J, Murmu MS, Biala Y, Weinstock M, Braun K. 2011. "Prenatal stress and neonatal handling induce sex-specific changes in dendritic complexity and dendritic spine density in hippocampal subregions of prepubertal rats" Neuroscience. 193:34-43.

Boldrini M, Hen R,Underwood MD, Rosoklija GB, Dwork AJ, Mann JJ, Arango V. 2012. "Hippocampal angiogenesis and progenitor cell proliferation are increased with antidepressant use in major depression" Biol Psychiatry. 72:562-571.

Bolshakov VY., Golan H., Kandel ER., Siegelbaum SA. 1997. "Recruitment of new sites of synaptic transmission during the cAMPdependent late phase of LTP at CA3-CA1 synapses in the hippocampus" Neuron. 19:635–651.

Bond NW., Di Giusto EL. 1977. "Prenatal alcohol consumption and open-field behaviour in rats: effects of age at time of testing" Psychopharmacology. (Berl), 52:311-312.

Bond NW. 1981. "Prenatal alcohol exposure in rodents: a review of its effects on offspring activity and learning ability" Aust J Psych. 33:331–344.

Bonthius DJ., West JR. 1990. "Alcohol-induced neuronal loss in developing rats: Increased brain damage with binge exposure" Alcohol Clin Exp Res. 14(1):107-118.

Bonthius DJ, West JR. 1991. "Permanent neuronal deficits in rats exposed to alcohol during the brain growth spurt" Teratology. 44:147-163.

Bonthius DJ, McKim R, Koele L, Harb H, Karacay B, Mahoney J, Pantazis NJ. 2004. "Use of frozen sections to determine neuronal number in the murine hippocampus and neocortex using the optical disector and optical fractionator" Brain Res Brain Res Protoc. 14:45-57.

Brien J., Loomis C., Tranmer J., McGath M. 1983. "Disposition of ethanol in human maternal venous blood and amniotic fluid" American Journal of Obstetrics and Gynecology. 146: 181-186.

Brown JP, Couillard-Després S, Cooper-Kuhn CM, Winkler J, Aigner L, Kuhn HG. 2003. "Transient expression of doublecortin during adult neurogenesis" J. Comp. Neurol. 467 (1): 1–10.

Bruel-Jungerman E, Davis S, Laroche S. 2007. "Brain plasticity mechanisms and memory: a party of four" Neuroscientist. 13(5):492-505.

Burrows RC., Shetty AK., Phillips DE. 1995. "Effects of prenatal alcohol exposure on the postnatal morphology of the rat oculomotor nucleus" Teratology. 51: 318–328.

Burwell RD., Witter MP., Amaral DG. 1995. "The perirhinaland postrhinal cortices of the rat: A review of the neuroanatomical literature and comparison with findings from the monkey brain" Hippocampus. 5:390–408.

Buss RR, Sun W, 2006. "Oppenheim RW. Adaptive roles of programmed cell death during nervous system development" Annu Rev Neurosc.i 29:1-35.

Calvet MC., Calvet J. 1984. "Computer assisted analysis of HRP labeled and Golgi stained Purkinje neurons" Progress in Neurobiology. 23: 251–272.

Carneiro LM, Diógenes JP, Vasconcelos SM, Aragão GF, Noronha EC, Gomes PB, Viana GS. 2005. "Behavioral and neurochemical effects on rat offspring after prenatal exposure to ethanol" Neurotoxicol Teratol. 27:585–592.

Cartwright MM., Tessmer LL., Smith SM. 1998. "Ethanol-induced neural crest apoptosis is coincident with their endogenous death, but is mechanistically distinct" Alcohol Clin Exp Res. 22(1):142–149.

Chang LR, Liu JP, Zhang N, Wang YJ, Gao XL, Wu Y. 2009. "Different expression of NR2B and PSD-95 in rat hippocampal subregions during postnatal development" Microsc Res Tech. 72(7):517-524.

Chang GQ, Karatayev O, Liang SC, Barson JR, Leibowitz SF. 2012. "Prenatal ethanol exposure stimulates neurogenesis in hypothalamic and limbic peptide systems: possible mechanism for offspring ethanol overconsumption" Neuroscience. 222:417-428.

Charness ME., Safran RM., Perides G. 1994. "Ethanol inhibits neural cell-cell adhesion" The Journal of Biological Chemistry. 269(12):9304–9309.

Chevaleyre V., Siegelbaum SA. 2010. "Strong CA2 pyramidal neuron synapses define a powerful disynaptic cortico-hippocampal loop" Neuron. 66:560–572.

Chicurel ME, Harris KM. 1992. "Three-dimensional analysis of the structure and composition of CA3 branched dendritic spines and their synaptic relationships with mossy fiber boutons in the rat hippocampus" J Comp Neurol. 325(2):169-182.

Chiu J, Brien JE, Wu P, Eubanks JH, Zhang L, Reynolds JN. 1999. "Chronic ethanol exposure alters MK-801 binding sites in the cerebral cortex of the near-term fetal guinea pig" Alcohol. 17:215–221.

Claiborne BJ., Amaral DG., Cowan WM. 1986. "A light and electron microscopic analysis of the mossy fibers of the rat dentate gyrus" J. Comp. Neurol. 246:435–458.

Claiborne BJ., Amaral DG., Cowan WM. 1990. "A quantitative three-dimensional analysis of granule cell dendrites in the rat dentate gyrus" J. Comp. Neurol. 302:206–219.

Clarke PGH. 1985. "Neuronal death in the development of the vertebrate nervous system" Trends Neurosci. 8:345-349.

Clausing P, Ferguson SA, Holson RR, Allen RR, Paule MG. 1995. "Prenatal ethanol exposure in rats: long-lasting effects on learning" Neurotoxicology Teratology. 17(5):545-552.

Climent E., Pascual M., Renau-Piqueras JC. Guerri C. 2002. "Ethanol exposure enhances cell death in the developing cerebral cortex: Role of Brain- Derived Neurotrophic Factor and its signaling pathways" Journal of Neuroscience Research. 68:213–225.

Cohen RS, Siekevitz P. 1978. " Form of the postsynaptic density. A serial section study" J Cell Biol. 78(1):36-46.

Coleman LA., Friedlander MJ. 2002. "Postnatal dendritic development of Y-like geniculocortical relay neurons" International Journal of Developmental Neuroscience. 20:137–159.

Coles C. 1994. "Critical Periods for Prenatal Alcohol Exposure" Alcohol Research and Health. 18(1):22–29.

Coombs JL., Van Der List D., Wang GY., Chalupa LM. 2006. "Morphological properties of mouse retinal ganglion cells" Neuroscience. 140:123–136.

Costa ET., Savage DD., Valenzuela CF. 2000. "A review of the effects of prenatal or early postnatal ethanol exposure on Brain Ligand-Gated Ion Channels" Alcoholism: Clinical and Experimental Research. 24(5):706-715.

Cotman CW, Matthews DA, Taylor D, Lynch G. 1973. "Synaptic rearrangement in the dentate gyrus: histochemical evidence of adjustments after lesions in immature and adult rats" Proc Natl Acad Sci U S A. 70(12):3473-3477.

Couillard-Despres S, Winner B, Schaubeck S, Aigner R, Vroemen M, Weidner N, Bogdahn U, Winkler J, Kuhn HG, Aigner L. 2005. "Doublecortin expression levels in adult brain reflect neurogenesis" Eur J Neurosci. 21(1):1-14.

Crain B, Cotman C, Taylor D, Lynch G. 1973. "A quantitative electron microscopic study of synaptogenesis in the dentate gyrus of the rat" Brain Res. 63:195-204.

Cronise K., Marino MD., Tran TD., Kelly SJ. 2002. "Critical periods for the effects of alcohol exposure on learning in rats" Behavioral Neuroscience. 105(1): 138-145.

Dailey ME., Smith SJ. 1996. "The dynamics of dendritic structure in developing hippocampal slices" J. Neurosci. 16:2983–2994.

Danglot L., Triller A., Marty S. 2006. "The development of hippocampal interneurons in rodents" Hippocampus. 16(12):1032-1060.

Darnaudéry M., Maccari S. 2008. "Epigenetic programming of the stress response in male and female rats by prenatal restraint stress" Brain Res Rev. 57:571-585.

Datta S, Siwek DF, Patterson EH, Cipolloni PB. 1998. "Localization of pontine PGO wave generation sites and their anatomical projections in the rat" Synapse. 30(4):409-423.

Davies DL, Smith DE. 1981." A Golgi study of mouse hippocampal CA1 pyramidal neurons following perinatal ethanol exposure" Neurosci Lett. 26:49-54.

Davis S, Butcher SP, Morris RG. 1992. "The NMDA receptor antagonist D-2-amino-5-phosphonopentanoate (D-AP5) impairs spatial learning and LTP in vivo at intracerebral concentrations comparable to those that block LTP in vitro" J Neurosci. 12(1):21-34.

DeKosky ST, Scheff SW. 1990. "Synapse loss in frontal cortex biopsies in Alzheimer's disease: correlation with cognitive severity" Ann Neurol. 27(5):457-464.

Deltour L., Ang HL., Duester G. 1996. "Ethanol inhibition of retinoic acid synthesis as a potential mechanism for fetal alcohol syndrome" The FASEB Journal. 10(9):1050-1057.

Demeter S., Rosene DL., Van Hoesen GW. 1985. "Interhemispheric pathways of the hippocampal formation, presubiculum and entorhinal and posterior parahippocampal cortices in the rhesus monkey: The structure and organization of the hippocampal commissures" J. Comp. Neurol. 233,30–47.

Dent JA., Galvin NJ., Stanfield BB., Cowan WM. 1983. "The mode of termination of the hypothalamic projection to the dentate gyrus: An EM autoradiographic study" Brain Res. 258:1–10.

Desmond NL., Levy WB. 1982. "A quantitative anatomical study of the granule cell dendritic fields of the rat dentate gyrus using a novel probabilistic method" J. Comp. Neurol. 212:131–145.

Dikranian K., Qin YQ., Labruyere J., Nemmers B., Olney JW. 2005. "Ethanol-induced neuroapoptosis in the developing rodent cerebellum and related brain stem structures" Developmental Brain Research. 155:1-13.

Dobbing J., Sands J. 1979. "Comparative aspects of the brain growth spurt" Early Human Development. 3:79–84.

Dobrossy MD, Drapeau E, Aurousseau , Le Moal M, Piazza PV, Abrous DN. 2003. "Differential effects of learning on neurogenesis: learning increases or decreases the number of newly born cells depending on their birth date" Mol Psychiatry. 8:974-982.

Dong H, Csernansky CA, Goico B, Csernansky JG. 2003. "Hippocampal neurogenesis follows kainic acid-induced apoptosis in neonatal rats" J Neurosci. 23:1742-1749.

Downing C, Balderrama-Durbin C, Hayes J, Johnson TE, Gilliam D. 2009. "No effect of prenatal alcohol exposure on activity in three inbred strains of mice" Alcohol Alcohol. 44(1):25-33.

Driscoll CD., Streissguth AP., Riley EP. 1990. "Prenatal alcohol exposure: Comparability of effects in humans and animal models" Neurotoxicology and Teratology. 12(3): 231–237.

Dunty WC., Chen S., Zucker RM., Dehart DB., Sulik KK. 2001. "Selective vulnerability of embryonic cell populations to ethanol-induced apoptosis: Implications for Alcohol-Related Birth Defects and Neurodevelopmental Disorder" Alcoholism: Clinical and Experimental Research. 25(10):1523-1535.

Dupret D, Fabre A, Dobrossy MD, Panatier A, Rodriguez JJ, Lamarque S, Lemaire V, Oliet SH, Piazza PV, Abrous DN. 2007. "Spatial learning depends on both the addition and removal of new hippocampal neurons". PLoS Biol 5:e214.

Dursun I, Jakubowska-Doğru E, Uzbay T. 2006. "Effects of prenatal exposure to alcohol on activity, anxiety, motor coordination, and memory in young adult Wistar rats" Pharmacol Biochem Behav. 85:345-355.

Dursun I, Jakubowska-Doğru E, van der List D, Liets LC, Coombs JL, Berman RF. 2011. "Effects of early postnatal exposure to ethanol on retinal ganglion cell morphology and numbers of neurons in the dorsolateral geniculate in mice" Alcohol Clin Exp Res. 35:2063-2074.

Edelmann L, Hanson PI, Chapman ER, Jahn R. 1995. "Synaptobrevin binding to synaptophysin: a potential mechanism for controlling the exocytotic fusion machine" EMBO J. 14(2):224-231.

Ehrlich I, Malinow R. 2004. "Postsynaptic density 95 controls AMPA receptor incorporation during long-term potentiation and experience-driven synaptic plasticity" J Neurosci. 24(4):916-927.

El-Falougy H, Benuska J. 2006. "History, anatomical nomenclature, comparative anatomy and functions of the hippocampal formation" Bratisl Lek Listy. 107(4):103-106.

El-Husseini AE, Schnell E, Chetkovich DM, Nicoll RA, Bredt DS. 2000. "PSD-95 involvement in maturation of excitatory synapses" Science. 290(5495):1364-1368.

Epp JR, Spritzer MD, Galea LAM. 2007. "Hippocampus-dependent learning promotes survival of new neurons in the dentate gyrus at a specific time during cell maturation" Neuroscience. 149:273-285.

Esposito MS, Piatti VC, Laplagne DA, Morgenstern NA, Ferrari CC, Pitossi FJ, Schinder AF. 2005. "Neuronal differentiation in the adult hippocampus recapitulates embryonic development" J Neurosci. 25:10074-10086.

Etkin A, Alarcón JM, Weisberg SP, Touzani K, Huang YY, Nordheim A, Kandel ER. 2006. "A role in learning for SRF: deletion in the adult forebrain disrupts LTD and the formation of an immediate memory of a novel context" Neuron. 50(1):127-143.

Fattori V., Abe S., Kobayashi K., Costa LG., Tsuji R. 2008. "Effects of postnatal ethanol exposure on neurotrophic factors and signal transduction pathways in rat brain" Journal of Applied Toxicology. 28:370-376.

Ferrer I, Galofre F, Lopez-Tejero D, Llobera M. 1988. "Morphological recovery of hippocampal pyramidal neurons in the adult rat exposed in utero to ethanol" Toxicology. 48:191-197.

Fiala JC, Feinberg M, Popov V, Harris KM. 1998. "Synaptogenesis via dendritic filopodia in developing hippocampal area CA1" J Neurosci. 18(21):8900-8911.

Finch DM. Babb TL. 1981. "Demonstration of caudally directed hippocampal efferents in the rat by intracellular injection of horseradish peroxidase" Brain Res. 214:405–410.

Fitting S, Booze RM, Hasselrot U, Mactutus CF. 2010. "Dose-dependent long-term effects of Tat in the rat hippocampal formation: a design-based stereological study" Hippocampus. 20:469-480.

Francis F, Koulakoff A, Boucher D, Chafey P, Schaar B, Vinet MC, Friocourt G, McDonnell N, Reiner O, Kahn A, McConnell SK, Berwald-Netter Y, Denoulet P, Chelly J. 1999. "Doublecortin is a developmentally regulated, microtubule-associated protein expressed in migrating and differentiating neurons" Neuron. 23(2):247-256.

Freund TF., Buzsaki G. 1996. "Interneurons of the hippocampus" Hippocampus. 6:345–470.

Funke L, Dakoji S, Bredt DS. 2005. "Membrane-associated guanylate kinases regulate adhesion and plasticity at cell junctions" Annu Rev Biochem. 74:219-245.

Fykse EM, Takei K, Walch-Solimena C, Geppert M, Jahn R, De Camilli P, Südhof TC. 1993. "Relative properties and localizations of synaptic vesicle protein isoforms: the case of the synaptophysins" J Neurosci. 13(11):4997-5007.

Gaarskjaer FB. 1978. "Organization of the mossy fiber system of the rat studied in extended hippocampi. II. Experimental analysis of fiber distribution with silver impregnation methods" J. Comp. Neurol. 178:73–88.

Gall C. 1984. "The distribution of cholecystokinin-like immunoreactivity in the hippocampal formation of the guinea pig: Localization in the mossy fibers" Brain Res. 306:73–83.

Gardoni F, Marcello E, Di Luca M. 2009. "Postsynaptic density-membrane associated guanylate kinase proteins (PSD-MAGUKs) and their role in CNS disorders" Neuroscience. 158(1):324-333.

Garner CC, Nash J, Huganir RL. 2000. "PDZ domains in synapse assembly and signalling" Trends Cell Biol. 10(7):274-280.

Ge S, Goh EL, Sailor KA, Kitabatake Y, Ming GL, Song H. 2006. "GABA regulates synaptic integration of newly generated neurons in the adult brain" Nature. 439:589-593.

Geinisman YL. deToledo-Morrell F. Morrell IS. Persina,. Beatty MA. 1996. "Synapse restructuring associated with the maintenance phase of hippocampal long-term potentiation" J. Comp. Neurol. 368:413– 423.

Gianoulakis C. 1990. "Rats exposed prenatally to alcohol exhibit impairment in spatial navigation test" Behav Brain Res. 36(3):217-228.

Gil-Mohapel J, Boehme F, Kainer L, Christie BR. 2010. "Hippocampal cell loss and neurogenesis after fetal alcohol exposure: insights from different rodent models" Brain Res Rev. 64:283-303.

Girard TA, Xing HC, Ward GR, Wainwright PE. 2000. "Early postnatal ethanol exposure has long-term effects on the performance of male rats in a delayed matching-to-place task in the Morris water maze" Alcohol Clin Exp Res. 24:300-306.

Gokcimen A, Ragbetli MC, Bas O, Tunc AT, Aslan H, Yazici AC, Kaplan S. 2007. "Effect of prenatal exposure to an anti-inflammatory drug on neuron number in cornu ammonis and dentate gyrus of the rat hippocampus: a stereological study" Brain Res. 1127:185-192.

Gonzales RB, DeLeon Galvan CJ, Rangel YM, Claiborne BJ. 2001. "Distribution of thorny excrescences on CA3 pyramidal neurons in the rat hippocampus" J Comp Neurol. 430(3):357-368.

Gonzàles-Burgos M, Alejandre-Gómez ME, Olvera-Cortés MI, Pérez-Vega S, Evans S, Feria-Velasco A. 2006. "Prenatal-through-postnatal exposure to moderate levels of ethanol leads to damage on the hippocampal CA1 field of juvenile rats: A stereology and golgi study" Neurosci Res. 56:400-408.

Goodlett CR, Marcussen BL, West JR. 1990. "A single day of alcohol exposure during the brain growth spurt induces brain weight restriction and cerebellar Purkinje cell loss" Alcohol. 7:107-114.

Goodlett CR, Peterson SD. 1995. "Sex differences in vulnerability to developmental spatial learning deficits induced by limited binge alcohol exposure in neonatal rats" Neurobiol Learn Mem. 64(3):265-275.

Goodlett CR, Johnson TB. 1997. "Neonatal binge ethanol exposure using intubation: timing and dose effects on place learning" Neurotoxicol Teratol. 19(6):435-446.

Goodlett CR, Pearlman AD, Lundahl KR. 1997. "Binge-like alcohol exposure of neonatal rats via intragastric intubation induces both Purkinje cell loss and cortical astrogliosis" Alcohol Clin Exp Res. 21:1010-1017.

Goodlett CR., Horn KH., Zhou FC. 2005. "Alcohol teratogenesis: Mechanisms of damage and strategies for intervention" Experimental Biology and Medicine (Maywood). 230: 394–406.

Gottlieb DI, Cowan WM. 1972. "Evidence for a temporal factor in the occupation of available synaptic sites during the development of the dentate gyrus" Brain Res. 41(2):452-456.

Gould E, Beylin A, Tanapat P, Reeves A, Shors TJ. 1999. "Learning enhances adult neurogenesis in the hippocampal formation" Nat Neurosci. 2:260-265.

Grabs D, Bergmann M, Schuster T, Fox PA, Brich M, Gratz M. 1994. "Differential expression of synaptophysin and synaptoporin during pre- and postnatal development of the rat hippocampal network" Eur J Neurosci. 6(11):1765-1771.

Guerri C. 2002. "Mechanisms involved in central nervous system dysfunctions induced by prenatal ethanol exposure" Neurotoxicity Research. 4(4):327-335.

Gulyas AI., Freund TF. 1996. "Pyramidal cell dendrites are the primary targets of calbindin D 28K-immunoreacte interneurons in the hippocampus" Hippocampus. 6:525–534.

Gundersen HJ, Jensen EB. 1987. "The efficiency of systematic sampling in stereology and its prediction" J Microsc. 147:229-263.

Gundersen HJG, Jensen EBV, Kieu K, Nielsen J. 1999. "The efficiency of systematic sampling in stereology-reconsidered" J Microsc. 193:199-211.

Haglund L., Swanson LW., Köhler C. 1984. "The projection of the supramammillary nucleus to the hippocampal formation: An immunohistochemical and anterograde transport study with the lectin PHA-L in the rat" J Comp Neurol. 229.171–185.

Halasy K., Miettinen R., Szabat E., Freund TF. 1992. "GABAergic interneurons are the major postsynaptic targets of median raphe afferents in the rat dentate gyrus" Eur J Neurosci. 4:144–153.

Halasy K., Buhl EH., Lorinczi Z., Tamas G.,Somogyi P. 1996. "Synaptic target selectivity and input of GABAergic basket and bistratified interneruons in the CA1 area of the rat hippocampus" Hippocampus. 6:306–329.

Halasy K., Hajszan T., Kovács EG., Lam TT., Leranth C. 2004. "Distribution and origin of vesicular glutamate transporter 2-immunoreactive fibers in the rat hippocampus." Hippocampus. 14(7):908-918.

Hall CS., Ballachey EL. 1932. "A study of the rat's behavior in a field: a contribution to method in comparative psychology" University of California Publications in Psychology. 6: 1–12.

Hamilton DA., Kodituwakku P., Sutherland RJ., Savage DD., 2003. "Children with fetal alcohol syndrome are impaired at place learning but not cued-navigation in a virtual Morris water task" Behavioral Brain Research. 143(1):85-94.

Hamilton GF, Murawski NJ, St Cyr SA, Jablonski SA, Schiffino FL, Stanton ME, Klintsova AY. 2011. "Neonatal alcohol exposure disrupts hippocampal neurogenesis and contextual fear conditioning in adult rats" Brain Res. 1412:88-101.

Han ZS., Buhl EH., Lorinczi Z., Somogy P. 1993. "A high degree of spatial selectivity in the axonal and dendritic domains of physiologically identified local-circuit neurons in the dentate gyrus of the rat hippocampus" Eur J Neurosci. 5:395–410.

Han JY., Joo Y., Kim YS., Lee YK., Kim HJ., Cho GJ., Choi WS., Kang SS. 2005 "Ethanol induces cell death by activating caspase-3 in the rat cerebral cortex" Molecules and Cells. 20(2):189-195.

Haring JH., Davis JN. 1985. "Retrograde labeling of locus coeruleus neurons after lesion-induced sprouting of the coeruleohippocampal projection" Brain Res. 360:384–388.

Harris KM., Stevens JK. 1989. "Dendritic spines of CA1 pyramidal cells in the rat hippocampus: Serial electron microscopy with reference to their biophysical characteristics" J Neurosci. 9:2982–2997.

Harris KM., Jensen FE., Tsao B. 1992. "Three-dimensional structure of dendritic spines and synapses in rat hippocampus (CA1) at postnatal day 15 and adult ages: Implications for the maturation of synaptic physiology and long-term potentiation" J Neurosci. 12:2685–2705.

Harris KM, Kater SB. 1994. "Dendritic spines: cellular specializations imparting both stability and flexibility to synaptic function" Annu Rev Neurosci. 17:341-371.

Harris E., Stewart M. 2001. "Propagation of synchronous epileptiform events from subiculum backward into area CA1 of rat brain slices" Brain Res. 895:41–49.

Harris E., Witter MP., Weinstein G., Stewart M. 2001. "Intrinsic connectivity of the rat subiculum. I. Dendritic morphology and patterns of axonal arborization by pyramidal neurons" J Comp Neurol. 436:490–505.

Hasselmo ME., Wyble BP. 1997. "Free recall and recognition in a network model of the hippocampus: simulating effects of scopolamine on human memory function" Behavioural Brain Research. 89:1–34.

Hastings NB., Gould E. 1999. "Rapid extension of axons into the CA3 region by adult-generated granule cells" J Comp Neurol. 413:146–154.

Hayashi A, Nagaoka M, Yamada K, Ichitani Y, Miake Y, Okado N. 1998. "Maternal stress induces synaptic loss and developmental disabilities of offspring" Int J Dev Neurosci. 16(3-4):209-216.

Hazlett JC., Farkas N. 1978. "Short axon molecular layer neurons in the opossum fascia dentata: A Golgi study" Brain Res. 143:355–360.

He J, Nixon K, Shetty AK, Crews FT. 2005. "Chronic alcohol exposure reduces hippocampal neurogenesis and dendritic growth of newborn neurons" Eur J Neurosci. 21:2711-2720.

Heaton MB., Paiva M., Madorsky I., Shaw G. 2003. "Ethanol effects on neonatal rat cortex: Comparative analyses of neurotrophic factors, apoptosis-related proteins, and oxidative processes during vulnerable and resistant periods" Developmental Brain Research. 145:249-262.

Henze DA, Cameron WE, Barrionuevo G. 1996. "Dendritic morphology and its effects on the amplitude and rise-time of synaptic signals in hippocampal CA3 pyramidal cells" J Comp Neurol. 369(3):331-344.

Herrera DG, Yague AG, Johnsen-Soriano S, Bosch-Morell F, Collado-Morente L, Muriach M, Romero FJ, Garcia-Verdugo JM. 2003. "Selective impairment of hippocampal neurogenesis by chronic alcoholism: protective effects of an antioxidant" Proc Natl Acad Sci U S A. 100:7919-7924.

Hjorth-Simonsen A, Jeune B. 1972. "Origin and termination of the hippocampal perforant path in the rat studied by silver impregnation" J Comp Neurol. 144(2):215-232.

Hjorth-Simonsen A, Zimmer J. 1975. "Crossed pathways from the entorhinal area to the fascia dentata. I. Normal in rabbits" J Comp Neurol. 161(1):57-70.

Hoge J, Kesner RP. 2007. "Role of CA3 and CA1 subregions of the dorsal hippocampus on temporal processing of objects" Neurobiol Learn Mem. 88:225–231.

Hosseini-Sharifabad M, Hadinedoushan H. 2007. "Prenatal stress induces learning deficits and is associated with a decrease in granules and CA3 cell dendritic tree size in rat hippocampus" Anat Sci Int. 82(4):211-217.

Hoyme HE, May PA, Kalberg WO, Kodituwakku P, Gossage JP, Trujillo PM, Buckley DG, Miller JH, Aragon AS, Khaole N, Viljoen DL, Jones KL, Robinson LK. 2005. "A practical clinical approach to diagnosis of fetal alcohol spectrum disorders: c Wattendorf larification of the 1996 institute of medicine criteria" Pediatrics. 115(1):39-47.

Hsiao SH., Parrish AR., Nahm SS., Abbott LC., McCoola BA., Fryea GD. 2002. "Effects of early postnatal ethanol intubation on GABAergic synaptic proteins" Developmental Brain Research. 138:177-185.

Hughes PD., Kim YN., Randall PK., Leslie SW. 1998. "Effect of prenatal ethanol exposure on the developmental profile of the NMDA receptor subunits in rat forebrain and hippocampus" Alcoholism: Clinical and Experimental Research. 22(6):1255-1261.

Hughes PD, Wilson WR, Leslie SW. 2001. "Effect of gestational ethanol exposure on the NMDA receptor complex in rat forebrain: from gene transcription to cell surface" Brain Res Dev Brain Res. 129(2):135-145.

Hunsaker MR, Lee B, Kesner RP. 2008. "Evaluating the temporal context of episodic memory: The role of CA3 and CA1" Behav Brain Res. 188:310–315.

Ieraci A., Herrera DG. 2007. "Single alcohol exposure in early life damages hippocampal stem/progenitor cells and reduces adult neurogenesis" Neurobiology of Disease. 26:597-605.

Ikonomidou C., Bittigau P., Ishimaru MJ., Wozniak DF., Koch C., Genz K. 2000. "Ethanol-induced apoptotic neurodegeneration and fetal alcohol syndrome" Science. 287: 1056–1060.

Inta D, Alfonso J, von Engelhardt J, Kreuzberg MM, Meyer AH, van Hooft JA, Monyer H. 2008. "Neurogenesis and widespread forebrain migration of distinct GABAergic neurons from the postnatal subventricular zone" Proc Natl Acad Sci U S A. 105:20994-20999.

Iqbal, U., Dringenberg, HC., Brien, JF., Reynolds, JN. 2004. "Chronic prenatal ethanol exposure alters hippocampal GABA$_A$ receptors and impairs spatial learning in the quinea pig" Behavioural Brain Research. 150(1-2):117-125.

Ishizuka N, Weber J, Amaral DG. 1990. " Organization of intrahippocampal projections originating from CA3 pyramidal cells in the rat" J Comp Neurol. 295(4):580-623.

Ishizuka N, Cowan WM, Amaral DG. 1995. "A quantitative analysis of the dendritic organization of pyramidal cells in the rat hippocampus" J Comp Neurol. 362(1):17-45.

Janz R, Südhof TC, Hammer RE, Unni V, Siegelbaum SA, Bolshakov VY. 1999. "Essential roles in synaptic plasticity for synaptogyrin I and synaptophysin I" Neuron. 24(3):687-700.

Jensen O., Lisman JE. 1996. "Hippocampal CA3 region predicts memory sequences: Accounting for the phase precession of place cells" Learning & Memory. 3:279–287.

Jia N, Yang K, Sun Q, Cai Q, Li H, Cheng D, Fan X, Zhu Z. 2010. "Prenatal stress causes dendritic atrophy of pyramidal neurons in hippocampal CA3 region by glutamate in offspring rats" Dev Neurobiol. 2:114–125.

Johnson TB., Goodlett CR. 2002. "Selective and enduring deficits in spatial learning after limited neonatal binge alcohol exposure in male rats" Alcoholism Clinical and Experimental Research. 26(1):83-93.

Jones DG, Harris RJ. 1995. "An analysis of contemporary morphological concepts of synaptic remodelling in the CNS: perforated synapses revisited" Rev Neurosci. 6(3):177-219.

Kallinikos P., Berhanu M., O"Donnell C., Boulton AJM., Efron N., Malik RA. 2004. "Corneal Nerve Tortuosity in Diabetic Patients with Neuropathy" Investigative Ophthalmology and Visual Science. 45(2): 418–422.

Kaplan MS, Bell DH. 1983. "Neuronal proliferation in the 9-month-old rodent-radioautographic study of granule cells in the hippocampus" Exp Brain Res. 52:1-5.

Keane B., Leonard B. 1989. "Rodent models of alcoholism: A review" Alcohol and Alcoholism. 24(4):299–309.

Kemp A, Manahan-Vaughan D. 2007. "Hippocampal long-term depression: master or minion in declarative memory processes?" Trends Neurosci. 30(3):111-118.

Kempermann G, Gast D, Kronenberg G, Yamaguchi M, Gage FH. 2003. "Early determination and long-term persistence of adult-generated new neurons in the hippocampus of mice" Development. 130:391-399.

Kennedy MB. 1998. "Signal transduction molecules at the glutamatergic postsynaptic membrane" Brain Res Brain Res Rev. 26(2-3):243-257.

Kesner RP, Hunsaker MR, Gilbert PE. 2005. "The role of CA1 in the acquisition of an object trace-odor paired associate task" Behav Neurosci. 119:781–786.

Kessey K, Trommer BL, Overstreet LS, Ji T, Mogul DJ. 1997. "A role for adenosine A2 receptors in the induction of long-term potentiation in the CA1 region of rat hippocampus" Brain Res. 756(1-2):184-190.

Kilic U, Yilmaz B, Ugur M, Yüksel A, Reiter RJ, Hermann DM, Kilic E. 2012. "Evidence that membrane-bound G protein-coupled melatonin receptors MT1 and MT2 are not involved in the neuroprotective effects of melatonin in focal cerebral ischemia" J Pineal Res. 52(2):228-235.

Kilic E., Elali A., Kilic L., Guo Z., Ugur M., Uslu U., Bassetti CL., Hermann DM. 2010. "Role of Nogo-A in neuronal survival in the reperfused ischemic brain" Journal of Cerebral Blood Flow and Metabolism. 30(5):969-984.

Kim E., Sheng M. 2004. "PDZ domain proteins of synapses" Nat Rev Neurosci. 5(10):771-781.

Kim KC., Go HS., Bak HR., Choi CS., Choi I, Kim P., Han SH., Han SM., Shin CY., Ko KH. 2010. "Prenatal exposure of ethanol induces increased glutamatergic neuronal differentiation of neural progenitor cells" Journal of Biomedical Science. 17:85.

Kirov SA, Sorra KE, Harris KM. 1999. Slices have more synapses than perfusion-fixed hippocampus from both young and mature rats" J Neurosci. 19(8):2876-2886.

Klintsova AY, Helfer JL, Calizo LH, Dong WK, Goodlett CR, Greenough WT. 2007. "Persistent impairment of hippocampal neurogenesis in young adult rats following early postnatal alcohol exposure" Alcohol Clin Exp Res. 31:2073-2082.

Koehl M, Lemaire V, Le Moal M, Abrous DN. 2009. "Age-dependent effect of prenatal stress on hippocampal cell proliferation in female rats" Eur J Neurosci. 29:635-640.

Köhler C., Steinbusch H. 1982. "Identification of serotonin and non-serotonin-containing neurons of the mid-brain raphe projecting to the entorhinal area and the hippocampal formation: A combined

immunohistochemical and fluorescent retrograde tracing study in the rat brain" Neuroscience. 7:951–975.

Köhler C., Swanson LW., Haglund L., Wu YY. 1985. "The cytoarchitecture, histochemistry, and projections of the tuberomammillary nucleus in the rat" Neuroscience. 16:85–110.

Kosaka T. 1983. "Axon initial segments of the granule cell in the rat dentate gyrus: Synaptic contacts on bundles of axon initial segments" Brain Res. 274:129–134.

Kosaka T., Hama K., Wu JY. 1984. "GABAergic synaptic boutons in the granule cell layer of rat dentate gyrus" Brain Res. 293:353–359.

Kosaka T., Hama K., Nagatsu I. 1987. "Tyrosine hydroxylaseimmunoreactive intrinsic neurons in the rat cerebral cortex" Exp Brain Res. 68:393–405.

Kostyuk PG. 1986. "Calcium channels in the cell membrane" Neurosci Behav Physiol. 16(5):401-410.

Kotch LE., Chen SY., Sulik KK. 1995. "Ethanol-induced teratogenesis: Free radical damage as a possible mechanism" Teratology. 53:128-136.

Krettek JE., Price JL. 1977. "Projections from the amygdaloid complex and adjacent olfactory structures to the entorhinal cortex and to the subiculum in the rat and cat" J Comp Neurol. 172:723–752.

Kuge T, Asayama T, Kakuta S, Murakami K, Ishikawa Y, Kuroda M, Imai T, Seki K, Omoto M, Kishi K. 1993. "Effect of ethanol on the development and maturation of synapses in the rat hippocampus: a quantitative electron-microscopic study" Environ Res. 62(1):99-105.

Laplagne DA, Espósito MS, Piatti VC, Morgenstern NA, Zhao C, van Praag H, Gage FH, Schinder AF. 2006. "Functional convergence of neurons generated in the developing and adult hippocampus" PLoS Biol. 4(12):e409.

Laurberg S. 1979. "Commissural and intrinsic connections of the rat hippocampus" J Comp Neurol. 184:685–708.

Laurberg S., Sorensen KE. 1981. "Associational and commissural collaterals of neurons in the hippocampal formation (hilus fasciae dentatae and subfield CA3)" Brain Res. 212:287–300.

Lee MH., Rabe A., 1999. "Infantile handling eliminates reversal learning deficit in rats prenatally exposed to alcohol" Alcohol. 18(1):49-53.

Lemaire V, Koehl M, Le Moal M, Abrous DN. 2000. "Prenatal stress produces learning deficits associated with an inhibition of neurogenesis in the hippocampus" Proc Natl Acad Sci U S A. 97:11032-11037.

Lemmens MA, Sierksma AS, Rutten BP, Dennissen F, Steinbusch HW, Lucassen PJ, Schmitz C. 2011. "Age-related changes of neuron numbers in the frontal cortex of a transgenic mouse model of Alzheimer's disease" Brain Struct Funct. 216:227-237.

Levy WB. 1996. "A sequence predicting CA3 is a flexible associator that learns and uses context to solve hippocampal-like tasks" Hippocampus. 6:579–590.

Li XG., Somogyi P., Ylinen A., Buzsaki G. 1994. "The hippocampal CA3 network: An in vivo intracellular labeling study" J Comp Neurol. 339:181–208.

Light KE., Brown DP., Newton BW., Belcher SM., Kane CJM. 2002. "Ethanol-induced alterations of neurotrophin receptor expression on Purkinje cells in the neonatal rat cerebellum" Brain Research. 924: 71–81.

Lisman JE. 1999. "Relating hippocampal circuitry to function: Recall of memory sequences by reciprocal dentate-CA3 interactions" Neuron. 22(2):233–242.

Lisman JE., Otmakhova NA. 2001. "Storage, recall, and novelty detection of sequences by the hippocampus: Elaborating on the SOCRATIC model to account for normal and aberrant effects of dopamine" Hippocampus. 11(5):551–568.

Lister JP., Blatt GJ., Debassio WA., Kemper TL., Tonkiss J., Galler JR., Rosene DL. 2005. "Effect of prenatal protein malnutrition on numbers of neurons in the principal cell layers of the adult rat hippocampal formation" Hippocampus. 15:393-403.

Lister JP., Tonkiss J., Blatt GJ., Kemper TL., DeBassio WA., Galler JR., Rosene DL. 2006. "Asymmetry of neuron numbers in the hippocampal formation of prenatally malnourished and normally nourished rats: a stereological investigation" Hippocampus. 16:946-958.

Livy DJ., Miller EK., Maier SE., West JR. 2003. "Fetal alcohol exposure and temporal vulnerability: effects of binge-like alcohol exposure on the developing rat hippocampus" Neurotoxicol Teratol. 25:447-458.

Lorento de No R. 1934. "Studies on the structure of the cerebral cortex. II. continuation of the study of the ammonic system" J Psychol Neurol. 46:113-177.

Low LK, Cheng HJ. 2006. "Axon pruning: an essential step underlying the developmental plasticity of neuronal connections" Philos Trans R Soc Lond B Biol Sci. 361:1531-1544.

Lucassen PJ., Bosch OJ., Jousma E., Krömer SA., Andrew R., Seckl JR., Neumann ID. 2009. "Prenatal stress reduces postnatal neurogenesis in rats selectively bred for high, but not low, anxiety: possible key role of placental 11beta-hydroxysteroid dehydrogenase type 2" Eur J Neurosci. 29:97-103.

Lukoyanov NV., Madeira MD., Paula-Barbosa MM. 1999. "Behavioral and neuroanatomical consequences of chronic ethanol intake and withdrawal" Physiol Behav. 66:337-346.

Luo J., Miller MW. 1998. "Growth factor-mediated neural proliferation: target of ethanol toxicity" Brain Res Brain Res Rev. 27(2):157-167.

Lyck L., Krøigård T, Finsen B. 2007. "Unbiased cell quantification reveals a continued increase in the number of neocortical neurons during early post-natal development in mice" Eur J Neurosci. 26:1749-1764.

Lynch G., Deadwyler S, Cotman G 1973. "Postlesion axonal growth produces permanent functional connections" Science. 180(4093):1364-1366.

Lynch MA., Voss KL., Rodriguez J., Bliss TV. 1994. "Increase in synaptic vesicle proteins accompanies long-term potentiation in the dentate gyrus" Neuroscience. 60(1):1-5.

Maciejewski-Lenoir D. 1993. "Chronic prenatal ethanol exposure does not affect the expression of selected genes in rat brain development" Alcohol Alcohol. 28(4):401-412.

Magloczky Z., Acsady L., Freund TF. 1994. "Principal cells are the postsynaptic targets of supramammillary afferents in the hippocampus of the rat" Hippocampus. 4:322–334.

Maier SE., Chen WJ., Miller JA., West JR. 1997. "Fetal alcohol exposure and temporal vulnerability regional differences in alcohol-induced microencephaly as a function of the timing of binge-like alcohol exposure during rat brain development" Alcohol Clin Exp Res. 21(8):1418-1428.

Maier SE., Miller JA., West JR. 1999. "Prenatal binge-like alcohol exposure in the rat results in region-specific deficits in brain growth" Neurotoxicol Teratol. 21:285-291.

Maier SE., West JR. 2001a. "Drinking patterns and alcohol-related birth defects" Alcohol Res Health. 25:168-174.

Maier SE., West JR. 2001b. "Regional differences in cell loss associated with binge-like alcohol exposure during the first two trimesters equivalent in the rat" Alcohol. 23:49-57.

Mameli M., Zamudio PA., Carta M., Valenzuela CF. 2005. "Developmentally regulated actions of alcohol on hippocampal glutamatergic transmission" J Neurosci. 25(35):8027-8036.

Mameli M., Valenzuela CF. 2006. "Alcohol increases efficacy of immature synapses in a neurosteroid-dependent manner" Eur J Neurosci 23(3):835-839.

Manns JR., Howard MW., Eichenbaum H. 2007. "Gradual changes in hippocampal activity support remembering the order of events" Neuron. 56:530–540.

Marrone DF., Petit TL. 2002. "The role of synaptic morphology in neural plasticity: structural interactions underlying synaptic power" Brain Res Brain Res Rev. 38(3):291-308.

Martin JC., Martin DC., Sigman G., Radov B. 1978. "Maternal ethanol consumption and hyperactivity in cross-fostered offspring" Physiol Psychol. 6:362–365.

Matsuzaki M., Ellis-Davies GC., Nemoto T., Miyashita Y., Iino M., Kasai H. 2001. "Dendritic spine geometry is critical for AMPA receptor expression in hippocampal CA1 pyramidal neurons" Nat Neurosci. 4(11):1086-1092.

Mattson SN., Riley EP., Jernigan TL., Garcia A., Kaneko WM., Ehlers CL., Jones KL. 1994. "A decrease in the size of the basal ganglia following prenatal alcohol exposure: a preliminary report" Neurotoxicol Teratol. 16:283-289.

Mattson SN., Schoenfeld AM., Riley EP. 2001. "Teratogenic effects of alcohol on brain and behavior" Alcohol Res Health. 25(3):185-191.

McAllister AK. 2000. "Cellular and molecular mechanisms of dendrite growth" Cereb Cortex. 10(10):963-973.

Fujioka A., McGinty JF., VanDerKooy D., Bloom FE. 1984. "The distribution and morphology of opioid peptide immunoreactive neurons in the cerebral cortex of rats" J Neurosci. 4:1104–1117.

Fujioka A., Fujioka T., Ishida Y., Maekawa T., Nakamura S. 2006. "Differential effects of prenatal stress on the morphological maturation of hippocampal neurons" Neuroscience. 141(2):907-915.

McKittrick CR., Magariños AM., Blanchard DC., Blanchard RJ., McEwen BS., Sakai RR. 2000. "Chronic social stress reduces dendritic arbors in CA3 of hippocampus and decreases binding to serotonin transporter sites" Synapse. 36(2):85-94.

Megías M., Emri Z., Freund TF., Gulyás AI. 2001. "Total number and distribution of inhibitory and excitatory synapses on hippocampal CA1 pyramidal cells" Neuroscience. 102(3):527-540.

Meyer LS., Riley EP. 1986. "Behavioral teratology of alcohol. In Riley EP, Vorhees CV (eds). Handbook of Behavioral Teratology" New York: Plenum. 101–140.

Mihalick SM., Crandall JE., Langlois JC., Krienke JD., Dube WM. 2001. "Prenatal ethanol exposure generalized learning impairment and medial prefrontal cortical deficits in rats" Neurotoxicol Teratol. 23:453-462.

Miki T., Harris SJ., Wilce PA., Takeuchi Y., Bedi KS. 2003. "Effects of alcohol exposure during early life on neuron numbers in the rat hippocampus. I. hilus neurons and granule cell" Hippocampus. 13:388-398.

Miles R., Toth K., Gulyas AI., Hajos N., Freund TF. 1996. "Differences between somatic and dendritic inhibition in the hippocampus" Neuron. 16:815–823.

Miller MW. 1988. "Effect of prenatal exposure to ethanol on the development of cerebral cortex: I. Neuronal generation" Alcohol Clin Exp Res. 12:440–449.

Miller MW. 1989. "Effect of prenatal exposure to ethanol on neocortical development: II. Cell proliferation in the ventricular and subventricular zones of the rat" J Comp Neurol. 278: 326–338.

Miller MW., Chiaia NL., Rhoades RW. 1990. "Intracellular recording and labeling study of corticospinal neurons in the rat somatosensory cortex: Effect of prenatal exposure to ethanol" Comp Neurol. 296:1–15.

Miller MW., Nowakowski RS. 1991. "Effect of prenatal exposure to ethanol on the cell cycle kinetics and growth fraction in the proliferative zones of fetal rat cerebral" Alcohol Clin Exp Res. 15 :229–232.

Miller MW. 1992. "Circadian rhythm of cell proliferation in the telencephalic ventricular zone: effect of in utero exposure to ethanol" Brain Res. 595(1):17-24.

Miller MW., Robertson S. 1993. "Prenatal exposure to ethanol alters the postnatal development and transformation of radial glia to astrocytes in the cortex" J Comp Neurol. 337:253-266.

Miller MW. 1995. "Generation of neurons in the rat dentate gyrus and hippocampus: effects of prenatal and postnatal treatment with ethanol" Alcohol Clin Exp Res. 19:1500-1509.

Minetti A., Arolfo MP., Virgolini MB., Brioni JD., Fulginiti S. 1996. "Spatial Learning in Rats Exposed to Acute Ethanol Intoxication on Gestational Day 8" Pharmacol Biochem Behav. 53:361-367.

Mirescu C., Gould E. 2006. "Stress and adult neurogenesis" Hippocampus. 16:233-238.

Montone KT., Fass B., Hamill GS. 1988. "Serotonergic and nonserotonergic projections from the rat interpeduncular nucleus to the septum, hippocampal formation and raphe: A combined immunocytochemical and fluorescent retrograde labelling study of neurons in the apical subnucleus" Brain Res Bull. 20:233–240.

Mooney SM. Miller MW. 2007. "Time-specific effects of ethanol exposure on cranial nerve nuclei: Gastrulation and neuronogenesis" Experimental Neurology. 205(1):56-63.

Moore RY., Ziegler B., Bayer SA. 1978. "Monoamine neuron innervation of the hippocampal formation: Alteration by neonatal irradiation" Exp Neurol. 60:318–326.

Moore DB., Madorsky I., Paiva M., Heaton MB, 2004. "Ethanol exposure alters neurotrophin receptor expression in the rat central nervous system: Effects of neonatal exposure" Journal of Neurobiology. 60(1):114-126.

Morris R. 1984. "Developments of a water-maze procedure for studying spatial learning in the rat" J Neurosci. Methods. 11:47–60.

Morris RG. 2006. "Elements of a neurobiological theory of hippocampal function: the role of synaptic plasticity, synaptic tagging and schemas" Eur J Neurosci. 23(11):2829-2846.

Morriset RA., Martin D., Wilson WA., Savage DD., Swartzwelder HS. 1989. "Prenatal exposure to ethanol decreases the sensitivity of the adult rat hippocampus to N-Methyl-D-Aspartate" Alcohol. 6(5):415-420.

Morrison JH., Benoit R., Magistretti PJ., Ling N., Bloom FE. 1982. "Immunohistochemical distribution of pro-somatostatinrelated peptides in hippocampus" Neurosci Lett. 34:137–142.

Morterá P, Herculano-Houzel S. 2012. "Age-related neuronal loss in the rat brain starts at the end of adolescence" Front Neuroanat. 6:45.

Moser MB, Trommald M, Andersen P. 1994. "An increase in dendritic spine density on hippocampal CA1 pyramidal cells following spatial learning in adult rats suggests the formation of new synapses" Proc Natl Acad Sci U S A. 91(26):12673-12675.

Mullany PM, Lynch MA. 1998. "Evidence for a role for synaptophysin in expression of long-term potentiation in rat dentate gyrus" Neuroreport. 9(11):2489-2494.

Mychasiuk R., Gibb R., Kolb B. 2011. "Prenatal bystander stress induces neuroanatomical changes in the prefrontal cortex and hippocampus ofdeveloping rat offspring" Brain Res. 1412:55-62.

Naber PA., Witter M. P., Lopes da Silva FH. 2000. "Differential distribution of barrel or visual cortex-evoked responses along the rostro-caudal axis of the peri- and postrhinal cortices" Brain Res. 877:298–305.

Nagahara AH, Handa RJ. 1997. "Fetal alcohol exposure produces delay-dependent memory deficits in juvenile and adult rats" Alcohol Clin Exp Res. 21:710-715.

Nakano T., Fujimoto T., Shimooki S., Fukudome T., Uchida T., Tsuji T., Mitsuyama Y., Akimoto H., Furukawa S. 1996. "Transient elevation of nerve growth factor content in the rat hippocampus and frontal cortex by chronic ethanol treatment" Psychiatry Clin Neurosci. 50(3):157-160.

Napper RM., West JR. 1995. "Permanent neuronal cell loss in the cerebellum of rats exposed to continuous low blood alcohol levels during the brain growth spurt: a stereological investigation" J Comp Neurol. 362:283-292.

Neese S., La Grange L., Trujillo E., Romero D., 2004. "The effects of ethanol and silymarin treatment during gestation on spatial working memory" BMC Complementary and Alternative Medicine. 4:4.

Nikonenko I., Boda B., Steen S., Knott G., Welker E., Muller D. 2008. "PSD-95 promotes synaptogenesis and multiinnervated spine formation through nitric oxide signaling" J Cell Biol. 183(6):1115-1127.

Nixon K., Crews FT. 2002. "Binge ethanol exposure decreases neurogenesis in adult rat hippocampus" J Neurochem. 83:1087-1093.

Nixon K., Hughes PD., Amsel A., Leslie SW. 2004. "NMDA receptor subunit expression after combined prenatal and postnatal exposure to ethanol" Alcoholism: Clinical and Experimental Research. 28(1):105-112.

Norman KA., O'Reilly RC. 2003. "Modeling hippocampal and neocortical contributions to recognition memory: A complementarylearning- systems approach" Psychological Review. 110:611–646.

Nyakas C., Luiten PGM., Spencer DG., Traber J. 1987. "Detailed projection patterns of septal and diagonal band efferents to the hippocampus in the rat with emphasis on innervation of CA1 and dentate gyrus" Brain Res Bull. 18:533–545.

Nyffeler M., Zhang WN., Feldon J., Knuesel I. 2007. "Differential expression of PSD proteins in age-related spatial learning impairments" Neurobiol Aging. 28(1):143-155.

Olney JW., Ishimaru MJ., Bittigau P., Ikondomidou C. 2000. "Ethanol-induced apoptotic neurodegeneration in the developing brain" Apoptosis. 5(6):515-521.

Olney JW., Tenkova T., Dikranian K., Labruyere J., Qin QY., Ikonomidou C., 2002a. "Ethanol-induced apoptotic neurodegeneration in the developing C57BL/6 mouse brain" Developmental Brain Research. 133:115-126.

Olney JW., Tenkova T., Dikranian K. 2002b. "Ethanol-induced caspase-3 activation in the in vivo developing mouse brain" Neurobiology of Disease. 9:205-219.

Olney JW., Wozniak DF., Farber NB., Jevtovic-Todorovic V., Bittigau P., Ikonomidou C. 2002c. "The enigma of fetal alcohol neurotoxicity" Annals of Medicine. 34:109-119.

Olney JW. 2004. "Fetal alcohol syndrome at the cellular level" Addiction Biology. 9:137-149.

O'Malley A., O'Connell C., Murphy KJ., Regan CM. 2000. "Transient spine density increases in the mid-molecular layer of hippocampal dentate gyrus accompany consolidation of a spatial learning task in the rodent" Neuroscience. 99(2):229-232.

Osborne GL., Caul WF., Fernandez K. 1979. "Behavioral effects of prenatal ethanol exposure and differential early experience in rats" Pharmacol Biochem Behav. 12:393–401.

Papa M, Bundman MC, Greenberger V, Segal M. 1995. "Morphological analysis of dendritic spine development in primary cultures of hippocampal neurons" J Neurosci. 15(1):1-11.

Papa M., Segal M. 1996. "Morphological plasticity in dendritic spines of cultured hippocampal neurons" Neuroscience. 71(4):1005-1011.

Parks EA., McMechan AP., Hannigan JH., Berman RF. 2008. "Environmental enrichment alters neurotrophin levels after fetal alcohol exposure in rats" Alcohol Clin Exp Res. 32(10):1741-1751.

Pauli J., Wilce P., Bedi KS. 1995. "Spatial Learning Ability of Rats Following Acute Exposure to Alcohol During Early Postnatal Life" Physiol Behav. 58(5):1013-1020.

Paxinos G., Watson C. 2007. "The rat brain in stereotaxic coordinates" USA: Academic Press. Figures:40-90.

Peng Y., Yang PH., Ng SSM., Wong OG., Liu J., He ML., Kung HF., Lin MCM. 2004. "A critical role of Pax6 in alcohol-induced fetal microcephaly" Neurobiology of Disease. 16(2):370–376.

Perez-Torrero E., Duran P., Granados P., Gutierrez-Ospina G., Cintra L., Diaz-Cintra S. 1997. "Effects of acute prenatal ethanol exposure on Bergmann glia cells early postnatal development" Brain Research. 746: 305–308.

Pickel VM., Segal M., Bloom FE. 1974. "A radioautographic study of the efferent pathways of the nucleus locus coeruleus" J Comp Neurol. 155:15–42.

Pierce DR., West JR. 1986. "Alcohol-induced microencephaly during the third trimester equivalent: relationship to dose and blood alcohol concentration" Alcohol. 3(3):185–191.

Pikkarainen M., Rönkkö S., Savander V., Insausti R., Pitkänen A. 1999. "Projections from the lateral, basal, and accessory basal nuclei of the amygdala to the hippocampal formation in rat" J Comp Neurol. 403(2):229-260.

Prendergast MA., Harris BR., Mullholland PJ., Blanchard JA., Gibson DA., Holley RC., Littleton JM. 2004. "Hippocampal CA1 region neurodegeneration produced by ethanol withdrawal requires activation of intrinsic polysynaptic hippocampal pathways and function of N-methyl-D-aspartate receptors" Neuroscience. 124(4):869-877.

Puglia MP., Valenzuela CF. 2010. "Repeated third trimester-equivalent ethanol exposure inhibits long-term potentiation in the hippocampal CA1 region of neonatal rats" Alcohol. 44(3):283-290.

Pyapali GK., Sik A., Penttonen M., Buzsaki G., Turner DA. 1998. "Dendritic properties of hippocampal CA1 pyramidal neurons in the rat: intracellular staining in vivo and in vitro" J Comp Neurol. 391(3):335-352.

Ramanathan R., Wilkemeyer MF., Mittal B., Perides G., Charness ME. 1996. "Alcohol inhibits cell-cell adhesion mediated by human L1" The Journal of Cell Biology. 133(5):381–390.

Ramón y Cajal S. 1911. "Histologie du Systeme Nerveux de l'Homme et des Vertebres" Maloine, Paris.

Randall CL., Anton RF., Becker HC., White NM. 1989. "Role of prostaglandins in alcohol teratogenesis" Annals of the New York Academy of Sciences. 562:178–182.

Ransdell JL., Faust TB., Schulz DJ. 2010. "Correlated Levels of mRNA and Soma Size in Single Identified Neurons: Evidence for Compartment-specific Regulation of Gene Expression" Front Mol Neurosci. 3:116.

Rao MS., Shetty AK. 2004. "Efficacy of doublecortin as a marker to analyse the absolute number and dendritic growth of newly generated neurons in the adult dentate gyrus" Eur J Neurosci. 19(2):234-246.

Redila VA., Olson AK., Swann SE., Mohades G., Webber AJ., Weinberg J., Christie BR. 2006. "Hippocampal cell proliferation is reduced following prenatal ethanol exposure but can be rescued with voluntary exercise" Hippocampus. 16(3):305-311.

Reyes E., Wolfe J., Savage DD. 1989. "The effects of prenatal alcohol exposure on radial arm maze performance in adult rats" Physiology and Behavior. 46(1):45-48.

Rietze R., Poulin P., Weiss S. 2000. "Mitotically active cells that generate neurons and astrocytes are present in multiple regions of the adult mouse hippocampus" J Comp Neurol. 424:397-408.

Riley JN., Moore RY. 1981. "Diencephalic and brainstem afferents to the hippocampal formation of the rat" Brain Res Bull. 6:437–444.

Riley EP., Thomas JD., Goodlett CR., Klintsova AY., Greenough WT., Hungund BL., Zhou F., Sari Y., Powrozek T., Li TK. 2001. "Fetal alcohol effects: mechanisms and treatment" Alcohol Clin Exp Res. 25:110-116.

Riley EP., McGee CL., Sowell ER., 2004. "Teratogenic effects of alcohol: A decade of brain imaging" American Journal of Medical Genetics Part C Seminars in Medical Genetics, 127(1):35–41.

Rice D., Barone S Jr. 2000. "Critical periods of vulnerability for the developing nervous system: evidence from humans and animal models" Environmental Health Perspectives. 108 (3): 511–533.

Rogers CJ., Hunter BE. 1992. "Chronic ethanol treatment reduces inhibition in CA1 of the rat hippocampus" Brain Res Bull. 28(4):587-592.

Ruan YW., Zou B., Fan Y., Li Y., Lin N., Zeng YS., Gao TM., Yao Z., Xu ZC. 2006. "Dendritic plasticity of CA1 pyramidal neurons after transient global ischemia" Neuroscience. 140(1):191-201.

Ryabinin AE., Cole M., Bloom FE., Wilson MC. 2006. "Exposure of neonatal rats to alcohol by vapor inhalation demonstrates specificity of microcephaly and purkinje cell loss but not astrogliosis" Alcohol Clin Exp Res. 19:784-791.

Sag C., Yokusoglu M., Cincik M., Ozkan M., Kayir H., Uzun M., Baykal B., Ozogul C., Baysan O., Uzbay IT. 2006. "The prevention of myocardial ultrastructural changes by perindopril, atenonol, and amlodipine in chronic alcohol administered rats" Pharmacol Res. 53:142-148.

Samudio-Ruiz SL, Allan AM, Sheema S, Caldwell KK. 2010. "Hippocampal N-methyl-D-aspartate receptor subunit expression profiles in a mouse model of prenatal alcohol exposure" Alcohol Clin Exp Res. 34(2):342-353.

Saunders DE., Zajac CS., Wappler NL. 1995. "Alcohol inhibits neurite extension and increases N-myc and c-myc proteins" Alcohol. 12(5):475-483.

Savoy-Moore RT., Dombrowski MP., Cheng A., Abel EA., Sokol RJ. 1989. "Low dose alcohol contracts the human umbilical artery in vitro" Alcoholism Clinical and Experimental Research. 13(1):40–42.

Scheff SW., Price DA. 2006 "Alzheimer's disease-related alterations in synaptic density: neocortex and hippocampus" J Alzheimers Dis. 9(3 Suppl):101-115.

Schmitz C., Rhodes ME., Bludau M., Kaplan S., Ong P., Ueffing I., Vehoff J., Korr H., Frye CA. 2002. "Depression: reduced number of granule cells in the hippocampus of female, but not male, rats due to prenatal restraint stress" Mol Psychiatry. 7:810–813.

Schlessinger AR., Cowan WM., Gottlieb DI. 1975. "An autoradiographic study of the time of origin and the pattern of granule cell migration in the dentate gyrus of the rat" J Comp Neurol. 159(2):149-175.

Schneider ML., Moore CF., Kraemer GW. 2004. " Moderate level alcohol during pregnancy, prenatal stress, or both and limbic-hypothalamic-pituitary-adrenocortical axis response to stress in rhesus monkeys" Child Dev. 75(1):96-109.

Seabold GK., Luo J., Miller MW. 1998. "Effect of ethanol on neurotrophin-mediated cell survival and receptor expression in cultures of cortical neurons" Brain Research Developmental Brain Research. 108(1-2):139-145.

Segal M. 2001. "New building blocks for the dendritic spine" Neuron. 31(2):169-171.

Segev I., Rall W. 1998. "Excitable dendrites and spines: earlier theoretical insights elucidate recent direct observations" Trends Neurosci. 21(11):453-460.

Sekino Y., Obata K., Tanifuji M., Mizuno M., Murayama J. 1997. "Delayed signal propagation via CA2 in rat hippocampal slices revealed by optical recording" J Neurophysiol. 78:1662–1668.

Seress L., Pokorny J. 1981. "Structure of the granular layer of the rat dentate gyrus: A light microscopic and Golgi study" J Anat. 133:181–195.

Seress L., Mrzljak L. 1987. "Basal dendrites of granule cells are normal features of the fetal and adult dentate gyrus of both monkey and human hippocampal formations" Brain Res. 405(1):169-174.

Seress L., Ribak CE. 1990. "Postnatal development of the light and electron microscopic features of basket cells in the hippocampal denstate gyrus of the rat" Anat Embryol. 181:547–565.

Shah KR., West M. 1984. "Behavioral changes in rat following perinatal exposure to ethanol" Neurosci Lett. 47:145–148.

Shibley IAJ., Pennington SN. 1997. "Metabolic and mitotic changes associated with the fetal alcohol syndrome" Alcohol and Alcoholism. 32 (4):423–434.

Silva-Gómez AB, Rojas D, Juárez I, Flores G. 2003. "Decreased dendritic spine density on prefrontal cortical and hippocampal pyramidal neurons in postweaning social isolation rats" Brain Res. 983(1-2):128-136.

Siew LK., Love S., Dawbarn D., Wilcock GK., Allen SJ. 2004. "Measurement of pre- and post-synaptic proteins in cerebral cortex: effects of post-mortem delay" J Neurosci Methods. 139(2):153-159.

Silberman Y., Shi L., Brunso-Bechtold JK., Weiner JL. 2008. "Distinct mechanisms of ethanol potentiation of local and paracapsular GABAergic synapses in the rat basolateral amygdala" J Pharmacol Exp Ther. 324(1):251-260.

Singh AK., Gupta S., Jiang Y., Younus M., Ramzan M. 2009. "In vitro neurogenesis from neural progenitor cells isolated from the hippocampus region of the brain of adult rats exposed to ethanol during early development through their alcohol-drinking mothers" Alcohol Alcohol. 44(2):185-198.

Sliwowska JH., Barker JM., Barha CK., Lan N., Weinberg J., Galea LA. 2010. "Stress-induced suppression of hippocampal neurogenesis in adult male rats is altered by prenatal ethanol exposure" Stress. 13:301-313.

Smith DE., Foundas A., Canale J. 1986. "Effect of perinatally administered ethanol on the development of the cerebellar granule cell" Experimental Neurology. 92: 491–501.

Smith AM., Pappalardo D., Chen WJ. 2008. "Estimation of neuronal numbers in rat hippocampus following neonatal amphetamine exposure: a stereology study" Neurotoxicol Teratol. 30:495-502.

Smith AM., Wellmann KA., Lundblad TM., Carter ML., Barron S., Dwoskin LP. 2012. "Lobeline attenuates neonatal ethanol-mediated changes in hyperactivity and dopamine transporter function in the prefrontal cortex in rats" Neuroscience. 206:245-254.

Snyder AK., Jiang F., Singh SP. 1992. "Effects of ethanol on glucose utilization by cultured mammalian embryos" Alcohol Clin Exp Res. 16(3):466-470.

Somogyi P., Freund TF., Hodgson AJ., Somogyi J., Berboukas D., Chubb IW. 1985. "Identified axo-axonic cells are immunoreactive for GABA in the hippocampus and visual cortex of the cat" Brain Res. 332:143–149.

Soriano E., Frotscher M. 1989. "A GABAergic axo-axonic cell in the fascia dentata controls the main excitatory hippocampal pathway" Brain Res. 503:170–174.

Sorra KE., Harris KM. 1993. "Occurrence and threedimensional structure of multiple synapses between individual radiatum axons and their target pyramidal cells in hippocampal area CA1" J Neurosci. 13:3736–3748.

Sorra KE., Harris KM. 1998. "Stability in synapse number and size at 2 hr after long-term potentiation in hippocampal area CA1" J Neurosci. 18:658–671.

Sousa N., Madeira MD., Paulo-Barbosa MM. 1998. "Effects of corticosterone treatment and rehabilitation on the hippocampal formation of neonatal and adult rats. An unbiased stereological study" Brain Research. 794:199-210.

Soussi R., Zhang N., Tahtakran S., Houser CR., Esclapez M. 2010. "Heterogeneity of the supramammillary-hippocampal pathways: evidence for a unique GABAergic neurotransmitter phenotype and regional differences" Eur J Neurosci. 32:771–785.

Spong CY., Abebe DT., Gozes I., Brenneman DE., Hill JM. 2001. "Prevention of fetal demise and growth restriction in a mouse model of fetal alcohol syndrome" J Pharmacol Exp Ther. 297(2):774-779.

Spruston N., McBain CJ. 2006. "Structural and functional properties of hippocampal neurons" In: Andersen P., Morris R., Amaral D., Bliss T. and O'Keefe J. (Eds.), The Hippocampus Book. Oxford University Press. pp:133-164.

Sreenathan RN., Padmanabhan R., Singh S. 1982. "Teratogenic effects of acetaldehyde in the rat" Drug and Alcohol Dependence. 9(4):339–350.

Staff NP., Jung HY., Thiagarajan T., Yao M., Spruston N. 2000. "Resting and active properties of pyramidal neurons in subiculum and CA1 of rat hippocampus" J Neurophysiol. 84:2398–2408.

Stensaas LJ. 1967. "The development of hippocampal and dorsolateral pallial region of the cerebral hemisphere in fetal rabbits. V. Sixty millimeter stage, glial cell morphology" J Comp Neurol. 131(4):423-436.

Stepanyants A., Tama´s G., Chklovskii DB. 2004. "Class-specific features of neuronal wiring" Neuron. 43: 251–259.

Storm-Mathisen J., Fonnum F. 1972. "Localization of transmitter candidates in the hippocampal region" Prog. Brain Res. 36:41–58.

Stratton K., Howe C., Battglia F. 1996. "Fetal alcohol syndrome: Diagnosis, epidemiology, prevention and treatment" National Academy Press, Washington, DC.

Südhof TC., Lottspeich F., Greengard P., Mehl E., Jahn R. 1987. "A synaptic vesicle protein with a novel cytoplasmic domain and four transmembrane regions" Science. 238(4830):1142-1144.

Sugita S., Janz R., Südhof TC. 1999. "Synaptogyrins regulate Ca2+-dependent exocytosis in PC12 cells" J Biol Chem. 274(27):18893-18901.

Swanson LW., Cowan WM. 1977. "An autoradiographic study of the organization of the efferent connections of the hippocampal formation in the rat" J Comp Neurol. 172:49–84.,

Swanson LW., Wyss JM., Cowan WM. 1978. "An autoradiographic study of the organization of intrahippocampal association pathways in the rat" J Comp Neurol. 181:681–716.

Swanson LW., Mogenson GJ., Simerly RB., Wu M. 1987. "Anatomical and electrophysiological evidence for a projection from the medial preoptic area to the 'mesencephalic and subthalamic locomotor regions' in the rat" Brain Res. 405(1):108-122.

Tamamaki N., Abe K., Nojyo Y. 1987. "Columnar organization in the subiculum formed by axon branches originating from single CA1 pyramidal neurons in the rat hippocampus" Brain Res. 412(1):156-160.

Tang YP., Shimizu E., Dube GR., Rampon C., Kerchner GA., Zhuo M., Liu G., Tsien JZ. 1999. "Genetic enhancement of learning and memory in mice" Nature. 401(6748):63-69.

Tapia-Arancibia L., Rage F., Givalois L., Dingeon P., Arancibia S., Beauge F. 2001. "Effects of alcohol on brain-derived neurotrophic factor mRNA expression in discrete regions of the rat hippocampus and hypothalamus" Journal of Neuroscience Research. 63(2):200-208.

Tarelo-Acuña L., Olvera-Cortés E., González-Burgos I. 2000. "Prenatal and postnatal exposure to ethanol induces changes in the shape of the dendritic spines from hippocampal CA1 pyramidal neurons of the rat" Neurosci Lett. 286(1):13-16.

Tarsa L., Goda Y. 2002. "Synaptophysin regulates activity-dependent synapse formation in cultured hippocampal neurons" Proc Natl Acad Sci U S A. 99(2):1012-1016.

Tenkova T., Young C., Dikranian K., Labruyere J., Olney JW. 2003. "Ethanol induced apoptosis in the developing visual system during synaptogenensis" Investigative Ophthalmology & Visual Science. 44(7):2809-2817.

Terry RD., Masliah E., Salmon DP., Butters N., DeTeresa R., Hill R., Hansen LA., Katzman R. 1991. "Physical basis of cognitive alterations in Alzheimer's disease: synapse loss is the major correlate of cognitive impairment" Ann Neurol. 30(4):572-580.

Thomas JD., Wasserman EA., West JR., Goodlett CR. 1996. "Behavioral deficits induced by bingelike exposure to alcohol in neonatal rats: importance of developmental timing and number of episodes" Developmental Psychobiology.29(5):433-452.

Toni N., Teng EM., Bushong EA., Aimone JB., Zhao C., Consiglio A., van Praag H., Martone ME., Ellisman MH., Gage FH. 2007. "Synapse formation on neurons born in the adult hippocampus" Nat Neurosci. 10:727-734.

Toth K., Freund TF. 1992. "Calbindin D28k-containing nonpyramidal cells in the rat hippocampus: Their immunoreactivity for GABA and projection to the medial septum" Neuroscience. 49:793–805.

Tran TD., Cronise K., Marino MD., Jenkins WJ., Kelly SJ. 2000. " Critical periods for the effects of alcohol exposure on brain weight, body weight, activity and investigation" Behav Brain Res. 116: 99–110.

Tran TD., Kelly SJ. 2003. "Critical periods for ethanol-induced cell loss in the hippocampal formation" Neurotoxicol Teratol. 25:519-528.

Treves A., Rolls ET. 1992. "Computational constraints suggest the need for two distinct input systems to the hippocampal CA3 network" Hippocampus. 2:189–199.

Treves A., Tashiro A., Witter ME., Moser EI. 2008. "What is the mammalian dentate gyrus good for?" Neuroscience.154: 1155-1172.

Trommald M., Vaaland J.L., Blackstad T., Andersen P. 1990. "Neurotoxicity of excitatory amino acids. In A. Guidotti and E. Costa (eds): Dendritic Spine Changes in Rat Dentate Granule Cells AssociatedWith Long-Term Potentiation" New York: Raven. Pp:163–174.

Trommald M., Jensen V., Andersen P. 1995. "Analysis of dendritic spines in rat CA1 pyramidal cells intracellularly filled with a fluorescent dye" J Comp Neurol. 353(2):260-274.

Trommald M., Hulleberg G. 1997. "Dimensions and density of dendritic spines from rat dentate granule cells based on reconstructions from serial electron micrographs" J Comp Neurol. 377(1):15-28.

Tsien RY., Bacskai BJ., Adams SR. 1993. " FRET for studying intracellular signalling" Trends Cell Biol. 3(7):242-245.

Uban KA., Sliwowska JH., Lieblich S., Ellis LA., Yu WK., Weinberg J., Galea LA. 2010. "Prenatal alcohol exposure reduces the proportion of newly produced neurons and glia in the dentate gyrus of the hippocampus in female rats" Horm Behav. 58(5):835-843.

Ulug S., Riley EP. 1983. "The effect of methylphenidate on overactivity in rats prenatally exposed to alcohol" Neurobehav Toxicol Teratol. 5:35–39.

Uylings HB., van Pelt J., Parnavelas JG., Ruiz-Marcos A. 1994. "Geometrical and topological characteristics in the dendritic development of cortical pyramidal and non-pyramidal neurons" Prog Brain Res. 102:109-123.

Uzbay IT., Kayaalp SO. 1995. "A modified liquid diet of chronic ethanol administration: Validation by ethanol withdrawal syndrome in rats" Pharmacological Research. 31 (1): 37–42.

Valtorta F., Pennuto M., Bonanomi D., Benfenati F. 2004. "Synaptophysin: leading actor or walk-on role in synaptic vesicle exocytosis?" Bioessays. 26(4):445-453.

Van Daal JHHM., Zanderink HEA., Jenks BG., van Abeelen JHF. 1989. "Distribution of dynorphin B and methionine–enkephalin in the mouse hippocampus: Influence of genotype" Neurosci Lett. 97:241–244.

Van den Hove DL., Steinbusch HW., Scheepens A., Van de Berg WD., Kooiman LA., Boosten BJ., Prickaerts J., Blanco CE. 2006. "Prenatal stress and neonatal rat brain development" Neuroscience. 137(1):145-155.

Van Praag H., Schinder AF., Christie BR., Toni N., Palmer TD., Gage FH. 2002. "Functional neurogenesis in the adult hippocampus" Nature. 415:1030–1034.

Vázquez-Roque RA., Ramos B., Tecuatl C., Juárez I., Adame A., de la Cruz F., Zamudio S., Mena R., Rockenstein E., Masliah E., Flores G. 2012. "Chronic administration of the neurotrophic agent cerebrolysin ameliorates the behavioral and morphological changes induced by neonatal ventral hippocampus lesion in a rat model of schizophrenia" J Neurosci Res. 90:288-306.

Veena J, Rao BS, Srikumar BN. 2011. "Regulation of adult neurogenesis in the hippocampus by stress, acetylcholine and dopamine" J Nat Sci Biol Med. 2:26-37.

Vertes RP. 1993. "PHA-L analysis of projections from the supramammillary nucleus in the rat" J Comp Neurol. 326:595–622.

Vertes RP., Fortin WJ., Crane AM. 1999. "Projections of the median raphe nucleus in the rat" J Comp Neurol. 407:555–582.

Vorhees CV. 1989. "A fostering/crossfostering analysis of the effects of prenatal ethanol exposure in a liquid diet on offspring development and behavior in rats" Neurotoxicol Teratol. 11:115–120.

Vorhees CV., Fernandez K. 1986. "Effects of short-term prenatal alcohol exposure on maze, activity, and olfactory orientation performance in rats" Neurobehav Toxicol Teratol. 8:23–28.

Warren KR., Foudin LL. 2001. "Alcohol-related birth defects--the past, present, and future" Alcohol Research and Health: The Journal of the National Institute on Alcohol Abuse and Alcoholism. 25(3): 153–158.

Watanabe Y., Gould E., McEwen BS. 1992. "Stress induces atrophy of apical dendrites of hippocampal CA3 pyramidal neurons" Brain Research. 588:341–345.

Waters EM., Mitterling K., Spencer JL., Mazid S., McEwen BS., Milner TA. 2009. "Estrogen receptor alpha and beta specific agonists regulate expression of synaptic proteins in rat hippocampus" Brain Res. 1290:1-11.

Wattendorf DJ., Muenke M. 2005. "Fetal Alcohol Spectrum Disorders" American Family Physician. 72 (2): 279–285.

Waltman R., Iniquez ES. 1972. "Placental transfer of ethanol and its elimination at term" Obstetrics and Gynecology. 40:180–185.

West JR. 1987. "Fetal alcohol-induced brain damage and the problem of determining temporal vulnerability: A review" Alcohol Drug Research. 7(5-6): 423-441.

West JR., Goodlett CR., Bonthius DJ., Pierce DR. 1989. "Manipulating peak blood alcohol concentrations in neonatal rats: Review of an animal model for alcohol-related developmental effects" Neurotoxicology. 10(3): 347–365.

West JR., Goodlett CR. 1990. "Teratogenic effects of alcohol on brain development" Ann Med. 22(5):319-325.

West JR., Goodlett CR., Bonthius DJ., Hamre KM., Marcussen BL. 1990. "Cell population depletion associated with fetal alcohol brain damage: mechanisms of BAC-dependent cell loss" Alcohol Clin Exp Res. 14:813-818.

West MJ., Slomankia L., Gundersen HJ. 1991. "Unbiased stereological estimation of the total number of neurons in the subdivisions of the rat hippocampus using the optical fractionator" Anat Rec. 231:482-497.

Westergren S., Rydenhag B., Bassen M., Archer T., Conradi NG. 1996. "Effects of prenatal alcohol exposure on activity and learning in Sprague-Dawley rats" Pharmacol Biochem Behav. 55:515–520.

Wozniak DF., Hartman RE., Boyle MP., Vogt SK., Brooks AR., Tenkova T., Young C., Olney JW., Muglia LJ. 2004. "Apoptotic neurodegeneration induced by ethanol in neonatal mice is associated with profound learning/memory deficits in juveniles followed by progressive functional recovery in adults" Neurobiol Dis. 17:403-414.

Whitaker-Azmitia PM., Druse M., Walker P., Lauder JM., 1996. "Serotonin as a developmental signal" Behavioral Brain Research. 73(1-2):19–29.

Wiedenmann B., Franke WW. 1985. "Identification and localization of synaptophysin, an integral membrane glycoprotein of Mr 38,000 characteristic of presynaptic vesicles" Cell. 41(3):1017-1028.

Wigal T., Amsel A. 1990. "Behavioral and neuroanatomical effects of prenatal, postnatal, or combined exposure to ethanol in weanling rats" Behav Neurosci. 104:116–126.

Wilkemeyer MF., Charness ME., 1998. "Characterization of ethanol-sensitive and insensitive fibroblast cell lines expressing human L1" Journal of Neurochemistry. 71(6):2382–2391.

Witter MP., Amaral DG. 2004. "Hippocampal formation," in The Rat Nervous System, ed. Paxinos G., editor. (Amsterdam: Elsevier), 637–703.

Woolley CS. 1998. "Estrogen-mediated structural and functional synaptic plasticity in the female rat hippocampus" Horm Behav. 34(2):140-148.

Wouterlood FG., Saldana E., Witter MP. 1990. "Projection from the nucleus reuniens thalami to the hippocampal region: Light and electron microscopic tracing study in the rat with the anterograde tracer Phaseolus vulgaris-leucoagglutinin" J Comp Neurol. 296:179–203.

Yanni PA., Lindsley TA. 2000. "Ethanol inhibits development of dendrites and synapses in rat hippocampal pyramidal neuron cultures" Brain Res Dev Brain Res. 120(2):233-243.

Young C., Klocke BJ., Tenkova T., Choi J., Labruyere J., Qin YQ., Holtzman DM., Roth KA., Olney JW. 2003. "Ethanol-induced neuronal apoptosis in vivo requires BAX in the developing mouse brain" Cell Death and Differentiation. 10:1148-1155.

Young C., Olney JW. 2005. "Neuroapoptosis in the infant mouse brain triggered by a transient small increase in blood alcohol concentration" Neurobiology of Disease. 22:548-554.

Young C., Roth KA., Klocke BJ., West T., Holtzman DM., Labruyere J.,Qin Y-Q., Dikranian K., Olney JW. 2005. "Role of caspase-3 in ethanol-induced developmental neurodegeneration" Neurobiology of Disease. 20:608-614.

Zhang FX., Rubin R., Rooney TA. 1998. "Ethanol induces apoptosis in cerebellar granule neurons by inhibiting insulin-like growth factor-1 signaling" Journal of Neurochemistry. 71(1):196–204.

Zhang ZW. 2004. " Maturation of layer V pyramidal neurons in the rat prefrontal cortex: intrinsic properties and synaptic function" J Neurophysiol. 91(3):1171-1182.

Zhang X., Sliwowska JH., Weinberg J. 2005. "Prenatal alcohol exposure and fetal programming: effects on neuroendocrine and immune function" Exp Biol Med (Maywood). 230:376–388.

Zhang XH., Wu LJ., Gong B., Ren M., Li BM., Zhuo M. 2008. "Induction- and conditioning-protocol dependent involvement of NR2B-containing NMDA receptors in synaptic potentiation and contextual fear memory in the hippocampal CA1 region of rats" Mol Brain. 1:9.

Zhao MG., Toyoda H., Lee YS., Wu LJ., Ko SW., Zhang XH., Jia Y., Shum F., Xu H., Li BM., Kaang BK., Zhuo M. 2005. "Roles of NMDA NR2B subtype receptor in prefrontal long-term potentiation and contextual fear memory" Neuron. 47(6):859-872.

Zhao C., Teng EM., Summers RG Jr., Ming GL., Gage FH. 2006. "Distinct morphological stages of dentate granule neuron maturation in the adult mouse hippocampus" J Neurosci. 26:3-11.

Zheng JQ. 1994. "Cortical projections from the reuniens nucleus of the thalamus in the rat" Kaibogaku Zasshi. 69:261–269.

Zhu PJ., Lovinger DM. 2006. "Ethanol potentiates GABAergic synaptic transmission in a postsynaptic neuron/synaptic bouton preparation from basolateral amygdala" J Neurophysiol. 96(1):433-441.

Zhu ZW., Xu Q., Zhao ZY., Gu WZ., Wu DW. 2011. "Spatiotemporal expression of PSD-95 in Fmr1 knockout mice brain" Neuropathology. 31(3):223-229.

Zimmer J. 1973. "Extended commissural and ipsilateral projections in postnatally deentorhinated hippocampus and fascia dentata demonstrated in rats by silver impregnation" Brain Res. 64:293-311.

Zimmer J., Hjorth-Simonsen A. 1975. "Crossed pathways from the entorhinal area to the fascia dentata. II. Provokable in rats" J Comp Neurol. 161(1):71-101.

Zimmerberg B., Sukel HL., Stekler JD. 1991. "Spatial learning of adult rats with fetal alcohol exposure: deficits are sex-dependent" Behav Brain Res. 42:49-56.

CURRICULUM VITAE

PERSONAL INFORMATION

Surname, Name: Elibol-Can, Birsen

Nationality: Turkish (TC)

Date and Place of Birth: 05 February 1982, Ankara

Phone: +90 533 231 07 23

Fax: +90 312 210 79 76

email: c.birsen@gmail.com

Foreign languages: English

EDUCATION

Degree	Institution	Year of Graduation
M.Sc.	METU, Dept. of Biological Sciences	2007
BS	METU, Dept. of Biological Sciences	2005

Conferences, Symposia, Trainings, and Workshops-Seminars:

1. European Molecular Biology Organization-Young Scientists Forum,Yeditepe University, İstanbul, Turkey, (2012, June)

2. Course of Microscopy, Imaging and Stereology, Hacettepe University, Ankara, Turkey (2012, January)

3. Turkish FEPS-Physiology Congress, Yeditepe University, İstanbul, Turkey (2011, September)

4. 36th National Congress of Physiology, Edirne, Turkey (2010, September)

5. 7th FENS Forum of European of Neuroscience, Amsterdam, The Netherlands, (2010, July)

6. 9th National Congress of Neuroscience, Yeditepe University, İstanbul, Turkey, (2010, April)

7. Certificate of Animal Use in Experimental Research, 80-hour course in Laboratory Animal Science, Yeditepe University, İstanbul, Turkey, (2009, November)

8. Neuroscience workshop on the effects of perinatal and adult ethanol intake on brain and behavior in animal models, METU, Ankara, Turkey, (2008, October)

9. 10th International Conference on Cognitive Neuroscience, Bodrum, Turkey, (2008, September)

10. Seminar on Stereological Methods in Clinical Experiments,Faculty of Medicine of Fatih University and Turkish Society for Stereology, (2008, May)

11. European Molecular Biology Organization-Young Scientists Forum, Boğaziçi University, İstanbul, Turkey, (2008, February)

12. 4th Ege Bingss, Innovative Neuromorfology and Neurostereology Course and Developmental, Degenerative and Restorative Neural Plasticity 4, (2007, June)

13. Noldus- Ethovision 3.1 Software User Training Meeting, Ankara, Turkey, (2006, April)

14. 5th National Congress of Neuroscience, Zonguldak Karaelmas University, Zonguldak, Turkey, (2006, April)

Awards/Honors and Scholorships :

* 2009, 8th National Congress of Geriatry, First Award of Scientific Research

* 2009, Middle East Technical University, Course Performance Award in PhD Program

* 2006, 6th National Congress of Geriatry, First Award of Poster Presentation

* 2007-2012, Scholorships of Tubitak (PhD)

Publications :

Journal Papers (SSCI, SCI, AHCI)
1. **Elibol-Can B**., Simsek-OzekN., Severcan M., Severcan F., Jakubowska-Dogru E. "Vitamin A deficiency induces structural and functional alterations in the molecular constituents of the rat hippocampus" in preparation.

2. **Elibol-Can B.,** Dursun I., Canan S., Jakubowska-Dogru E. "Changes in hippocampal cell counts and volumes during the first two postnatal months in control and fetal alcohol rats: A stereological study" submitted to *Journal of Neuroscience Research.*

3. Dursun I., Jakubowska-Dogru E., van der List D., **Elibol-Can B.,** Chapman B., Qi L., Berman RF. "Effects of Early Postnatal Alcohol Exposure on the Developing Retinogeniculate Projections in C57BL/6 Mice" *Alcohol*, in press.

4. **Elibol-Can B.,** Jakubowska-Dogru E., Severcan M., Severcan F. "The effects of short-term chronic ethanol intoxication and ethanol withdrawal on the molecular composition of the rat hippocampus by FT-IR spectroscopy" *Alcoholism Clinical and Experimental Research*, 35(11):2050-62, 2011.

5. Isik At, Celik T, Ulusoy G, Ongoru O, **Elibol B,** Doruk H, Bozoglu E, Kayir H, Mas Mr, Akman S. "Curcumin Ameliorates Impaired Insulin/Igf Signalling And Memory Deficit in A Streptozotocin-Treated Rat Model", *Age (Dordr).* 31(1):39-49, 2009.

Conference Papers

1. Severcan M., Severcan F., Jakubowska-Dogru E., **Elibol-Can B.,** Simsek-Ozek N.Vitamin A deficiency-induced alterations and the protective role of Vitamin A supplementation in protein secondary structure of rat hippocampus, OMICS Group Conferences, International Conference on Pathology, J Clin Exp Pathol 2012, 2:5, USA, August, 2012

2. Eyuboglu S., Kılıc U., Ugur M., Seker B., **Can B**., Fındık S., Yılmaz B., Kılıc E., Effects of Melatonin and Memantine on Brain Injury and Intracellular Signaling: Roles of Akt, p38, p21, and ERK1/2 phosphorylation, British Society for Neuroendocrinology Annual Meeting Abstract Book, pp:50, England, July, 2011.

3. Eyuboglu S., Ugur M., Kılıc U., Cumbul A., Cevreli B., **Can B**., Yılmaz B., Kılıc E., Anti-Oksidant Melatonin ve NMDA Antagonisti Memantin Kombinasyonunun Beyin Felci Sonucu Oluşan Beyin Hasarı ve Ödemine Olan Etkileri, 36th National Congress of Physiology Abstract Book, S26, pp:60, Edirne, September, 2010.

4. **Can B**., Dursun I., Uysal A.K., Canan S., Jakubowska-Dogru E.,Investigation of Morphological Regeneration in The Neonatal Rat Hippocampus After Fetal Alcohol Administration, 7th FENS Forum of European of Neuroscience, Abstract Book, vol.5, 115.19, The Netherlands, July 2010.

5. **Elibol-Can B**., Dursun I., Uysal A.K., Canan S., Jakubowska-Dogru E., The Effects of Prenatal Exposure to Ethanol on the Morphology of Developing Rat Hippocampus, 9th National Congress of Neuroscience, Turkish Journal of Neurology, 16(1), pp:239, İstanbul, April 2010.

6. Işık, AT., Bozoğlu, E., Çelik, T., Ural, AU., Ulusoy, MG., Akdağ, E., **Elibol, B.,** Streptozotosinle Oluşturulan Deneysel Alzheimer Hastalığı Modelinde Mezenkimal Kök Hücre Tedavisi, 8th National Congress of Geriatry Abstract Book pp:102-3, Fethiye, October 2009.

7. Jakubowska-Doğru E., **Elibol B.,** Arıtan B., Sezer M., Kaya Z., Tufanlı Ö., Ragbetli M., Kaplan S., Study on the Potential Effects of Fetal Exposure to Diclofenac Sodium (Voltaren) on Brain Morphology and Behaviour in Young Wistar Rats. 9th International Congress of Polish Neuroscience Society. Acta Neurobiol. Exp. 69(3): P355, Poland, September, 2009.

8. Severcan F., **Elibol B**., Jakubowska-Doğru E., Effects of Binge-Like Ethanol Administration on Macromolecule Profiles in The Hippocampus of Young-Adult Wistar Rats as Assessed by FT-IR Spectroscopy. 9th International Congress of Polish Neuroscience Society. Acta Neurobiol. Exp. 69(3): P350, Poland, September, 2009.

9. Dursun I., **Elibol, B.,** Jakubowska-Dogru, E.,Uzbay, U., Confounding Factors, Gender and Age, in the Research of Fetal Ethanol Effects on Animal Behavior, Alcoholism: Clin. And Exp. Res. 33(6):35A, RSA Congress, San Diego, June 2009.

10. Dursun, I., **Elibol, B**., Uzbay, T., Jakubowska-Dogru, E., Animal's Gender And Age At Testing Are Critical Factors in Evaluation of Fetal Ethanol Effects on Behavior, 8th National Congress of Neuroscience, Neuroanatomy 8, Pp:185-6, Bolu, April 2008.

11. **Elibol B.,** Jakubowska-Doğru E., Severcan F., Effects of Chronic Ethanol Cohsumption on Memory and Molecular Changes in Hippocampus of Young Adult Wistar Rats, 10th International Conference on Cognitive Neuroscience, Frontiers in Human Neuroscience Abstract Book, p. 291, Bodrum, September 2008,

12. Jakubowska-Doğru E., Wesierska M., **Elibol B.,** Güven Ş., Role Of Perirhinal Cortex İn The Short-Term Auditory Recognition Memory İn Rat. Proc. 8th International Congress of The Polish Neuroscience Society, Acta Neurobiol. Exp. 67(3) P.:296, P4.04, Poland, September 2007.

13. Isık AT., Celik T., Ulusoy G., Ongoru O., **Elibol B.,** Bozoglu E., Doruk H., Mas MR. Streptozotosinle Olusturulan Alzheimer Hastalığı Modelinde Curcuminin Etkinliği. 6th National Congress of Geriatry Abstract Book p:89, Antalya, October 2006.

14. A. Isik, T. Celik, G. Ulusoy, H. Doruk, E. Bozoglu, O. Ongoru, **B. Elibol,** S. Akman, M. Mas, P4-374: Curcumin Reverses İmpaired İnsulin/Igf Signaling And Memory İn Streptozotocin İnduced Memory Deficit. Alzheimer&Aposs And Dementia, Volume 4, Issue 4, Pages T783-T784.

15. Jakubowska-Doğru E., **Elibol B.,** Dursun I., Severcan F. Effects of Chronic Alcohol Intake and Withdrawal on Memory and Brain Protein and Lipid Profiles Assessed by FT-IR

Technique in Young Adult Wistar Rats. The 5th International Congress of Pathophysiology, Chinese J. Pathophysiol. 22: 437, China, July 2006.

16. Jakubowska-Doğru E., Wesierska M., **Elibol B.,** Günay G. Preliminary study on the involvement of perirhinal cortex in the short-term auditory recognition memory in rat. The 5th National Congress of Neuroscience, Neuroanatomy 5 supply P.63, Zonguldak, April 2006,